The Molecular Mechanisms of Bacterial Virulence Factors that Modulate Host Haemostatic Factors

Sophie Elizabeth Cherrington

Submitted in accordance with the requirements for the degree of
Doctor of Philosophy

The University of Leeds
School of Medicine

Based at and funded by

NIBSC, Hertfordshire

Department of Biotherapeutics

February 2022

The candidate confirms that the work submitted is her own and that appropriate credit has been given where reference has been made to the work of others.

Acknowledgements

First, I would like to thank my supervisors Dr. Craig Thelwell (NIBSC), Professor Helen Philippou (University of Leeds), and Dr. Azhar Maqbool (University of Leeds) for their continued guidance, support, and scientific expertise throughout my PhD. I am extremely grateful to Craig for his motivation and positivity. His guidance has shaped me to be a better scientist.

I would like to thank individuals of LICAMM who always made me feel welcome during my visits to University of Leeds. Dr. Lewis Hardy assisted me for 2 weeks with the scanning electron microscopy (SEM) and inverted laser scanning confocal microscopy (LSCM) work. He provided valuable laboratory guidance that enabled me to continue the LSCM experiments back at NIBSC. I would also like to thank Dr. Fraser Macrae who demonstrated bacterial migration assays allowing me to adapt at NIBSC, and Dr. Cédric Duval who provided me protocols for the permeation experiments.

At NIBSC, I would like to thank Dr. Robert J Francis for providing extensive training on the upright LSCM and Imaris software. I would also like to thank Dr. Kirsty MacLellan-Gibson for providing training on the SEM at NIBSC and, although the work did not reach my thesis, thank you for helping me learn freeze-fracturing as an alternative for critical point drying.

Thank you to all of my colleagues and friends at NIBSC, particularly in the Haemostasis section. Dr. Stella Williams, Dr. Helen Wilmot, and Dr. John Hogwood, our chats were always a welcome distraction! A special thank you to Dr. Sanj Raut and Andrew Riches-Duit, whom I have had the pleasure of working with for the last 12 months whilst I have been writing my thesis.

I would like to say thank you to my friends and family. A special mention to Martina Krištof, Kiera Burns, and Andrew Tung Yep for the numerous coffee and lunch breaks which kept me going during the busiest of weeks, and to Abi Tindell (Thank you for also listening to me vent on numerous occasions about experimental failures!), Kirsty Wilkinson and Emily Bainbridge who, despite the 200 mile distance, still managed to keep in touch every day for the last 4 years making it a much easier transition moving into a new county alone. Finally, Chris McSorley thank you for the unconditional support (and the constant reminders that I should be writing my thesis!), even during the days when I must have been unbearable to live with. I could not have done this without you all, thank you.

Abstract

Group A Streptococcus (GAS) express an arsenal of virulence factors that interact with the host haemostatic system. Streptokinase (SK) from GAS activates human plasminogen, which degrades fibrin clots to facilitate bacterial dissemination. GAS strains have been divided into evolutionary clusters based upon SK sequence variation. Unlike Cluster 1 SK, Cluster 2 variants have very little activity against plasminogen alone and depend on stimulation by co-factors (e.g., fibrin(ogen)). Cluster 2 SK variants also appear to correlate with cell-surface M-like proteins: SK2a with M1 (fibrinogen-binding) and SK2b with PAM (plasminogen-binding).

We have shown that plasminogen activation rates using rSK2b are stimulated by rPAM following a template model, suggesting rPAM binding sites are present on rSK2b. Maximum stimulation was found using immobilised rPAM indicating an important role for cell-surface plasmin generation by rSK2b. M1 is known to be cleaved from GAS cell-surface and form a supramolecular complex with fibrinogen, capable of activating neutrophils and platelets creating a hypercoagulable state. Fibrin was the most potent stimulator of rSK2a activity, and fibrin(ogen) stimulation of rSK2a was independent of rM1. The impact of rM1-bound fibrinogen on fibrin clot formation was investigated using microscopy, permeation assays and thromboelastometry, which revealed increasing rM1 produces heterogeneous clots with irregular fibre bundles, compacted fibrin with increased porosity and susceptibility to lysis. rM1 also disrupted the formation of the protective fibrin film and reduced mechanical clot strength. M1-bound fibrinogen at infection sites may contribute to the severity of infection by forming fibrin clots with a compromised protective film, that are mechanically weaker, more porous, and less resistant to lysis by plasmin.

Currently no vaccine exists for GAS and reduced susceptibility to antibiotics has been observed. Targeted therapies against M1 and SK (or to counter the haemostatic processes they interrupt) could provide a novel therapeutic strategy for treating GAS diseases and sequalae.

List of Figures

List of Tables

Abbreviations

6-AHA	6-aminohexanoic acid
aPTT	Activated partial thromboplastin time
BCA	Bicinchoninic Acid
BSA	Bovine serum albumin
ClfA	Clumping factor A
Coa	Coagulase
CovRS	Control of virulence two-component signalling system
ECM	Extracellular matrix
EGF	Epidermal growth factor
EP	European Pharmacopoeia
FBS	Fetal bovine serum
FDA	US Food and Drug Administration
FgD	Fibrinogen D domain
FnBPB	Fibronectin-binding protein B
FpA	Fibrinopeptide A
FpB	Fibrinopeptide B
FT	Flow through
GAS	Group A Streptococcus
GPIb/IX/V complex	Glycoprotein Ib-IX-V complex
GPVI	Glycoprotein VI
HA capsule	Hyaluronic acid capsule
HBP	Heparin binding protein
HMWK	High-molecular weight kininogen
HPLC	High-performance liquid chromatography
HSA	Human serum albumin
IgG	Immunoglobulin G
IPTG	Isopropyl ß-D-1-thiogalactopyranoside
LB	Luria broth
LBS	Lysine binding sites
LSCM	Laser Scanning Confocal Microscopy
LTA	Lipoteichoic acid
MCF	Maximum clot firmness
mga	Multiple gene regulator
NBS	Non- binding surface
NETs	Neutrophil extracellular traps
nm	Nanometre
PAI-1	Plasminogen activator inhibitor- 1
PAM	Plasminogen binding Group A streptococcal M-like protein
PAp	Pan-apple domain
PBS	Phosphate-buffered saline
PK	Prekallikrein
pNa	p-nitroaniline

PolyP	Polyphosphates
RBC	Red blood cell
ROTEM	Rotational thromboelastometry
sc-tPA	Single chain tissue plasminogen activator
sc-uPA	Single-chain urokinase-type plasminogen activator
SDS-PAGE	Sodium dodecyl sulphate–polyacrylamide gel electrophoresis
SEM	Scanning Electron Microscopy
SfbI	Streptococcal fibronectin-binding protein I
SK	Streptokinase
SLO	Streptolysin-O
SPR	Surface plasmon resonance
STSS	Streptococcal toxic shock syndrome
TAFI	Thrombin-activatable fibrinolysis inhibitor
TCS	Two-component regulatory systems
tc-tPA	Two chain tissue plasminogen activator
tc-uPA	Two-chained urokinase-type plasminogen activator
TF	Tissue factor
TFPI	Tissue factor pathway inhibitor
THY	Todd Hewitt Broth, yeast extract
tPA	Tissue plasminogen activator
uPA	Urokinase-type plasminogen activator
UV	Ultraviolet
vWbp	Von Willebrand factor binding protein
vWF	Von Willebrand binding factor
WHO	World health Organisation

Chapter 1 Introduction

1.1 Physiological Haemostasis

Haemostasis is a tightly regulated process requiring a delicate balance between coagulation (intrinsic and extrinsic pathways), anticoagulation and fibrinolysis to prevent excessive thrombosis or bleeding upon vascular injury. There are two main stages of haemostasis, primary and secondary. Primary haemostasis refers to platelet aggregation and initial platelet plug formation in response to a disrupted or damaged blood vessel. Secondary haemostasis is the proteolytic activation of circulating coagulation factors with the ultimate goal of fibrin formation to stabilise the blood clot, control bleeding and prevent microbial invasion (Gale, 2011); the first principles of which were described in 1964 when Davie and Ratnoff outlined the cascade of proenzymes, describing the activation of serine proteases downstream as a waterfall (Davie and Ratnoff, 1964).

1.1.1 Primary haemostasis

Under normal circumstances and blood flow, platelets circulate in the bloodstream for 5-7 days at ~150-450 x 10^9/L and do not adhere to surfaces or aggregate together. Due to the shear forces within the blood vessel and presence of the blood components, platelets flow within close proximity to the vessel wall which allows platelets to react quickly upon injury. Platelets respond to vascular injury in several stages; beginning with immediate adhesion to the exposed subendothelial extracellular matrix to limit haemorrhage. Under shear pressure, adhesion occurs via von Willebrand binding factor (vWF) forming a

bridge between subendothelial collagen and platelet glycoprotein Ib-IX-V complex (GPIb/IX/V complex) on the platelet surface. The exposed collagen also binds directly to platelet integrin α2β1 and glycoprotein VI (GPVI). As vWF binds to collagen, it is the shear stress of the flowing blood that exposes cryptic binding sites on vWF A1 domain for GPIb (part of the GPIb/IX/V complex). This leads to platelet activation and degranulation occurs to release α-granules and dense granules. Platelets begin to aggregate forming a vascular seal. Activated platelets change their shape from a discoid shape to elongated cells to maximise the subepithelial surface coverage and allow a tight fit. Platelet aggregation is strengthened by connections between the platelet receptor aIIbβ3 bound to fibrinogen, vWF, fibronectin or vitronectin (Pryzdial et al., 2018, Holinstat, 2017, Yun et al., 2016, Clemetson, 2012). The platelet plug is then stabilised by an insoluble fibrin scaffold, generated by secondary haemostasis.

1.1.2 Secondary haemostasis

The coagulation cascade has been traditionally classified into the intrinsic and extrinsic pathways, both of which join at the common pathway during factor X activation. Figure 1 demonstrates a schematic diagram of these two mechanisms for blood clotting initiation. Each zymogen in the cascade is depicted as a Roman numeral, with a lower case ‘a’ once the protein has been proteolytically converted to the active enzyme.

1.1.2.1 Extrinsic pathway

The extrinsic pathway is triggered upon exposure to a transmembrane protein known as tissue factor (TF) following vascular injury (Grover and Mackman, 2018). TF is a glycoprotein, expressed by a wide variety of cells including adventitial cells surrounding all blood vessels, in keratinocytes in the skin, and in a variety of epithelial layers (Drake et al., 1989, Wilcox et al., 1989, Fleck et

al., 1990). Furthermore, TF expression is particularly abundant in anatomic sites where haemorrhage is likely to be fatal to the host, such as the kidneys and brain (Fleck et al., 1990, Drake et al., 1989). Circulating blood cells and cells that are exposed to blood, do not normally express TF to prevent inappropriate activation in a healthy individual (Wilcox et al., 1989).

TF binds to either the circulating zymogen coagulation factor FVII (FVII) or the active form FVIIa with a high affinity, resulting in a 1:1 stoichiometry. FVII is rapidly converted to FVIIa by TF through the cleavage of a single peptide bond (Nemerson and Repke, 1985). The TF:FVIIa complex then proteolytically cleaves coagulation factor X (FX) into its active form, FXa, which along with activated coagulation factor V (FVa) can trigger the formation of thrombin as described in section 1.1.2.3. The TF:FVIIa complex can be inhibited by tissue factor pathway inhibitor (TFPI), which exists as two isoforms; TFPIα and TFPIβ (Piro and Broze, 2005).

1.1.2.2 Intrinsic pathway

The intrinsic pathway, or contact pathway, is known to be activated *in vitro* by contact with negatively charged surfaces such as ellagic acid, glass and diatomaceous earth (Colman and Schmaier, 1997). These non-physiological modes of activation are commonly used in clinical plasma clotting tests known as the activated partial thromboplastin time (aPTT). The assay is routinely used as a diagnostic tool to screen for coagulation defects in the intrinsic pathway, such as haemophilia A (FVIII deficiency), B (FIX deficiency) or C (FXI deficiency). More recently, *in vivo* candidate activators of the intrinsic pathway have been proposed; such as extracellular nucleic acids (Kannemeier et al., 2007), inorganic polyphosphate (polyP) (Muller et al., 2009) and bacterial surface proteins (Herwald et al., 1998, Nickel and Renne, 2012).

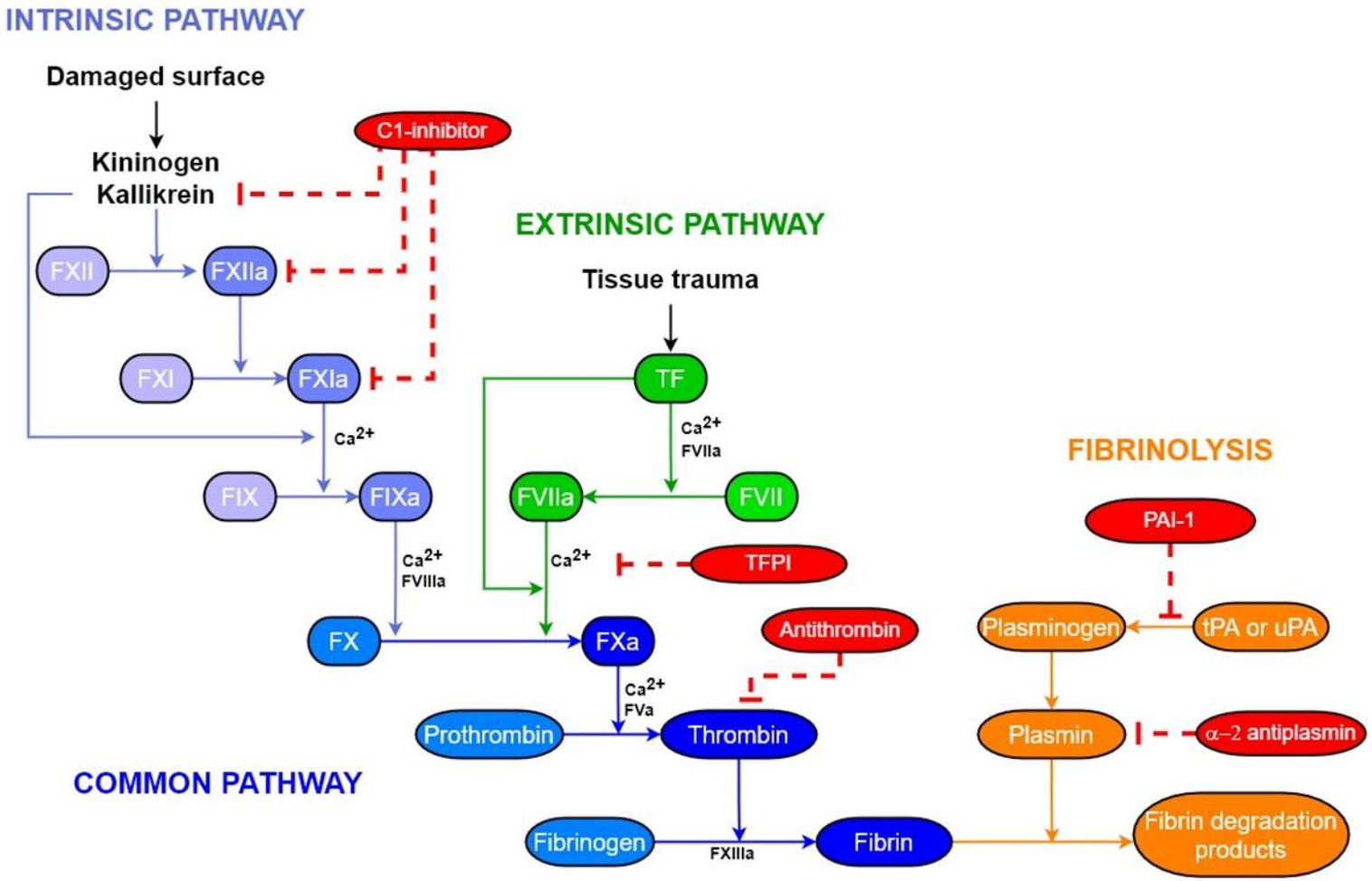

Figure 1 Schematic representation of coagulation, fibrinolysis, and natural inhibitors. The coagulation cascade has been traditionally classified into two pathways, the intrinsic system (purple boxes and lines) and the extrinsic system (green boxes and lines). These two pathways converge at the common pathway (blue boxes and lines) leading to the activation of factor X (FX) and the generation of thrombin which is required for the ultimate goal of fibrin clot formation. Fibrinolysis (Orange boxes and lines) is initiated by plasminogen activators converting plasminogen to the active serine protease plasmin, degrading fibrin into the degradation products. Inhibitors are indicated in red boxes with dashed lines. Coagulation factors are indicated by 'F' followed by Roman numerals. Active coagulation factors are indicated by the additional 'a'

Following binding to surfaces, FXII undergoes a conformational change leading to autoactivation. FXIIa cleaves prekallikrein (PK) to generate active kallikrein; which in turn activates additional FXII in a positive feedback loop (Muller et al., 2011). Kallikrein, a trypsin-like serine protease, simultaneously cleaves high-molecular-weight kininogen (HMWK), releasing bradykinin, which stimulates the release of tissue plasminogen activator (tPA). Activated FXIIa converts FXI to FXIa, which then activates FIX to FIXa. FIXa then forms an 'intrinsic tenase' with FVIIIa, which activates FX to FXa, before the intrinsic and extrinsic pathways converge at the common pathway (section 1.1.2.3) (Smith et al., 2015). Recently, a new branch of the intrinsic coagulation cascade has also been identified. Kearney et al., and others have demonstrated that kallikrein can activate FIX directly, thus bypassing FXI (Kearney et al., 2021b, Visser et al., 2020, Noubouossie et al., 2020). The intrinsic pathway is regulated by C1-inhibitor, which is a protease capable of inhibiting FXIIa, kallikrein and FXIa (Zeerleder, 2011).

Whilst the intrinsic pathway is known to play an important role in clot formation *in vitro*, it has not been well characterised *in vivo.* Humans and mice with FXII deficiencies do not bleed abnormally, despite having prolonged aPTT times (Ratnoff and Colopy, 1955). Furthermore, individuals lacking PK or HMWK do not have impaired coagulation and are only diagnosed upon routine screening (Renne et al., 2012). This has caused much debate over the contribution of the intrinsic pathway to normal haemostasis and led to the hypothesis that the extrinsic (TF) pathway is the main pathway that initiates fibrin formation *in vivo.* This is supported by data that shows decreased levels of TF in murine models leads to an increase in bleeding (Monroe et al., 2010) and a complete absence

of TF is fatal, indicating TF is essential for development and survival (Mackman, 2004).

The intrinsic pathway is however very important in inflammatory response and host defence due to the release of the proinflammatory neuropeptide, bradykinin. Bradykinin causes vasodilation, enhanced vascular permeability and vascular leakage in blood vessels (Shigematsu et al., 2002, Han et al., 2002, Proud and Kaplan, 1988). Furthermore, the intrinsic pathway produces PK, which can activate the alternate complement pathway by proteolytic activation of factor C3 (DiScipio, 1982). PK can also activate pro-urokinase or plasminogen and initiate fibrinolysis (Maas et al., 2011, Ichinose et al., 1986).

1.1.2.3 Common Pathway

The intrinsic and extrinsic pathways converge at the common pathway where FX is converted to FXa. FXa forms a prothrombinase complex with FVa which proteolytically converts prothrombin to thrombin (Adams and Huntington, 2016). Thrombin is a multifunctional serine protease and is considered to play a key function in haemostasis. Thrombin converts soluble fibrinogen to insoluble fibrin (as described in section 1.1.3) and enhances its own generation through the activation of FV, FVIII and FXI in a positive feedback loop, resulting in a large thrombin ‘burst’. Thrombin also activates FXIII to FXIIIa, a member of the transglutaminase family of enzyme, which crosslinks and stabilises fibrin clots. Overall, thrombin has been found to have 13 different roles in haemostasis (Lane et al., 2005, Posma et al., 2016). Thrombin activity is inhibited directly by antithrombin, a member of the serine protease inhibitor (serpin) family. When thrombin is bound to its cofactor thrombomodulin, an endothelial cell thrombin receptor, it is capable of activating protein C, which along with its cofactor,

protein S, proteolytically inactivates FVa and FVIIIa (Crawley et al., 2007). Therefore, thrombin also aids in its own attenuation.

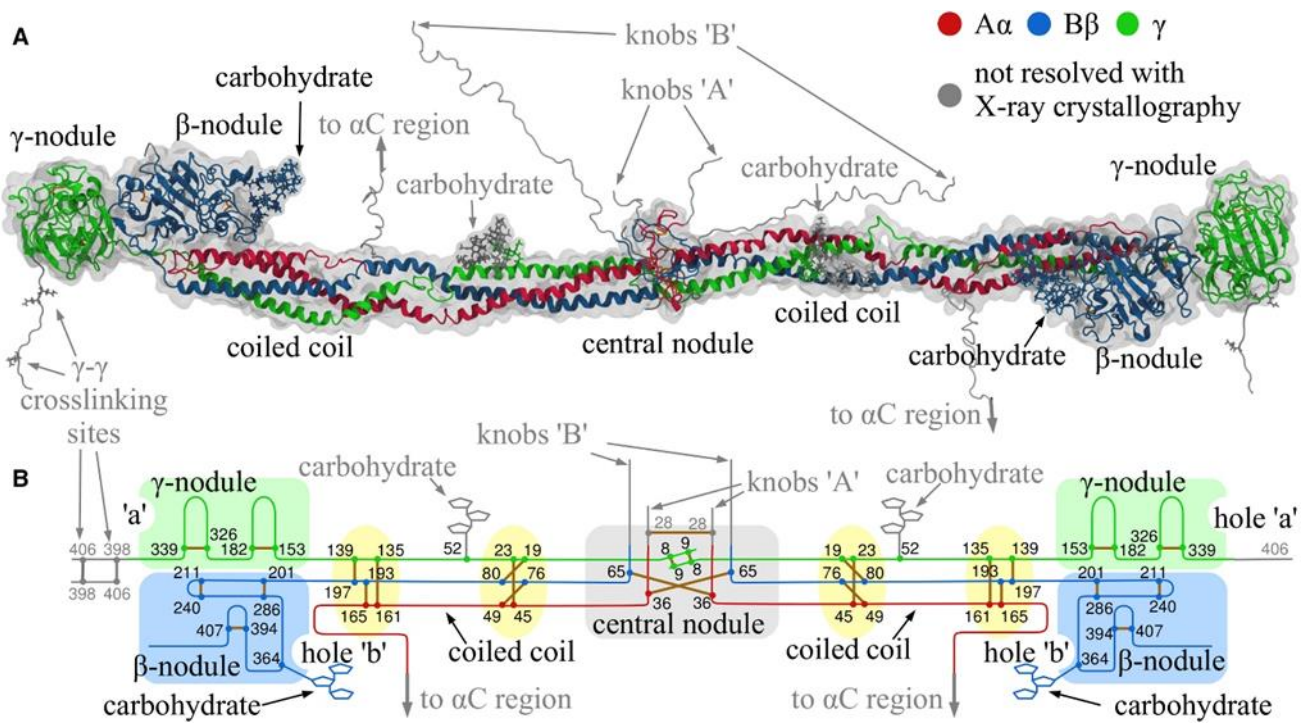

Figure 2 Structure of human fibrin(ogen) (A) Crystal structure of approximately two thirds of human fibrinogen has been shown by X-ray crystallography (PBD Entry: 3GHG). Aα chains are highlighted in red, Bβ chains in blue and γ chains in green. Additional portions of the structure highlighted in grey, such as knobs 'A' and knobs 'B', have been computationally reconstructed and have not been resolved by X-ray crystallography. **(B)** Schematic of fibrin(ogen) structure held together with 29 disulphide bonds (yellow), with the γ-γ crosslinking sites highlighted (Imaged reused from (Zhmurov et al., 2016) with permission from Elsevier Ltd; Licence number: 5141310838873)

1.1.3 Fibrin(ogen) structure

Human fibrinogen is a 340-kDa glycoprotein, which circulates in the blood at 2-4 mg/ml. Structural data collected from X-ray crystallography, transmission electron microscopy and atomic force microscopy has demonstrated that fibrinogen monomers are trinodular, elongated, 45 nm in length and ~2-5 nm in diameter (Weisel et al., 1985, Williams, 1981, Fowler and Erickson, 1979, Hall and Slayter, 1959). More than two thirds of the human fibrinogen structure has been resolved by X-ray crystallography to date (Madrazo et al., 2001, Brown et al., 2000, Yee et al., 1997, Spraggon et al., 1997) and the unresolved portions have been computationally reconstructed (Figure 2A, (Zhmurov et al., 2016)) to gain a complete molecular structure. Fibrinogen is composed of two sets of

three distinct disulphide- linked polypeptide chains, appointed Aα, Bβ and γ, which consists of 610, 461 and 411 amino acids, respectively (Weisel, 2005) (Figure 2). The six fibrinogen chains are in a complex with their N-terminal in a central 'E region' which extends outward in a coiled-coil E domain consisting of a triple α-helical structure. The coiled-coils contain a hinge point, located near the residue γAsn52 (Figure 2B), which determines the flexibility of fibrinogen molecules both in solution (Zuev et al., 2017) and bound to a surface (Kohler et al., 2015). The C termini of the Bβ and γ chains form globular regions known as βC and γC modules, respectively. These nodules were named the D regions. The C termini of the Aα chains extend from the D region by approximately 400 amino acids, forming a highly flexible series of repeats followed by a globular αC region. Due to the flexible nature of these regions they could not be resolved by crystallography, however Protopopova et al. obtained images using high resolution atomic force microscopy (Protopopova et al., 2015, Protopopova et al., 2017). The nomenclature representing the fibrinogen polypeptide chain as $(A\alpha\ B\beta\ \gamma)_2$ arises from the designation of the fibrinopeptides A and B (FpA and FpB) on the N-terminal ends of the Aα and Bβ chains, respectively (Medved et al., 2009).

1.1.3.1 Fibrin clot polymerisation

During coagulation, fibrin polymerisation and arrangement is stimulated upon cleavage of the 16-residue FpA and 14-residue FpB chains of fibrinogen, from the N-terminal Aα and Bβ chains, respectively. In solution, FpA is initially cleaved at a faster rate than FpB producing fibrin monomers. The enzymatic cleavage of FpA exposes a new glycine (Gly)-proline(Pro)-arginine(Arg) motif (knobs 'A' in the central E region, Figure 2), which binds with a high affinity to holes 'a' of neighbouring fibrin monomers 'D regions' (Erickson and Fowler,

1983, Yang et al., 2000, Kostelansky et al., 2002). The holes ‘a’ are located on the γ-chains between residues γ290-379 and include the amino acids γAsp364, γArg375, γHis340, γGln329 and γLys338 (Everse et al., 1998, Litvinov et al., 2021). The complementary ‘A:a’ knob: hole interactions between the molecules results in the formation of a half-staggered fibrin dimers (Figure 3). A third fibrin monomer joins the half-staggered molecule producing an end-to-end junction, where the lateral D regions form the D:D interface. The D:D interactions, involving residues γ275, γ308 and γ309, are weak and are the first to break apart in the fibrin structure (Zhmurov et al., 2011, Mullin et al., 2002, Marchi et al., 2006, Bowley et al., 2009, Hirota-Kawadobora et al., 2004). Additionally, at the inter-strand D:E:D interfaces, residues αVal20-Lys29 (adjacent to the knob ‘A’ sequence) interacts with residues γAsp298-Phe304, γAsn319-Asn325, and γGln329 in the γ-nodule next to hole ‘a’. There are also binary contacts between residues αLeu54, αGlu57, αPhe62, αArg65, γGln33, γAsp37, and γGln47 in the coiled-coil region and γGln329-Asp330 in the γ-nodule (Zhmurov et al., 2016). Fibrin monomers continue to join longitudinally to the two- stranded trimer oligomers. The oligomers begin to aggregate laterally once they reach a length of 0.5-0.6 μm, containing 20-25 half-staggered fibrin monomers, forming protofibrils (Chernysh et al., 2011).

As the fibrin assembles, the rate of FpB release increases, reaching maximum when polymerisation is almost complete suggesting that FpB is preferentially released from polymers (Weisel et al., 1993, Erickson and Fowler, 1983). However in surface attached fibrinogen, FpB is cleaved at a faster rate than FpA (Riedel et al., 2011) suggesting that the increased rate is due to the conformation of fibrinogen and the accessibility of thrombin to the fibrinopeptides. Despite these observations, the physiological role for B:b

interactions remains unclear. It has been proposed that FpB plays a role in lateral aggregation of protofibrils as it has been shown that when FpA is cleaved, but FpB release is inhibited, the fibrin fibres are thinner (Blomback et al., 1978). Additionally, B:b knob: hole interactions have been found to contribute to the fibrin clots susceptibility to lysis by plasmin (Doolittle and Pandi, 2006).

The flexible globular αC regions of fibrinogen have also been proposed to enhance lateral aggregation of the fibrin protofibrils (Weisel and Medved, 2001, Tsurupa et al., 2011) and have been shown to interact resulting in the formation of αC polymers (Figure 3). Similar to B:b knob: hole interactions, when the αC region was absent or shorter in length, the resultant clots had thinner fibres with increased branch points and enhanced fibrinolysis suggesting impaired lateral aggregation of the protofibrils (Collet et al., 2005, Ping et al., 2011, Protopopova et al., 2017). However, in the absence of A:a or B:b knob: hole interactions the αC regions interactions appear to be too unstable and did not show any signs of polymerisation (Duval et al., 2020).

As the fibrin clot continues to aggregate laterally, forming thicker fibres, and grow in length, the fibrin fibres also begin to branch forming a three-dimensional network. There are two main types of branching points, ‘bilateral junction’ and ‘trimolecular junction’. A ‘bilateral’ junction can form when two protofibrils join to form a four-stranded fibril before diverging into two separate protofibrils (Mosesson et al., 1993). A ‘trimolecular junction’, also known as a ‘equilateral junction’, forms when a fibrin monomer joins by only a single γ-nodule, and can begin the formation of a new two-stranded protofibril (Fogelson and Keener, 2010).

A recent study from *in vitro* and *in vivo* experiments demonstrated that following a skin wound, a fibrin film forms at the air-liquid interface. The film is a continuous layer that covers the external surface of the clot, which is distinct from the fibrin network underneath. The film is thought to form a protective layer between the blood and the air, retain blood cells and provide the first line of defence against microbial invasion (Macrae et al., 2018).

During and after polymerisation, the fibrin clot is stabilised by covalent crosslinking from the plasma transglutaminase, factor XIIIa. The D:D interface between two fibrin monomers are cross-linked by an intermolecular ε-(γ-glutamyl)-lysyl isopeptide bond between γLys406 of one γ chain and γGln398/399 of another γ chain. Additional crosslinking is catalysed between lysine and glutamine residues in the αC regions within protofibrils and in the inter-protofibril space (Matsuka et al., 1996). The α and γ chains, but not β chains, can also be crosslinked resulting in the formation of α -polymers (McKee et al., 1970) and α-γ-heterodimers (Standeven et al., 2007). The covalent crosslinking makes the fibrin polymerisation irreversible, and the fibrin clot becomes mechanically stiff. Additionally, the incorporation of plasmin inhibitors, α_2-antiplasmin (Sakata and Aoki, 1980) and plasminogen activator inhibitor-1 (PAI-1) (Ritchie et al., 2001, Ritchie et al., 2000), forms a mechanically and chemically stable clot, that is more resistant to fibrinolysis.

Fibrinogen is a highly abundant plasma protein which plays many key roles in haemostasis. Whilst its primary role is to provide a scaffold for blood clots, by providing mechanical strength, fibrin also serves as a mesh for recruitment of leukocytes to the point of injury. Therefore, fibrin(ogen) is also involved in inflammation, angiogenesis and importantly microbial wound protection; through entrapment within networks and the formation of a fibrin sheet on the surface of

clots forming a physical barrier (Gaertner and Massberg, 2016, Kearney et al., 2021a, Macrae et al., 2018).

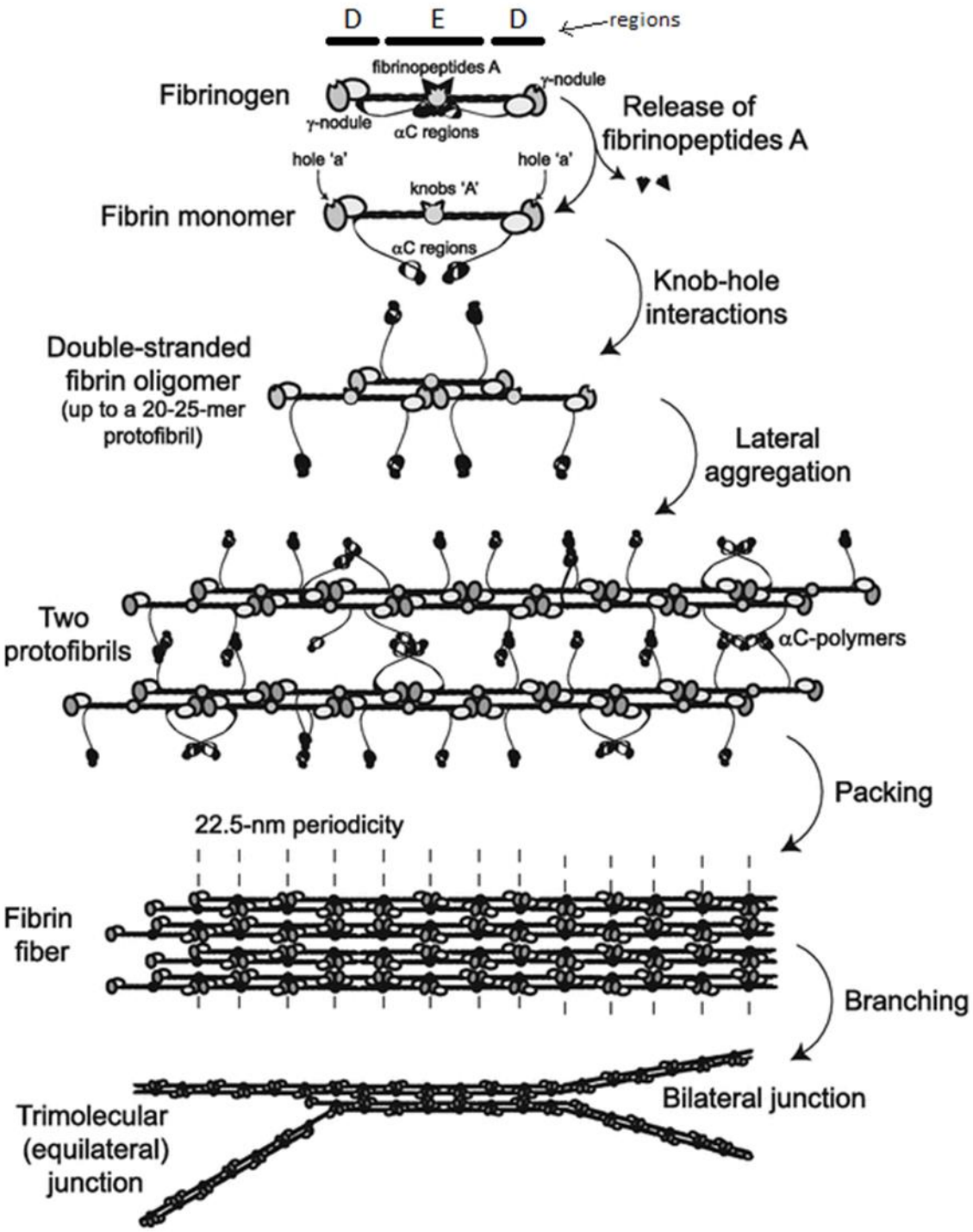

Figure 3 Fibrin(ogen) polymerisation and clot formation Fibrinopeptides are cleaved by thrombin, exposing knobs A and B. Upon cleavage, knob-hole interaction between other fibrin monomers, and dimers, occur giving rise to oligomers (a trimer is shown), which elongates to produced two-stranded protofibrils composed of half-staggered molecules. The protofibrils aggregate laterally to make fibres. The process is enhanced by interactions by the αC regions and formation of the αC-polymers. Branch points initiate by the divergence of two protofibrils and the splitting of each strand of a single protofibril. Imaged modified from (Weisel and Litvinov, 2017) with permission from Springer Nature; Licence number: 5174140750828).

1.1.4 Fibrinolysis

Fibrinolysis is the proteolytic breakdown of fibrin by the enzyme plasmin. As with the coagulation cascade, fibrinolysis is a tightly regulated process involving cofactors and inhibitors. Plasminogen is a 92 kDa zymogen of the serine protease plasmin, an enzyme consisting of an N-terminal Pan-apple domain (PAp; ~1-77), 5 Kringle domains (~78-542) and an active serine protease site (562-791) (Law et al., 2012, Castellino and Ploplis, 2005). The Kringle domains 1, 2, 4, and 5 contain a DXD/motif, which is thought to mediate binding to fibrin fibres, receptors on cell surfaces and activators or inhibitors via C- terminal lysine residues. However, in the Kringle 3 domain, the motif contains a mutation from DXD to DXK, and does not bind to lysine residues *in vitro* (Law et al., 2012, Christen et al., 2010). Plasminogen circulates in its native form, a 791-residue glycoprotein, known as glu-plasminogen because of the N-terminal glutamic acid residue. The native form can be modified to a more open, readily activatable conformation known as lys-plasminogen, through the digestion by trace plasmin between residues Arg67-Met68, Lys76-Lys77, or Lys77-Val78 releasing the PAp domain, also known as the activation peptide (Lahteenmaki et al., 2001). It is important to note, that only Kringle 1 is exposed in the glu-plasminogen due to the closed conformation, suggesting this domain plays a pivotal role in initial recruitment of plasmin(ogen) to fibrin or binding partners (Xue et al., 2012, Law et al., 2012). Conversion to plasmin is initiated through the cleavage of the peptide bond Arg560- Val561 by host plasminogen activators (Robbins et al., 1967, Holvoet et al., 1985), The cleavage exposes the serine protease catalytic triad, His603, Asp646 and Ser741, and results in a double-stranded plasmin molecule held together by disulphide bonds (Saksela, 1985). The plasmin light chain contains the catalytic site, whilst the heavy chain

contains the Kringle domains. Due to the closed conformation in Glu-plasminogen, the Arg560-Val561 bond is shielded from cleavage by Kringle 3 and Kringle 4 loops (Law et al., 2012). However, the more open conformation, Lys-plasminogen, is activated 10-20 times more readily (Holvoet et al., 1985, Hoylaerts et al., 1982, Markus et al., 1979). Thus, suggesting that there is a direct connection between conformation of the plasminogen and activation activity.

1.1.4.1 Fibrin degradation by plasmin

There have been at least 34 different plasmin cleavage sites identified on fibrin(ogen), leaving a series of fibrin degradation products during lysis. Plasmin cleaves the AαLys583 bond in circulating fibrinogen which leaves a C-terminal lysine. The αC-domains in fibrin are one of the first sites to be degraded by plasmin through the cleavage of αLys206 and αLys230. This is followed by the removal of a peptide from the N-terminal of the β-chain and cleavage of the coiled coil connecter of the E and D domains at αLys81, βLys122, γLys59 or αArg104, βLys133, γLys63. In FXIIIa cross-linked fibrin, fragments known as D-dimers are released, which are used clinically to identify and diagnose thrombosis (Cesarman-Maus and Hajjar, 2005, Longstaff and Kolev, 2015, Hudson, 2017).

1.1.4.2 Mammalian plasminogen activators

The major mammalian plasminogen activators include tissue- type plasminogen activator (tPA) and urokinase- type plasminogen activator (uPA). Both plasminogen activators are used clinically as a therapeutic thrombolytics (e.g. tPA: alteplase or uPA: saruplase) (Weisel and Litvinov, 2008), and as such the mechanism of action of these enzymes is well characterised. tPA is primarily synthesised and released by endothelial cells as a single chain, 527-amino

acid, glycoprotein. The glycoprotein contains five structural domains: a finger domain, an epidermal growth factor-like cassette, two Kringle structures and a serine protease domain (Pennica et al., 1983, Lamba et al., 1996). The half-life of tPA is exceptionally short, approximately 4 minutes in circulation, and it is primarily found in complex with its inhibitor, PAI-1 (Levin and del Zoppo, 1994, Mutch and Booth, 2016, Booth et al., 1987, Stalder et al., 1985). Unlike other serine proteases, such as uPA, the single-chain tPA (sc-tPA) is an active enzyme and can activate plasminogen, so it is not a true zymogen (Madison and Sambrook, 1993). However, cleavage of the peptide bond between Arg275 and Ile276 by plasmin, converts sc-tPA into a two-chain tPA (tc-tPA), and increases plasminogen activation rates by 3-10 fold, in the absence of fibrin (Rijken et al., 1982, Hoylaerts et al., 1982). The presence of fibrin increases the plasminogen activation activity of tPA by 100- to 1000- fold, and the catalytic rates for both sc-tPA and tc-tPA are comparable (de Vries et al., 1991, Rijken et al., 1982, Hoylaerts et al., 1982). Additionally, plasminogen increases the affinity of tPA for fibrin by approximately 20-fold (Ranby et al., 1982), due to the formation of a ternary complex. Despite minor structural differences, fibrinogen has been observed to stimulate tPA to different levels as a result of testing under different conditions, with values varying from no further stimulation (Hoylaerts et al., 1982, Medved and Nieuwenhuizen, 2003), to 5-fold (Eastman et al., 1992) to 25-fold (Stewart et al., 1998).

Plasminogen activation by tPA in the presence of fibrin occurs in two phases. The first phase occurs upon fibrin cleavage by trace plasmin and subsequent exposure of C- terminal lysine residues which provide tPA and plasminogen binding sites. During this stage the typical tPA K_m value is ~1 μM plasminogen (sc-tPA: 1.05 μM, tc-tPA: 0.99 μM) and the K_{cat} is ~0.2 s^{-1} (sc-tPA: 0.18 s^{-1}, tc-

tPA: 0.16 s^{-1}) (Hoylaerts et al., 1982, Norrman et al., 1985). As surface-bound plasmin begins to form, more fibrin is cleaved and new C-terminal lysine residues are exposed, forming a positive feedback loop. This provides more binding sites for plasminogen and tPA, and results in the K_m values for tPA ~100 nM (sc-tPA: 0.07 μM, tc-tPA: 0.06 μM) whilst the K_{cat} remains constant (Norrman et al., 1985, Suenson et al., 1984).

The main fibrin binding sites in tPA are primarily in the finger domain and Kringle 2 (de Vries et al., 1991). Kringle 2 domain plays a role in C-terminal lysine binding, whilst the finger domain binds to a region in the γ-nodule in a lysine-independent mechanism or to amyloid-like cross-beta structures. Additionally, multiple studies have demonstrated that the finger domain plays the major role in the initial interaction of fibrin binding (Gebbink, 2011, Grailhe et al., 1994, Silva et al., 2012, Longstaff et al., 2011).

uPA is primarily produced by monocytes, macrophages and epithelium cells as a 411-residue single chain, zymogen (sc-uPA) (Manchanda and Schwartz, 1990, Grau and Moroz, 1989, Larsson et al., 1984). sc-uPA is activated through cleavage of the Lys158 and Ile159 peptide bond by trace plasmin or kallikrein; converting sc-uPA to a disulphide linked two-chained uPA (tc-uPA) (Suenson et al., 1984). tc-uPA also exists as a high and low molecular weight enzyme formed by plasmin cleavage between Lys135 and Lys136. Both forms have the ability to activate plasminogen, however only the high-molecular weight uPA binds to the uPA receptor (uPAR, (Cesarman-Maus and Hajjar, 2005))

uPA has three domains: an epidermal growth factor (EGF) domain (10-43), a Kringle (50-132), and a serine protease domain (159-411) (Huai et al., 2006). uPA primarily activates cell-surface bound plasminogen however it can also

activate plasminogen in solution (Mutch and Booth, 2016). sc-uPA shows ~100-fold increase in activity when surface bound, whilst tc-uPA does not show any further increase in activity (Baeten et al., 2010, Manchanda and Schwartz, 1991). Unlike tPA, the uPA Kringle has no binding sites for fibrin and a low affinity for fibrin (Cesarman-Maus and Hajjar, 2005). However, tc-uPA activates glu-plasminogen at a 10-fold higher rate in the presence of fibrin (Cesarman-Maus and Hajjar, 2005), potentially due to a conformational change in plasminogen upon fibrin binding. There has been much debate about the importance and role that uPA plays in fibrinolysis; fibrin deposition was observed in uPA knockout mice, suggesting uPA is essential for regulating baseline fibrin homeostasis and showing that uPA plays an critical role in fibrinolysis (Bugge et al., 1996, Carmeliet et al., 1994).

1.1.4.3 Fibrinolysis modulators

There are a number of inhibitors that moderate the activity of fibrinolytic components to prevent excessive plasmin generation. Thrombin-activatable fibrinolysis inhibitor (TAFIa) cleaves C-terminal lysine and arginine residues in fibrin, which reduces the binding sites for plasminogen and plasmin and the positive feedback loops which stimulate fibrinolysis (Wang et al., 1998a). The two most critical serpins are PAI-1, an inhibitor of t-PA and uPA, and α_2-antiplasmin, which directly inhibits plasmin. Fibrin clots are key activation sites for fibrinolysis and upon binding, plasmin is protected from inhibition from α_2-antiplasmin. Thus, fibrinogen and fibrin increase activation of plasminogen to plasmin and aid in their own dissolution (Chapin and Hajjar, 2015, Kimura and Aoki, 1986, Plow and Collen, 1981).

1.1.4.4 Fibrin clot structure

Fibrin clot structure is characterised by the fibre thickness, strength, and pore size, which can be assessed using a variety of *in vitro* techniques. Measuring clot turbidity changes using light scattering, at 350, 405 or 600 nm, can provide important information on clot structure (Wolberg et al., 2002). The lag phase of the curve reflects the time required for protofibrils to grow to a sufficient length to begin lateral aggregation, whilst the maximum absorbance of the clot reflects the fibrin fibre cross-sectional area and the number of protofibrils per fibre (Carr and Hermans, 1978, Wolberg et al., 2002). However, the reproducibility of turbidity results can be relatively poor, particularly in plasma clots, as other components in a clot can alter the clot structure without altering the fibre diameter (Pieters et al., 2020).

Addition of plasminogen and plasminogen activators to turbidimetric experiments can provide additional information on the fibrin clot lysis rates. The simplest method is to report the time to 50% lysis or time between 50% clotting and 50% lysis time. The addition of plasminogen activators with a chromophoric substrate for plasmin to the surface of a pre-formed fibrin clot incorporating plasminogen can provide information on the plasminogen activation rates of plasminogen activators such as tPA, or uPA. However, fibrinolysis methods are notoriously difficult to standardised (Longstaff, 2018a).

Fibrin ultrastructure is most commonly examined using scanning electron microscopy (SEM). SEM works at a high magnification and provides great spatial resolution of the surface of the clot, allowing the measurement of fibrin diameter, pore size, fibre density and branching angles. However, this technique requires fixation and dehydration steps which can create preparation artefacts to the final network morphology. Laser Scanning Confocal Microscopy

(LSCM) overcomes this limitation by imaging fluorescently labelled fibrin clots in a fully hydrated state. Although LSCM has lower resolution, in comparison to SEM, this optical imaging technique allows visualisation deep into the specimen and the ability to construct a 3D representation of a sample (Collet et al., 2000b, Blomback et al., 1989). Additionally, LSCM can be used to follow fibrinolysis using Ibidi microslides (Varju et al., 2015).

The local conditions present during fibrin polymerisation strongly influences the final clot structure including the temperature (Nair et al., 1986), pH (Ferry and Morrison, 1947, Weisel and Nagaswami, 1992), ionic strength (Nair et al., 1986) and concentrations of calcium (Carr et al., 1986, Hardy et al., 1983), buffers (Kurniawan et al., 2017) or albumin (Galanakis et al., 1987, Wilf et al., 1985). Additionally, fibrin fibres produced from using citrated plasma have larger fibre diameters compared to those produced using purified fibrinogen (Carr, 1988) due to the presence of circulating plasma molecules. For example, the presence of antithrombin inhibits free thrombin, which lowers the apparent thrombin concentration causing increased clotting times and thicker fibrin fibres (Carr, 1988, Elgue et al., 1994, Naski and Shafer, 1991, Shah et al., 1987, Torbet, 1986). Additionally, the presence of albumin, γ-globulin, and haemoglobin decreases lag times, which has been hypothesised to be due to their influence on macromolecular interactions during clotting (Torbet, 1986, Wilf et al., 1985, Wolberg and Campbell, 2008).

Fibrinogen and thrombin concentrations have been recognised as important modulators of fibrin clot structure. At a constant fibrinogen concentration, an increased thrombin causes a decrease in lag phase and maximum absorbance, which indicates thinner fibrin fibres. SEM analyses of fibrin clots with high thrombin concentrations reveal dense, highly branched networks of thinner

fibres; whilst low concentrations of thrombin produce fibrin clots with unbranched networks of thick fibres (Carr and Hermans, 1978, Wolberg, 2007, Domingues et al., 2016). A study conducted by Wolberg et al. (Wolberg et al., 2003) found elevated prothrombin levels increases the rate of thrombin generation leading to the formation of densely packed fibrin clots with thinner fibres. Similarly, at a constant thrombin concentration, increasing the fibrinogen concentration produces denser, highly branched, fibrin networks with longer fibres (Weisel and Nagaswami, 1992). The Darcy constant (Ks), which is a measure of the clot porosity, or permeability, is inversely related to the fibrinogen and thrombin concentrations (Blomback and Okada, 1982, Blomback et al., 1989). At high concentrations of fibrinogen or thrombin, clots are less permeable, as indicated by a decrease in Ks.

Previous *in vitro* studies have indicated that fibrin clots composed of thick fibres and loose networks are more susceptible to fibrinolysis. Turbidity, LSCM and mechanical (elastometry) lysis assays have demonstrated that clots formed at higher ionic strengths, lower fibrinogen concentrations or lower thrombin concentrations produce thick fibres which were more susceptible to lysis than when the clots were composed of thin fibres, and dense network (Carr and Alving, 1995, Collet et al., 2000a, Campbell et al., 2009, Machlus et al., 2011, Gabriel et al., 1992). Furthermore, patients with thin, closely spaced fibres have reported hypofibrinolysis, supporting the *in vitro* studies that have indicated that thinner fibres are more resistant to lysis (Fatah et al., 1996, Collet et al., 1993). However, whilst fibrin clots composed of thick fibres and loose network are lysed at a quicker rate than a dense network of thin fibres, at the individual fibre level thin fibres were found to cleave faster than thicker fibres (Collet et al., 2000a). Therefore, it is likely that the permeation of the plasminogen activators

or plasmin into a clot network plays an important role in determining fibrinolysis rates.

1.2 Haemostasis in host defence

The haemostasis system also acts as a host defence mechanism to protect the integrity of the vascular system by providing a barrier to infection upon tissue injury. During bacterial infections, the haemostasis system cooperates with the inflammatory cascade, complement system and coagulation cascade to eradicate pathogens. However, a common mechanism employed by pathogenic bacteria is to express virulence factors that seize control of the host haemostatic system to elude host defences and enter sterile tissue.

1.2.1 Bacterial contact system activation

As described in section 1.1.2.2, the intrinsic cascade (or contact system) is activated in the presence of negatively charged surfaces, such as a bacterial surface proteins. Both gram negative bacteria and gram-positive bacteria are known to bind components of the contact system. It has been demonstrated that contact factors HMWK, FXII, FXI and PK bind to the surface of *Escherichia coli* and some *Salmonella* spp via the cell surface expressed amyloid fibres (curli organelles) or thin aggregative fimbriae (Herwald et al., 1998, Ben Nasr et al., 1996). Gram negative bacteria such as Group G *Streptococci* (via the protein FOG and protein G (Wollein Waldetoft et al., 2012) which are a novel fibrinogen binding surface proteins and immunoglobulin-binding proteins, respectively), *Staphylococcus aureus* and *Streptococcus pneumoniae* (Ben Nasr et al., 1996) also bind components of the contact system via cell surface binding proteins. Additionally, M proteins from most *Streptococcus pyogenes* strains have been found to bind kininogens (Ben Nasr et al., 1995) and in particular contact factor HMWK (BenNasr et al., 1997).

Some bacteria have been shown to release cysteine proteases that are able to proteolytically cleave FXII or plasma PK, thus indirectly releasing bradykinin. This includes Arg-gingipains from *Porphyromonas gingivalis* (Imamura et al., 1995*)* and the *Vibrio vulnificus* proteinase (Molla et al., 1989). In contrast, other bacterial cysteine proteinases such as SpeB from *Streptococcus pyogenes* (Herwald et al., 1996) and staphophains from *Staphylococcus aureus* (Imamura et al., 2005) are able to directly cleave HMWK to release bradykinin. High bradykinin plasma levels have been noted as a biomarker for *Staphylococcus aureus* induced sepsis (Mattsson et al., 2001). In relation to *Streptococcus pyogenes* pathogenesis, it has been proposed that the recruitment of high amounts of HMWK by M proteins could lead to a localised 'burst' in bradykinin, by the action of SpeB. This would subsequently lead to increased vascular permeability and high amounts of plasma proteins and nutrients into the site of infection (Herwald et al., 1996). M proteins are known to play major roles in *Streptococcus pyogenes* pathogenesis which is described further in section 1.4.2.

1.2.2 Fibrin(ogen) protective barrier

The ultimate goal of the coagulation cascade is the generation of fibrin. Fibrin plays a vital role in preventing haemorrhage and allowing vessel repair following injury, and also acts as a barrier to physically entrap and prevent the spreading of pathogens (Kearney et al., 2021a, Macrae et al., 2018). Fibrinogen deficient mice show a significantly compromised pathogen clearance. This was indicated by the increased dissemination of bacteria and mortality in fibrinogen deficient mice (α-chain knockout, causing immunologically undetectable levels of β and γ chain (Suh et al., 1995) or ancrod depletion methods), in comparison to wild type or heterozygous mice (Claushuis et al., 2017, Sun et al., 2009, Mullarky et

al., 2005, Luo et al., 2011). Additionally, in murine models with normal fibrinogen levels but impaired fibrin generation due to anticoagulant treatment, a marked increase in infection related mortality is observed (Claushuis et al., 2017, Mullarky et al., 2005, Luo et al., 2011) signifying the importance of fibrin in host defence against microbial invasion.

However, the host fibrin can also be exploited by virulence factors expressed by pathogenic bacteria to aid in dissemination and survival of the organism. Formation of localised fibrin network at the site of infection can be detrimental to the host, as it can allow the accumulation of large numbers of bacteria whilst protecting them from clearance by the immune system. Whilst inside the fibrin clot, the bacteria can proliferate leading to the formation of abscesses.

Staphylococcus aureus has evolved the ability to hijack the host fibrin(ogen) system and form a 'shield' (Thomer et al., 2013, Guggenberger et al., 2012) around the bacterium through the secretion of two coagulases; von Willebrand factor binding protein (vWbp) and Coagulase (Coa) (Bjerketorp et al., 2004, McAdow et al., 2012). Thus, protecting the bacterium from the immune system and phagocytosis (Crosby et al., 2016). Mature Coa protein consists of an N terminal D1D2 domain, followed by a linker region and tandemly repeated fibrinogen-binding motif (Panizzi et al., 2006, Panizzi et al., 2004). Coa nonproteolytically activates prothrombin (Thomer et al., 2016) through the insertion of N-terminal amino acid residues Ile1- Val2 of the D1D2 domain into the Ile16 pocket of prothrombin; resulting in a conformational change and an active Coa-prothrombin complex formation, called staphylothrombin, which is then capable of cleaving fibrinogen to generate fibrin. Coa protein structure (Panizzi et al., 2006) and interactions with prothrombin is well characterised, therefore much of our understanding of the mechanism of action of

Staphylococcus aureus fibrin formation is based upon coagulase activation of prothrombin. However, structural predictions shows that despite the N-terminal half of vWbp sharing only 30% amino acid identity to the N terminal region of Coa (Bjerketorp et al., 2004), the N terminal is composed of primarily alpha helices resembling the structure of the Coa segment; suggesting a similar prothrombin activation mechanism occurs with vWbp (Friedrich et al., 2003, Thomas et al., 2019). The C-terminal portion of vWbp lacks further resemblance to Coa, and instead a unique vWF binding site exists (Cheng et al., 2010, Bjerketorp et al., 2002). Additionally, the formation of vWF truncations revealed that fibrinogen binding predominantly occurs via the N-terminal portion of vWbp (Thomas et al., 2019).

The two coagulases are thought to result in the formation of two distinct types of fibrin network. In a murine abscess model of *Staphylococcus aureus* infection, antibody staining revealed intense Coa staining co-localised with prothrombin and fibrinogen in the pseudocapsule surrounding the staphylococcal abscess community. The vWbp staining was found throughout the abscess lesions, but also accumulated at the peripheral of the abscess lesions, another layer of fibrinogen/fibrin, predominantly co-localised with fibrinogen and prothrombin (Cheng et al., 2010). Furthermore, in a 3D-Collagen Fibrinogen *in vitro* culture model, Coa was also involved in the formation of a fibrin pseudocapsule, whilst the vWbp was required for the formation of the extended microcolony-associated meshwork. Both types of fibrin, vWbp and Coa-generated, were shown to hinder neutrophils from attacking the bacteria by forming a barrier (Guggenberger et al., 2012) supporting the idea that both coagulases are critical for *Staphylococcus aureus* pathogenicity. In preclinical models involving *Staphylococcus aureus* vWbp and Coa knock-out mutants, the virulence was

severely attenuated with their ability to cause skin infections (Vanassche et al., 2011, Malachowa et al., 2016), catheter infections (Vanassche et al., 2013) or sepsis (McAdow et al., 2011). Additionally, inducing expression of coagulases in a usually non-invasive species of *Staphylococcus*, *Staphylococcus simulans*, transformed the bacterium into a pathogen that could survive in the bloodstream and cause infection (Yu et al., 2017).

Staphylococcus aureus also expresses another virulence factor known as clumping factor A (ClfA); a surface bound protein capable of binding to the fibrinogen γ-chain. The ClfA aids in bacterial adhesion to endothelial cells under shear conditions and the binding of fibrinogen protects against phagocytosis (Claes et al., 2018, McDevitt et al., 1997, Higgins et al., 2006). *In vitro* binding studies and *in vivo* studies of St*aphylococcus aureus* adhesion to murine mesenteric circulation demonstrated that secreted vWbp interacts with ClfA and host vWF, to form a complex which anchors the bacteria to vascular endothelium under shear stress (Claes et al., 2017). Additionally, the ClfA-fibrinogen complex has been found to activate platelets by engaging the platelet integrin GPβ/IIIa through a fibrinogen bridge and the IgG platelet receptor, which subsequently promotes thrombus formation (Loughman et al., 2005). Furthermore, the ClfA binding to fibrinogen mediates bacterial clumping, which has been shown previously to protect the *Staphylococcus aureus* from neutrophil-dependent (Kapral, 1966) and extracellular phospholipase A_2-dependent (Dominiecki and Weiss, 1999) killing; acting as a barrier to these agents. Fibrinogen- induced clumping results in a phenotypic switch from a primarily adhesive bacteria to an invasive pathogen (Rothfork et al., 2003). Murine models expressing mutant fibrinogen lacking the *Staphylococcus aureus*

Clfa binding motif, but with full fibrin clotting function, exhibited reduced bacterial burdens and significantly reduced organ damage (Flick et al., 2013).

Another virulence factor which binds fibrin is the M1 protein from *Streptococcus pyogenes.* Cell-bound M1 prevents phagocytosis of *Streptococcus pyogenes* by binding fibrinogen which inhibits complement and antibody deposition (Carlsson et al., 2005, Sandin et al., 2006). The M1 protein can be cleaved from the cell surface by *Streptococcal pyogenes* proteases, such as SpeB, and host neutrophil proteases resulting in soluble M1 (It is not currently known how host neutrophil proteases cleave M1 protein from the cell surface) (Berge and Bjorck, 1995a, Herwald et al., 2004). The M1 forms a pathological cross-like network with fibrinogen (Macheboeuf et al., 2011) which capable of activating neutrophils; triggering the release of heparin binding protein and subsequently vascular leakage (Herwald et al., 2004). M1 binding fibrinogen is explained in more detail in section 1.4.2.1.

1.2.3 Bacterial clot degradation

Soluble fibrinogen or insoluble fibrin can physically entrap pathogens within the infected tissue to limit growth and prevent dissemination. Cross-linking of the fibrin fibres by FXIIIa immobilises pathogens within the networks to aid in clearance (Dickneite et al., 2015).

The surface bound M1 protein from *Streptococcus pyogenes* has been shown to be cross-linked by FXIIIa to the fibrin network, following activation of the clotting system at the bacterial surface via the intrinsic pathway. The bacteria were observed in tissue biopsies from patients with streptococcal necrotising fasciitis, to be cross-linked to the fibrin networks (Loof et al., 2011). Additionally, in murine skin and soft tissue of *Streptococcus pyogenes* (M1 serotype)

infection models, using FXIII-deficient mice led to increased signs of inflammation, and elevated bacterial dissemination (Loof et al., 2011, Deicke et al., 2016). The FXIII-deficient mice showed an impaired survival in comparison to the wild-type mice, with significantly higher bacterial loads found in the blood and spleens 72 hours post-infection with *Streptococcus pyogenes* (Deicke et al., 2016). Thus, suggesting a protective role for FXIIIa in infection. FXIIIa has previously been shown to cross-link *Escherichia coli* and *Staphylococcus aureus* via cell surface bound proteins to the fibrin clot (Wang et al., 2010b).

Many bacteria produce virulence factors that can counteract the coagulation pathway and prevent entrapment by fibrin. One mechanism is to induce fibrinolysis through the expression of plasminogen activators. Group A, C and G streptococci secretes a plasminogen activator known as streptokinase which, despite its name, is not an enzyme and it does not proteolytically activate plasminogen. Instead, streptokinase forms a 1:1 complex with plasminogen, inducing a conformation change in the plasminogen activation pocket thus converting it into an active form (Boxrud et al., 2001, Wang et al., 2000). The streptokinase-plasminogen complex is protected from inhibition by the plasmin specific inhibitor, α_2-antiplasmin (Wiman, 1980). *Streptococcus pyogenes* also express cell surface M proteins or M-like proteins that are capable of binding to fibrinogen or plasminogen (Zhang et al., 2012). Fibrinogen is also thought to act as a template for plasminogen binding, thus streptokinase aids in plasmin recruitment at the cell surface forming a proteolytic coat to aid in dissemination (Glinton et al., 2017)**.**

Staphylokinase, produced by *Staphylococcus aureus*, is another nonproteolytic plasminogen activator, however unlike streptokinase, staphylokinase has a low affinity for plasminogen and cannot activate plasminogen directly. Instead

staphylokinase binds strongly to trace amounts of pre-activated plasmin forming a staphylokinase-plasmin complex capable of cleaving plasminogen to generate more plasmin (Collen et al., 1993, Grella and Castellino, 1997). Additionally, the complex is inhibited by α_2-antiplasmin (Lijnen et al., 1991b). *Staphylococcus aureus* also expresses the cell surface bound fibronectin-binding protein B (FnBPB) which can bind both fibrinogen and plasminogen simultaneously. Recruitment of cell surface plasminogen can then be activated by staphylokinase (Pietrocola et al., 2016).

Another example of a bacteria plasminogen activator is the 'Pla' protease expressed by *Yersinia pestis,* the causative agent of the bubonic plague. Unlike streptokinase and staphylokinase, the Pla protease can proteolytically activate plasminogen by the same peptide bond as the human plasminogen activators uPA and tPA. Additionally, Pla protease rapidly cleaves and inhibits the action of PAI-1, and the plasmin inhibitor α_2-antiplasmin (Korhonen et al., 2013).

Many bacteria, such as *Escherichia coli* (Lahteenmaki et al., 1993, Parkkinen et al., 1991, Korhonen et al., 1997) *, Salmonella typhimurium* (Kukkonen et al., 1998, Korhonen et al., 1997), *Neisseria meningitides* (Ullberg et al., 1992) *Borrelia burgdorferi* (Fuchs et al., 1994), do not have their own plasminogen activators and instead bind plasminogen at the cell surface and rely on host plasminogen activators to recruit and generate cell surface plasmin.

Many different bacteria have evolved virulence factors to bind and interact with the host haemostatic system, to both stimulate the coagulation cascade, and subsequent fibrin formation, or to initiate fibrinolysis. Plasmin generation at the cell surface not only prevents entrapment of the bacterium within fibrin clots, but aids in dissemination via the degradation of connective tissue and extracellular

matrix and protects from immune proteins (Lahteenmaki et al., 2001). This project will be primarily focussed on the clinically important *Streptococcus pyogenes* virulence factors.

1.3 Group A Streptococcus

Streptococci strains were traditionally identified (designated by a letter) upon serologic reactivity of specific carbohydrate antigens on the bacterial cell wall by the Lancefield system (Lancefield, 1933). Group B, C and G *Streptococci* were originally recognised as animal pathogens; however they were subsequently found to colonise humans asymptomatically or cause zoonotic diseases in humans (Turner et al., 2019, Raabe and Shane, 2019). Group A Streptococcus (GAS) or *Streptococcus pyogenes* is a strictly human pathogen capable of causing both mild, superficial infections and life-threatening invasive diseases. Despite the species name being derived from Greek words meaning pus (pyo)–forming (genes), clinical manifestations of this bacterium are one of the most diverse of any human pathogen (Carapetis et al., 2005). Whilst many cases of GAS infections are localised throat and skin infections such as impetigo and pharyngitis. Ineffective treatment can result in postinfectious nonsuppurative and suppurative (pus-forming) sequela including rheumatic heart disease, post-streptococcal reactive arthritis, and post-streptococcal glomerulonephritis. Furthermore, GAS causes invasive infections such as necrotising fasciitis, septic shock and streptococcal toxic shock syndrome (STSS), all of which are associated with high morbidity and mortality rates (Cunningham, 2000, Walker et al., 2014).

1.3.1 Transmission

Whilst GAS is known to colonise the oropharynx, genital mucosa, rectum and skin, the carrier status is poorly understood (Martin, 2016, DeMuri and Wald, 2014). Humans are the only known natural reservoir of GAS, with the mode of

transmission primarily being through respiratory droplets and with direct contact from broken skin with infected sores (Walker et al., 2014). Additionally, although not as common, food-borne transmission of GAS have been reported (Avire et al., 2021).

1.3.2 Epidemiology

The global impact of GAS and consequential diseases remains relatively unknown due to gaps in the data available and underreporting of acute and chronic cases, leading to the current disease burden being underestimated (World Health Organisation, 2005). However, GAS remains listed by the World Health Organisation (WHO) amongst the top ten causes of human mortality from infectious diseases. The last review conducted by WHO in 2005 estimated that there were approximately 18.1 million existing cases of invasive GAS, with a further 1.78 million new cases occurring each year, accounting for 517,000 deaths annually. The majority of deaths being caused by rheumatic heart disease, followed by invasive GAS diseases then acute post-streptococcal glomerulonephritis. Additionally, there were over 111 million prevalent cases of streptococcal skin infections and 616 million new cases of pharyngitis each year (World Health Organisation, 2005, Carapetis et al., 2005). Furthermore, mortality rates for necrotising fasciitis and STSS range from between 30-60%, even with aggressive treatments (Stevens and Bryant, 2016)

GAS cases began falling in industrialised countries from the 20th century, mainly due to improved living conditions, reduction in poverty and development of antibiotics (Ralph and Carapetis, 2013). However, during the 1980's a global, significant resurgence of severe and fatal forms of invasive GAS diseases began reappearing with the emergence of hypervirulent mutant and novel strains, e.g., M1T1 strain (Aziz and Kotb, 2008, Barnett et al., 2018). Recent

genomic analysis of invasive GAS infections from industrialised populations have found that the *emm1* strains are the most common type associated in epidemiological investigations (Gherardi et al., 2018, Nelson et al., 2016, Luca-Harari et al., 2009, O'Grady et al., 2007) (Further information on *emm* types can be found in section 1.4.2). Furthermore, before the SARS-CoV-2 pandemic and consequential reduction in case reporting, increased social distancing and hand hygiene measures, the United Kingdom was experiencing the seventh consecutive season of elevated scarlet fever and invasive GAS infection cases (Public Health England, 2020). GAS has remained highly prevalent in developing countries, indigenous populations and amongst low socioeconomic areas in developed countries, particularly in the elderly, children, and young adults. This is thought to be caused by poor living conditions, including overcrowding, leading to more social contact within these populations (Avire et al., 2021). Therefore, GAS remains a significant public health issue.

1.3.3 Treatment

Currently GAS is believed to be fully sensitive to penicillin, despite reports of resistance in acute infections increasing to almost 40% in some regions of the world (Sela and Barzilai, 1999, Brook, 2013, Passali et al., 2007). GAS is also often treated with other β-lactam antibiotics such as amoxicillin and cephalosporins (Walker et al., 2014). However, a recent study has found two GAS isolates with a mutation in the penicillin-binding protein PBP2x gene, leading to a reduced susceptibility to β-lactam antibiotics (Vannice et al., 2020). The same mutation was originally observed in *Streptococcus pneumoniae*, which eventually lead to penicillin resistance (Grebe and Hakenbeck, 1996). In cases where penicillin allergies are a factor, antibiotics such as clindamycin and

macrolides are used. However, bacterium resistance against both treatments has also been reported (DeMuri et al., 2017).

Despite a global demand, there is currently no vaccine for GAS prevention. GAS vaccine development has been ongoing for over 100 years, in the 1940's young adults were injected with whole, killed bacteria. The vaccines were highly reactogenic and did not prevent GAS disease. In 1969, a GAS vaccination human trial resulted in serious adverse effects in 3 out of 21 volunteers, whom developed acute rheumatic fever (Massell et al., 1969). This lead to safety concerns and in 1979, the US Food and Drug Administration (FDA) prohibited the use of GAS organisms and their derivatives in any GAS vaccine (US Food and Drug Administration, 2005). The human vaccination trial was subsequently investigated. It was discovered that the 3 volunteers had documented GAS infections prior to the onset of acute rheumatic fever and all were siblings. The siblings had been exposed to high doses of a crude M protein vaccine formulation, leading to the development of the symptoms. The FDA therefore revised the ban in 2006 and allowed purified GAS antigens to be used as vaccine candidates (US Food and Drug Administration, 2005). However, by this time, there had not been a vaccine trial reported in 25 years. Another major issue with vaccine development is antibody cross-reactivity with human organs, particularly cardiac proteins (Giffard et al., 2019). The first evidence of which was observed in mice immunised with GAS components leading to anti-streptococcal antibodies cross-reacting with ventricular myosin (Krisher and Cunningham, 1985) To date, two GAS vaccine candidates have completed human trials (Pastural et al., 2020, Sekuloski et al., 2018). However, GAS isolates frequently undergo genetic recombination events, resulting in the emergence of new strains. Therefore, there has only been 13 possible antigenic

proteins which are over 99% conserved amongst all GAS isolates globally (Davies et al., 2019).

In the absence of a vaccine and an observed decrease in susceptibility to antibiotics, there is a clear need for increased research efforts to uncover novel therapeutic targets for treatment of GAS diseases and sequalae. The first steps of which would be to better understand the pathogenesis of the organism.

1.4 Virulence factors of GAS

1.4.1 CovR/S regulon

Tight control of virulence factor expression is essential to GAS pathogenesis as regulation of different factors during infection enables the bacterium to adapt to a wide range of environmental stressors. The **t**wo **c**omponent regulatory **s**ystems (TCS) are a critical mechanism that enables a broad-spectrum of bacteria to detect and respond to a wide range of environmental stimuli. TCS are typically composed of a membrane-embedded histidine kinase regulatory responder and a response regulator (Zschiedrich et al., 2016, Gao and Stock, 2009).

In GAS, ~13 TCS regulators are known (Churchward, 2007) with the **c**ontrol **o**f **v**irulence two-component signalling system (CovRS) being the most well characterised. CovRS plays a key role in GAS pathogenesis, regulating ~15% of the GAS genome. CovRS is required for survival of the organism as it responds to environmental stress conditions such as increased temperatures, high salt concentration, low pH and iron starvation (Froehlich et al., 2009, Dalton and Scott, 2004). CovS is the membrane-bound sensor kinase that auto-phosphorylates (or dephosphorylates) the CovR response regulator, to enhance (or reverse) the repression of its gene targets (Dalton and Scott, 2004). The CovRS positively regulates the cysteine protease SpeB, whilst negatively regulating other virulence factors including the hyaluronic acid capsule, streptokinase, streptolysin O (SLO), Immunoglobulin G (IgG)- degrading enzyme and DNase Sda1 (Levin and Wessels, 1998, Sumby et al., 2006, Vega et al., 2016).

A number of hypervirulent GAS isolates have been characterised with inactivation mutations in the CovRS systems. It has been proposed that when experiencing environmental stressors during infection, the GAS isolates are selectively pressured towards those that have a mutated *CovS* component (Cole et al., 2011). Several hypervirulent GAS strains have been isolated with mutations in the *CovS* gene that prevents the activity of the CovR regulator (Sumby et al., 2006, Maamary et al., 2010, Tatsuno et al., 2013, Bao et al., 2016, Liang et al., 2013). For example, a murine survival study with the skin-tropic GAS strain AP53 showed that the lethality of the bacteria was increased upon switching from an AP53/CovS+ to AP53/CovS-. The mutation led to a decrease in SpeB and increase in hyaluronic acid capsule in the AP53/CovS- strain (Liang et al., 2013). SpeB is required for establishment of localised infection, including a role in evading host autophagy pathway (Barnett et al., 2013), degradation of epithelial tight junctions (Sumitomo et al., 2013) and complement proteins (Honda-Ogawa et al., 2013).

Later on in infection, environmental pressures result in selection pressure towards the CovRS mutants which results in a downregulation in the cysteine protease SpeB and an upregulation in the hyaluronic acid capsule, streptokinase, SLO, IgG- degrading enzyme and DNase Sda1. The hyaluronic acid capsule aids in resistance to opsonophagocytosis (Dale et al., 1996, Wessels et al., 1991). The invasive M1T1 GAS serotype survival was promoted within neutrophil extracellular traps (NETs) through the inhibition of the human cathelicidin (Cole et al., 2010). NETs are secreted from activated neutrophils, and are composed of DNA, histones, granule proteases and antimicrobial agents, which aid in the entrapment and killing of gram-positive and gram-negative bacteria (Brinkmann et al., 2004). The hyaluronic capsule was found to

be essential for full virulence in M1T1 serotype strains of subcutaneous and intraperitoneal models of GAS infection (Ashbaugh et al., 1998, Wessels et al., 1991, Moses et al., 1997).

SLO is a secreted, cholesterol-dependent exotoxin that has been shown to form large pores in host cell membranes (Bhakdi et al., 1985). SLO plays multiple roles in pathogenesis, including induction of apoptosis in host epithelial cells, neutrophils, and macrophages (Timmer et al., 2009, Bricker et al., 2002). The DNase Sda1 facilitates GAS escape from NETs by degrading the DNA framework (Walker et al., 2007).

Mutations in the CovR or CovS also prevent the cleavage of key proteins such as M proteins from the cell surface (Macheboeuf et al., 2011) and prevents the degradation of streptokinase and host coagulation factors such as fibrinogen and plasminogen. Plasmin generation at the cell surface of GAS allows the bacterium to degrade host tissue barriers and disseminate beyond site of localised infection to the bloodstream, leading to systemic dissemination (Walker et al., 2007, Cole et al., 2011).

1.4.2 M proteins

M proteins are one of the most extensively studied virulence factors found on the surface of GAS. During the course of infection, M proteins play various roles to aid bacterial dissemination including adherence to host epithelial cells (Okada et al., 1995, Ellen and Gibbons, 1972), intracellular invasion of host cells (Cue et al., 2000), immune evasion (Oehmcke et al., 2010) and microcolony formation (Frick et al., 2000). Furthermore, a subcutaneous mouse model of invasive GAS disease found M proteins to be essential for full virulence (Ashbaugh et al., 1998).

M proteins extend approximately 500 Å outwards from the GAS cell surface and are between 350-450 amino acid consisting of distinct tandem repeating domains (Hollingshead et al., 1986, Fischetti, 1989). It is believed that M proteins exist as amphipathic α-helical parallel coiled coils, although little rigorous data is available on the majority of isolated M proteins (Fischetti, 1989). The N-terminus contains the hypervariable region, followed by A and B domains and a highly conserved C, D and Pro/Gly sites (Figure 64B). The C- terminus contains a 'LPXTG' motif for anchoring to the cell wall peptidoglycan, providing GAS with a hair- like surface (Ghosh, 2018, Qiu et al., 2018).

Traditionally, GAS strains were serotyped based upon serological sensitivity against the extremely variable N terminal region. However, advances in DNA-sequencing technology resulted in a development of a method for determining the M type of GAS from the sequence of the M protein (Facklam et al., 2002, Johnson et al., 2006). GAS strains are therefore commonly typed based upon the 5' variable region of the *emm* gene encoding the M protein, with ~ 234 distinct *emm* types been defined (Bessen, 2016). Additionally, GAS strains can also be classified by the *emm* gene chromosomal arrangement in the multiple gene activator (mga) regulon. Five different chromosomal patterns were found to exist, Patterns A-E, based upon the presence and arrangement of the M-proteins and M-like proteins (Bessen et al., 1996).

1.4.2.1 M1 protein and fibrinogen

As highlighted in section 1.3.2, *emm 1* strains are overrepresented in invasive GAS diseases. The *emm 1* strains contain an M1 protein on the cell surface of GAS which has been found to bind to host fibrinogen with a high affinity; with an equilibrium constant of 1.1×10^{10} M^{-1} (Akesson et al., 1994). Whilst this has been proposed to camouflage the GAS from opsonophagocytic killing (Ringdahl

et al., 2000, Carlsson et al., 2005) and to promote cell surface plasmin generation (Glinton et al., 2017); M1 can be released from GAS through cleavage by SpeB (Berge and Bjorck, 1995a) or by neutrophil proteinases (Herwald et al., 2004).

The soluble M1 protein retains functional activity and has been found to bind to fibrinogen in solution. The M1-fibrinogen complex is capable of activating polymorphonuclear neutrophils, through the cross-linking of β_2-integrins. The activated neutrophils then release heparin binding protein, a potent vasodilator, subsequently inducing vascular leakage (Herwald et al., 2004). Heparin binding protein and vascular leakage is a strong indicator of sepsis and circulatory failure (Linder et al., 2009) and a common symptom of STSS; with patients requiring 10/20 litres/day of intravenous fluids (Herwald et al., 2004). A murine model of subcutaneous *Streptococcus pyogenes* infection found that M1 protein was present in the lungs and vascular leakage occurred before bacteria was found in the bloodstream or lungs. Using confocal microscopy, Herwald et al. demonstrated that infected soft tissue from a patient with necrotising fasciitis and STSS, showed soluble M1 protein colocalised with fibrinogen (Herwald et al., 2004). Underlining the pathophysiological significance of this complex in infection.

The M1-fibrinogen complex is capable of binding to the fibrinogen receptor, GPIIb/IIa on platelets and inducing platelet activation (Shannon et al., 2007). Activation can only occur when immunoglobulin G (IgG) antibodies against M1 are already present in plasma, usually during invasive infections. The IgG antibodies bind to the M1 – fibrinogen complex, where the F_c region is exposed and recognised by the platelet IgG receptor (FcγRII). The simultaneous interaction between the fibrinogen and IgG receptor subsequently leads to

platelet activation. Under normal circumstances the fibrinogen platelet receptor has a low affinity for fibrinogen and can only bind immobilised fibrinogen suggesting M1 binding leads to conformational changes in fibrinogen. The activated platelets release their pro-inflammatory granule contents and form complexes with neutrophils and monocytes; activating both cell types and redistributing tissue factor to the surface creating a hypercoagulable state (Shannon et al., 2007). Shannon et al. used tissue biopsies collected from the soft tissue of severe infection of M1 isolates which demonstrated that activation of platelets led to platelet aggregation, colocalised with M1 (Shannon et al., 2007). The platelet rich thrombi are then deposited in the microvascular. In invasive GAS infections, thrombi are often found to occupy diverse tissue locations (Barker et al., 1987, Ashbaugh et al., 1998).

The crystal structure of a partial M1-fibrinogen complex has been resolved by X-ray crystallography (Figure 4). The M1 protein fragment ($M1^{BC1}$, (residues 132-263, ~17 kDa)) contain; the B repeats which bind to the fibrinogen; the S region which has been found to bind IgG and enhance the release of HBP through FcγRII; and the first C repeat domain. The fibrinogen fragment contains the D domain (~86 kDa) (Macheboeuf et al., 2011). M1 protein has previously been shown to contain two fibrinogen binding B domains, B1 and B2 (Akesson et al., 1994) (Ringdahl et al., 2000). As shown in Figure 4, the M1 fragment was found to be surrounded by four fibrinogen fragment D molecules, in a cross-like pattern. There are four B repeats due to M1 protein existing as a dimer (so two B repeats per chain), explaining the 2:4 $M1^{BC1}$: fibrinogen D complex of the ~380 kDa complex. The B1 repeats bind two fibrinogen D molecules and are orientated ~180º to each other. The B1 and B2 repeats are 28 amino acids apart, and roughly one-quarter turn of the coiled-coil superhelix. This allows the

second couple of fibrinogen fragments to be orientated ~90º, creating the cross-like pattern (Macheboeuf et al., 2011). The binding sites are represented in Figure 5. Residues in the B1 and B2 repeats from both helices of the coiled coils and every heptad position (a-g) contributes to fibrinogen D domain binding (Figure 5b). Within the fibrinogen D domain, β and γ chains are involved in M1-fibrinogen binding. As shown in Figure 5b, βArg169, βGlu173, βArg176, and γArg108, γTyr109, γSer116 are involved in the M1-fibrinogen binding. Additionally, the site at which M1 binds fibrinogen D domain is quite distant (~90 Å) from the fibrinogen γC globular head which has been found to bind β_2 integrins (Medved et al., 1997, Macheboeuf et al., 2011).

Previous studies have introduced mutations into the fibrinogen binding coiled-coil B repeats (GAS M1*), which demonstrated a decrease in fibrinogen binding *in vitro*. The mutants also displayed an impaired ability to adhere to and invade cultured human endothelial cells and were more readily killed in whole blood or isolated neutrophils (Uchiyama et al., 2013). In the same study, Uchiyama et al. also used murine models to investigate bacterial survival with wild-type GAS strains and GAS M1* mutant strains. They found that the M1-fibrinogen interactions help GAS to resist NET-mediated neutrophil clearance from blood and M1 protein decreases GAS's susceptibility to the antimicrobial peptide cathelicidin, which is a key component of NETs.

Fibrinogen has also been shown to interact with other M proteins which have B-repeat regions including M5, M6, M12, M14, M18, M19, M23, M54 and M57 (Sanderson-Smith et al., 2014, Glinton et al., 2017). The B repeats are variable in amino acid sequence and do not share a high sequence identity, for example M5 has only 24% sequence identity to M1 B-repeat regions (Ringdahl et al., 2000). To date, all M proteins have been found to bind to the fibrinogen D

domain, as noted by binding and dissociation kinetics (Glinton et al., 2017). However, structural data has not been resolved for the majority of the M proteins therefore the fibrinogen binding mechanism is unknown.

In conclusion, massive dysregulation of the pro- and anti-coagulation equilibrium is a central finding in sepsis and severe GAS infection (Stevens, 2001) with microthrombi often found at the site of infection and at distant sites. Whilst M1 has previously been shown to bind to fibrinogen, the consequences of this in relation to coagulation, particularly fibrin formation, are poorly investigated and understood.

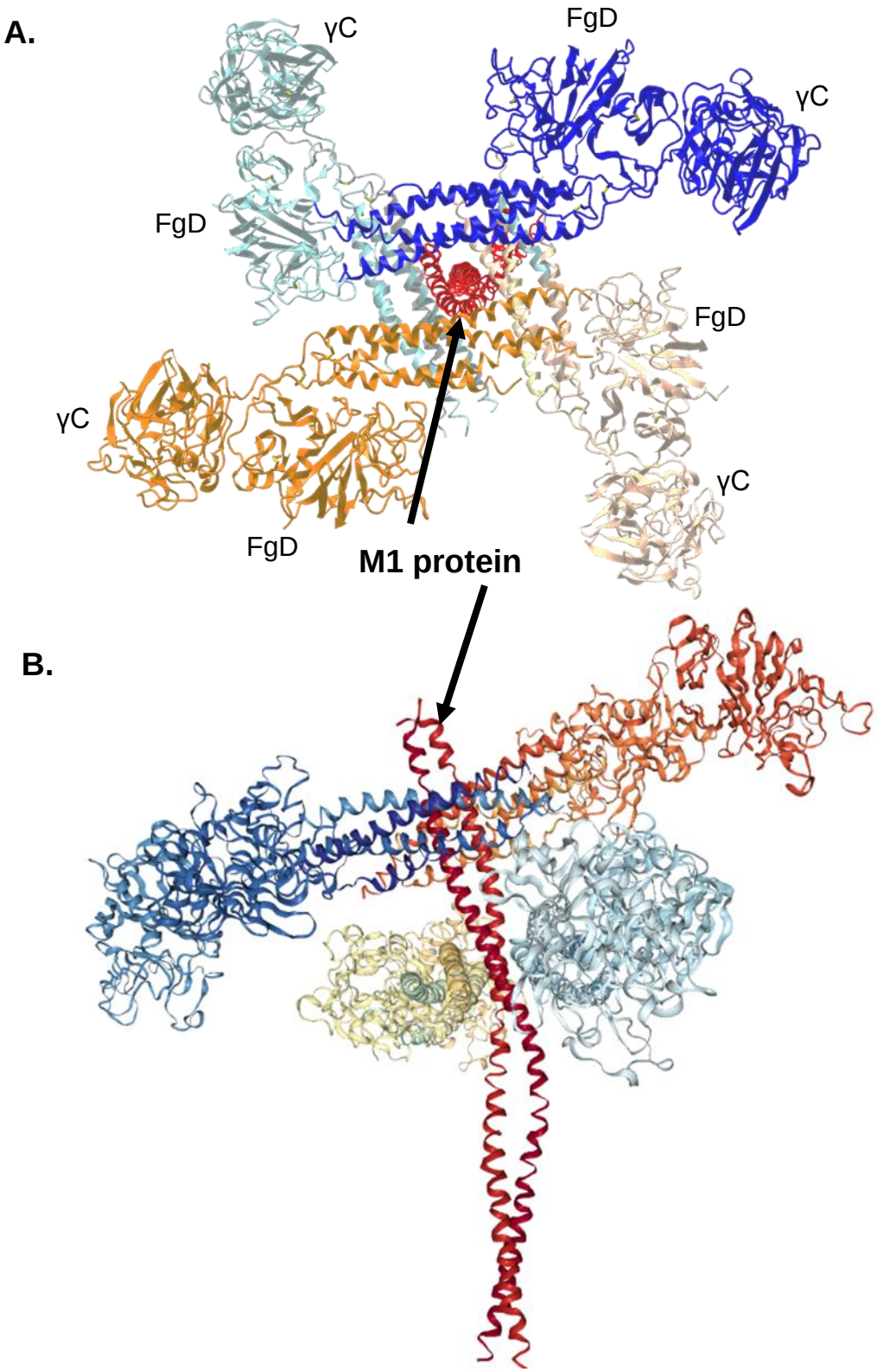

Figure 4 Fibrinogen binding to streptococcal M1 protein The M1BC1 protein (residues 132-263, ~17 kDa) and four fibrinogen fragment D domain structure (~86 kDa) in ribbon representation. PBD: 2XNX. The M1 protein binds fibrinogen in a cross-like pattern, as shown from the representative structure from above. Fibrinogen D domain (FgD) and γC modules are labelled. **(A.)** The B1 repeats bind two fibrinogen D molecules and are orientated ~180º to each other. The B1 and B2 repeats are 28 amino acids apart, and roughly one-quarter turn of the coiled-coil superhelix, as demonstrated in **(B.)**

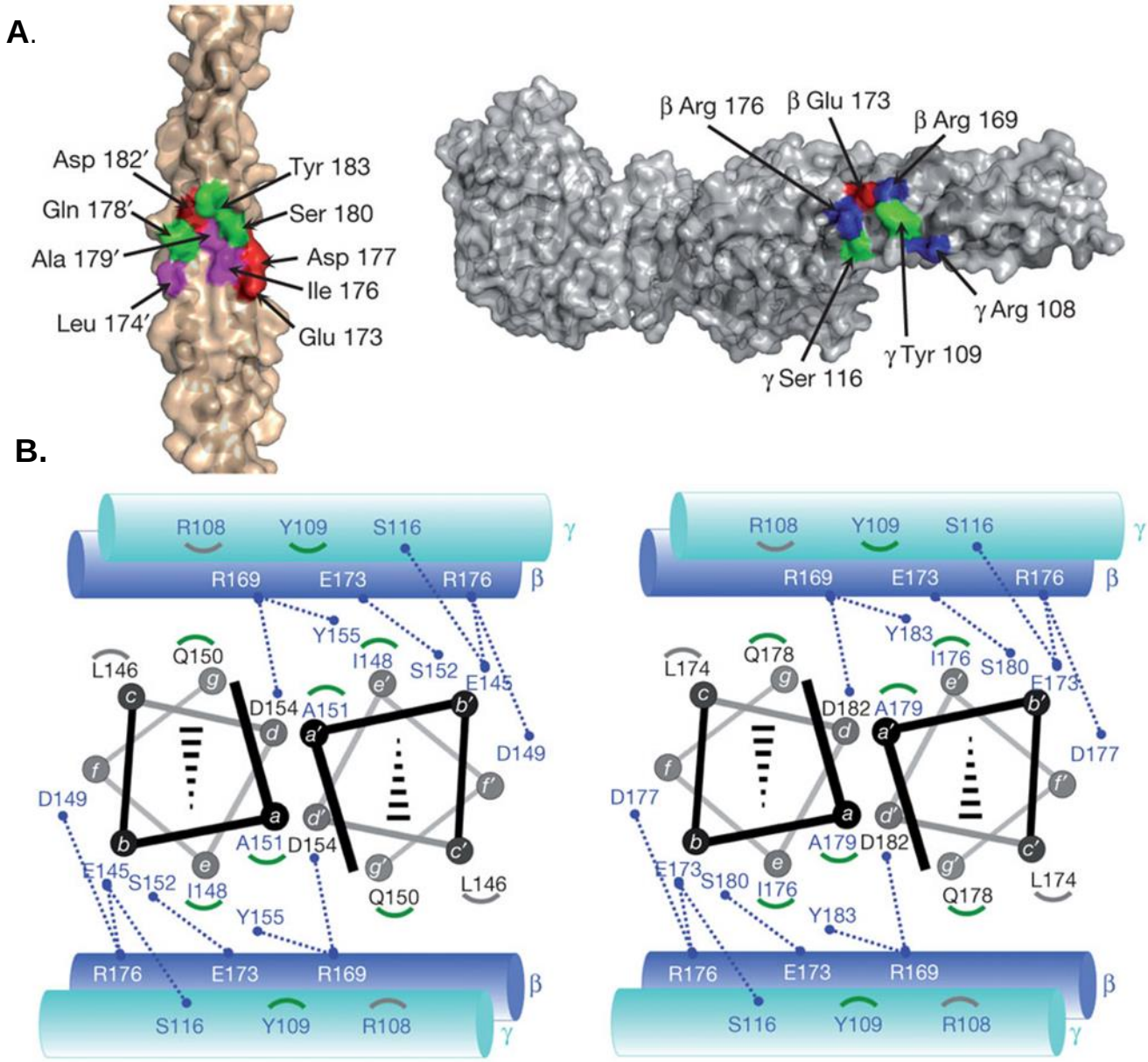

Figure 5 M1-fibrinogen complex. A. Interface between M1BC1 B2 domain (left, primed numbers refer to one helix and non-primed the opposing helix) and fibrinogen D domain (right). **B**. Diagram of the residues between M1BC1 B1 (left) and B2 (right) in the helical projections and the fibrinogen D domains (cylinders, γ- chain in blue-green and β chain in blue). Blue dotted lines connect residues with polar contacts and grey and green arcs correspond to M1 residues making van der Waals contacts to fibrinogen γ 108 and 109, respectively. *(Imaged reused from (Macheboeuf et al., 2011) with permission from Springer Nature; Licence number: 5171060068100)*

1.4.3 Streptokinase

Streptokinase is a single-chain 414 amino acid protein composed of three distinct domains: α (1-150), β (151-287) and γ (288-414) (Wang et al., 1998b, Kalia and Bessen, 2004). Unlike host plasminogen activators, uPA and tPA, streptokinase lacks any proteolytic activity and instead forms a stable 1:1 stoichiometric complex with plasminogen to form an active streptokinase-plasminogen complex. This complex can then activate further plasminogen molecules to generate the formation of the serine protease, plasmin. The streptokinase-plasminogen complex is believed to generate an active site through the N-terminal Ile1 residue of streptokinase forming a salt bridge with Asp740 of plasminogen to induce a conformational change. A mechanism termed 'molecular sexuality' and 'N terminal insertion hypothesis' (Bode and Huber, 1976, Jackson and Tang, 1978). Deletion of the amino terminal Ile1 has previously been shown to prevent the formation of the streptokinase-plasminogen complex and is therefore critical for activation of plasminogen to generate plasmin and supports the 'molecular sexuality' hypothesis (Wang et al., 1999, Wang et al., 2000). Additionally, equilibrium and kinetic studies showed that streptokinase mutants without the amino terminal Ile1 displayed no detectable conformational activation of plasminogen despite retaining affinity of native streptokinase (Boxrud et al., 2001).

Binding and kinetic studies have shown that streptokinase binds to the closed conformation glu-plasminogen with a dissociation constant of 130 ± 76 nM, and this binding is independent of lysine binding sites (LBS). However, streptokinase binds to lys-plasminogen in a LBS dependent manner with a ~13-20-fold higher affinity (10 ± 3 nm) which is reduced to similar levels to glu-

plasminogen upon saturation with **6**-aminohexanoic acid (6-AHA), a lysine analogue (Boxrud et al., 2004, Boxrud et al., 2000). Additionally, streptokinase displays a significantly higher affinity for native plasmin than glu-plasminogen and lys-plasminogen, with dissociation constants of 12 ± 4 pM (~800 and ~11,000-fold higher affinity, respectively) (Boxrud et al., 2000). This results in the formation of streptokinase-plasmin complexes following plasminogen activation (Nolan et al., 2013). Streptokinase-plasmin and streptokinase-plasminogen activity cannot be regulated by host plasmin inhibitors, such as α_2-antiplasmin (Lijnen et al., 1991a, Wiman, 1980), thus leading to uncontrolled plasmin generation and subsequent degradation of fibrin clots and extracellular matrix, promoting bacterial dissemination (Parry et al., 2000).

Mechanism of action of streptokinase is mainly understood based upon a group C streptokinase, from the H46a strain of *Streptococcus equisimilis*, which was the first streptococcal gene to be cloned and sequenced (Malke et al., 1985, Malke and Ferretti, 1984). Streptokinase H46a is a clinically important plasminogen activator, remaining one of the most widely used thrombolytic agents for the treatment of myocardial infarction worldwide (Thelwell and Longstaff, 2014).

Although streptokinase variants have been shown to be highly conserved with Group C streptokinase displaying 85% amino acid sequence identity to Group A *Streptococcus* streptokinase, the small sequence differences appear to contribute to different plasminogen activation properties (Huang et al., 1989). Phylogenetic analysis of streptokinase from diverse strains of Group A *Streptococcus* indicate that β-domain sequence variation can divide the streptokinase into 3 distinct clusters ((Figure 6) 1, 2a and 2b). Interestingly, phylogenetic studies have also found that streptokinase clusters were

associated with tissue specific *emm* patterns of the bacterium (McArthur et al., 2008).

Streptokinase 2a (SK 2a)- expressing strains are secreted from nasopharyngeal isolates and are commonly associated with a fibrinogen binding M protein such as M1. The streptokinase 2a has low plasminogen activation activity in solution, however is stimulated by fibrinogen and maximally stimulated by fibrin (Huish et al., 2017) resulting in localised plasmin generation at host fibrin barriers. Streptokinase 2b (SK 2b)-expressing strains are released from skin-tropic isolates expressing plasminogen- binding M proteins, such as PAM (Kalia and Bessen, 2004, Hynes and Sloan, 2016). PAM can bind plasminogen to the cell surface of GAS and increase its activation rate by SK 2b. PAM bound plasmin also protects the enzyme from inhibition by α2-antiplasmin (Lottenberg et al., 1992). Plasminogen bound to cell-surface receptors such as PAM, or ligands such as fibrin, change conformation to an 'open' conformation that is much more susceptible to activation (Castellino and Ploplis, 2005). Cluster 1 streptokinase appear to behave like group C streptokinase, whereby Cluster 1 can activate plasminogen free in solution and does not appear to coincide with particular M- proteins or require co-factors for full activity (Figure 7A) (McArthur et al., 2008). The plasminogen activation by Cluster 1 streptokinase would not be localised like Cluster 2 streptokinase therefore leading to systemic plasmin generation. The soluble plasmin would not be protected by cell-surface receptors or ligands and be rapidly inactivated by α_2-antiplasmin. This may explain why Cluster 1 expressing *Streptococci* are less commonly associated with invasive infections (Zhang et al., 2014).

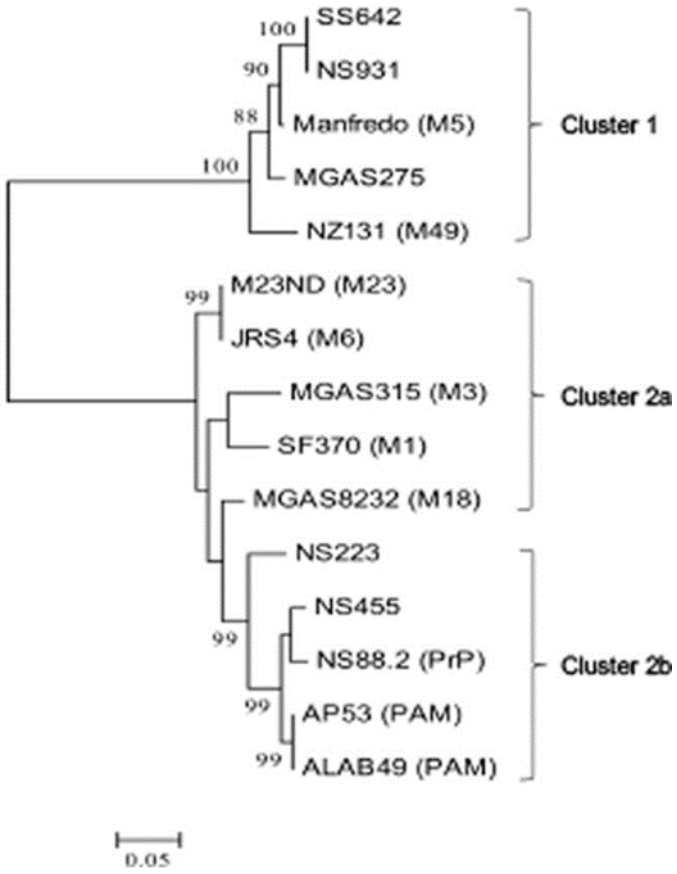

Figure 6 Phylogenetic analysis of streptokinase β- domains. The streptokinase β-domains were aligned using BLAST multiple sequence alignment tool (NCBI). The phylogenetic tree was constructed by the neighbour-joining method using MEGA. Bootstrap values (500 replicates) are indicated at the nodes. Scale bar= 0.05 substitution per site. *The figure and analysis were reused from (Glinton et al., 2017).*

1.4.3.1 Streptokinase 2a and M1

SK 2a displays low plasminogen activation activity in solution, approximately 5-fold lower than the well characterised therapeutic Group C Streptococcus, H46a strain (12.4 IU/μg compared to 58.2 IU/μg, respectively), and is only weakly stimulated by fibrinogen. However, turbidity lysis experiments have demonstrated that fibrin is a potent stimulator of SK 2a activity, with specific activities ~14-fold higher than streptokinase H46a strain (Huish et al., 2017). M1 protein is a particularly important M protein due to the connection with the

unusual prevalence and severe invasive manifestations of the M1T1 strain (Aziz and Kotb, 2008). M1 binds fibrinogen with a high affinity, and is thought to provide a template for plasminogen acquisition at the cell surface through the formation of a trimolecular complex (Figure 7B) (Glinton et al., 2017). The proposed model suggests that this complex then stimulates the formation of plasmin by SK 2a. Binding to the cell surface fibrinogen also protects GAS from the immune response and phagocytosis by encapsulating the bacteria and by promoting plasmin generation which can break down complement factor components such as C3b (Agrahari et al., 2016). M1 can be cleaved from the cell surface by the *Streptococcal* protease SpeB. The free M1 can bind to fibrinogen in solution to form a supramolecular network and has been known to contribute to the pathophysiology of streptococcal toxic shock syndrome (Macheboeuf et al., 2011). The significance of M1- bound fibrinogen, either at the cell surface or free in solution following cleavage for plasminogen- activation by SK 2a is not fully understood.

1.4.3.2 Streptokinase 2b and PAM

SK 2b secreting GAS strains are unique in that they directly interact with human plasminogen, through their associated M protein, PAM. PAM bound-plasminogen is activated by SK 2b, resulting in the formation of plasmin, thus providing the GAS with a proteolytic ‘coat’. Two pathways for this plasmin acquisition have been proposed: In the first pathway PAM directly binds plasminogen which is sequentially activated by SK 2b to generate plasmin at the cell surface (Figure 7D). In the second proposed pathway, plasminogen binds to fibrinogen which is activated by SK 2b, forming a trimolecular complex. The generated plasmin is then bound to the cell surface via the cell surface bound PAM (Figure 7C) (Zhang et al., 2012). The cell- bound protease is then

employed to dissolve host fibrin clots, degrade extracellular matrix and cellular tight junctions to allow the invasion of GAS into sterile deep tissues of the host (Qiu et al., 2018). PAM is approximately 42 kDa single-chain protein that, as a mature protein, exists as a dimer. Unlike M1, PAM isn't thought to be released from the cell surface by the protease, SpeB (Mayfield et al., 2014).

It was discovered that PAM binds to plasminogen Kringle 2 domain via the N terminal a1a2 repeats (Wistedt et al., 1998, Wistedt et al., 1995). X-ray crystallography (PBD code: 1I5K) (Rios-Steiner et al., 2001) and high resolution NMR analysis (PDB code 2KJ4) (Wang et al., 2010a) on truncated peptides PAM-type M proteins demonstrated that the interaction between PAM and plasminogen is mediated by the lysine binding sites of Kringle 2 along with a1 or a1 and a2 pseudo-Lysine sites found in the A domain of PAM (Rios-Steiner et al., 2001, Wang et al., 2010a, Wistedt et al., 1998, Qiu et al., 2018, Quek et al., 2019, Yuan et al., 2019). PAM has been categorised into three different classes based upon the amino acid sequences in plasminogen binding A domain, Class I, II, III. Class I PAMs contain two tandem repeats in the A domain for example A1A2, (PAM_{AP53}) expressed in the invasive AP53 strain. Class II isolates lack one of the domains, for example NS88.2 ($PAM_{NS88.2}$) and SS1448 (PAM_{SS1448}), both only contain the A2-repeat. Class III PAMs contain both the A1A2 repeats but also contain a VHD or DHD tripeptide at the COOH-termini of their A1-repeats (Qiu et al., 2020). However, structural analysis has revealed the a2 domain has a 5-fold higher affinity for plasminogen Kringle 2 domain than a1; which has been further supported by biophysical and biochemical experiments where the affinity for plasminogen was ~3-times higher (Quek et al., 2019). Despite PAM's pathological significance the structural data available is still

limited due to the use of truncated proteins so it is still not clear the exact binding mechanisms of PAM to plasminogen.

Numerous studies involving measuring streptokinase activity in culture supernatants, chromogenic solution assays and SPR analysis have indicated that SK 2b cannot effectively activate plasminogen in solution, displaying approximately 29 to-35- fold lower affinity for plasminogen in comparison to other streptokinase variants (Cook et al., 2012, McArthur et al., 2008). However, SK 2b activity is greatly enhanced in the presence of PAM and further still in the presence of fibrinogen. Recently SPR and chromogenic studies have demonstrated that PAM binding to the lysine binding site of plasminogen, relaxes the conformation of plasminogen and greatly enhances the activation rate of plasminogen by SK 2b (Ayinuola et al., 2021b). Additionally, murine models of GAS infection have revealed that the virulence of the bacterium is severely attenuated upon knockout of the PAM gene, in PAM-expressing strains (Sanderson-Smith et al., 2008, Chandrahas et al., 2015). Furthermore, when PAM was replaced with M1, the SK 2a associated M protein, there was no significant activation of SK 2b. Current understanding of plasminogen acquisition by SK 2b expressing strains is limited, proposed mechanisms suggest that in order for optimal plasminogen activation a trimolecular complex of streptokinase-plasminogen-fibrinogen must be formed bound to the M protein (Zhang et al., 2012, Chandrahas et al., 2015). The relationship between streptokinase sequence variations, M- like protein association and bacteria pathogenicity is not fully understood at the molecular level.

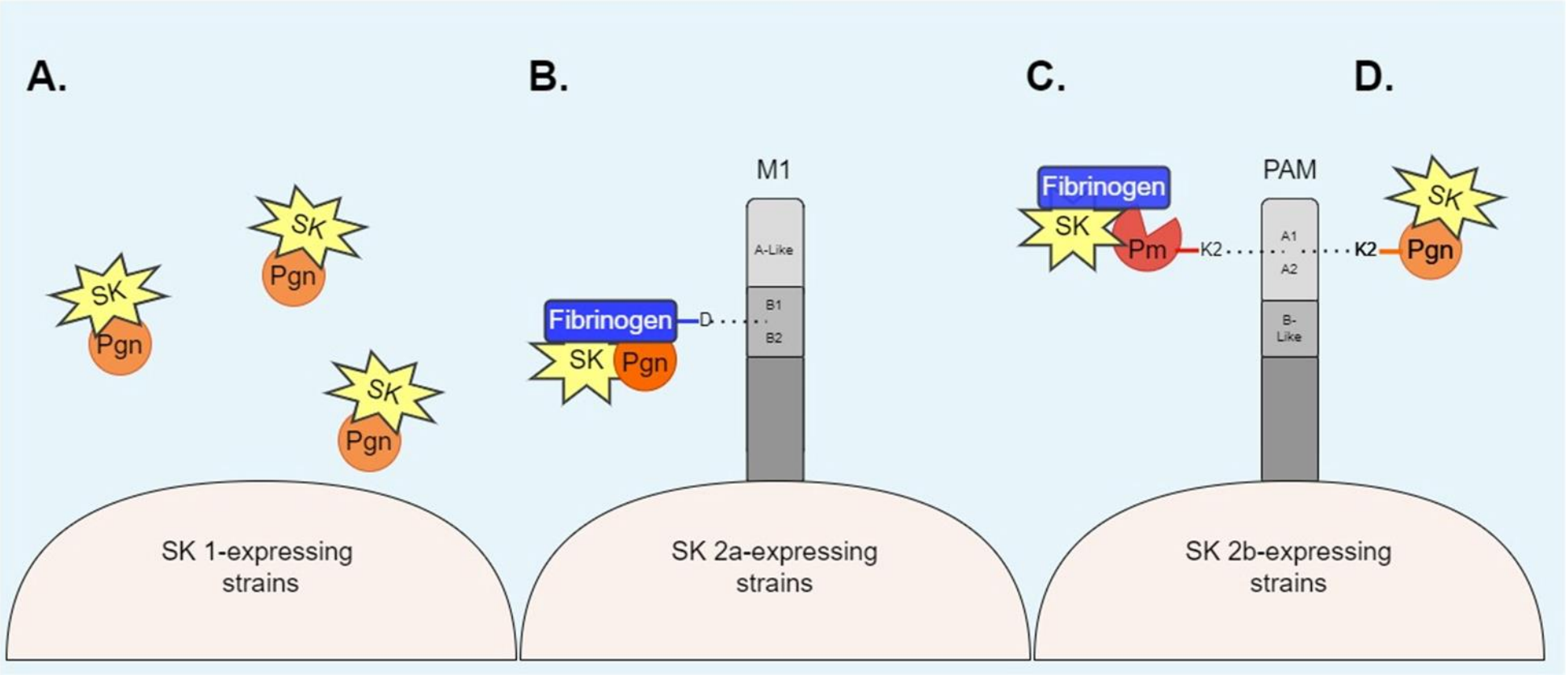

Figure 7 Schematic diagram of proposed mechanism of cell surface plasmin acquisition of GAS expressing streptokinase Cluster 1, 2a and 2b with associated M proteins. Cluster 1 streptokinase (SK) -expressing strains do not require M proteins or ligands for full activity and can activate plasminogen (pgn) free in solution. **(A.)** Streptokinase 2a- expressing strains contain the cell surface bound M1 protein which can bind fibrinogen D domain via the B1B2 domain of M1. The fibrinogen is thought to act as a template for plasmin (pm) generation, forming a trimolecular complex with SK 2a **(B.)** Two pathways are proposed for cell surface plasmin acquisition by SK 2b expressing strains. In the first pathway, plasminogen binds to fibrinogen in solution and is activated by SK 2b forming a trimolecular complex. The resulting Kringle 2 (K2) domain of plasmin is then bound to the A1A2 domain of PAM **(C.)** In the second pathway, plasminogen K2 domain directly binds to PAM A1A2 and is activated by SK 2b **(D.)**

1.4.4 Summary and Project aims

Invasive GAS serotypes express both cell-surface and secreted virulence factors that facilitate host interactions and aids in the dissemination of bacteria beyond point of infection. This project will be primarily focussed on the interaction of two virulence factors of GAS, the M protein (section 1.4.2) and streptokinase (section 1.4.3) with the human haemostasis system.

As previously highlighted, the *emm 1* serotypes are overly represented in invasive GAS disease. This serotype contains a cell-bound M1 protein, which is cleaved by a GAS protease, SpeB, at earlier stages of infection (Cole et al., 2011). The soluble M1 protein has been previously shown to form a complex with fibrinogen that is capable of activating neutrophils and platelets. However, the impact of M1 protein on fibrin clot formation properties has not previously been investigated.

Streptokinase mechanism of action is mainly understood based upon the well characterised therapeutic Group C streptokinase, H46a. Whilst GAS displays 85% amino acid sequence identity to the Group C Streptokinase, the small sequence differences appear to translate to very different plasminogen activation properties (Huang et al., 1989). Furthermore, phylogenetic analysis of the streptokinase β-domain from diverse strains of GAS have indicated that streptokinase divide into 3 distinct evolutionary clusters, 1, 2a and 2b (McArthur et al., 2008). The Cluster 2a SK displays very little activity in solution and is maximally stimulated by fibrin (Huish et al., 2017). Cluster 2b expressing strains display almost no activity in solution but are stimulated by the associated M protein, PAM, and further still by fibrinogen (Cook et al., 2012, McArthur et al.,

2008, Ayinuola et al., 2021b). Phylogenetic analysis also indicated that the Cluster 2 SK are associated with specific *emm* patterns of the bacterium, with SK 2a commonly coinciding with the fibrinogen binding M1 protein and 2b with plasminogen binding PAM (McArthur et al., 2008). Cluster 1 SK, behave very similar to Group C SK H46a in that they are not commonly associated with M proteins and optimally activate plasminogen in solution (McArthur et al., 2008). It has been proposed that the Cluster 2 streptokinase utilise the associated M proteins for cell-surface plasmin generation by forming a trimolecular complex with plasminogen-fibrinogen-streptokinase thus forming a proteolytic coat for dissemination beyond point of infection (McArthur et al., 2008). However, current understanding of plasmin acquisition is limited, and the relationship between streptokinase sequence variations, M-like protein association and bacterial pathogenicity is not fully understood at the molecular level.

The aims of the project are as follows;

A. Investigate the impact of M1 protein on fibrin clot formation, properties, and fibrinolytic potential
B. Investigate the functional relationship between streptokinase variants, and associated M-like proteins.

Specific aims and objectives will be stated in each chapter introduction (Section 3.1 and 4.1).

Chapter 2 Materials and Methods

2.1 Consumables

Unless otherwise stated, all chemicals and reagents were purchased from Sigma Aldrich

2.2 Buffer preparation

Buffer	Concentration	Reagent
Buffer A pH 7.8 room temperature	0.5 M	Tris(hydroxymethyl) aminomethane
	1 M	Hydrochloric acid
Buffer B	10 mM	Buffer A
	100 mM	Sodium Chloride
	0.01 % (v/v)	10 % Tween 20
Buffer C	n/a	Buffer B
	1 mg/ml	Human Serum Albumin (HSA)
Buffer D (Overlay)	40 mM	Buffer A
	100 mM	Sodium Chloride
	0.01% (v/v)	Tween 20
Buffer E (Ni NTA plates)	40 mM	Buffer A
	100 mM	Sodium Chloride
	0.05% (v/v)	Tween 20
	10 mM	Imidazole
Buffer F (Pull-down)	20 mM	Tris/ HCl (pH 7.4 at RT)
	150 mM	Sodium Chloride
	40 mM	Imidazole
Buffer G elution	20 mM	Tris/ HCl (pH 7.4 at RT)
	150 mM	Sodium Chloride
	500 mM	Imidazole

Dialysis buffer pH 7.4 room temperature	20 mM	Tris/ HCl pH 7.4 (at room temp)
	150 mM	Sodium Chloride
Halo activation mixture	15% (v/v)	Innovin
	67 mM	Calcium Chloride
Todd-Hewitt Yeast broth	37 g / Litre	Todd Hewitt Broth (Millipore)
	2 g / Litre	Yeast extract
Sterile C-media pH 7.5 (As per **(Gera and McIver, 2013)**)	0.5% (w/v)	Protease Peptone 3 (Difco)
	1.5% (w/v)	Yeast Extract
	17 mM	Sodium Chloride
	0.4 mM	Magnesium sulfate
	10 mM	Dipotassium Phosphate
Profinity eXact wash buffer, pH 7.2	0.1 M	Sodium Phosphate, pH 7.2
	2 M	Urea
Profinity eXact elution buffer, pH 7.2	0.1 M	Sodium Phosphate, pH 7.2
	2 M	Urea
	0.25 M	Sodium Fluoride
SUMOstar wash buffer, pH 7.2	0.5 M	Sodium Chloride
	0.02 M	Tris/ HCl, pH 7.2
	0.04 M	Imidazole
SUMOstar elution buffer, pH 7.2	0.5 M	Sodium Chloride
	0.02 M	Tris/HCl, pH 7.2
	0.6 M	Imidazole

Table 1 Composition of frequently used buffers prepared during the project

2.3 Cloning and Transformation

2.3.1 SK2b and PAM Synthesis

Commercial gene synthesis of SK 2b and PAM sequences (from *Streptococcus pyogenes* strain, NS88.2- accession numbers: JX898186 and AAQ64526.2, respectively) with an additional N-terminal Profinity eXact fusion-tag (Biorad) was performed by GenScript Biotech (Piscataway, NJ, USA). The PAM sequence also included a C- terminal 6 x Histidine tag for experimental purposes. Both sequences were codon optimised for expression in an *E. coli* expression system. The sequences were provided as lyophilised plasmid constructs cloned into a pET 27b (+) expression vector containing a kanamycin selection marker. The plasmids were reconstituted in ddH_20 to a final concentration of 100 ng/ml ready for transformation into chemically competent cells.

Primers were also designed as a contingency plan to sub-clone the SK 2b sequence into a pE-SUMO vector, following the previous success of SK 2a in this system (Huish et al., 2017). Primers were designed using vector NTI and a 100 µM cartridge purified stock was ordered from Sigma Aldrich.

2.3.2 Transformation of SK2b and PAM constructs

Autoclaved LB agar was supplemented with 50 µg/ml kanamycin and poured into triple vent petri dishes. Rosetta^{TM} 2 (DE3) (Merck Millipore), T7 Express LysY (New England Biolabs) and Top10 (OneShot ®) chemically competent *E. coli* cells were thawed slowly on ice. Competent cells (50 µl) and 2 µl of plasmid (from section 2.3.1) was transferred to a pre-chilled 0.5 ml Eppendorf, gently mixed and returned to ice for 15 minutes. The mixture was then quickly transferred to a 42ºC water bath for 120 seconds, then immediately returned to

the ice for a further 2 minutes. SOC medium (800 µl) was then added to the transformation mixture and bacteria was left to recover at 37ºC, shaking at 250 rpm for 60 minutes. Transformed cells were spread onto LB agar plates, with appropriate antibiotic and incubated overnight at 37°C.

The following day, two colonies from each agar plate were picked and inoculated into 10 ml LB (50 µg/ml kanamycin) and incubated overnight at 37°C/ 250 rpm. Glycerol stocks were prepared as 1 ml aliquots to a final concentration of 15% glycerol and stored at -80°C.

2.4 Protein Expression and Purification

Expression constructs of recombinant streptokinase 2a (rSK 2a) and rM1 were provided as Rosetta 2^{TM} glycerol stocks by C. Thelwell (NIBSC), containing an N- terminal SUMOstar fusion protein or Profinity eXact tag respectively. Additionally, rSK H46a was provided as a lyophilised protein, calibrated to have the same potency and specific activity of the WHO 3rd International Standard SK (00/464) used in previous work (Huish et al., 2017).

Bacteria was recovered from the glycerol stocks by inoculating 10 ml of LB (with appropriate antibiotic, see Table 2) with a sterile inoculating loop containing a scrape of the frozen stock. This was grown to saturation (overnight at 37ºC, shaking at 250 rpm). Pre-warmed LB broth (supplemented with appropriate antibiotics) was inoculated with a 1:50 ml dilution of the overnight culture, and placed shaking at 250 rpm/ 37ºC until the culture reached an optical density (600 nm) of ~0.5- 0.7.

Recombinant protein expression was induced by the addition of IPTG to a final concentration of 0.4 mM and incubated for a further 4 hours shaking at 250 rpm.

The cultures were harvested by centrifugation at 4355 g for 20 minutes at 4°C. The pellets, containing the expressed protein of interest were stored at -40°C.

2.4.1 Affinity Chromatography

Harvested frozen bacterial pellets were thawed then weighed and chemically lysed at ambient temperature using 4 ml B-PER reagent (Thermo Fisher Scientific, Massachusetts, US) per gram of pellet. DNase I solution (Thermo Fisher Scientific, Massachusetts, US) and lysozyme solution (Thermo Fisher Scientific, Massachusetts, US) were added to a final concentration of 5 U/ml, and 0.1 mg/ml respectively. After 15 minutes at ambient temperature the soluble and insoluble fractions were harvested by centrifugation at 16,000 x g for 20 minutes.

Prior to loading samples onto the respective columns, all buffer and protein samples were de-gassed in an ultrasonication water bath, and vacuum filtered through a 0.45 µM nitrocellulose filter membrane (Sigma Aldrich, Missouri, US).

2.4.1.1 Profinity eXact

The Profinity eXact system utilises an immobilised, extensively engineered subtilisin protease, originally obtained from *Bacillus subtilis*. The protease recognises and vigorously binds to the N- terminal co-expressed affinity tag of the recombinant proteins. The tag cleavage reaction is highly specific and self-initiates once triggered by a triggering ion (F^-, N_3^-, NO_2^-, Cl^-). To ensure the highest purification yields were obtained, all buffers containing these ions were removed and substituted with sodium phosphate.

Fusion proteins with an N- terminal Profinity eXact tag expressed as insoluble inclusion bodies. The pellets were washed with a 1:10 dilution (with sodium phosphate) of B-PER reagent and solubilised with a denaturant buffer

containing 4 M urea. Samples were diluted with 0.1 M sodium phosphate down to 2 M urea. The sample was centrifuged at 16,000 x g for 20 minutes to remove any remaining cell debris. The insoluble fraction was supplemented with cOmplete^{TM} Protease Inhibitor (Roche, Basel, Switzerland) and stored at 4°C until purification.

Recombinant proteins were purified on an ÄKTA purifier 10 (GE Healthcare Life Sciences, Chicago, US) using a 5 ml Bio-Scale^{TM} Mini Cartridge. The column was equilibrated with 10 column volumes (CV) of Profinity eXact wash buffer (Table 1) and protein was loaded at 1 ml/min. The column was then washed with an additional 10 CV of wash buffer at 10 ml/min to limit non-specific binding. The cartridge was equilibrated with 2 CV of Profinity eXact elution buffer and incubated at ambient temperature for 30- 60 minutes. The bound proteins were then eluted by resuming the flow of elution buffer (1 ml/min) until the optical density (280 nm) reached a baseline UV. The protein was collected automatically in 0.5 ml aliquots.

2.4.1.2 SUMOstar fusion proteins

Proteins expressed with the SUMOstar affinity tag were purified by IMAC Ni^{2+} affinity chromatography using a 1 ml HisTrap FF crude column (GE Healthcare Life Sciences, Chicago, US). This system binds the protein using the hexahistidines at the N-terminus of the SUMOstar fusion protein.

Imidazole was added to proteins prior to purification, to a final concentration of 40mM, to limit non-specific binding to the column. The column was equilibrated with 10 CV of SUMOstar wash buffer and protein was loaded at 1 ml/min. The column was then washed with an additional 10 CV of SUMOstar wash buffer at

3 ml/min. The bound proteins were eluted with an imidazole gradient ranging from 40 mM to 600 mM at 1 ml/min for 10 minutes.

The SUMOstar fusion tag system required an additional tag removal step using SUMOstar protease 1. Optimal results were observed following cleavage overnight at room temperature in the presence of 2 mM DTT. Tag removal efficiency was confirmed by SDS-PAGE analysis. The cleaved SUMOstar tag was removed from the protein by binding the tag and protease to magnetic Ni-NTA beads (Thermo Fisher Scientific, Massachusetts, US) and incubating the sample for 1 hour. The protein of interest was retrieved by removing and retaining the supernatant from the Ni-NTA resin.

All proteins were dialysed overnight against 20 mM Tris/ HCl, 150 mM NaCl, pH 8 (4ºC). Protein concentrations were determined by BCA protein assay (Pierce, Massachusetts, US) and amino acid analysis (Alta Bioscience Ltd, Redditch, UK) (as per section 2.4.2). Several batches were made and pooled together for all recombinant proteins, so all assays could be performed on the same pooled protein batch.

2.4.2 Protein quantification

2.4.2.1 BCA analysis

Protein quantification by BCA analysis was performed using a Pierce™ BCA Protein Assay Kit, as per manufacturer's instructions. The protein to be quantified was prediluted 1:2 and 1:4 then 25 µl (including an undiluted neat sample) was added to the wells of a Corning™ 96-well NBS plate. A standard dilution range (0-500 µg/ml) was prepared by diluting bovine serum albumin (BSA) with the same diluent as the protein sample and 25 µl was placed into the well. A BCA working reagent was prepared by mixing 50 parts BCA reagent A with 1 part of

BCA reagent B. The reaction was initiated through the addition of 200 µl of BCA working reagent to each sample or standard well. The 96-well plate was then incubated at 37ºC, shaking at 250 rpm for 30 minutes. The absorbance was then read at 562 nm on a plate reader.

The blank standard replicates were subtracted from each standard and unknown standard replicate. A standard curve was prepared by plotting the blank-corrected 562 nm measurement for each BSA sample against its concentration in µg/ml. The standard curve was then used to determine protein concentration of each unknown sample.

2.4.3 SDS- PAGE

SDS- PAGE (**S**odium **D**odecyl **S**ulfate **P**oly**A**crylamide **G**el **E**lectrophoresis) samples were prepared with 20 µl sample, 8 µl 1 x NuPAGE™ LDS sample buffer and 3 µl NuPAGE™ sample reducing agent. The samples were centrifuged briefly and heated to 70ºC for 10 minutes. 1x Bolt™ MES SDS running buffer (400 ml) was prepared from a 20x stock solution and poured into a mini gel tank containing a Bolt™ 4-12% Bis-Tris gel. Samples (30 µl) were loaded into the gel alongside 10 µl of SeeBlue™ Plus2 Pre-stained protein standard. Gels were run at a constant voltage of 200 V for 35 minutes. Gels were stained in an electric eStain® 2.0 protein staining device (GenScript Biotech, Piscataway, NJ, USA) for 6 minutes. The gel is placed between an eStain® cathode pad, containing Coomassie blue dye, and an eStain® anode pad. The device sends a voltage through the pads driving negatively charged Coomassie blue dye into the gel matrix to bind the proteins and out of the protein gel into the anode pad to destain. Gels can be visualised immediately and imaged using PXi Touch system with GeneSys® software.

2.5 Fibrin clot properties

2.5.1 Whole Blood Collection

Whole blood samples were taken from volunteer donors at NIBSC by an onsite phlebotomist into falcon tubes containing 0.109 M trisodium citrate, with the use of a tourniquet. The blood was mixed at a 1-part citrate to 9-part whole blood ratio. Blood samples were not stored overnight and were disposed of at the end of each day. All blood donations followed the regulations of the granted Human tissue act.

2.5.2 Permeability Assays

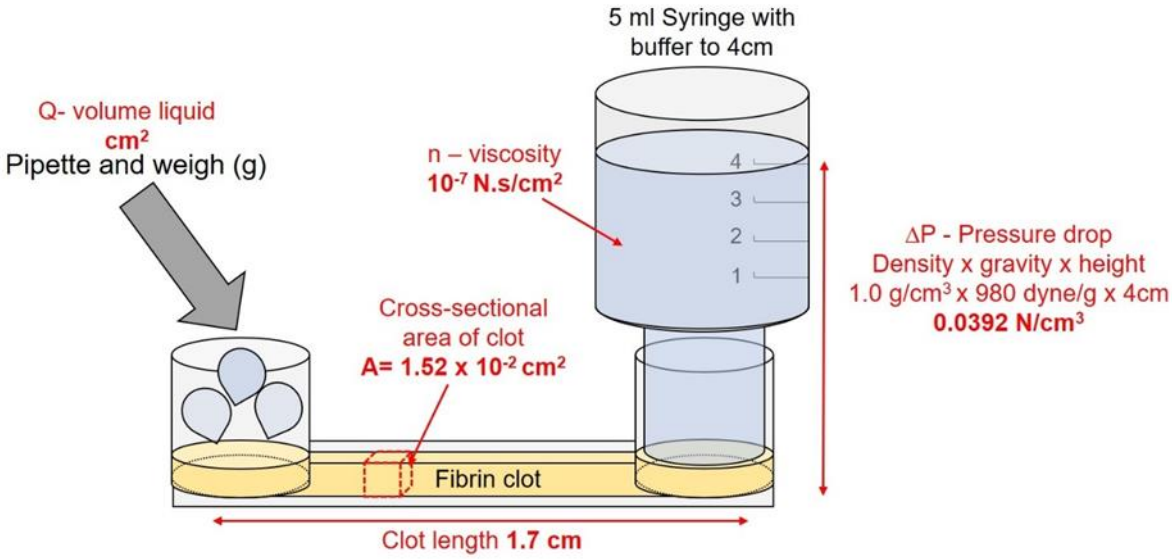

Figure 8 Schematic representation of permeation assay experimental set-up, with important measurements used in calculation of fibrin clot pore size.

Permeation assays were used to determine the pore size of the fibrin network in the presence of rM1. Purified fibrin clots were prepared in 0.5 ml Eppendorf's by preincubating 70 µl of 3 mg/ml purified fibrinogen (Calbiochem®, plasminogen-depleted), and rM1 (0 µg/ml – 60 µg/ml). Samples were incubated for 5 minutes before 30 µl of activation mixture (0.2 IU/ml thrombin (01/578) and 5 mM

calcium chloride) was added to initiate clotting. Plasma fibrin clots were prepared in 0.5 ml Eppendorf's by preincubating 50 µl of plasma with 25 µl of rM1 (0 µg/ml – 60 µg/ml) followed by 25 µl of activation mixture as above.

Immediately, 25 µl of the clotting mixture was transferred to 3 channels in an uncoated IBIDI µ-slide VI 0.4 (Thistle Scientific, Glasgow, Scotland), as shown in Figure 10B. Slides were placed into a humidity chamber and incubated at 37ºC for two hours.

Once the clots had formed, Buffer B (Table 1) was carefully added to one side of the channel and a 5 ml syringe was slowly attached, ensuring no bubbles formed. The syringe was filled to the 4 cm mark and the clot was washed for 30 minutes.

Liquid was removed from the opposite end of the channel and the syringe was refilled to the 4 cm mark. The volume of liquid was then weighed every 15 minutes, for 60 minutes (1 g = 1 ml = 1 cm^3). A constant pressure head was maintained by keeping the buffer level at the 4 cm mark.

Pore size of the fibrin clots were determined by calculating the permeation co-efficient (Darcy's constant, Ks);

$$K_s = \frac{Q\ x\ n\ x\ L}{t\ x\ A\ x\ \Delta P}$$

Where, Q = volume of permeated buffer (cm^2); n= viscosity of buffer (10^{-2} poise = 10^{-7} N.s/cm^2); L= length of clot (1.7 cm); t= time (s); A= cross-sectional area of clot ($1.52x10^{-2}$ cm^2); ΔP= Pressure drop (0.0392 N/cm^2), as demonstrated in Figure 8.

2.5.3 Rotational Thromboelastography

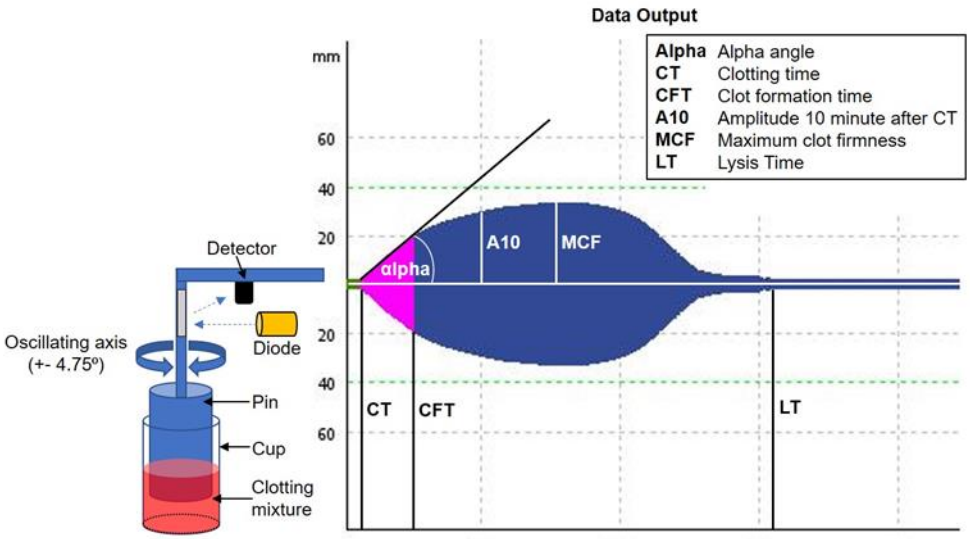

Figure 9 Basic diagram of experimental set up including a typical ROTEM® TEMogram with the main parameters.

Rotational thromboelastography (ROTEM) is a point of care instrument that measures clotting and lysis potential of a patient's blood. A cup containing 340 µl of sample (300 µl fibrinogen source (plasma or whole blood), 40 µl rM1 (0- 60 µg/ml) mixed with test activator (lyophilised EXTEM-S/ FIBTEM-S/INTEM-S)) remains fixed whilst a pin suspended into the cup, oscillates 4.75º every 6 seconds with a constant force. As the clot forms, the resistance to movement of the pin is detected optically and converted into a TEMogram (Figure 9). The main parameters obtained from these TEMograms are:

- **Clotting time (CT):** The time (s) to initiate clotting and begin clot polymerisation (clot firmness 2 mm) from the start of measurement.
- **Clot formation time (CFT):** The time (s) to reach a clot firmness of 20 mm from the initiation of clotting.

- **Alpha angle (α-angle):** The angle of tangent between the start of measurement (0 mm) and the curve when clot firmness is 20 mm. This parameter reflects the kinetics of clot formation. It is a measurement of the rapidity of fibrin polymerisation and stabilisation of the clot through cross-linking by FXIIIa.
- **Amplitude after 10 minutes (A10):** This is directly related to the maximum clot firmness; it is a measurement of how firm (mm) the clot is after 10 minutes.
- **Maximum clot firmness (MCF):** This is the maximum clot amplitude (mm) obtained during the test. It reflects the strength of the clot overall and is an indication of the platelet number, fibrinogen level and fibrin cross-linking.
- **Lysis time (LT):** The time taken (s), from clotting time, until the clot firmness is decreased to 10% of the maximum clot firmness during fibrinolysis**.**

ROTEM measures coagulation through a variety of tests. The most relevant for this project are the INTEM, EXTEM and FIBTEM tests. The INTEM assay provides similar information to an APTT test, it is activated using phospholipids and ellagic acid. The intrinsic pathway is activated, therefore can identify deficiencies in this cascade. The EXTEM assay is activated by tissue factor, which initiates the extrinsic clotting cascade. It can therefore identify deficiencies in factors VII, IX, X and prothrombin. The EXTEM assay is also the most sensitive test to fibrinolysis. The FIBTEM test is an EXTEM based assay, however the addition of cytochalasin D, inhibits the platelets to produce a clot tracing that isolates the contribution of fibrinogen. The ROTEM device can analyse 4 samples simultaneously.

2.5.4 Scanning Electron Microscope

Scanning electron microscopy (SEM) was used to investigate the architecture of the fibrin clots. SEM generates images of the surface of the clot by scanning the sample with a focused high-energy beam of electrons. A high-resolution image is then generated from two types of electrons, backscattered and secondary electrons, 'reflected' from the sample. The electron column needs to be kept under vacuum; therefore, the sample preparation includes fixation and dehydration of the specimen.

Fibrin clots were prepared in 0.5 ml Eppendorf tubes by combining 0.2 IU/ml thrombin (01/578), 5 mM calcium chloride and rM1 (0, 3.75, 15 and 60 µg/ml) with 50% plasma to a volume of 100 µl. Immediately, 75 µl of this clotting mixture was transferred to a 1.5 ml Eppendorf lid, which had been pierced several times prior with a needle and wrapped in parafilm to prevent leakage. The clots were then allowed to form in a humidity chamber at 37ºC for 2 hours.

After 2 hours, parafilm was removed and the clots were placed in a beaker and fixed overnight with 2% Glutaraldehyde then washed for 20 minutes three times in 50 mM sodium cacodylate buffer (pH 7.4). The samples were then dehydrated using a series of increasing acetone concentrations (30, 50, 60, 70, 80, 90, 95% and (3x) 100% acetone for 15 minutes per acetone concentration). The plasma clots were transferred to fresh 100% acetone and left overnight. The clots were critically point dried by Martin Fuller of the Astbury Biostructure Laboratory, University of Leeds. Briefly, liquid acetone was replaced with liquid CO_2, and heated to 31ºC under 1200psi to remove excess liquid. Samples were then mounted onto 12.5 mm diameter aluminium specimen stubs with adhesive carbon tabs (AgarScientific Ltd., Stansted, UK). The samples were sputter coated with 10 nm thick layer of iridium using a SC7620 mini sputter coater

(Quorum Technologies Ltd, West Sussex, UK). Clots were imaged at a minimum of three areas at x1000, x5000, x10,000 and x20,000 magnifications using Hitachi SU8230 (FESEM) scanning electron microscope (assisted by Lewis Hardy, University of Leeds).

2.5.5 Laser Scanning Confocal Microscopy

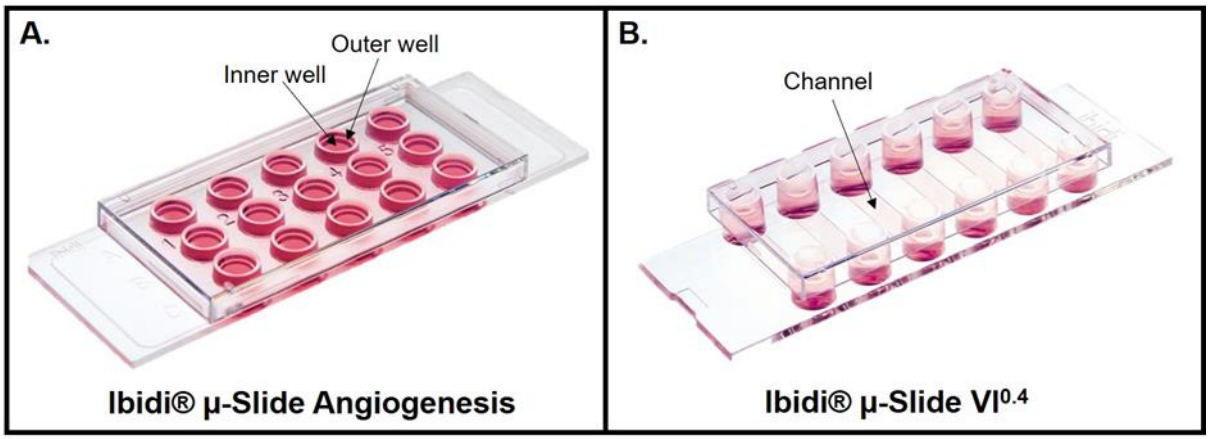

Figure 10: Representative images of Ibidi® µ-Slides used in this project. Images of slides obtained from Ibidi® official website.

The structure of the fibrin clots was also investigated using laser confocal scanning microscopy (LSCM). LSCM generates an image, built up pixel-by-pixel from emitted photons from fluorophores added to the samples. This is achieved by passing a laser beam through a light source aperture which has been focused by the objective lenses into a small region of the sample of interest. Although the resolution of LSCM is poorer than SEM (maximum resolution of ~200 nm in comparison to 1- 10 nm), LSCM allows for the visualisation of samples in fully hydrated conditions, and the reconstruction of z-stacks generates 3D images.

Fibrinogen (3 mg/ml) (Calbiochem®, plasminogen depleted) or frozen plasma was spiked with an Alexa Fluor 594- fibrinogen conjugate to a final concentration of 0.25 mg/ml. The fibrin clots were then formed in 0.5 ml

Eppendorf tubes by combining plasma or fibrinogen mixture (to a final concentration 20% plasma or 0.6 mg/ml fibrinogen and 0.05 mg/ml Alexa Fluor 594 conjugate) with rM1 (0- 60 µg/ml), 0.2 IU/ml thrombin (01/578) and 5 mM calcium chloride to a total volume of 100 µl.

2.5.5.1 Imaging fibrin network

Clotting mixture, 20 µl, (from section 2.5.5) was transferred into three inner wells of an uncoated Ibidi® µ-Slide angiogenesis (Figure 10A) and immediately placed into a dark humidity chamber to clot for one hour at 37ºC. Slides were placed on to the Galvo stage of a Leica TCS SP8X MP OPO Spectral confocal microscope and imaged using a 63 x water immersion objective (Leica, HC PL APO CS2 63X/1.20) with the following parameters;

Parameter	Setting
Resolution	16-bit
Size	872 x 872 pixels
z-stack	20 µm
Slices	58
Pinhole	1.0 Airy
Zoom	X2
Line average	4

Fibrin network images were processed in image J. Images were smoothed using a gaussian filter (1.0) and brightness was auto adjusted. The z- stacks were flattened into a 2D image and the pseudo-colour was amended by changing the lookup table (LUT) to ‘RainbowRGB’. Fibrin density was determined by applying a grid overlay of two lines spanning horizontally and vertically across the image then counting the number of fibres that cross these lines (Figure 11). The clot densities, between fibrin clots containing rM1, were compared to the control using an ordinary one-way ANOVA with Dunnett’s multiple comparisons test in GraphPad Prism (v. 8.1.1).

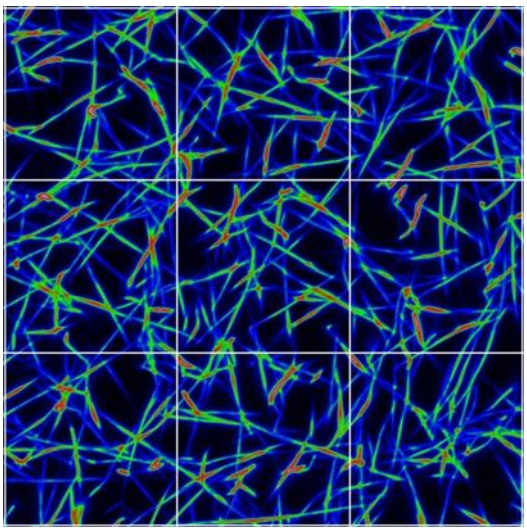

Figure 11 Representative image of fibrin clot processing. Z-stacks were flattened to a 2D image, smoothed with a gaussian filter and LUT were amended to RainbowRGB. Fibrin density was calculated from a grid overlay, counting the fibres that crossed each line.

2.5.5.2 Imaging fibrin film

15 µl of the clotting mixture (from section 2.5.5) was transferred into three channels of an uncoated Ibidi® µ-Slide VI$^{0.4}$ (Figure 10B). The maximum capacity of the Ibidi® µ-Slide VI$^{0.4}$ is 30 µl, therefore half filling the channels allowed for the fibrin clot film to form due to the presence of an air-liquid interface (Macrae et al., 2018). The slides were immediately placed into a dark humidity chamber to clot for one hour at 37ºC. Fibrin films were imaged using Leica TCS SP8X MP OPO Spectral confocal microscope and the fibrin film was located. The films were imaged using a 63x water immersion objective (Leica, HC PL APO CS2 63X/1.20) with the following parameters:

Parameter	Setting
Resolution	16-bit
Size	1024 x 1024 pixels
z- stack	20 µm
Slices	58
Pinhole	1.0 Airy

A 3D image of the fibrin film was constructed using Imaris 9.3.1 software (Bitplane). Images were smoothed with a gaussian blur filter then 3D isosurface rendering was performed using the 'surfaces' tool in the software. The surfaces were created by manually adjusting the threshold (background subtraction) to fill in the volume of the image. The surface was pseudo-coloured to a 'spectrum' LUT and represents intensity of the fibrin. The minimum and maximum intensities were amended to 0 and 20000, respectively, for each image.

2.6 Streptococcus pyogenes Growth and Maintenance

2.6.1 Bacterial Reconstitution and Stocks

A *Streptococcus pyogenes* strain from each evolutionary cluster (Cluster 1 strain: ATCC® BAA-1633™, Cluster 2a strain: ATCC® 700294™ and Cluster 2b strain: ATCC® BAA-1323™) was obtained as lyophilised bacteria from LGC (Teddington, UK.). The bacteria were reconstituted with 500 µl of pre-warmed Todd-Hewitt-Yeast (THY) broth and allowed to rehydrate for 10 minutes. Reconstituted bacteria were streaked, with a sterile inoculating loop, onto blood agar plates (Tryptic Soy Agar (TSA) with sheep blood, Thermo Fisher Scientific, Massachusetts, US) and incubated overnight at 37ºC with 5% CO_2. Reconstituted bacteria (100 µl) were stored in Protect Select cryobeads, by removing 100 µl of the media and inverting three times to mix the bacteria culture with the beads. After 10-minute incubation, all liquid was removed and the cryobeads were stored at -80ºC. The following day, the cryobeads were used to streak blood agar plates to ensure bacteria was compatible.

2.6.2 Gram staining

An individual cryobead, stored at -80ºC, was used to streak a blood agar plate and incubated statically at 37ºC, with 5% CO_2, overnight. The following day, an

individual colony was picked from the plate, with a sterile inoculating loop, and an emulsion was made in 10 µl of distilled water on a 1 mm glass slide. The bacteria emulsion was left to air dry for approximately 20 minutes then fixed with 10 µl of methanol. The fixed samples were flooded with crystal violet dye for 30 seconds then gently rinsed with distilled water. Gram's iodine (iodine and potassium iodide) was added to the sample to act as a mordant, by forming a larger crystal violet- iodine complex which is insoluble in water. Following another rinse with distilled water, the sample was flushed with a decolourising agent, containing a mixture of 95% ethanol and acetone. The decolourising agent dehydrates the peptidoglycan layer, trapping the crystal violet- iodine complex in Gram positive cells and washes away the complex in Gram negative cells. The sample is washed with distilled water and flooded with safranin, a weaker counterstain, that stains the cells red when crystal violet is not present. Finally, the samples were rinsed a final time and blotted dry. The bacteria were viewed under a benchtop microscope with a x100 lens to check staining, cell morphology and for contamination.

2.6.3 *Streptococcus pyogenes* Growth Curves

An individual cryobead, stored at -80ºC, was used to streak a blood agar plate and incubated statically at 37ºC, with 5% CO_2, overnight. The following day a sterile inoculating loop was used to pick an individual colony from the blood agar plate and was resuspended in 1000 µl of sterile THY media, in a Corning® Costar® TC-treated 24-well plate, and placed back at 37ºC, 5% CO2, overnight. Sterile THY broth (200 µl), in a fresh sterile 96-well plate, was inoculated with 4 µl (1:50 ml) of the overnight culture. Plates were covered with Axygen® Ultraclear sealing film, to mimic growth in a sealed tube, and read kinetically on

a BMG FluorStar Omega plate reader with the following conditions:

Condition	Setting
Wavelength	600 nm
Temperature	37ºC
Number of Cycles	40
Cycle Times	1800 s
Shaking Frequency	400 rpm
Shaking mode	Double orbital
Additional Shaking before reading	10 s
Number of flashes per well	20

Due to GAS being non-motile, bacteria settles to the bottom of the well, and aggregates during growth, therefore oscillation of the plate is essential to ensure accurate turbidity measurements. Growth curves were then generated using the software associated with the BMG FLUOstar® Omega plate reader and exported to Microsoft Excel.

2.7 Enzyme assay systems

2.7.1 Solution Plasminogen Activation Assay

Plasminogen activation activity of the streptokinase variants was determined against the WHO 3rd International Standard SK (WHO 3rd IS SK 00/464, NIBSC, South Mimms, UK) in accordance to the European Pharmacopoeia (EP)[1].

Plasmin generation was measured using the chromogenic substrate S2251 (Val-leu-lys-p-nitroaniline·2HCl; Chromogenix, Milan, Italy), which is cleaved by plasmin to release p-nitroaniline (pNa) (Figure 12). This is a chromophoric group that can be monitored kinetically and is directly proportional to plasminogen activation. A substrate solution was prepared by diluting S2251

[1] Streptokinase concentrated solution 07/2008: 0356 Ph Eur 9th Edition. Strasbourg, France: Council of Europe; 2013

and plasminogen (HYPHEN-BioMed) to a final concentration of 0.6 mM and 100 nM, respectively, with Buffer B (Table 1). A dose-response of streptokinase (4.8, 2.4, 1.2 and 0.6 IU/ml, unless otherwise stated) was prepared in Buffer B solution, with the addition of HSA (Buffer C, Table 1) and maintained in a microtiter plate at 37ºC. Plasminogen activation was initiated by mixing the streptokinase with activation mixture to a final volume of 100 µl per well in a Corning™ 96- well non-binding surface (NBS) plate. Reactions were measured using a plate reader containing a thermostat (Molecular Devices Thermomax, using Softmax software, MDC, Stanford, CA, USA) at an OD_{405} with 30 second intervals for 90 minutes at 37°C.

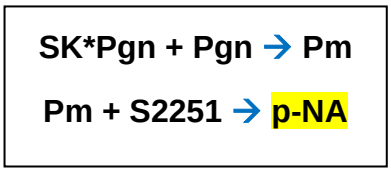

Figure 12 ***pNa generation is directly proportional to pgn activation.*** *p-NA is measured at an OD_{405} for 5400 seconds. Plasmin production is calculated from the plots of absorbance/ time^2.*

The raw data generated by Softmax Pro v5.0 (Molecular Devices) software was uploaded to an R script, written by Dr. Colin Longstaff (Biotherapeutics Division, National Institute for Biological Standards and Control, South Mimms, Hertfordshire, United Kingdom), which calculates zymogen activation rates (Longstaff, 2016b). The initial rates of reaction of plasmin production were calculated from the gradient of transformed plots of absorbance (where the substrate and plasminogen were less than 10% consumed) verses time^2 (s).

2.7.2 Clot- overlay assay

Plasminogen activation in the presence of fibrin was measured by using a clot-overlay assay, in which a mixture of the plasminogen activator and S2251 were

added to the surface of a preformed clot then monitored kinetically. Fibrin clots were formed in a Corning™ 96-well NBS plate at 37ºC (unless otherwise stated) to a total volume of 60 µl by combining 3 mg/ml fibrinogen (plasminogen depleted, Calbiochem®) with 5 mM calcium chloride, 100 nM plasminogen and 0.5 IU/ml thrombin (01/578). Clotting reagents were diluted with Buffer D (Table 1) in order to produce clear fibrin clots that would not affect the kinetic readings of pNa generation (Longstaff and Whitton, 2004). Clots were formed for 60 minutes. A dilution range of plasminogen activator (described in the methods of each chapter, (Section 3.2.1 and 4.2.4)) was prepared separately in the empty wells, using Buffer D with the addition of 1 mg/ml HSA, and combined with 0.6 mM S2251. Clot lysis, and plasminogen activation, were initiated by transferring 40 µl of the plasminogen activator-S2251 solution to the surface of the preformed clots. Reactions were read immediately using a plate reader containing a thermostat at two absorbances (OD_{405} and OD_{650}) for 300 minutes with 30 second intervals at 37ºC. The raw data was exported to Microsoft Excel (Redmood, Washington, USA) and each well was corrected by subtracting the initial absorbance value from each time point (due to initial absorbance differences under certain conditions tested). The absorbance at (3x) 650 nm was then subtracted from the absorbance at 405 nm to eliminate kinetic anomalies created from bubbles as the clot lyses. The normalised data was then uploaded to the R script which calculates the initial rates of reactions of plasmin production as per section 2.7.1.

2.7.3 Clot- lysis assay

Fibrinolysis of the fibrin clots was measured kinetically with turbidity assays. Plasminogen activator is combined with fibrinogen, plasminogen, and thrombin to form a clot that is lysed evenly throughout. This is to better represent the

physiological haemostasis in comparison to adding plasminogen activator to a preformed clot (as per section 2.7.2). Fibrin clots were formed in a Corning™ NBS 96- well NBS plate at 37ºC. All clotting mixtures were diluted with Buffer B, unless otherwise stated (Table 1). A dilution range of SK (2.4- 0.3 IU/ml, diluted with Buffer C) was combined with 3 mg/ml fibrinogen (plasminogen depleted, Calbiochem™) to a final volume of 60 µl. Fibrinolysis was initiated immediately through the addition of 40 µl activation mixture (0.05 IU/ml thrombin (01/578), 5 mM calcium chloride and 100 nM plasminogen). Reactions were measured kinetically on a Molecular Devices Thermomax plate reader for 7 hours with 30 second intervals at an absorbance of 350 nm. As the reaction proceeds, the insoluble fibrinogen is converted to soluble fibrin and polymerises, simultaneously with SK activating plasmin. Fibrin clotting and lysis was monitored through measuring turbidimetric changes in the microtitre plate wells. The raw data was exported to Microsoft Excel, and each well was corrected by subtracting the initial absorbance value from each time point. The data was then uploaded to an R script to analyse clotting and lysis data (Longstaff, 2016a). The R script can determine multiple parameters from the raw data such as max absorbance, area under the curve, time between clotting and 50% lysis, time to 50% lysis from peak, time to full lysis and time to max absorbance.

2.7.4 Halo Assay

Clot lysis data was obtained for whole blood samples using Halo assays (Bonnard et al., 2017). A clot is formed from whole blood around the bottom edge of a microtiter well, and a plasminogen activator is added to initiate lysis. The blood clot dissolution is then monitored kinetically using a plate reader. Whole blood clots were formed by depositing 5 µl of activation mixture (15% Innovin v/v- and 67-mM calcium chloride diluted with Buffer B) to the bottom

edge of a Falcon® 96-well clear flat bottom microplate. The droplet is then spread around the bottom edge of the well with the tip of a p100 micropipette tip containing 25 µl of citrated whole blood. The blood is released slowly and combined with the activation mixture to initiate clotting. Halo shaped whole blood clots form due to the fluidic cohesion effect and are left to polymerise for 30 minutes at 37ºC. A streptokinase dilution range (4.8- 0.6 IU/ml, with Buffer C) was prepared then carefully added down the side of each well, ensuring the clots are not dislodged. Reactions were monitored on a FluorStar® Omega microplate reader (BMG LANTECH Ltd.) with 5 second orbital shaking at 200 rpm. The plate was read at an OD_{510} for 300 minutes with 30 second intervals. Each experiment contained a negative control (lysis mixture did not contain plasminogen activator) and positive control (Blood was not activated with clotting mixture, instead this is substituted with Buffer B). The raw data was exported to Microsoft Excel then uploaded to a Halo analysing R script (Longstaff, 2018b). The script corrects the data by zeroing each well by its initial absorbance, then calculates several parameters from the raw data such as time to 50% lysis, area under the curve and max absorbance.

2.7.5 Surface Immobilised Assays

Cell surface plasmin generation, in the presence of M proteins, was simulated by binding the M proteins to a Pierce™ nickel coated 96-well plates utilising the co-expressed C-terminal histidine tags. Plasmin generation was then monitored kinetically following addition of plasminogen activators and a chromogenic substrate. The maximum binding capacity of the plates is ~9 pmol His-tagged protein (27kDa) per well, therefore M protein concentration was calculated to be in excess of the maximum. M protein (10 mM rPAM and 11 mM rM1, 100 µl per well) was bound to the plates for 1 hour, shaking. When M proteins were not

included in the well, the nickel was saturated with His tagged albumin (15 µg/ml, ProSci^{TM}, Poway, CA, USA.). Excess protein was removed, and the wells were washed three times with Buffer E (Table 1). The reaction was initiated through the addition of 0.6 mM S2251, 100 nM plasminogen and a dilution range of streptokinase. The reaction was then immediately measured at OD_{405} for 90 minutes at 37ºC on a Molecular Devices Thermomax plate reader. The raw data was exported to an excel document and was uploaded to the R script which calculates the initial rates of reactions of plasmin production as per section 2.7.1.

2.8 Parallel Line Bioassay

Potency estimates of the streptokinase variants were calculated in international units (IU) relative to the WHO 3rd IS SK (00/464). Each assay system included at least 4 streptokinase doses, made up in 2 replicate series for each sample. The calculated data from the R- scripts were entered into CombiStats^{TM} (v6.0, EDQM, Strasbourg, France), a program for statistical analysis of data from biological dilution or potency assays. The resultant dose-responses were fitted to a parallel-line model to estimate potencies and 95% confidence intervals. CombiStats^{TM} (Figure 13) performs various statistical tests to ensure the assay is valid. A non-linearity and non-parallelism at the 5% significance level is deemed significant and subsequently the assay was determined to be invalid, and the potency cannot be determined. Additionally, regression must be significant for the assay to be deemed valid. Specific activities for each streptokinase were then calculated in IU/µg using the estimated potencies and protein concentrations determined from amino acid analysis.

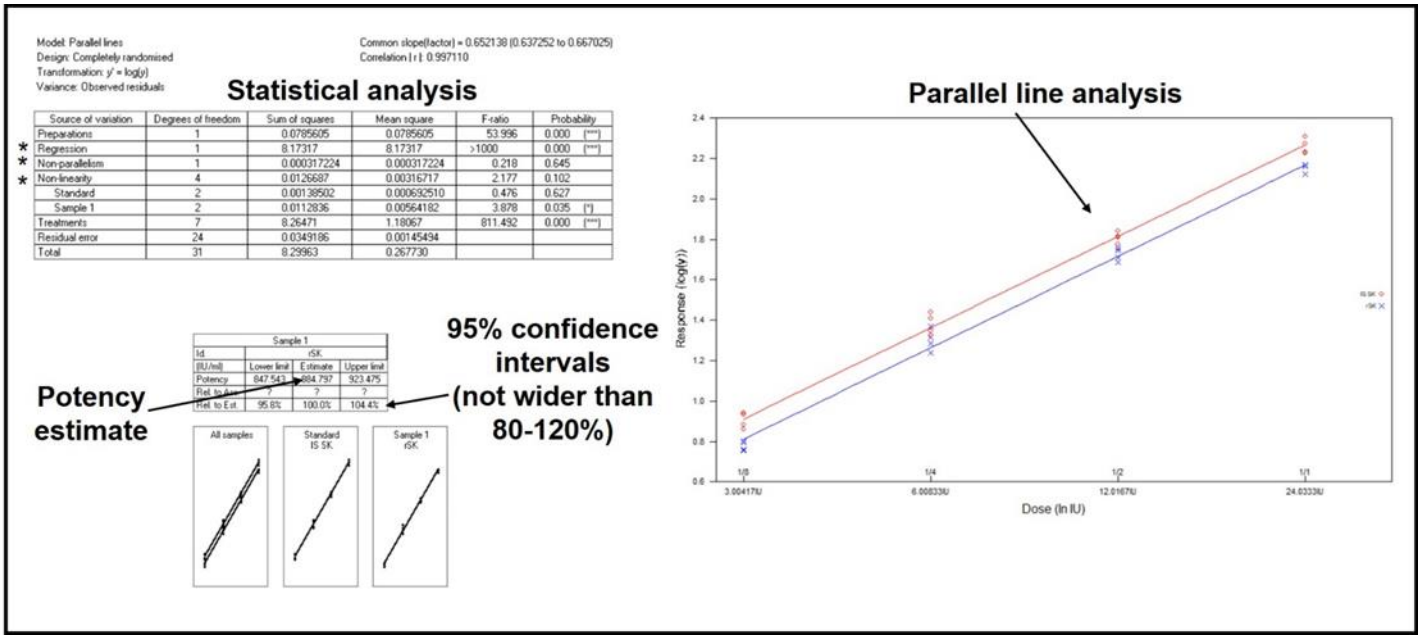

Figure 13 Representative parallel line bioassay analysis

Recombinant protein	**Tag**	**Selectable Marker**	**Expression system**	**~ MW with tag (kDa)**	**Source and form**
M1	Profinity eXact™	Ampicillin 100 µg/ml	Rosetta™ 2 (DE3)	62	C. Thelwell expression construct
SK 2a	SUMOstar™	Ampicillin 100 µg/ml	T7 Express LysY	62	C. Thelwell expression construct
PAM	Profinity eXact™	Kanamycin 50 µg/ml	Rosetta™ 2 (DE3)	50	Genscript Biotech Lyophilised plasmid
SK 2b	Profinity eXact™	Kanamycin 50 µg/ml	Rosetta™ 2 (DE3)	56	Genscript Biotech Lyophilised plasmid
rSK H46a	SUMOstar™	Ampicillin 100 µg/ml	T7 Express LysY	62	S. Huish Lyophilised protein (Huish et al., 2017)

Table 2 Recombinant proteins expressed for this work

Chapter 3 Impact of M1 protein on fibrin clot formation, properties, and structure

3.1 Introduction

During early GAS infection, it is proposed that the CovRS operon responds to environmental stressors and represses the synthesis of many key virulence factors, such as the hyaluronic acid and streptokinase, whilst upregulating the bacterial protease SpeB (Cole et al., 2011). SpeB cleaves M proteins from the GAS cell-surface resulting in soluble, functionally active M protein at the site of infection. Soluble M1 protein, from the leading invasive GAS serotype, has previously been shown to bind fibrinogen forming a pathological supramolecular complex (Section 1.4.2.1) capable of activating neutrophils and inducing vascular leakage, a common symptom of STSS (Herwald et al., 2004, Macheboeuf et al., 2011). The complex is also capable of activating platelets resulting in aggregation and platelet rich microthrombi at sites of infection and at distant sites (Shannon et al., 2007). Although M1 has previously been shown to bind fibrinogen, the consequences of this in relation to coagulation, particularly fibrin clot formation, are poorly investigated and understood.

The specific objectives were;

1. To express recombinant M1 protein (rM1) using an *E. coli* expression system and to purify rM1 using affinity chromatography.
2. To validate rM1 as being representative of the native GAS virulence factor by SDS-PAGE analysis (to confirm protein size) and using LSCM and pull-down assays to assess the fibrinogen-binding properties of rM1.

3. To determine the impact of rM1 protein on fibrin clot formation, using turbidity assays to investigate lag times and maximum absorbance in purified and plasma clots, and using KC4 delta and rotational thromboelastography (ROTEM) to assess mechanical clot formation by measuring the physical resistance of purified, plasma and whole blood clots.
4. To investigate the fibrin clot stability in the presence of rM1 by measuring the physical resistance of purified, plasma and whole blood clots in the presence of rM1 using ROTEM.
5. To assess the impact of rM1 on fibrin clot structure using clot permeation assays to measure the purified and plasma clot porosity. To investigate the plasma clot architecture in the presence of rM1 using laser scanning confocal microscopy (LSCM) and scanning electron microscopy (SEM). To calculate clot density using the LSCM images. To investigate the impact of rM1 protein on fibrin clot cross-linking by FXIIIa by densitometry analysis of the alpha-polymer chains, D-dimer ELISA plate assays and FXIIIa activity kits.
6. To determine the impact of rM1 protein on fibrin clot fibrinolytic potential using turbidimetric lysis assays in a purified system, by measuring time to 100% lysis. To investigate fibrinolysis of whole blood clots incorporating rM1 using Halo microtitre plate assays. Host and bacterial plasminogen activators were used in this system. To calculate time to 100% lysis by measuring physical resistance of the clot using ROTEM. Purified clot overlay assays, using a substrate specific for plasmin, were used to

assess the impact of rM1 on plasminogen activation activities of host plasminogen activators, uPA and tPA.

7. To examine the impact of rM1 protein on fibrin clot film formation, the protective external layer on the surface of a clot, using LSCM to visualise the impact of rM1 protein on plasma fibrin clot film formation.
8. To develop bacterial migration assays from previous literature (Macrae et al., 2018), for the purpose of investigating GAS movement through purified fibrin clots in the presence of rM1 protein

3.2 Methods

3.2.1 Protein expression and purification

As per section 2.4

3.2.2 Pull-down assay

Pull-down assays were employed to investigate protein- protein interactions between fibrinogen and rM1 (Figure 14). Fibrinogen (plasminogen depleted, Calbiochem®) and rM1 protein (diluted with Buffer B to final concentration of 1 mg/ml and 12.5 µg/ml, respectively) were combined in a 0.5 ml Eppendorf to a total volume of 200 µl and incubated for one hour at room temperature. HisPur™ magnetic Ni-NTA beads (Thermo Scientific™) were prepared by equilibrating with 400 µl of Buffer F wash buffer (Table 1) three times. The rM1, and associated proteins, were captured utilising the C-terminal co-expressed histidine tag through the addition of 100 µl of HisPur™ magnetic Ni-NTA beads. The samples were then incubated at room temperature on a roller mixer for 60 minutes. Beads were collected by placing the Eppendorfs in a magnetic stand and the supernatant was removed and retained for analysis. Magnetic beads were then washed 4 times with 1000 µl Buffer F wash buffer. Bound proteins were eluted through the addition of 50 µl of Buffer G elution buffer and placed on a rotating mixer roller for 30 minutes. Finally, the beads were boiled for 5 minutes, and the supernatant was removed and resolved by SDS-PAGE analysis as per section 2.4.3.

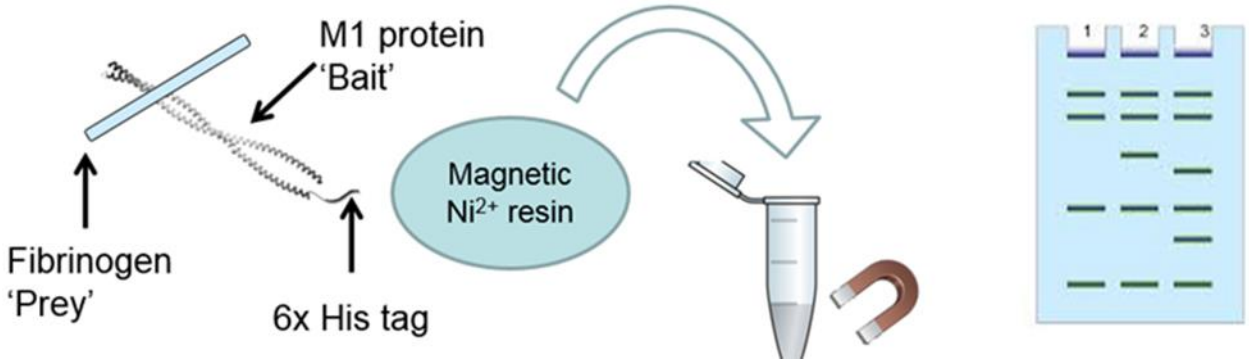

Figure 14 Schematic representation of pull-down assay. M1 proteins with a C-terminal His-tag (bait) and associated proteins (prey) are captured by magnetic nickel resin. Following washes to remove non-specific binding, the protein is eluted and resolved by SDS-PAGE analysis.

3.2.3 Turbidimetric clotting and fibrinolysis assays

Turbidity experiments were performed as per section 2.7.3 with minor adjustments. Fibrin clots were formed in a Corning™ NBS clear 96- well plate at 37ºC. A dilution range of rM1 (0.94- 60 µg/ml) and 0.2 IU/ml 3rd IS SK (00/464) was combined with 0.05 IU/ml thrombin (01/578) and 5 mM calcium chloride to a final volume of 60 µl. The reaction was initiated with 40 µl of 3 mg/ml fibrinogen (plasminogen depleted, Calbiochem®) and 8.2 µg/ml plasminogen (HYPHEN BioMed). Where stated in results, plasminogen and streptokinase was not included, and replaced with Buffer B, in order to investigate clotting profiles alone. Turbidity measurements were immediately monitored at 405 nm, for 5 hours with 10 second intervals on a Molecular Devices Thermomax plate reader. The reaction proceeded at 37ºC. The raw data was exported to Microsoft Excel, and each well was corrected by subtracting the initial absorbance value from each time point. The data was then uploaded to an R script to analyse clotting and lysis (Shiny app, (Longstaff, 2016a)). The R script calculated maximum absorbance, time between clotting and lysis and time to 100% lysis. The data was also used to manually calculate lag phase, which

represents fibrinopeptides being cleaved before lateral aggregation. The lag phase for this project was defined as the time from point 0 until the absorbance reached 0.01.

3.2.3.1 M1 and fibrinogen turbidimetric analysis

Turbidimetric analysis of M1 and fibrinogen interactions was performed using a Molecular Devices Thermomax plate reader. A dilution range of rM1 protein (62-1.88 µg/ml) was added to a Corning™ NBS clear 96- well plate at 37ºC. The reaction was initiated with 3 mg/ml fibrinogen. Turbidity measurements were immediately monitored at 405 nm, for 40 minutes with 30 second intervals on a Molecular Devices Thermomax plate reader. A control was included without the presence of rM1 protein.

3.2.1 Fibrin clot overlay assays

Fibrin clot overlay assays were performed as per section 2.7.2 with minor adjustments. Fibrin clots were pre-formed in a Corning™ NBS clear 96-well plate to a total volume of 60 µl at 37ºC by combining a dilution range of rM1 (0-30 µg/ml), 3 mg/ml fibrinogen (plasminogen depleted, Calbiochem®) with 5 mM calcium chloride, 100 nM plasminogen and 0.5 IU/ml thrombin (01/578). The clotting reagents were diluted with Buffer D (Table 1) in order to produce clear fibrin clots. Clots were formed at 37ºC for 60 minutes. Host plasminogen activator (64 IU/ml WHO 2nd International Standard uPA (11/184) or 200 IU/ml WHO 3rd International Standard tPA (98/714)) was prepared in a separate microtitre plate, by diluting with Buffer D with the addition of 1 mg/ml human serum albumin. Plasminogen activators were combined with 0.6 mM S2251 and plasminogen activation was initiated by transferring 40 µl of the mixture to the surface of the preformed clots. Reactions were read using a plate reader at two absorbances (OD_{405} and OD_{650}) for 300 minutes with 30 second intervals at

37ºC. The raw data was exported to Microsoft Excel and each well was subtracted by the initial absorbance value from each time point. The normalised absorbance at (3x) 650 nm was then subtracted from the absorbance at 405 nm then uploaded to the R script which calculated the initial rates of reaction of plasmin generation as per section. The potencies and specific activities were then calculated as per section 2.8

3.2.2 Coagulation analysis using KC4 Delta

Thrombin clotting time was measured on a KC4 Delta coagulometer, a semi-automated mechanical clot detection analyser. Fibrin clots were formed in a cuvette, containing a steel metal ball, to a final volume of 300 µl. Plasma (50%) or 3 mg/ml fibrinogen (plasminogen depleted, Calbiochem®) and a dilution range of rM1 (0.94-60 µg/ml) was added to the cuvette and the reaction was initiated through the addition of 0.5 IU/ml thrombin (01/578). A control was included in both plasma and purified conditions without the presence of rM1. Clot formation was defined as the time (s) taken for the fibrin clot to displace the steel ball from the magnetic sensor situated in the KC4 coagulometer. For the plasma conditions, the rM1 protein concentration was adjusted to reflect the decreased plasma concentration in experimental conditions.

3.2.3 Rotational Thromboelastography

Viscoelastic properties of fibrin clots in the presence of rM1 were measured using ROTEM as per section 2.5.3. An additional condition was included to investigate the effects of rM1 on purified fibrin clots. Briefly, 3 mg/ml fibrinogen (plasminogen depleted, Calbiochem®) and a dilution range of rM1 (1.88- 60 µg/ml) was added to the ROTEM cup. Fibrin clot formation was initiated through the addition of 0.5 IU/ml thrombin (01/578) and 5 mM calcium chloride. All

reagents were preincubated at 37ºC prior to use. Where stated in results, 8.2 µg/ml plasminogen (HYPHEN BioMed) and 0.15 IU/ml 3rd IS SK (00/484) was added to the activation mixture to measure fibrinolysis. The reaction was monitored for 1 hour and the raw data was exported to Microsoft excel. The following parameters were compared to the 0 µg/ml control using an ordinary one-way ANOVA with Dunnett's multiple comparisons test in GraphPad Prism (v. 8.1.1); Maximum Clot Firmness (MCF), alpha angle (α-angle) and time to 100% lysis (LT).

3.2.4 FXIII fibrin cross-linking

3.2.4.1 SDS-PAGE analysis

Fibrin cross-linking by FXIII was examined by SDS-PAGE analysis. All protein concentrations were reduced for optimal separation on the gels, however molar concentrations were kept the same. Fibrin clots were prepared in 0.5 ml Eppendorf tubes to a final volume of 10 µl by combining 0.75 mg/ml fibrinogen (plasminogen depleted, Calbiochem®) with a dilution range of rM1 protein (15 – 0.117 µg/ml). The reaction was initiated with the addition of 0.05 IU/ml thrombin (01/578) and 1.25 mM calcium chloride. A FXIIIa inhibitor, T101, was included as a control. Eppendorf's were placed in an incubator at 37ºC for 2 hours to allow fibrin clots to form. Reactions were stopped through the addition of 2 x Bolt™ LDS sample buffer and 2 x Bolt™ Sample Reducing Agent and boiled at 95ºC for 5 minutes. 10 µl of Buffer B (Table 1) was added and samples were loaded on a Bolt™ 4-12% Bis-Tris gel and stained as per section 2.4.3. Alpha-polymer bands were used an indication of fibrin cross-linking by FXIIIa and were analysed by densitometry analysis using ImageJ software.

3.2.4.2 D- Dimer analysis

Cross-linking of fibrin clots by FXIIIa was also investigated using a ZYMUTEST D-Dimer ELISA assay. The ELISA quantifies the concentration of D-Dimers, a degradation product of cross-linked fibrin, following fibrinolysis of the clots. Fibrin clots were prepared in 0.5 ml Eppendorf's to a final volume of 10 µl, all dilutions were performed using Buffer B (Table 1). 3 mg/ml fibrinogen (plasminogen depleted, Calbiochem®) and a concentration range of rM1 protein (0.94- 60 µg/ml) was combined and the reaction was initiated with an activation mixture comprising 0.2 IU/ml thrombin (01/578), 5 mM calcium chloride and 8.2 µg/ml plasminogen (HYPHEN BioMed). Fibrin clots were placed at 37ºC to form for 2 hours. Fibrinolysis was stimulated through the addition of 4.8 IU/ml 3rd IS streptokinase (00/464) to the surface of each preformed clot and incubated at 37ºC overnight.

The ELISA was performed using a micro-ELISA plate coated with a purified murine monoclonal antibody that is specific for D-Dimer detection. The lysed fibrin clots were diluted 1/50,000, with the kits sample diluent, and 200 µl was added to the wells of a micro-ELISA plate and incubated at room temperature for 1 hour, shaking. A dilution range of plasma D-Dimer calibrator was also prepared and run alongside the samples. The wells were washed 5 times with 1 x wash solution and 200 µl of Anti-(H)-D-Dimer-HRP immunoconjugate was introduced to the micro-ELISA plate. The plate was then incubated at room temperature for 1 hour, shaking. The wells were washed 5 times with wash solution and 200 µl of 3', 3', 5, 5'- tetramethylbenzidine solution (containing hydrogen peroxide) was added to each sample. After exactly 5 minutes, 50 µl of stop solution (0.45 M sulphuric acid) was added to each well and colour was left

to stabilise for 10 minutes. The reaction was measured at 450 nm using a Molecular Devices ThermoMax plate reader. D-Dimer concentrations were estimated by forming a calibration curve with the dilution range of D-Dimer calibration samples (0- 200 ng/ml) and test samples were interpolated. The concentrations obtained were then multiplied by the dilution factors (x50,000) in order to calculate final D-Dimer concentration.

3.2.4.3 FXIIIa activity assay

FXIIIa activity in the presence of rM1 was measured using an AbCam Factor FXIIIa activity kit (ab241013) as per the manufacturers protocol. The assay uses the transglutaminase activity of the FXIIIa to cross-link an amine-containing substrate to a glutamine-containing substrate. This cross-linking reactions results in the release of ammonia, which is quantified using a colorimetric assay through the action of glutamate dehydrogenase indicator. The glutamate dehydrogenase converts NADPH to $NADP^+$ resulting in a decrease in absorbance. Although buffer and probe constituents are not stated in the manufacturers protocol, previous ammonia release assays removed fibrinogen by bentonite treatment and activated the FXIIIa with thrombin and calcium (Katona et al., 2012) .

Samples were prepared to a volume of 25 µl in a Corning™ NBS clear 96- well plate by adding 20% plasma (or 4.4 µg/ml native human FXIII protein (ab62427)) to a dilution range of rM1 protein (0-60 µg/ml). A FXIIIa positive control was included through the addition of 0.008 Loewy U/µl of FXIIIa enzyme solution. Additionally, a negative control was included by spiking the plasma (or purified FXIII protein) with 5mM of the FXIIIa inhibitor, iodoacetamide. A standard dilution range was prepared using ammonium chloride solution (0-50 nmol NH_4Cl) and run alongside the samples. Reactions were activated with the

addition of 100 µl activation mixture (constituting 25 µl FXIIIa activation buffer, 25 µl FXIIIa reaction buffer, 48 µl detection buffer and 2 µl FXIIIa probe per well). Measurements were immediately monitored at 340 nm for 2 hours with 20 second intervals.

3.2.4.3.1 FXIIIa activity data analysis

An ammonium sulphate standard curve was created by first obtaining the absorbance at 30 minutes for each concentration and corrected by subtracting the 0-standard control. The absolute value of ΔOD340 was plotted against the nmol of the NH_4Cl as per Figure 15A. The linear region of each plasma samples kinetic curve (as demonstrated in Figure 15B) was determined. The ΔOD340/ΔT(min) was then calculated for each plasma sample and FXIII inhibitor control. Each plasma sample was corrected by subtracting the ΔOD340/ΔT(min) of the FXIII inhibitor control. Finally, the FXIIIa activity was calculated using the following equation:

$$FXIIIa\ activity\ \frac{PEU}{(dL)} = \frac{B\ x\ 1000\ x\ 100}{A\ x\ C\ x\ X\ x\ 108}$$

Where, B is the corrected plasma FXIIIa activity as calculated above (ΔOD340/ΔT(min)), A is the slope of the standard curve (example is provided in Figure 15A. 1/slope), C is 1.2 (nmol/Loewy U, correction factor for the amount of ammonia under assay conditions), X is the volume of plasma (µl) included in the assay.

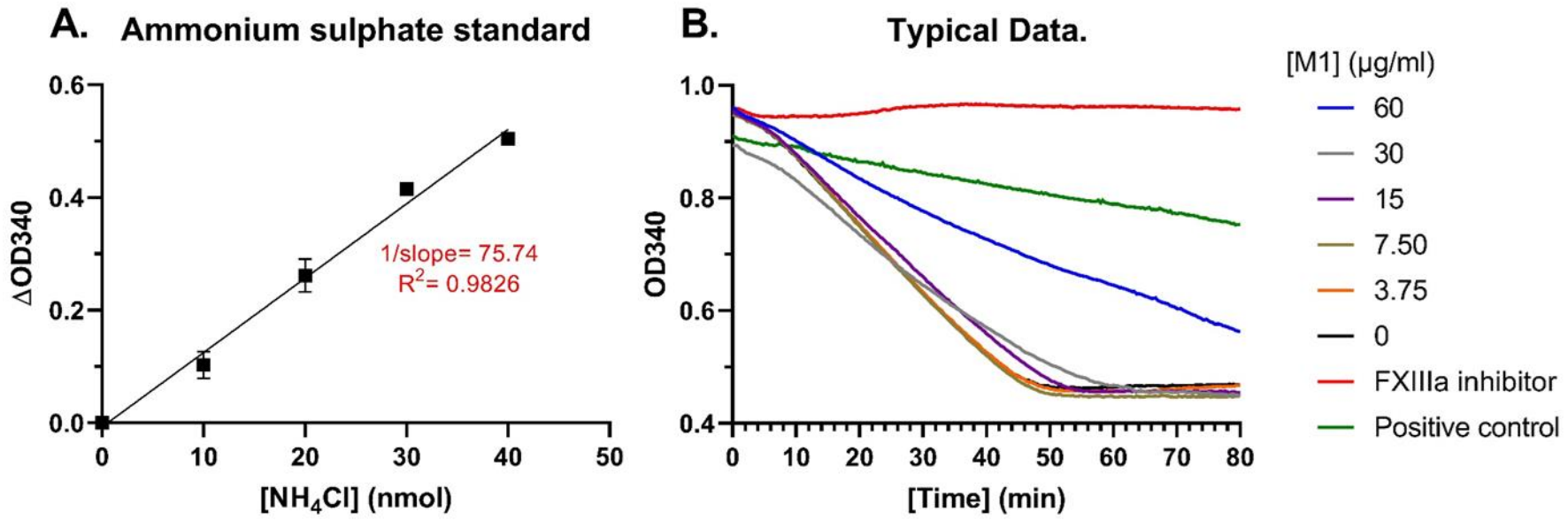

Figure 15 AbCam FXIIIa activity kit (ab241013) data analysis. A. Typical standard curve for ammonium sulphate concentrations. Absorbances for each NH4Cl concentration are obtained at t=30 minutes and corrected by subtracting the 0-standard control. Absolute values of ΔOD340 are plotted against ammonium sulphate concentration. **B.** Representative data demonstrating typical kinetic progressive curves for plasma with a dilution range of rM1. A negative (FXIIIa inhibitor, iodoacetamide) and positive control (purified human FXIIIa) were included for comparison.

3.2.5 Permeation experiments

Permeation assays were performed in order to determine the pore size of the fibrin network in the presence of rM1 protein, as per section 2.5.2. In brief, fibrin clots were formed in 0.5 ml Eppendorf's, to a final volume of 100 µl, by combining 3 mg/ml fibrinogen (plasminogen depleted, Calbiochem®) and rM1 (0- 60 µg/ml). Following a 5-minute incubation, the reaction was initiated through the addition of activation mixture (0.2 IU/ml thrombin (01/578) and 5 mM calcium chloride). Plasma fibrin clots were prepared in 0.5 ml Eppendorf's by preincubating 50 µl of plasma with 25 µl of rM1 (0 µg/ml – 60 µg/ml) followed by 25 µl of activation mixture as above Immediately, 25 µl of clotting mixture was transferred to an uncoated IBIDI µ-slide VI 0.4 (Thistle Scientific, Glasgow, Scotland) and incubated for 2 hours. A syringe was attached to the IBIDI slides, and the fibrin clots were washed with Buffer B for 30 minutes. The syringe was filled to the 4 cm mark and liquid was removed and weighed every 15 minutes for 1 hour.

Pore size was calculated from the following equation:

$$K_s = \frac{Q\ x\ n\ x\ L}{t\ x\ A\ x\ \Delta P}$$

Where, Q = volume of permeated buffer (cm^2); n= viscosity of buffer (10^{-2} poise = 10^{-7} N.s/cm^2); L= length of clot (1.7 cm); t= time (s); A= cross-sectional area of clot ($1.52x10^{-2}$ cm^2); ΔP= Pressure drop (0.0392 N/cm^2), as demonstrated in Figure 8.

3.2.6 Laser Scanning Confocal Microscopy

LSCM was used to investigate the architecture of the clots in fully hydrated conditions as per section 2.5.5. 3 mg/ml purified fibrinogen (plasminogen depleted, Calbiochem®), or human plasma, was spiked with 0.25 mg/ml Alexa

Fluor 594- fibrinogen conjugate. Fibrin clots were formed by combining the plasma or purified fibrinogen mixture (to a final concentration 20% plasma or 0.6 mg/ml fibrinogen and 0.05 mg/ml Alexa Fluor 594 conjugate) with rM1 (0- 60 µg/ml), 0.2 IU/ml thrombin (01/578) and 5 mM calcium chloride to a total volume of 100 µl.

Fibrin clot network was imaged by transferring 20 µl of the clotting mixture to three inner wells of an uncoated Ibidi® µ-Slide angiogenesis (Figure 10A). Clots were left to form in a dark humidity chamber at 37ºC for 2 hours. The network was then imaged using a X63 water immersion lens (Leica, HC PL APO CS2 63X/1.20) with the following parameters:

Parameter	Setting
Resolution	16-bit
Size	872 x 872 pixels
z-stack	20 µm
Slices	58
Pinhole	1.0 Airy
Zoom	X2
Line average	4

Fibrin clot film was imaged by half filling an uncoated Ibidi® µ-Slide VI$^{0.4}$ (Figure 10B) with 15 µl of the clotting mixture. Clots were then formed in a dark humidity chamber at 37ºC for 2 hours then imaged using a x63 water immersion lens (Leica, HC PL APO CS2 63X/1.20) with the following parameters:

Parameter	Setting
Resolution	16-bit
Size	1024 x 1024 pixels
z- stack	20 µm
Slices	58
Pinhole	1.0 Airy

Images were processed in ImageJ as per section 2.5.5.1 and section 2.5.5.2

3.2.7 Scanning Electron Microscopy

Fibrin clot architecture was investigated using SEM as per section 2.5.4. Fibrin clots were made to a final volume of 100 µl by combining 0.2 IU/ml thrombin (01/578), 5 mM calcium chloride and rM1 (0, 3.75, 15 and 60 µg/ml) with 50% human plasma. 75 µl of the clotting mixture was immediately transferred to a pierced 1.5 ml Eppendorf lid. Fibrin clots were placed into a humidity chamber at 37ºC for 2 hours then fixed overnight with 2% Glutaraldehyde. Samples were then washed for 2 minutes, 3 times, with 50 mM sodium cacodylate buffer (pH 7.4) then dehydrated using increasing serial concentrations of acetone (0-100%). Clots were transferred to fresh 100% acetone and incubated overnight. Clots were critically point dried then coated with a 10 nm layer of iridium using a SC7620 mini sputter coater (Quorum Technologies Ltd, West Sussex, UK). Samples were then imaged, in at least three areas, at a magnification of x1000, x5000, x10,000 and x20,000.

3.2.8 Bacterial Migration Assays

An individual Protect Select cryobead, containing *Streptococcus pyogenes* from section 2.6.1, was used to streak two blood agar plates then placed statically in an incubator at 37ºC/ 5% CO_2, overnight. An individual colony was picked from the plate, with a sterile inoculating loop, and used to inoculate 1000 µl of sterile THY media (with 20 µg/ml neomycin) in a Corning® Costar® Tissue Culture-treated 24-well plate. The plate was then placed back at 37ºC, 5% CO2, overnight. An individual colony from each plate was also gram stained as per section 2.6.2.

The following day, the cell count was calculated for each bacterium (~3.6 x 10^8 to 8.5 x 10^8 cells/ml) by measuring the OD600, and inputting to an online calculator (agilent). If multiple bacterial strains were being used, the cell count was normalised with sterile PBS for each strain. The bacteria (1000 µl) were dyed with 10 µl of 100 µM Molecular Probes™ BacLight™ Green Bacterial Stain and incubated for 15 minutes at room temperature. The bacteria were pelleted by centrifugation at 15,000 x G for 60 seconds, the supernatant was removed, and the bacteria was re-suspended in 1 ml of C- media (with 20 µg/ml neomycin) (Table 1). The cell count (OD600) and fluorescence (Ex 480 Em 516) of the bacteria was measured.

Fibrin clots in the presence of rM1 were formed in Falcon™ cell culture inserts (with 0.8-µm pores). The inserts were parafilmed to keep the clotting mixture in the well. Purified fibrinogen (3 mg/ml), incorporating increasing concentrations rM1 protein (0-60 µg/ml), was initiated with 0.2 IU/ml thrombin (01/578) and 5 mM calcium chloride. Immediately, 100 µl of the clotting mixture was transferred to the culture insert and placed in a humidity chamber at 37ºC for 2 hours then the parafilm was removed.

Sterile THY media (1000 µl, with 20 µg/ml neomycin) was transferred into Corning® Costar® TC-treated 24-well plate and the Falcon™ cell culture inserts containing the fibrin clots (incorporating 0-30 µg/ml M1) were placed inside. Labelled *Streptococcus pyogenes* (300 µl), in C- media, was carefully placed on the surface of each clot. A blank was included for each experiment, where C-media was used instead of labelled bacteria to check for cross-contamination. Immediately, a T0 reading was taken by removing 100 µl of media from underneath the insert and reading at an OD600 and Abs 480 EM 516. The 24-well plate was placed statically at 37ºC 5% CO_2 and readings were taken for up

to 49 hours. Each time media was replaced. A schematic of the experimental set up is demonstrated in Figure 16

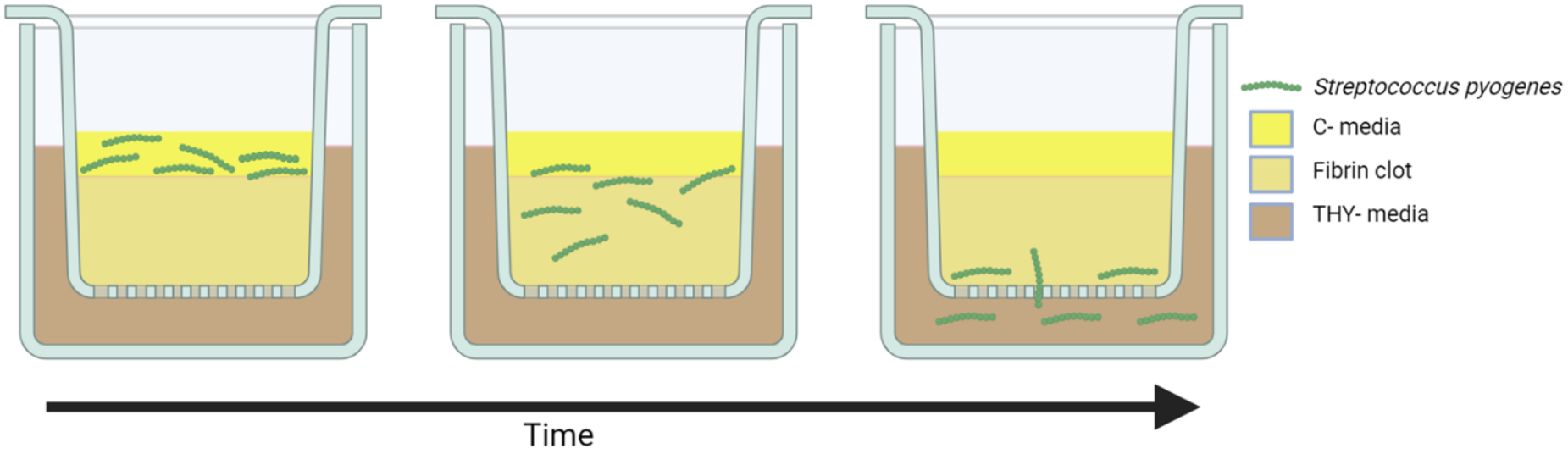

Figure 16 Schematic of experimental set-up of bacterial migration assays. Purified fibrin clots, incorporating rM1 (0-30 µg/ml) and initiated with thrombin, were formed in Falcon™ cell culture inserts (with 0.8-µm pores). Following a 2-hour incubation in a humidity chamber at 37ºC, Probes™ BacLight™ Green labelled Streptococcus pyogenes in a low carbohydrate C-media was added to the surface of each clot. The inserts were placed in 24-well plates with rich THY-media and labelled bacteria migration was monitored over 49 hours by measuring the fluorescence (Ex 480 Em 516) and absorbance (OD600) of the THY-media at time points.

3.3 Results

3.3.1 Protein expression and purification

As per section 4.3.2

3.3.2 M1 protein binds fibrinogen

To validate rM1 as functionally representative of the native GAS virulence factor, fibrinogen-binding by rM1 was investigated.

3.3.2.1 Pull down assay

A pull-down assay was developed to confirm the interaction between rM1 and fibrinogen. rM1 protein was incubated with an 11:1 molar excess of fibrinogen prior to the addition of Ni-NTA beads, to capture rM1 via its His-tag and any proteins associated with rM1. Controls were also set up with rM1 alone, fibrinogen alone and a blank with no added protein. The unbound and bound fractions were visualised by SDS PAGE as shown in Figure 17A. Fibrinogen alone was shown not to bind to the Ni-HTA resin (lane 7) and was predominantly found in the unbound fraction (lane 4) indicating that fibrinogen does not readily bind to the nickel resin. When rM1 was included, fibrinogen co-eluted with rM1 (lane 5) and was also present in the unbound fraction (lane 2) due to the molar excess of fibrinogen over the rM1 concentration. Co-elution of fibrinogen with rM1 indicates that the rM1 protein binds fibrinogen and is therefore functional.

3.3.2.2 Turbidity profile of rM1 and fibrinogen

It was observed during sample preparation for the pull-down assay, that mixing purified fibrinogen with high rM1 concentrations (without the presence of thrombin) resulted in a viscosity change in the sample. The gel -like substance that formed was similar in appearance to a fibrin clot. To investigate this further,

purified fibrinogen (3 mg/ml) and rM1 (0.94-62 µg/ml) were combined in a microtiter plate and absorbance change was monitored kinetically at 405 nm. An increase in turbidity of the sample was observed at rM1 concentrations greater than 15.5 µg/ml (Figure 17B) with 62 µg/ml reaching a maximum absorbance of ~0.08. Lower concentrations of rM1 appeared to result in a lag, before the absorbance of the sample increased, indicating a longer running time may have shown an increase in absorbance below 15 µg/ml rM1. Despite the increased turbidity, the maximum absorbance observed when rM1 binds fibrinogen was at least 10-fold lower than when fibrin is formed by the addition of thrombin under the same conditions (Figure 19C).

3.3.2.3 Visualisation of M1-bound fibrinogen

The nature of the rM1-fibrinogen complex was further investigated using laser scanning confocal microscopy (LSCM). Alexa Fluor 594 was added to human plasma to fluorescently label the fibrinogen, prior to the addition of increasing concentrations of rM1. As shown in Figure 17C, with the addition of rM1 dense clusters of fibrinogen are formed with increased fluorescence intensity. At the higher rM1 concentrations these clusters appear to aggregate forming networks with no apparent uniform order.

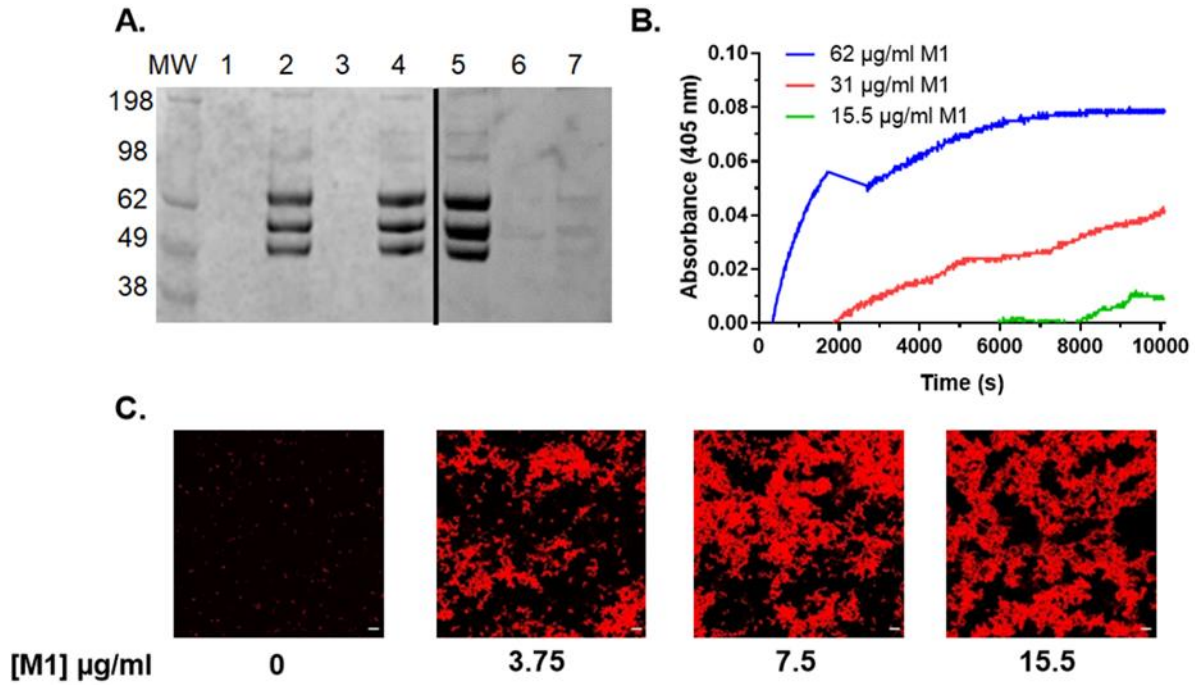

Figure 17 GAS M1 protein binds fibrinogen. A. SDS PAGE analysis of bound and unbound fractions from a pull- down assay to demonstrate fibrinogen (α-chain ~63.5 kDa, β-chain ~56 kDa, γ- chain ~47 kDa) binds to rM1 (54 kDa). Lanes 1- 4 show the unbound protein fractions (blank, rM1-bound fibrinogen, rM1, and fibrinogen respectively). Lanes 5-7 show proteins eluted from the Ni-NTA beads following boiling (rM1-bound fibrinogen, rM1, and fibrinogen, respectively). **B.** Turbidity increase (OD405) observed following addition of 3 mg/ml fibrinogen to dilution range of M1 (62-0.97 µg/ml) **C.** LSCM of plasma with the addition of increasing concentrations of rM1. Fibrinogen was fluorescently labelled with Alexa Fluor 594. Scale bar: 20 µm

3.3.3 Measuring the impact of M1 protein on fibrin clot formation

3.3.3.1 Turbidimetric assessment of fibrin clot formation and lysis

The impact of rM1 on fibrin clot formation and lysis was investigated using turbidimetric assays. Purified fibrinogen (3 mg/ml) was preincubated with varying concentrations of rM1 (1.88-60 µg/ml) in a microtitre plate. Fibrin clot formation was initiated by the addition of human thrombin; for fibrinolysis assays, streptokinase and plasminogen were also included. Clot formation (and lysis) were monitored kinetically by measuring absorbance changes at 405 nm. Representative clotting and fibrinolysis curves (Figure 18) show that increasing rM1 concentrations results in apparent reduced maximum clotting absorbances and reduced lysis times

The clotting experiments were repeated in both purified fibrinogen and human plasma. The clotting profiles were analysed using specialised software to calculate lag times (time taken for an initial absorbance increase of 0.01 absorbance units) and maximum absorbance. As shown in Figure 19A, a significant decrease in lag time was observed at an rM1 concentration of 0.94 µg/ml in purified conditions (70.5 ± 2.9%, relative to the control, 0 µg/ml M1). Lag times were further reduced with increasing rM1 concentrations up to a maximum of a 6- fold decrease at 15 µg/ml rM1 compared to the control (16.75± 2.39%, relative to the 100% 0 µg/ml control). However, when the lag time was measured in plasma (Figure 19B), no significant differences were observed at any concentration.

The maximum absorbance of purified fibrin clots decreased in a dose dependant manner as rM1 concentrations increased Figure 19C. A 1.5-fold decrease was observed at 60 µg/ml rM1 compared to the control (OD 0.81 ±

0.03 and OD 1.28 ± 0.02, respectively). The maximum absorbance also showed a dose-dependent decrease in plasma Figure 19D, to a maximum of 2.4-fold difference at 60 µg/ml rM1 compared to the control (OD 0.16 ± 0.013 and OD 0.38 ± 0.01, respectively)

3.3.3.2 Mechanical assessment of clot formation

Clot formation was investigated by measuring the physical resistance of purified and plasma clots using a KC4 delta coagulometer. Plasma or 3 mg/ml purified fibrinogen in the presence of rM1 (0.94-60 µg/ml) was activated with 0.5 IU/ml thrombin (01/578). Time to clotting was defined as the time (in seconds) to displace the steel ball from a magnetic sensor using thrombin time (TT) assays. A control was included for both plasma and purified conditions without the presence of rM1 protein. The data was presented as clot formation time (s), with the standard error of the mean. The validity of the data was assessed using an ordinary one-way ANOVA, with a Dunnett's post-hoc test (99% confidence interval) to compare each rM1 concentration with the 0 µg/ml control of plasma or purified conditions. Using purified fibrinogen (Figure 20) rM1 concentrations below 7.5 µg/ml produced consistent clot formation times of ~ 30.4 ± 0.3 seconds. Concentrations of rM1 at and above 7.5 µg/ml resulted in extended clot formation times: 34.03 ± 1.8 seconds at 7.5 µg/ml ($p=0.44$) increasing to 69.4 ± 0.77 seconds at 60 µg/ml ($p= <0.0001$, relative to the purified control, 30.4 ± 0.3) representing a 2.3-fold increase. A similar trend was observed when human plasma was used, with extended clotting times at 7.5 µg/ml rM1 (33.9 ± 0.61 seconds vs 30.03 ± 0.5 seconds, $p=0.08$) increasing to a maximum of ~2-fold at 60 µg/ml (58.28 ± 1.34 seconds, $p= <0.0001$ relative to the plasma control, 30.03 ± 0.5 seconds). Above 7.5 µg/ml, the plasma condition displayed a faster clotting time in comparison to the purified condition (at 15 µg/ml: 35.25

± 1.15 seconds verses 57.65 ± 3.30 seconds, respectively; at 30 µg/ml: 48.50 ± 2.16 seconds verses 61.70 ± 1.43 seconds, respectively; at 60 µg/ml: 58.28 ±1.34 seconds verses 69.40 ± 0.77 seconds, respectively).

Viscoelastic properties of the fibrin clots were measured using rotational thromboelastography (ROTEM), a clinical point of care instrument used to measure the clotting and lysis potential of a patient's blood. More parameters can be derived from this technique, compared to the KC4 delta analysis, because a pin constantly rotates to measure physical resistance as the clot forms. These parameters are shown in the TEMogram (Figure 21A).

The α-angle represents the speed of fibrin formation and cross-linking. A purified condition was first used to measure the effect of rM1 on fibrin formation. Fibrin clots were formed with purified fibrinogen (3 mg/ml) in the presence of rM1 protein (1.88-30 µg/ml) and activated with 0.5 IU/ml thrombin (01/578). In purified conditions, (Figure 21B), the α-angle decreased with increasing concentrations of rM1 and was significant at 15 µg/ml rM1 (23.25 ± 2.75 º verses 36.875 ± 1.445 º, p= 0.0025) and above when assessed by one-way ANOVA followed by a Dunnett's test. The largest decrease in α-angle was at 30 µg/ml, with a ~2-fold decrease in comparison to the control (19.25 ± 3.065 and 36.875 ± 1.445, respectively, p= 0.0001).

The intrinsic clotting cascade was investigated with whole blood, in the presence of rM1 (3.6-30 µg/ml), stimulated with ellagic acid using an INTEM-s assay. As shown Figure 21C, a significant decrease in α-angle was observed at 13.3 µg/ml, compared to the control (57.7 ± 3.5 º verses 75.4 ± 0.56 º, p=0.0003), with the largest decrease at 30 µg/ml rM1 (31.8 ± 6.3 verses 75.4 ± 0.56 º, p=0.0001).

The extrinsic clotting cascade was investigated with whole blood, in the presence of rM1 (3.6-30 µg/ml), stimulated with tissue factor using an EXTEM-s assay. Under normal clotting conditions with whole blood (Figure 21D), there was significant differences in fibrin polymerisation kinetics. A decrease in α-angle above 7.2 µg/ml rM1, compared to the control (60.8 ± 1.7 º vs 68.8 ± 1.03 º, p= 0.0046) was observed, with the largest decrease at 30 µg/ml rM1 (25.8 ± 2.2 º vs 68.8 ± 1.03 º, p= < 0.0001). The α-angle could not be derived from whole blood clots formed in the presence of 60 µg/ml rM1 due to the TEMogram reading not reaching an amplitude of 20 mm. The ROTEM delta software does not calculate further data such as the CFT and α-angle.

3.3.3.3 Mechanical assessment of clot stability

The physical resistance of purified fibrinogen, plasma, and whole blood clots in the presence of increasing concentrations of rM1 protein (1.88- 60 µg/ml) was investigated using ROTEM. A control was included consisting of purified fibrinogen, plasma, or whole blood without the presence of rM1 protein (0 µg/ml) and used as a comparison for the rM1 protein increasing concentrations. The maximum clot firmness (MCF), calculated from the maximum amplitude of the TEMogram (Figure 22A), measures the overall stability of the clot. The data was presented as MCF (mm) with standard error of mean. The statistical significance of the data was tested using a One-Way ANOVA with a Dunnett post-hoc test. A purified system (Figure 22B) was first used to investigate the effect of rM1 protein on fibrin clots. Fibrin clots were formed with 3 mg/ml fibrinogen, in the presence of rM1 (1.88-60 µg/ml) and activated with the addition of 0.5 IU/ml thrombin (01/578). As shown in Figure 22A, a dose-dependent reduction in clot strength in comparison to the 0 µg/ml rM1 control was observed with increasing concentrations of rM1, and almost undetectable

levels at 60 µg/ml rM1 (31.42 ± 0.57 mm and 2.25 ± 1.32 mm respectively, p= <0.0001). The extrinsic clotting cascade was investigated with whole blood, in the presence of rM1 (3.6-30 µg/ml), stimulated with tissue factor using an EXTEM-s assay. As shown in Figure 22D there was a decrease in the MCF with increasing levels of rM1. At 13.3 µg/ml rM1 there is a 1.4-fold decrease in MCF of whole blood clots in comparison to the 0 µg/ml rM1 control (41.67 ± 2.29 mm vs 56.88 ± 0.78 mm, respectively, p= <0.0001), with the largest decrease (3.1-fold) observed at 30 µg/ml rM1 (18.43 ± 2.01 mm vs 56.88 ± 0.78 mm, respectively, p= <0.0001).

Whole blood and plasma clots in which platelets were inhibited with cytochalasin-D (isolating the contribution of fibrinogen) were further investigated using the fibrin-based FIBTEM assay (Figure 22B). A significant decrease of MCF was observed from 3.6 µg/ml rM1 in both plasma (1.3-fold) and whole blood conditions (1.4-fold) in comparison to the control (14.33 ± 0.33 mm vs 18.14 ± 0.74 mm (p= 0.0007), and 7.20 ± 0.42 mm vs 10 ± 0.414 mm (p= <0.0001), respectively). The largest decrease was observed at 30 µg/ml rM1, with almost undetectable levels in both the whole blood condition, 1.43 ± 0.37 mm (p= <0.0001), and plasma, 6.0 ± 0.41 mm (p= 0.0001).

The intrinsic clotting cascade was investigated with whole blood, in the presence of rM1 (3.6-30 µg/ml), stimulated with ellagic acid using an INTEM-s assay. As shown in Figure 22C, there is a dose dependent decrease in MCF with increasing M1 concentrations, producing a similar profile to the EXTEM based assay (Figure 22D). At 13.3 µg/ml rM1 protein there is a 1.5-fold decrease in MCF of whole blood clots in comparison to the 0 µg/ml rM1 control (37.56 ± 2.24 mm vs 57.28 ± 0.94 mm, respectively, p= <0.0001). The largest increase was observed at 30 µg/ml rM1 with a 2.91-fold decrease in MCF in

comparison to the control (19.67 ± 3.27 mm vs 57.28 ± 0.94 mm, respectively, p= <0.0001).

In summary, as shown in Figure 22 addition of soluble rM1 protein to purified fibrinogen, plasma and whole blood results in fibrin clots that are significantly weaker.

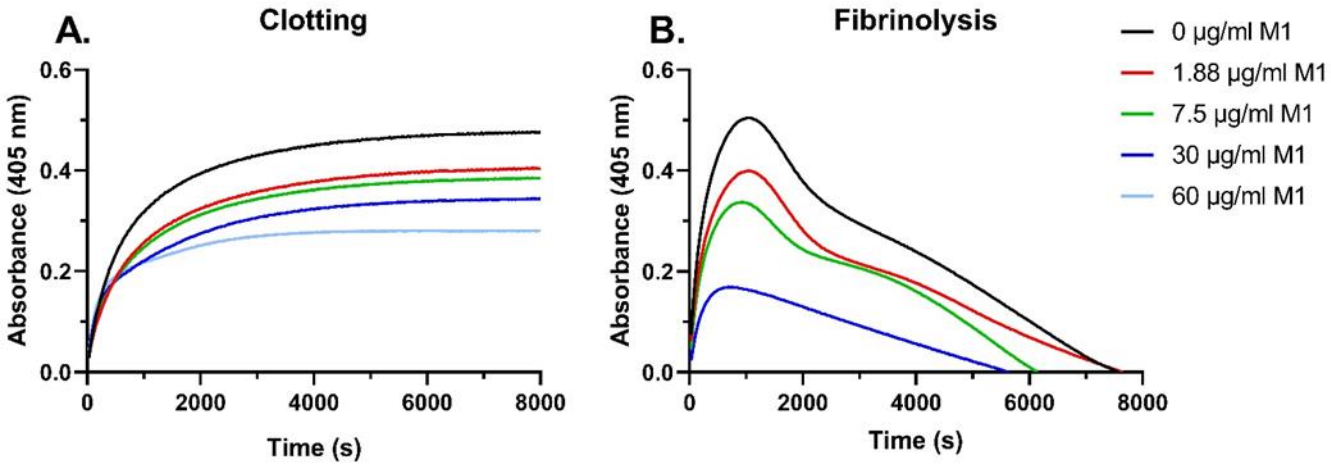

Figure 18 Representative clotting and lysis profiles in the presence of rM1 Typical clotting **(A.)** and fibrinolysis **(B.)** curves are shown for the WHO 3rd International Standard Streptokinase (00/464) in varying concentrations of M1 protein (0- 60 µg/ml)

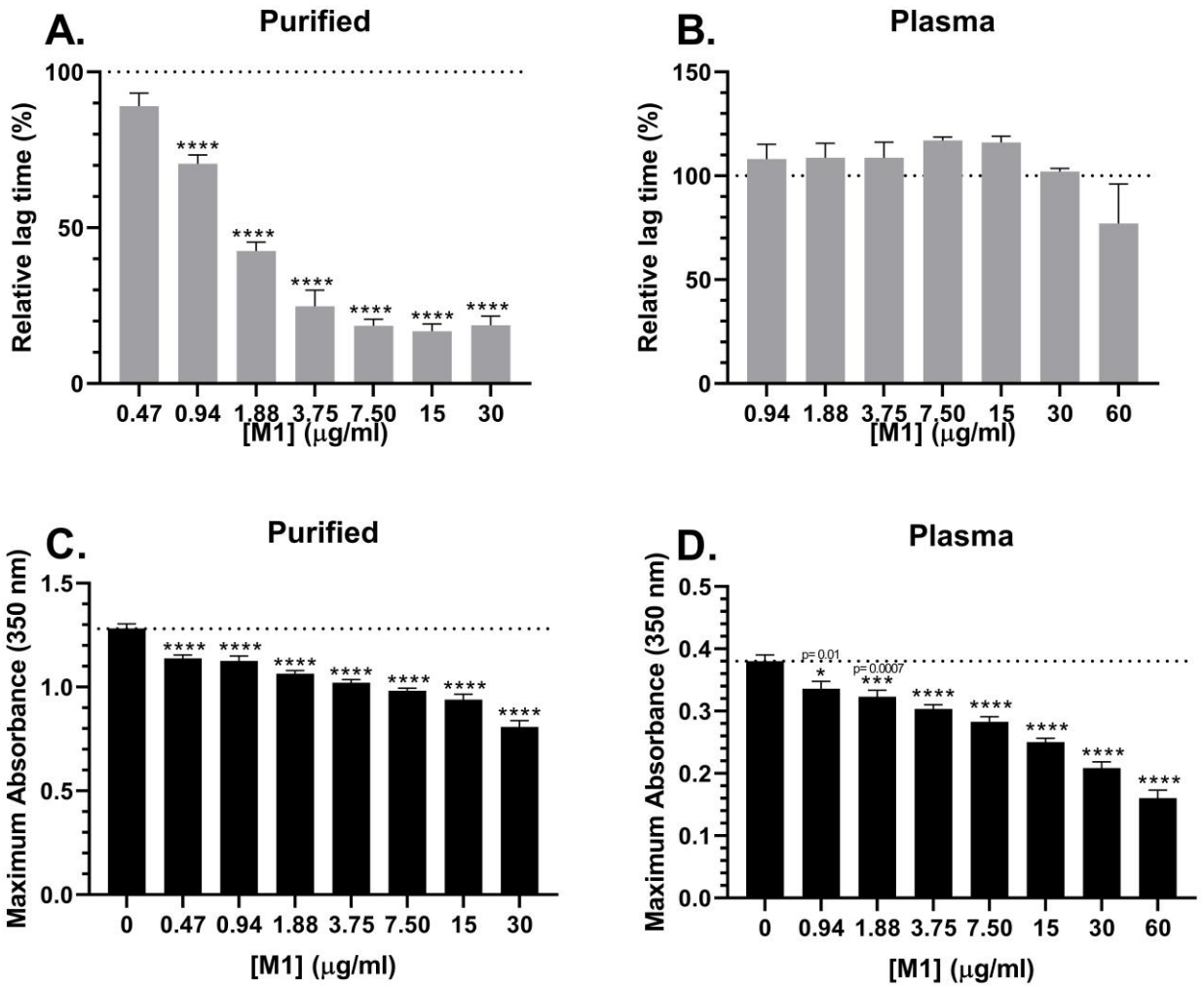

Figure 19 Parameters calculated from clotting turbidity curves. Parameters calculated from the fibrinolysis profiles **(Figure 18)** in purified **(A. & C.)** and plasma conditions **(B. & D.).** Lag times were manually calculated and defined as the time (s) for the absorbance to reach 0.01. The data is displayed in **A. & B.**, relative to the control 0 µg/ml as depicted by the dotted line at 100%. Maximum absorbance was determined from the curves and the raw data was plotted as per **C. & D.** Error bars represent SEM. (* $p < 0.05$, ** $p < 0.01$, *** $p < 0.001$, **** $p < 0.0001$, One-way ANOVA with Dunnett post-hoc test) n=4

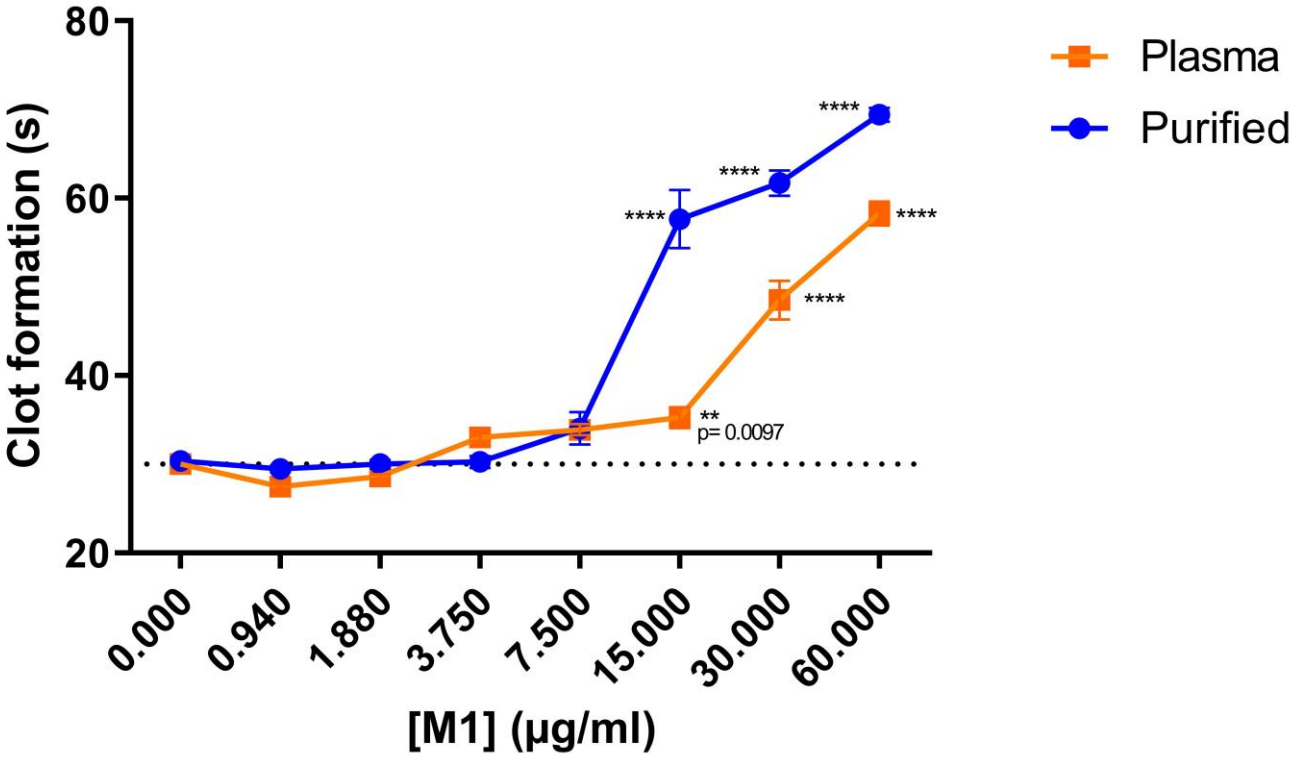

Figure 20 KC4 clotting time analysis in the presence of increasing rM1 concentrations Clotting times of purified fibrinogen and plasma were determined using thrombin time (TT) assay with a micro-mechanical clot detection KC4 coagulometer in varying concentrations of M1 (0-60 µg/ml). Dotted line indicates clot formation time at 0 µg/ml rM1. Error bars represent SEM. (* $p < 0.05$, ** $p < 0.01$, *** $p < 0.001$, **** $p < 0.0001$, One-way ANOVA with Dunnett post-hoc test, relative to purified or plasma 0 µg/ml condition) n=4

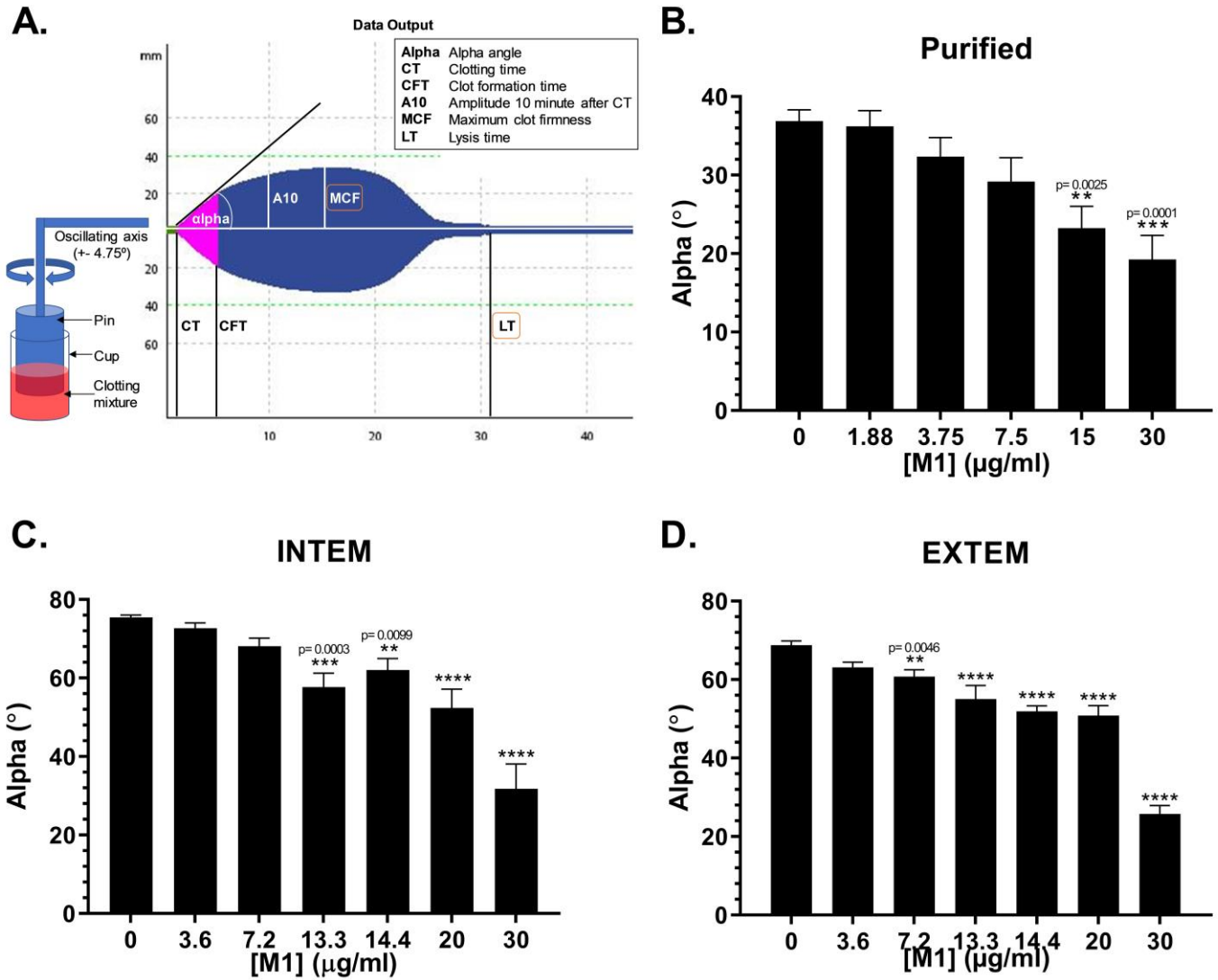

Figure 21 Viscoelastic analysis of fibrin clots in the presence of rM1 protein (1.88-30 µg/ml) A. Basic diagram of experimental set up, with a typical ROTEM® temogram. Mechanical resistance of the clots was measured with addition of thrombin, **(B.)**, an intrinsically activated INTEM assay **(C.)** or an extrinsically activated EXTEM assay **(D.)** performed using ROTEM. Alpha angle (α-angle) is shown. Error bars represent SEM. (* $p < 0.05$, ** $p < 0.01$, *** $p < 0.001$, **** $p < 0.0001$, One-way ANOVA with Dunnett post-hoc.) N= 9 for whole blood conditions or N= 6 for purified conditions.

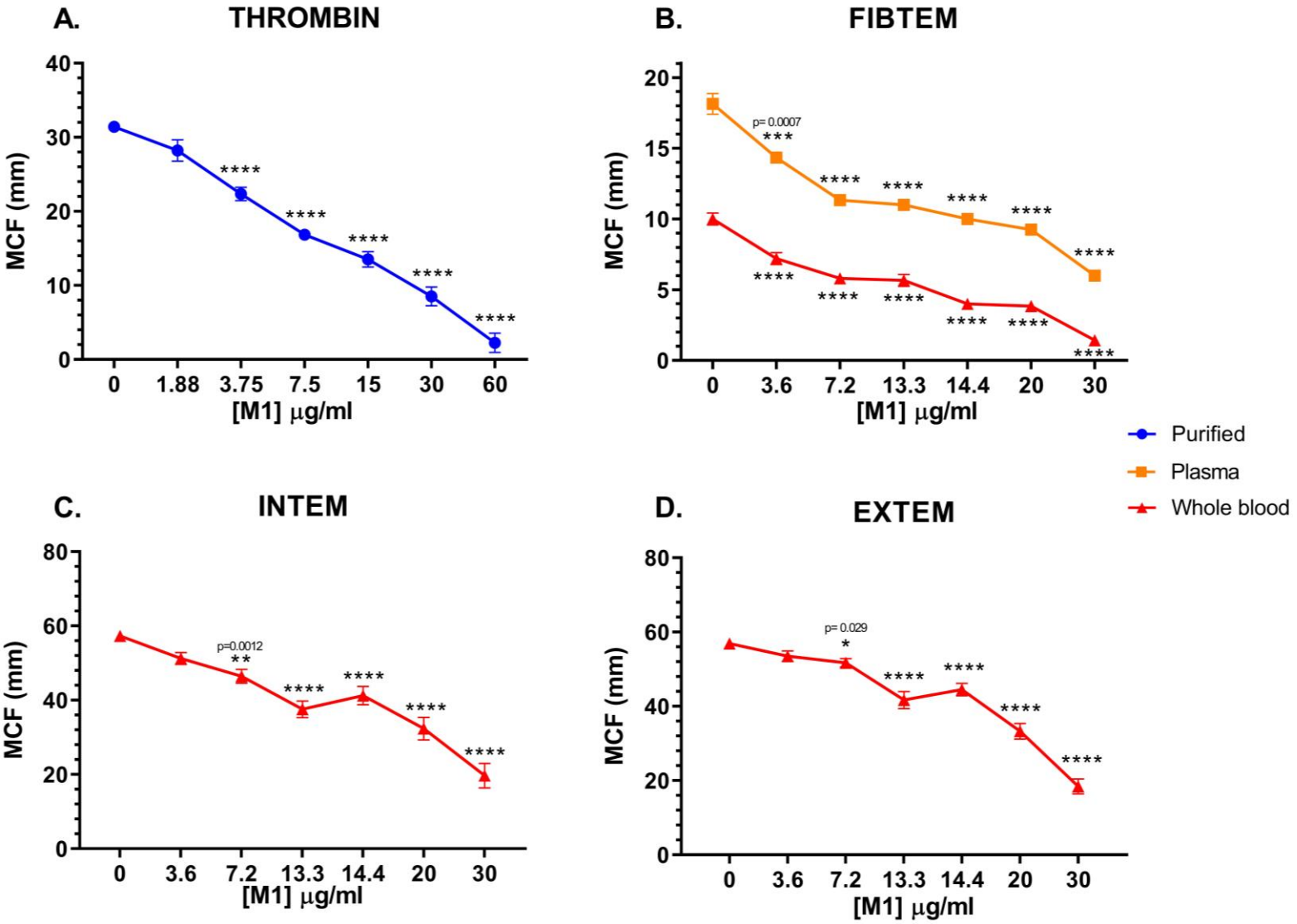

Figure 22 Maximum Clot Firmness of purified, plasma and whole blood clots in the presence of increasing concentrations of rM1 (1.88- 30 µg/ml) Physical strength of the clots were measured with addition of thrombin, **(A.)**, a fibrin based FIBTEM assay **(B.)**, an intrinsically activated INTEM assay **(C.)** or an extrinsically activated EXTEM assay **(D.)** performed using ROTEM ®. Maximum clot formation (mm) after 1 hour is shown. Error bars represent SEM. (* $p < 0.05$, ** $p < 0.01$, *** $p < 0.001$, **** $p < 0.0001$, One-way ANOVA with Dunnett post-hoc test, relative to each condition 0 µg/ml.) n=≥3

3.3.4 Assessing the impact of M1 protein on fibrin clot structure

3.3.4.1 Fibrin clot porosity

Clot permeation assays were used to determine the porosity of purified and plasma clots with increasing concentrations of rM1 (3.75-60 µg/ml). Purified and plasma fibrin clots were formed in uncoated IBIDI µ-slides through the addition of 3 mg/ml purified fibrinogen or frozen pooled plasma, respectively, incorporating rM1 (3.75-60 µg/ml). Clots were initiated with 0.2 IU/ml thrombin (01/578) and left to polymerise for 2 hours. Following washes, liquid was permeated through the clots under a constant hydrostatic pressure for 1 hour, and liquid was removed and weighed every 15 minutes. Permeation coefficients (Ks) were calculated from the assays, which is a direct measure of the average pore size of the fibrin network. A control was included in all experiments without the presence of rM1 protein (0 µg/ml) and used for comparison purposes. At lower concentrations of purified (Figure 23A) and plasma fibrin clots (Figure 23C) there are no significant differences in comparison to the control. However, at 3.75 µg/ml, purified fibrin clots showed a non-significant 1.4-fold decrease in permeability in comparison to the control (2.6 ± 0.365 Ks (x 10 -9 cm^2) verses 3.65 Ks ± 0.361 (x 10 -9 cm^2), respectively). Similarly, plasma fibrin clots with the addition of 3.65 µg/ml rM1 showed a non-significant ~1.3-fold decrease in permeability in comparison to the control (6.68 ± 1.47 Ks (x 10 -9 cm^2) verses 8.54 ± 0.893 Ks (x 10 -9 cm^2)). Above 23 µg/ml rM1 a gradual increase in porosity was observed in both purified and plasma conditions. At 34 µg/ml rM1 a 2.6- fold increase in clot porosity was seen in purified conditions (9.64 ± 1.38 Ks (x 10 -9 cm^2) verses 3.65 ± 0.36 Ks (x 10 -9 cm^2), respectively, p=0.0426), up to a maximum of ~12- fold increase at 60 µg/ml rM1 (42.53 ± 3.97 Ks (x 10 -9 cm^2) verses 3.65 ± 0.36 Ks (x 10 -9 cm^2), respectively. p= <0.0001.)

A similar trend was observed in plasma conditions, demonstrating a non-significant 2.7-fold increase in porosity at 34 µg/ml rM1 (23.31 ± 2.4 Ks (x 10 -9 cm^2) verses 8.54 ± 0.89 Ks (x 10 -9 cm^2), respectively. p= 0.96.). The increase in plasma clot porosity was up to a maximum of ~15-fold increase at 51 µg/ml rM1 in comparison to the control (131.04 ± 27.51 Ks (x 10 -9 cm^2) verses 8.54 ± 0.89 Ks (x 10 -9 cm^2), respectively. p= <0.0001.)

Addition of higher concentrations of rM1 led to an increase in inter-experimental variability between repeats suggesting that homogeneous clots are not formed.

3.3.4.2 FXIIIa cross-linking

The change in clot porosity suggests a modification of the fibrin structure. The effect of rM1 protein on fibrin cross-linking by FXIIIa was investigated as a potential explanation for this. Fibrin clots, in the absence and presence of varying concentrations of rM1, were reduced then subjected to SDS-PAGE analysis (Figure 24). The impact of rM1 protein on fibrin clot cross-linking by FXIIIa was then investigated by densitometry analysis of the alpha polymer chains (Figure 25A). A FXIIIa inhibitor, known as T101, was also included as a control for the absence of fibrin crosslinking. The data was presented as relative band density, with the standard error of the mean, and validity of the data was assessed using an ordinary one-way ANOVA, with a Dunnett's post-hoc test (99% confidence interval) to compare each M1 concentration with 0 µg/ml condition. A dose-dependent decrease in alpha-polymer density was observed at rM1 concentrations above 1.88 µg/ml up to 60 µg/ml where cross-linking was almost completely inhibited (0.049 ± 0.029 relative band density, p= 0.0027). At lower concentrations of rM1 protein (0.48- 1.88 µg/ml) an initial increase in band density was observed. The initial increase was up to a maximum of 1.8-fold ±

0.422 (p= 0.0099) at 0.48 µg/ml rM1, indicating an increase in cross-linking by FXIIIa.

A D-dimer ELISA plate assay was also used to further investigate fibrin clot cross-linking by FXIIIa. The ELISA plate assay quantifies D-dimer concentration, a degradation product of cross-linked fibrin, in fibrin clots lysed through the addition of plasminogen activators and plasminogen. As shown in Figure 24B, a similar trend as the densitometry analysis was observed. Above 15 µg/ml rM1 an overall dose dependant decrease in D-dimer concentration was observed, up to a 3.6-fold decrease at 60 µg/ml rM1 (0.794 ± 0.137 mg/ml verses 2.86 ± 0.218 mg/ml, P= <0.0001.). Additionally, consistent to the densitometry analysis data an initial increase in D-dimer concentration was observed. Between 1.88 µg/ml and 3.75 µg/ml rM1, there was a significant increase in D-dimer concentration up to ~1.4-fold increase at 1.88 µg/ml rM1 (3.93 ± 0.295 mg/ml and 2.86 ± 0.218 mg/ml, respectively. P= 0.0019).

The FXIIIa experiments above gave an indication of the impact of rM1 protein on cross-linking of fibrin clots by FXIIIa. However, the experiments do not provide information on whether the effect is due to direct inhibition of FXIIIa or due to structural changes. The impact of rM1 protein on FXIIIa activity was therefore investigated using a Factor FXIIIa activity kit method. The kit measures FXIIIa activity by quantifying the release of ammonia, a biproduct of the cross-linked amine-containing substrate to a glutamine-containing substrate. A positive control was included in all experiments consisting of 0.008 Loewy U/µl of FXIIIa enzyme solution. As shown in Figure 26, there are no significant differences in FXIIIa activity with increasing concentrations of rM1 protein in plasma. The highest concentrations of rM1 have previously shown the most dramatic differences in cross-linking by FXIIIa in comparison to the control,

however this does not appear to be a direct inhibition of enzyme activity (4.42 ± 0.76 and 4.58 ± 0.79, respectively).

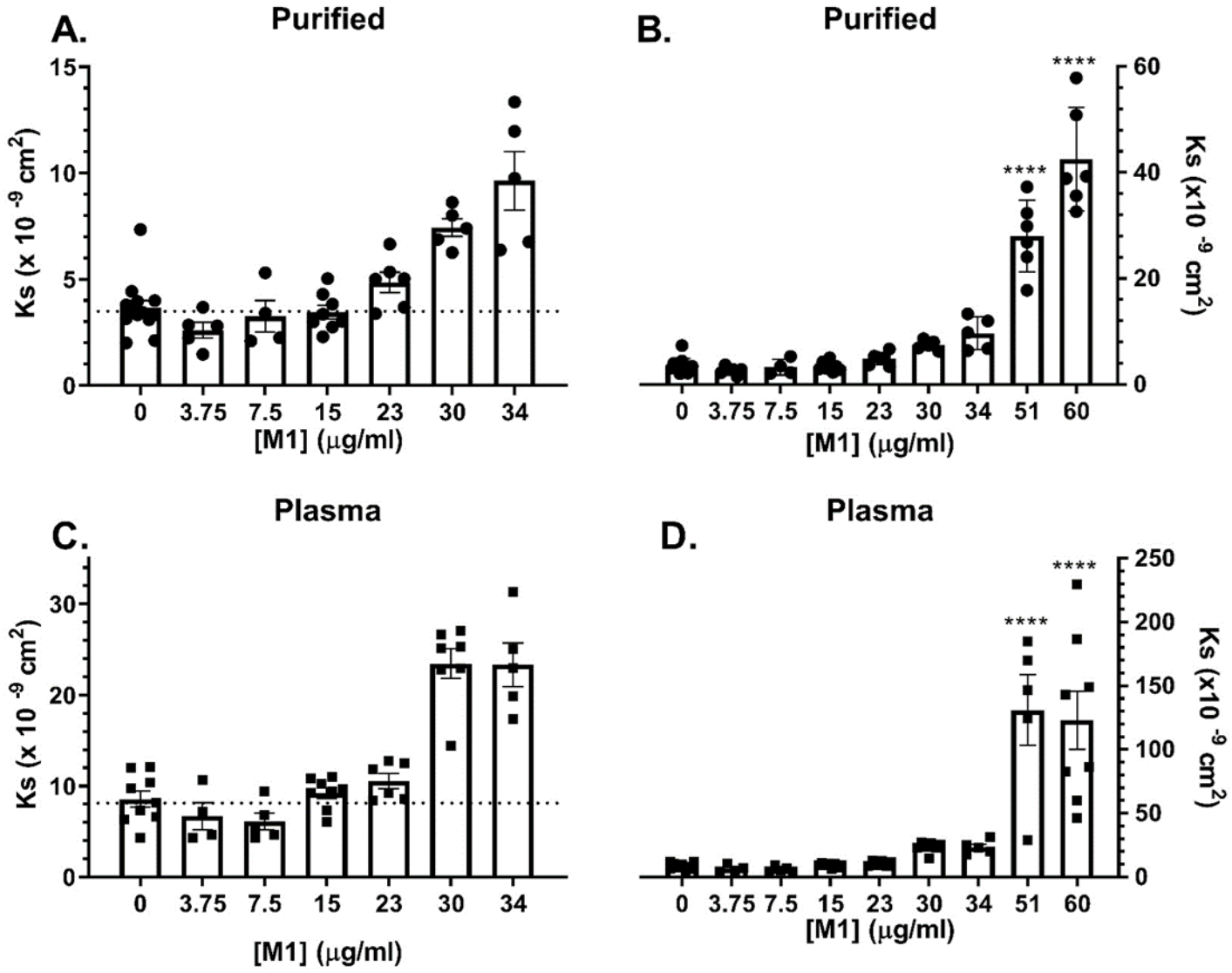

Figure 23 Fibrin clot permeability experiments in the presence of rM1 Porosity (Darcy's constant, Ks (x10-9cm2)) of purified **(A. & B.)** and plasma **(C. & D.)** fibrin clots, formed with thrombin, in the presence of varying concentrations of rM1 (3.75-60 µg/ml). Please note, graphs (A & B) and (B & D) are the same graphs with increased concentrations for better visualisation. Error bars represent SEM. (**** $p < 0.0001$, One-way ANOVA with Dunnett post-hoc test.) N= >3

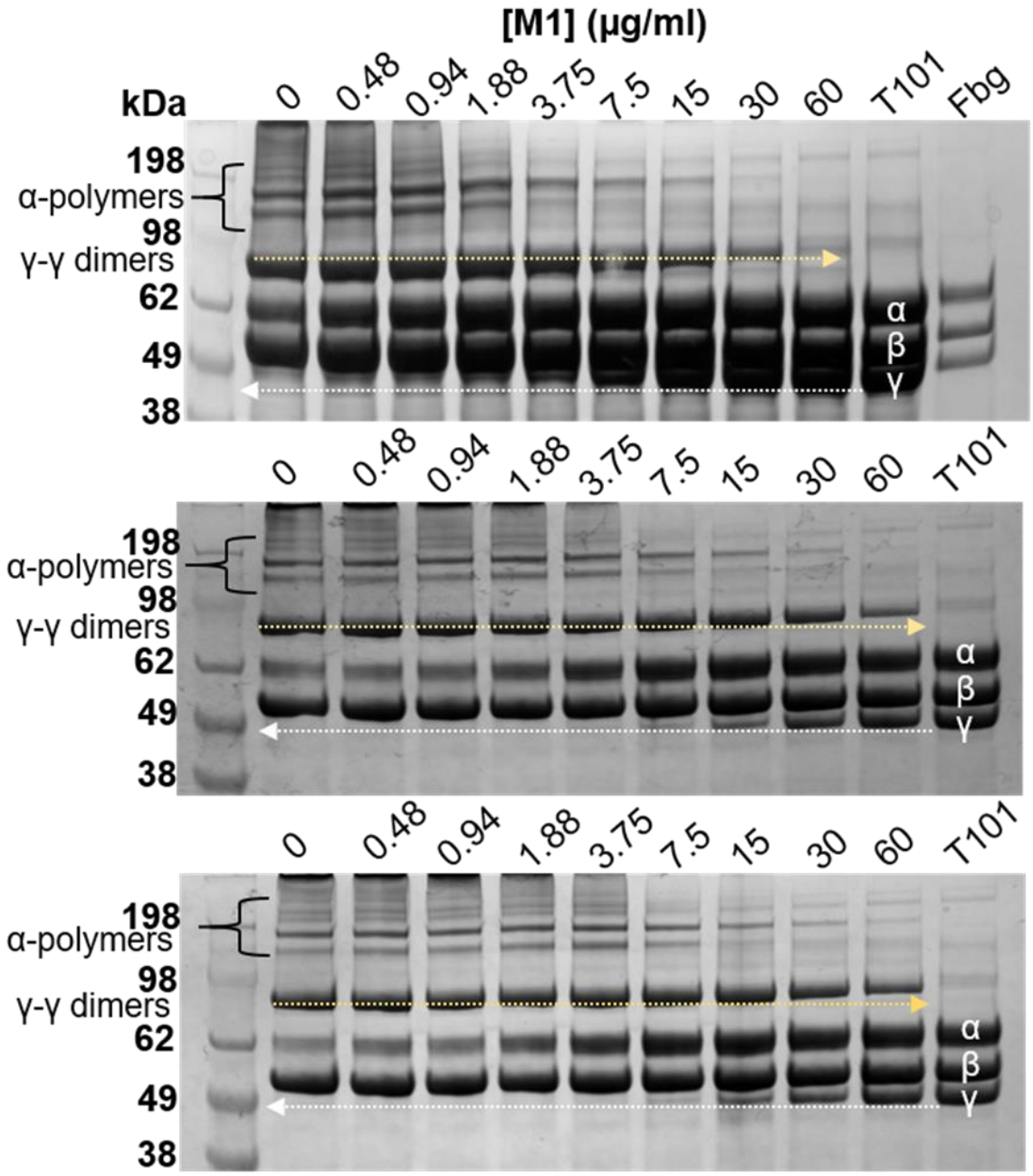

Figure 24 SDS PAGE analysis of fibrin crosslinking by FXIIIa in presence of rM1 Fibrin cross-linking by FXIIIa was investigated using 4-12% Bis-Tris SDS-PAGE analysis for reactions containing 3 mg/ml purified fibrinogen (containing small amounts of contaminating FXIII) preincubated with 5 mM calcium and varying concentrations of M1 (0-60 µg/ml). Reactions were initiated with 0.2 IU/ml thrombin. A FXIIIa inhibitor, T101, was included for comparison. Yellow dotted lines indicate γ-γ dimers, whilst the white dotted line indicates fibrin γ chain. N=3

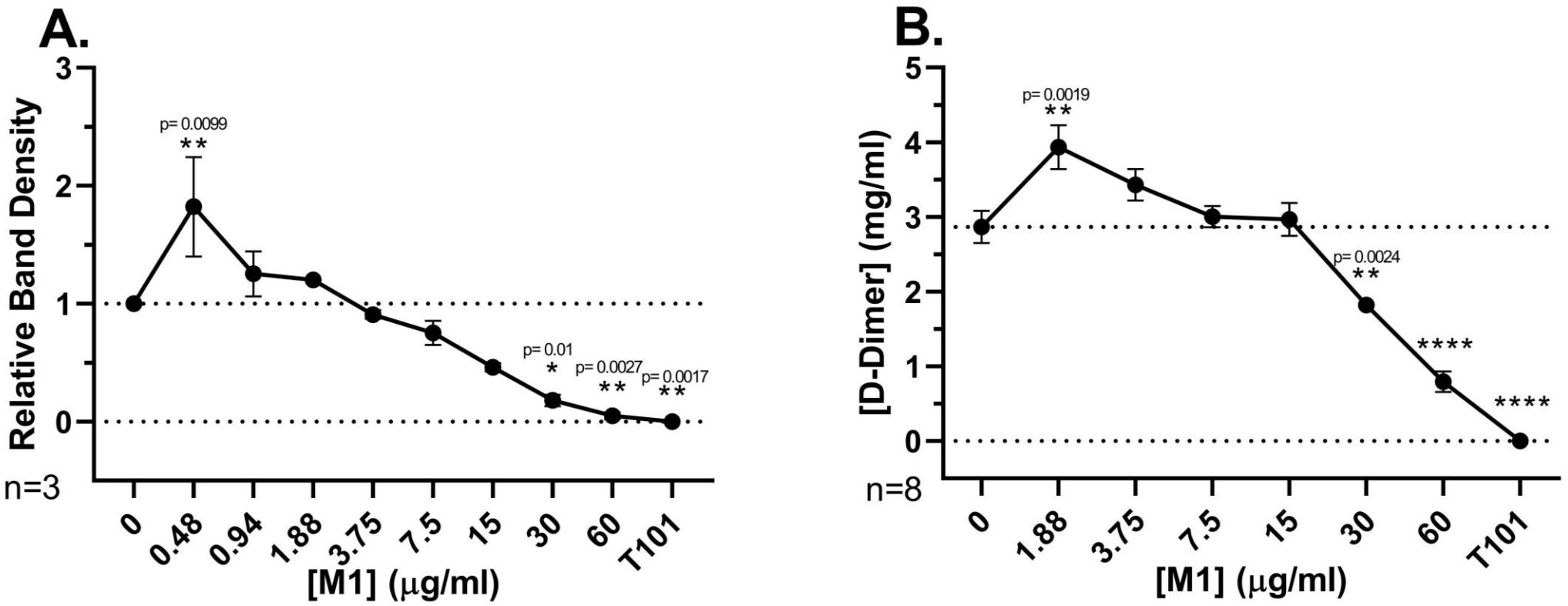

Figure 25 Fibrin clot cross-linking by FXIIIa. **A.** The α- polymer chains from the SDS-PAGE **(**Figure 24**)** were chosen as an indicator of cross-linking and analysed using densitometry. Band density, relative to 0 µg/ml M1, was plotted against rM1 concentration. Dotted line at 1. represents full cross-linking relative to no M1, whilst the dotted line at .0 represents no formation of alpha polymers **B.** Fibrin clots were formed with varying concentration of rM1 then lysed overnight with plasmin activated by plasminogen activators. D-Dimer concentration was then quantified by an ELISA plate assay and plotted as mg/ml of D-Dimer. Error bars represent SEM. (* $p < 0.05$, ** $p < 0.01$, *** $p < 0.001$, **** $p < 0.0001$, One-way ANOVA with Dunnett post-hoc test.) n=≥3

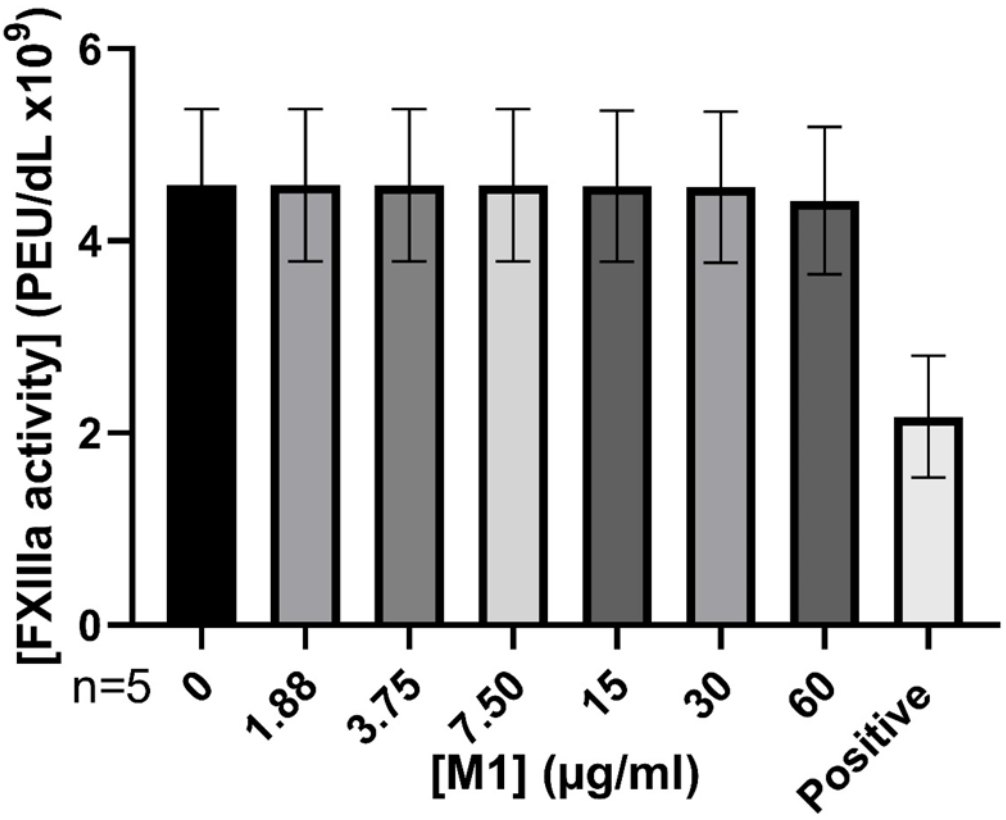

Figure 26 FXIIIa activity in the presence of rM1 (1.88-60 µg/ml) Plasma FXIIIa activity in the presence of rM1 (1.88-60 µg/ml) was calculated using an AbCam Factor FXIIIa activity kit method. Error bars represent SEM. (No significant differences were found between the M1 concentrations using One-way ANOVA with Dunnett post-hoc test.) N=5

3.3.4.3 Investigating the impact of rM1 on fibrin clot architecture

3.3.4.3.1 Scanning Electron Microscopy

Fibrin clot architecture was investigated in human plasma using scanning electron microscopy. As shown in the representative images (Figure 27), rM1 protein modifies the fibrin structure. At lower concentrations of rM1 (1.88 µg/ml), the fibrin fibres appear more densely packed with an apparent decrease in the size of the pores, which is consistent with the porosity data (section 3.3.4.1). The white arrows demonstrate the formation of irregular fibre bundles and compacted fibrin that are not present in the control condition (0 µg/ml rM1). At the highest concentration of rM1 protein the overall clot network structure is lost. However, it is important to note that even at the highest concentrations of rM1 protein fibrin fibres are still being formed despite the lack of structure. Due to preparation artefacts causing plasma proteins or the fibrin film to adhere to the fibrin, the fibrin fibre diameters could not be measured. Although SEM generates a high-resolution image of the clot network, a limitation of this technique is that the samples need to be dehydrated during the sample preparation leading to the unwanted preparation artefacts. Additional experiments were therefore needed to confirm the observations in a hydrated system.

3.3.4.3.2 Laser Scanning Confocal Microscopy

The native, fully hydrated structure of plasma fibrin clots was investigated using laser scanning confocal microscopy (LSCM) with a fluorescently labelled fibrinogen conjugate, Alexa fluor 594. A 20 µm slice was taken for each fibrin network condition, and the resultant 58 stacks were compacted into a 2D image. As shown in Figure 28, addition of rM1 protein results in the formation of heterogeneous clots with irregular fibre bundles and compacted fibrin. At lower

concentrations of rM1 (0.59- 9.4 µg/ml) individual fibres were visible allowing for further analysis of fibrin density. The fibrin fibre count per 90 µm (Figure 29) demonstrated significant differences in fibrin density with the addition of rM1 in comparison to the control. At lower concentrations of rM1, a denser clot was formed with a 2.2- fold increase in fibrin fibre count at 2.35 µg/ml rM1 (52.25 ± 1.29 fibres verses 23.88 ± 0.91 fibres, $p < 0.0001$). Above 2.35 µg/ml rM1 there is a gradual decrease in density although still significantly higher (1.6- fold) than the control condition at 9.4 µg/ml (38.58 ± 1.04 fibres verses 23.88 fibres, $p < 0.0001$). At rM1 concentrations above 9.4 µg/ml data cannot be obtained because of fibrin clustering and the limited resolution of confocal microscopy. However, consistent with the SEM images, visually there is a decrease in clot density with increased fibrin clusters and larger pores. The intensity of the fibrin fibre clusters increases with higher rM1 protein concentrations suggesting an increase in clustering of the fibres. Consistent with the SEM data, higher concentrations of rM1 protein leads to the eventual loss of the overall clot structure.

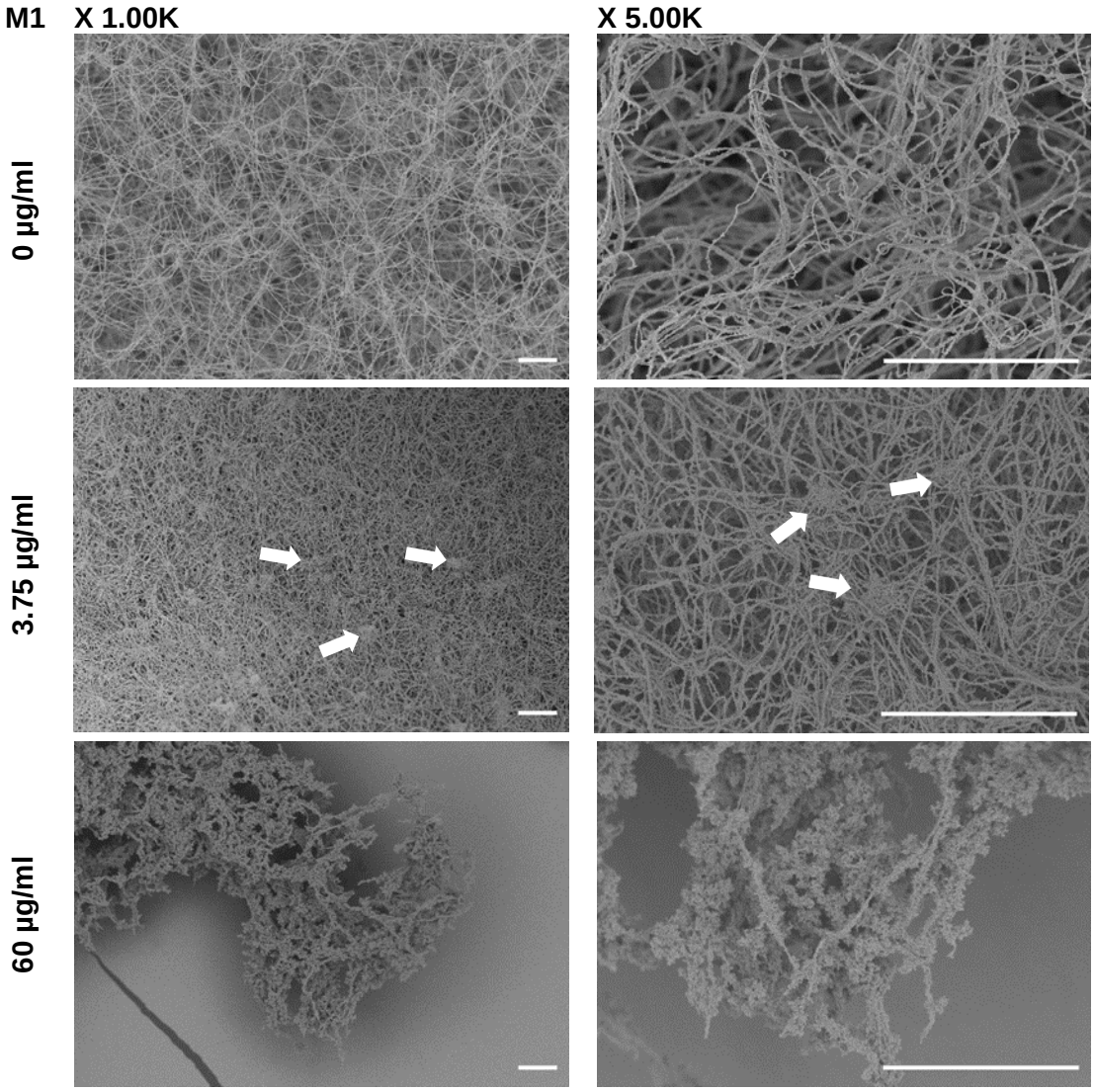

Figure 27 Scanning Electron Microscopy of plasma fibrin clot architecture in the presence of rM1 (0-60 µg/ml). Fibrin clots, incorporating rM1 (0, 3.75 or 60 µg/ml) were formed in perforated Eppendorf lids then fixed, dehydrated, critically point dried and coated with 10 nm iridium. The plasma clots were then imaged using scanning electron microscopy. Arrows indicate the formation of irregular fibre bundles and compacted fibrin. Scale bar: 10 µm. n=3

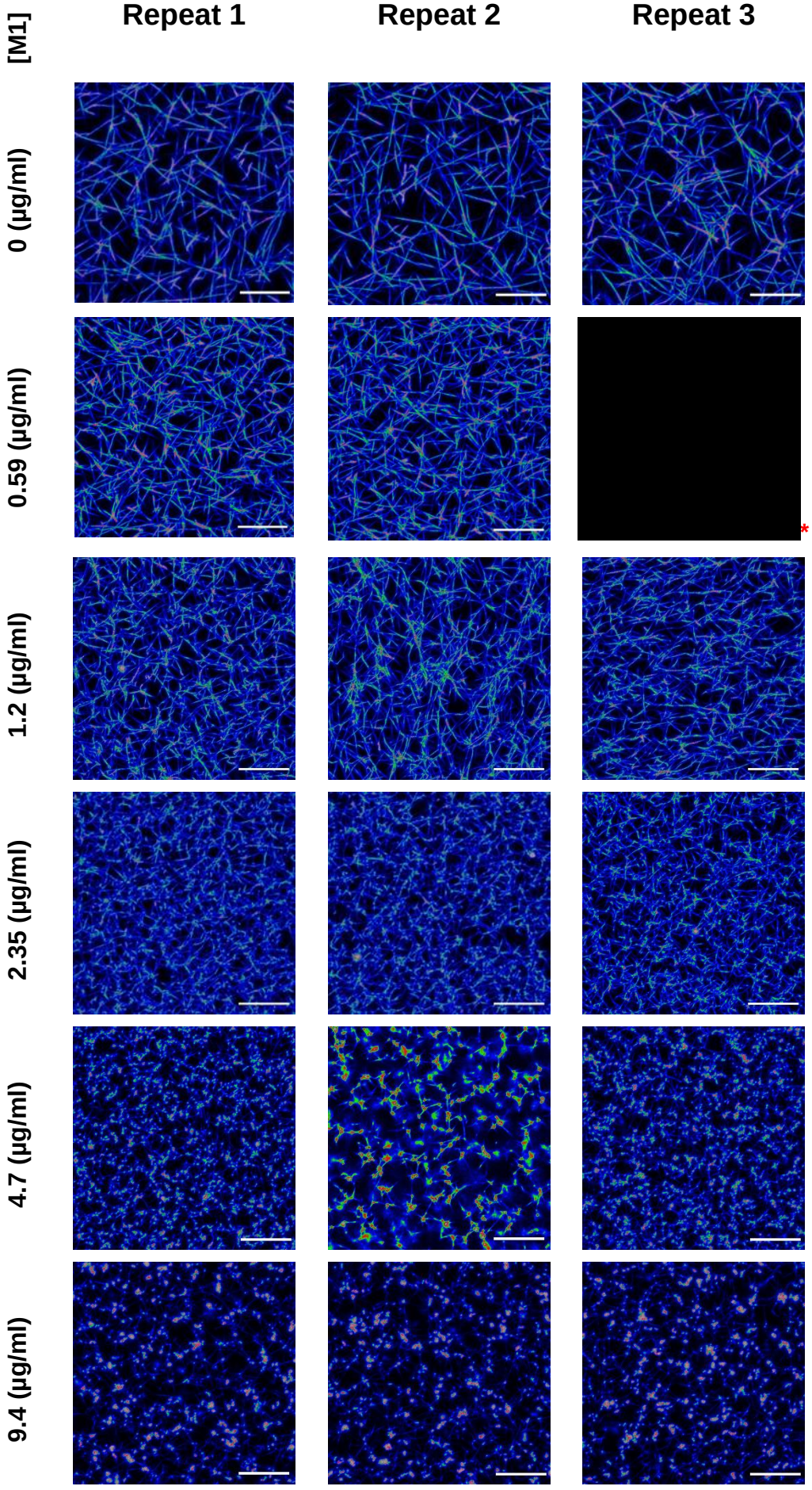
[M1]
Repeat 1
Repeat 2
Repeat 3
0 (µg/ml)
0.59 (µg/ml)
1.2 (µg/ml)
2.35 (µg/ml)
4.7 (µg/ml)
9.4 (µg/ml)
*

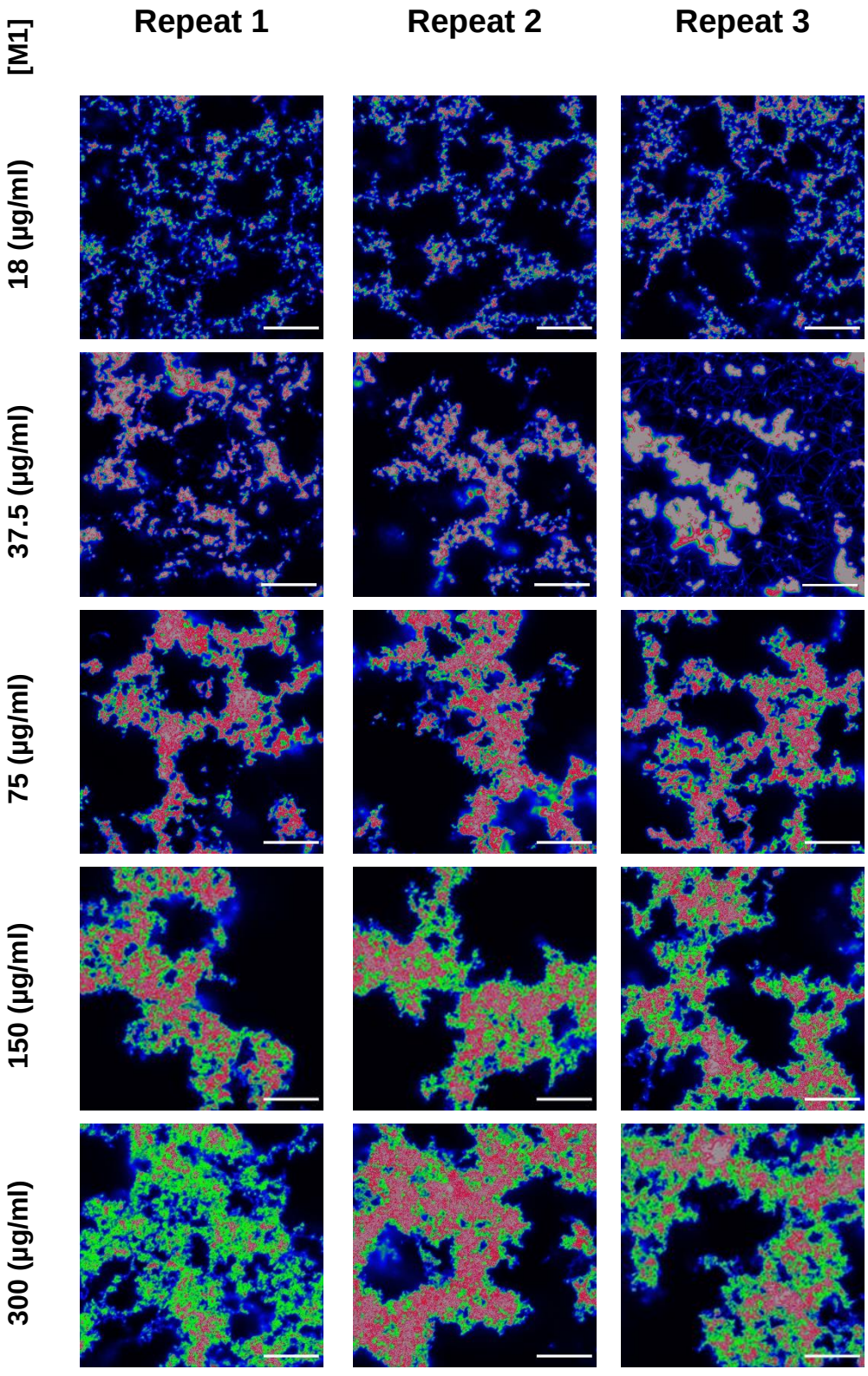

Figure 28 Laser Scanning Confocal Microscopy (LSCM) of plasma fibrin fibres Fibrin fibres were formed through the addition of thrombin in the presence of varying concentrations of rM1 protein (0-300 µg/ml). Fibrinogen was fluorescently labelled with Alexa Fluor 594. Scale bar: 20 µm. (* Excluded due to user error)

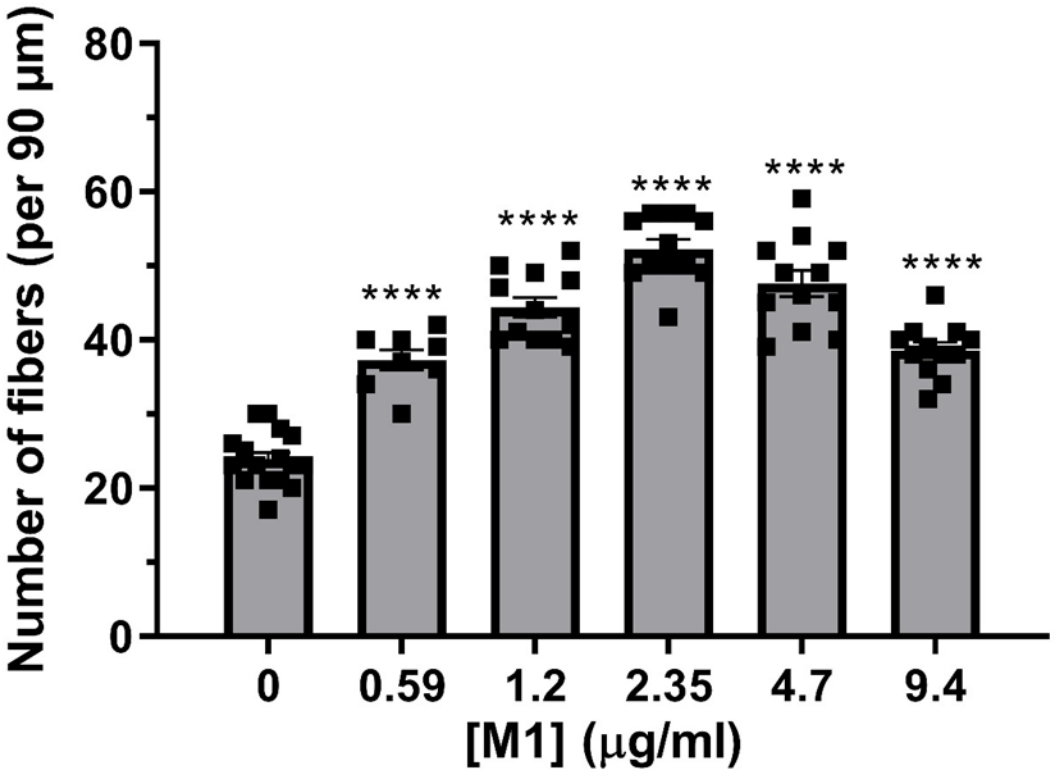

Figure 29 Fibrin fibre density of plasma clots with rM1. Fibrin fibre density was measured from LSCM images **Figure 28**. Error bars represent SEM. (**** $p < 0.0001$, One-way ANOVA with Dunnett post-hoc test.).

3.3.5 Investigating the impact of M1 protein on fibrin clot fibrinolytic potential

The impact of rM1 on fibrin clot susceptibility to lysis was investigated using turbidimetric clot formation and lysis assays in a purified system. Clotting of 3 mg/ml purified fibrinogen, incorporating rM1 concentrations (0-30 µg/ml) and 8.3 µg/ml plasminogen, was initiated by the addition of 0.05 IU/ml thrombin. A plasminogen activator was also incorporated, WHO 3rd IS Streptokinase ((00/464) 0.225 IU/ml), to accelerate plasmin generation and initiate lysis. The clotting and lysis profiles were monitored by measuring turbidity changes kinetically. As shown in Figure 30A, there is an initial non-significant 1.1-fold decrease in lysis time at 0.94 µg/ml rM1 in comparison to the control (5037.50 ± 264 seconds and 5602.50 ± 210 seconds, respectively). However, overall, there was no significant differences in time to 100% lysis in purified turbidimetric plate assays.

Fibrin clot susceptibility to lysis was also investigated by measuring the mechanical strength of the clot using ROTEM analysis. Purified clots with increasing concentrations of rM1 (0-30 µg/ml) and 9.3 µg/ml plasminogen were formed with 0.5 IU/ml thrombin and 1 IU/ml 3rd International Standard Streptokinase (00/464) to initiate lysis. The lysis time was then obtained from the subsequent TEMograms. As shown in Figure 30B, there were no significant differences observed between lysis time for purified conditions. This is consistent with the turbidimetric data, as even at the highest concentrations of rM1 no significant differences were observed in comparison to the control (1947.50 ± 39.79 seconds and 2233.29 ± 72.75 seconds, respectively).

An extrinsically activated EXTEM assay, in which coagulation is initiated by the addition of tissue factor, was used to measure fibrinolysis in whole blood conditions with the addition of increasing concentrations of rM1 (0-30 µg/ml) and 1 IU/ml 3rd International Streptokinase (00/464) to initiate lysis (Figure 30D). A nonsignificant decrease in lysis time was observed with increasing concentrations of rM1 up to 1.88 µg/ml, which reduced the lysis time by approximately 1.5-fold compared to the control with no rM1 added (1641.3 ± 195.6 seconds and 2428.5 ± 304.0 seconds, respectively. P=0.0391). Above this concentration a dose-dependent decrease in lysis time was observed up to a maximum of 2.2-fold decrease at 30 µg/ml rM1 compared to the control (1080 ± 126.7 seconds and 2428.5 ± 304.0 seconds, respectively. P= 0.0008). Lysis data for 60 µg/ml rM1 could not be obtained due to the TEMogram output not reaching an amplitude of 20 mm. This signifies a significantly weak clot and other data points, such as lysis time, is not calculated by the ROTEM delta software.

A microtitre plate-based halo assay was used to investigate further the impact of rM1 on whole blood clot lysis. Clotting of whole blood (5%) with varying concentrations of rM1 (0.48-30 µg/ml) was initiated with 15% v/v Innovin reagent (recombinant human tissue factor). The clots were formed around the edges of the microtitre plate wells forming a ‘halo’ ring. Once clotted, a lysis solution was added to the clots, consisting of 0.75 IU/ml 3rd International Standard streptokinase to activate plasminogen and begin lysis. The degradation of the halo clots was then monitored by measuring turbidity changes, in a BMG FluorStar® Omega plate reader, as blood progressively lyses into the centre of the well. As shown in Figure 30C, the halo assay results show a similar trend to the whole blood ROTEM analysis. A 1.2-fold decrease in

time to 100 % lysis was observed at 0.94 µg/ml rM1 compared to the control with no rM1 (2391 ± 135.0 seconds and 2967 ± 245.7 seconds, respectively, p= 0.0405). At 1.88 µg/ml rM1 the difference increased to ~1.7-fold (1767 ± 155.3 seconds and 2967 ± 245.7 seconds, respectively, p <0.0001) up to a maximum of 2.7-fold at 7.5 µg/ml rM1 (1104 ± 73.5 seconds, p= <0.0001). Above this concentration, time to 100% lysis begins increasing slowly in a dose-dependent manner. However, in comparison to 0 µg/ml, there is still a 2.6-fold and 2.2-fold decrease in time to 100% lysis in the presence of 15 µg/ml (2967 ± 245.7 seconds and 1153 ± 49.8 seconds) and 30 µg/ml (2967 ± 245.7 seconds and 1308 ± 66.7 seconds), respectively.

3.3.5.1 Assessing the impact of M1 on plasminogen activation

There are several possible explanations for the reduced lysis times found with increasing rM1 protein concentrations. To determine if changes to rates of plasminogen activation contribute to the apparent increase in susceptibility to lysis, plasminogen activation was measured directly using clot overlay assays. Fibrin clots were formed with 3 mg/ml purified fibrinogen, incorporating a range of rM1 concentrations (1.88-30 µg/ml). Plasminogen (8.2 µg/ml), host plasminogen activators, 64 IU/ml WHO 2nd International Standard uPA (11/184) or 200 IU/ml WHO 3rd International Standard tPA (98/714), and a chromogenic substrate (S2251), specific to plasmin, were added to the surface of the preformed clot to initiate lysis. As plasmin is generated, the chromogenic substrate is cleaved to release a chromophoric group which was monitored kinetically at 405 nm, and the rate is used as a measure of plasminogen activation. The assay was also monitored at 650 nm to remove background noise caused by lysis of the purified clots; each well was corrected by normalising by this absorbance. Specific activities were calculated relative to

the host plasminogen activator condition without the presence of rM1 (0 µg/ml) and presented as fold-change as per Figure 31. The host plasminogen activators, urokinase plasminogen activator (uPA) and tissue plasminogen activator (tPA), showed no significant differences in plasminogen activation activity with increasing concentrations of rM1. uPA shows a non-significant decrease in plasminogen activation activity with an average of 0.88-fold change at all rM1 concentrations. tPA does not display any differences in activation activity at any concentration of rM1. The assays were also repeated with a fixed concentration of streptokinase (4.8 IU/ml) over a dilution range of rM1 protein (1.88- 30 µg/ml) as per section 4.3.4.3. However, no particular trend was observed with streptokinase variants activity with increasing concentrations of rM1 protein (Figure 55).

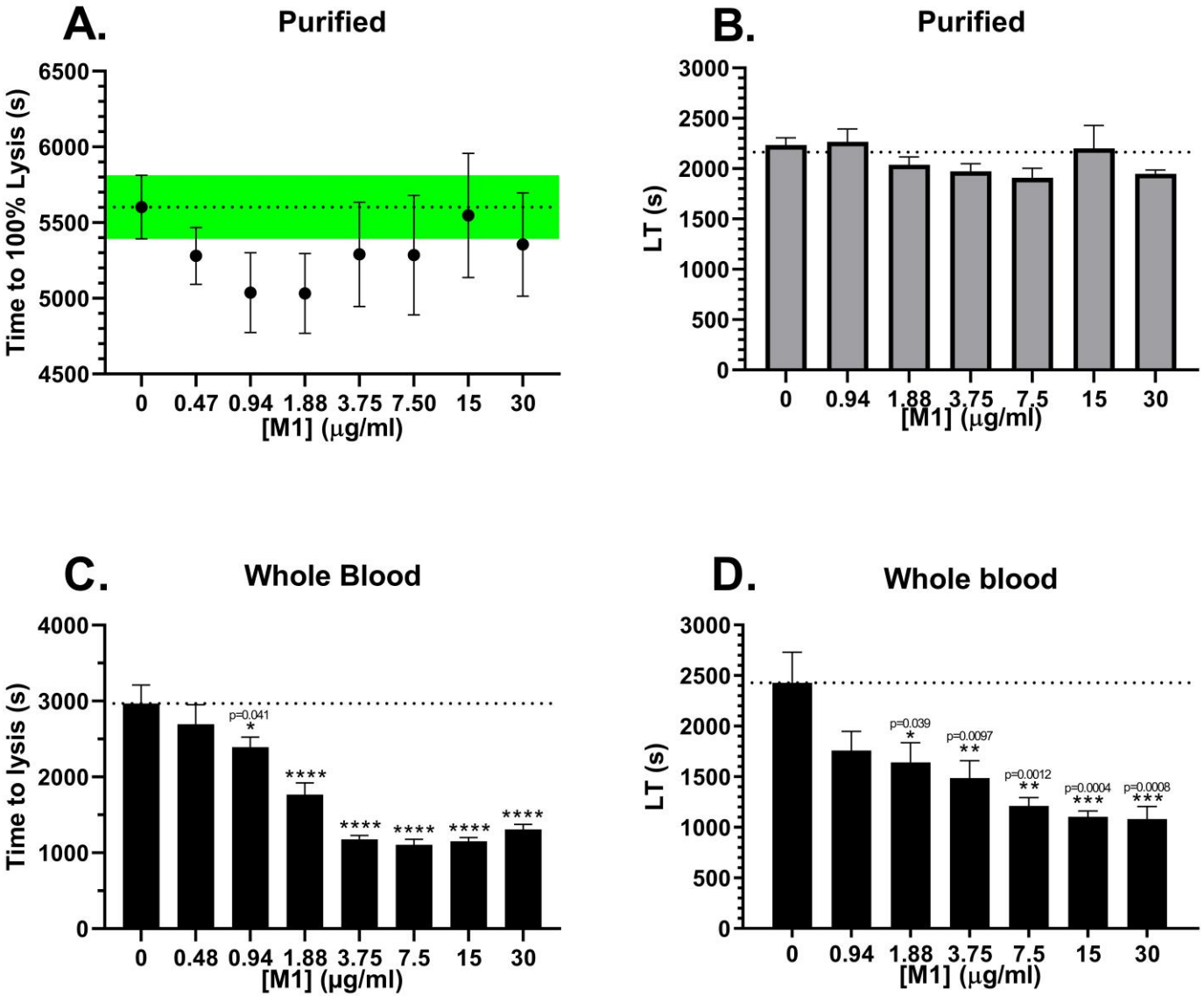

Figure 30 Fibrinolytic potential of fibrin clots measured using a microtitre plate assay **(A. & C.)** and ROTEM analysis **(B. & D.).** Whole blood was activated with tissue factor **(C. & D.)** whilst purified clots were activated with thrombin **(A. & B.)**. The lysis time was then derived from the ROTEM TEMogram **(B. & D.)** or presented as time to reach 100% lysis in the microtitre assays **(A. & C.). C.** represents a halo assay, whilst **A.** represents a purified turbidity assay. Error bars represent SEM. (**** $p < 0.0001$, One-way ANOVA with Dunnett post-hoc test.).

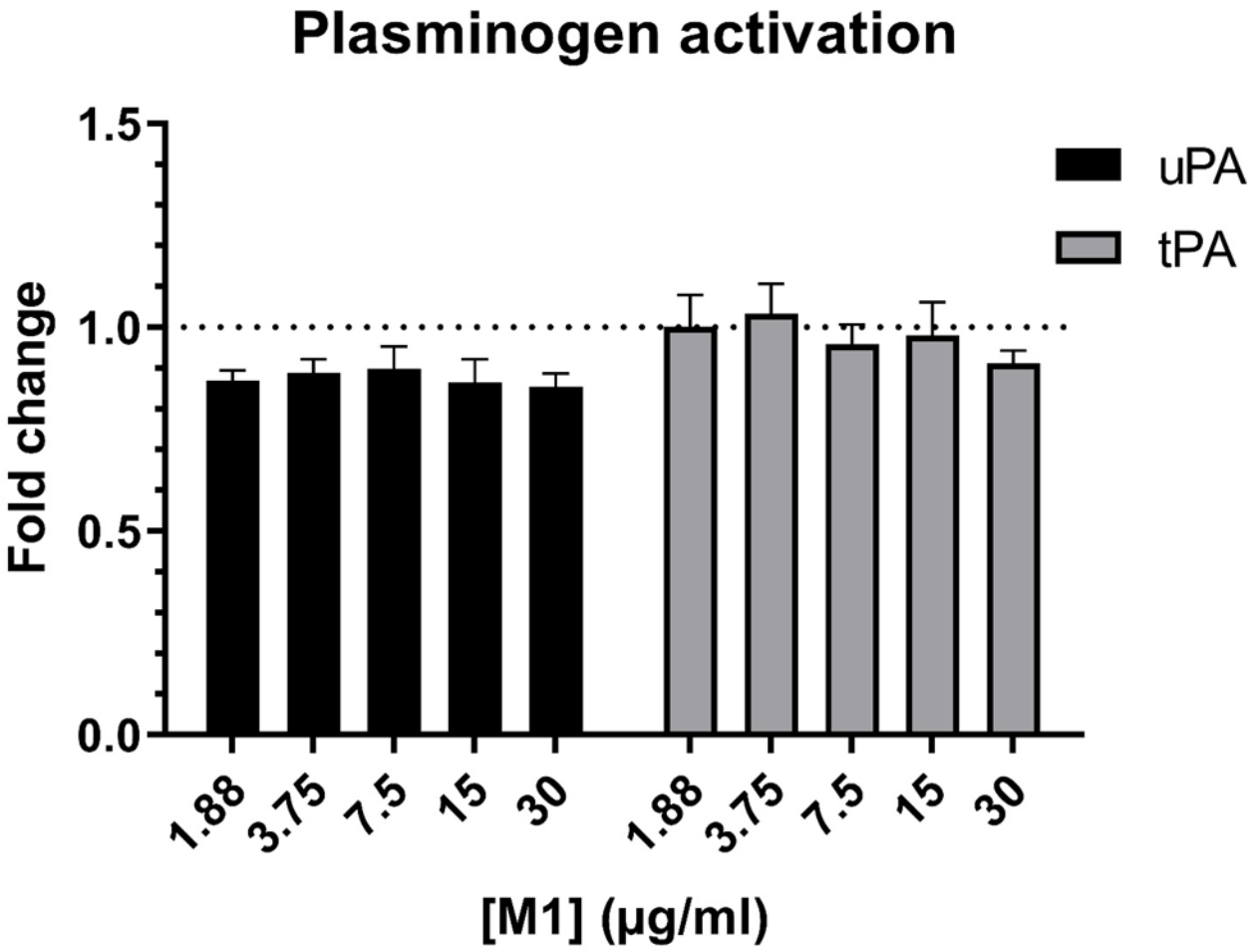

Figure 31 Plasminogen activation activity of host plasminogen activators in the presence of rM1 Glu-plasminogen activity of host plasminogen activators, uPA and tPA, was investigated in the presence of increasing concentrations of rM1 (1.88-30 µg/ml) using the chromogenic solution assay against S2251. Specific activities were calculated relative to the WHO 2nd International Standard uPA (11/184) or 200 IU/ml WHO 3rd International Standard tPA (98/714), respectively, using parallel line bioassay analysis, and presented as fold change. The dotted line indicates uPA and tPA without the presence of rM1. n=≥4 (No significant differences were found between M1 concentrations using One-way ANOVA with Dunnett post-hoc test.)

3.3.6 Assessing the impact of M1 protein on fibrin film formation

Laser scanning confocal microscopy was used to visualise the impact of rM1 protein on fibrin clot film formation. Figure 32 shows an LSCM image of a fibrin clot formed with 20% plasma, in the absence or presence of 1.88 µg/ml rM1, initiated with 0.2 IU/ml thrombin (01/578). The protective fibrin film which forms at the external surface of the clot is indicated by the yellow arrow. The fibrin film forms a continuous layer which is distinct from the fibrin fibre network underneath. The fibrin film has multiple physiological roles including retaining blood cells within the clot and providing a first line of defence against microbial invasion. It was therefore important to investigate the impact of rM1 protein on fibrin film formation. As shown by Figure 32, even low levels of rM1 protein appeared to disrupt the formation of the fibrin film. A 3D image was then constructed of the film, by taking a 20 µm slice of each condition. As shown in Figure 33, the fibrin film is demonstrated in the control condition with a red arrow. The colour indicates the intensity of the labelled fibrin. In the control condition the fibrin film is red, demonstrating a high density of fibrin. As the rM1 protein increases the number of pores in the film also increased, determined visually. The intensity of the film gradually decreases until at the highest concentration of rM1 protein (60 µg/ml), the film is no longer distinguishable from the fibrin network underneath.

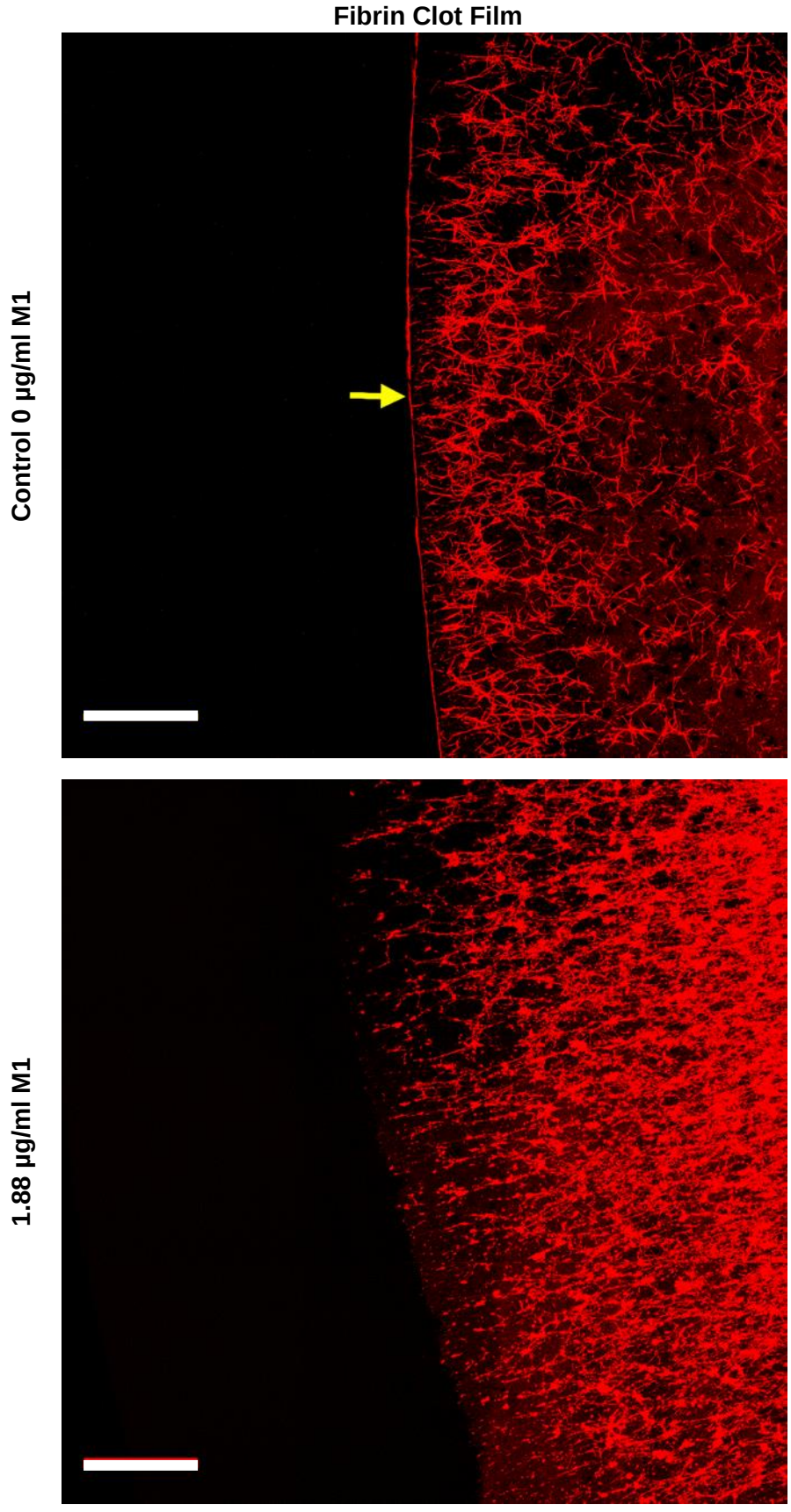

Figure 32 LSCM of plasma fibrin film with and without the presence of rM1 Fibrin fibres were formed through the addition of thrombin in the presence or absence of 1.88 µg/ml rM1 Fibrinogen was fluorescently labelled with Alexa Fluor 594 Scale bar: 20 µm. Assisted by Lewis Hardy, University of Leeds.

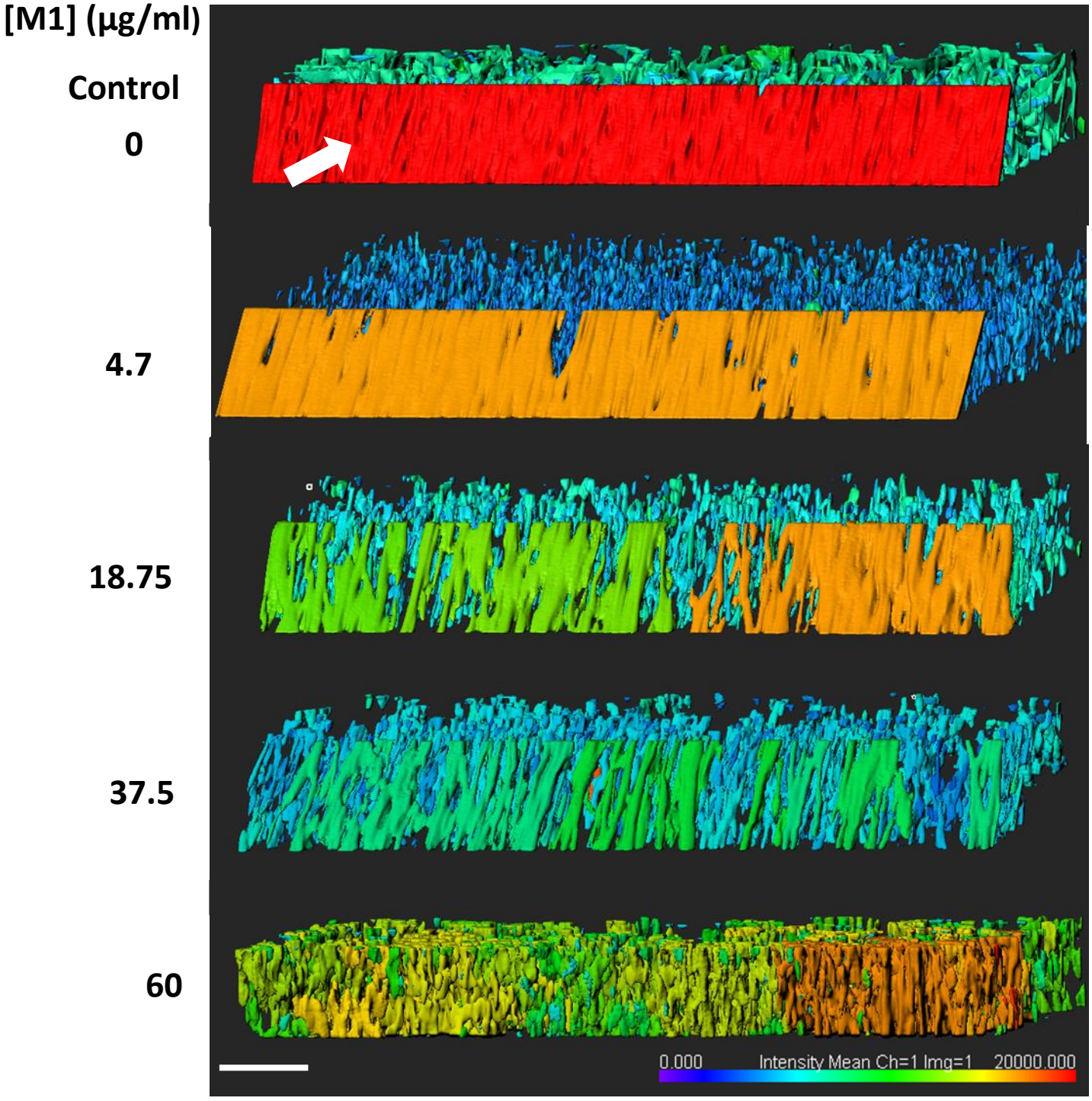

Figure 33. LSCM of plasma fibrin biofilm with increasing concentrations of rM1 (4.7-60 µg/ml). Fibrinogen was fluorescently labelled with Alexa Fluor 594. Images were constructed in Imaris software. Scale bar: 20 µm Fibrin biofilm (arrow) forms a continuous layer on the surface of the clot, distinct from the fibrin fibers underneath. Presence of M1 alters fibrin fiber properties and disrupts the formation of the fibrin biofilm. N=3

3.3.7 Pilot bacterial migration assays

Group A *Streptococcus pyogenes,* Cluster 1, 2a and 2b (section 2.6.1), were obtained as lyophilised bacteria from LGC (Teddington, UK). Following reconstitution in THY media and storage in Protect Select cryobeads, bacterial fitness growth curves assays were performed and gram staining before development of bacterial migration assays.

3.3.7.1 Group A Streptococcus growth curves

Streptococcus pyogenes, Cluster 1, 2a or 2b, was streaked on blood agar plates then incubated statically overnight at 37ºC/ 5% CO_2. One of the colonies was picked and used to inoculate 1000 µl THY media, or C-media, then incubated statically overnight at 37ºC/ 5% CO_2. The following day, 4 µl of the overnight culture was used to inoculate 200 µl of sterile THY, or C-media, (1:50 dilution) in a 96-well plate. Plates were sealed with Axygen® Ultra Clear sealing film, then growth was measured kinetically (OD600) at 37ºC on BMG FluorStar Omega plate for 22 hours as per section 2.6.3. The plates were oscillated before each reading as *Streptococcus pyogenes* is a non-motile bacterium and settles to the bottom of the well. A blank well was included for each condition to ensure no cross-contamination occurred.

As shown in Figure 34A, Cluster 1 and 2b *Streptococcus pyogenes,* displayed similar growth rates. The log phase for each strain started after ~1 hour, with Cluster 1 peaking after 9.5 hours (OD600: 0.635 ± 0.014), and Cluster 2b after 10 hours (OD600: 0.663 ± 0.023). Cluster 2a showed slower growth rates, starting log phase after ~1 hour but peaking around 16.5 hours (OD600: 0.616 ± 0.019).

Bacterial migration assay experiments required *Streptococcus pyogenes* to be grown in two types of media, a rich THY medium and a carbohydrate poor, peptide rich C-media (Table 1). The experiment was therefore repeated with Cluster 2a *Streptococcus pyogenes* grown in the different media types. *Streptococcus pyogenes* was overnight cultured in either C-media or THY media. The overnight culture was then used to inoculate sterile media (1:50) in a 96-well plate and measured kinetically (OD600) at 37ºC on BMG FluorStar Omega plate for 22 hours as per section 2.6.3. As shown in Figure 34B, when *Streptococcus pyogenes* was overnight cultured in C-media and then inoculated into the low nutrient C-media (• C-C), there is a delay in log phase of ~3 hours (OD600: 0.038 ± 0.003). When the bacterium was overnight cultured in THY medium, the log phase started ~1.5 hours when inoculated into either C-media (■ THY-C) or THY media (▲THY-THY) (OD600: 0.031 ± 0.004 and 0.037 ± 0.006, respectively). The • C-C condition peaked at 13.5 hours (OD600: 0.429 ± 0.009), whilst ■ THY-C peaked at ~7.5 hours (OD600: 0.470 ± 0.016) and ▲THY-THY at ~9 hours (OD600: 0.532 ± 0.020).

For all further experiments, *Streptococcus pyogenes* were overnight cultured in THY media before inoculation in C-media.

3.3.7.2 Gram stain of Group A Streptococcus

Streptococcus pyogenes was streaked on blood agar plates then incubated statically overnight at 37ºC/ 5% CO_2. The following day, one of the colonies was picked and gram stained to check morphology and for contamination before use in migration assays. Representative images are shown in Figure 35. Group A Streptococcus are Gram-positive cocci therefore stain purple when Gram-stained. Group A *Streptococcus* can be seen occurring in long chains (>5

cocci), short chains, pairs and individually. Whilst some clustering has occurred, this is likely due to the bacterial smear being applied slightly too thick to the glass slide during preparation. Overall, there appears to be no contaminating bacteria present.

3.3.7.3 Pilot migration assay data

Bacterial migration assays were developed to investigate the movement of *Streptococcus pyogenes* through fibrin clots with increasing concentrations of rM1 protein. Fibrin clots were formed in Falcon™ Cell Culture Inserts by adding 3 mg/ml fibrinogen, incorporating 0-30 µg/ml M1, then initiated with 0.2 IU/ml thrombin (01/578) and 5 ml calcium chloride. After 2 hours incubation, labelled *Streptococcus pyogenes* Cluster 2a was added to the surface of the clot and the cell culture inserts were placed in 24-well plates with 1000 µl rich THY-media in the wells. An initial fluorescence (Ex 480 Em 516) and absorbance (OD600) reading were taken, then the plates were placed statically at 37ºC/ 5% CO2. Fluorescence and absorbance were then measured for up to 49 hours to quantify bacterial movement through the clot. Data was corrected by subtracting the buffer absorbance and fluorescence from each data point. The control for this experiment was 0 µg/ml rM1. A blank was included to ensure no cross-contamination, where bacteria was replaced with C-media. Each condition was performed in duplicate. Due to time limitations and issues arising with the development of the experiments Figure 36 is pilot data and only represents one experiment.

As shown in Figure 36B, bacteria perforation is first observed in the 30 µg/ml rM1 and 7.5 µg/ml rM1 conditions after approximately 20 hours (OD600: 0.122 ± 0.094 and 0.128 ± 0.122, respectively.). Whilst the fluorescent readings (Figure 36A) shows consistent data, that bacteria perforation is first observed in

the 30 µg/ml rM1 condition, the labelled bacteria is not observed until around 30 hours after experimental start (6.32 ± 3.1 RFU). Additionally, labelled bacteria in the 7.5 µg/ml rM1 condition does not appear to perforate the clot until ~45 hours after the start of the experiment (4.03 ± 0.86 RFU). According to the absorbance data, Figure 36B, bacteria perforation was next seen in fibrin clots incorporating 0.47 µg/ml rM1 protein after 24 hours (OD: 0.118 ± 0.037). The control fibrin and fibrin incorporating 1.88 µg/ml M1 showed bacterial perforation after ~ 26 hours according to the absorbance data (OD600: 0.139 ± 0.035 and 0.148 ± 0.014, respectively). The fluorescence data does not show any labelled bacteria perforating the clots until after 45 hours for both the control and 1.88 µg/ml condition (3.44 ± 0.17 and 2.45 ± 0.57 RFU, respectively). The blank condition did not show any sign of cross-contamination throughout and remained at ~0 OD and RFU. At the end of the experiment, a sample of the remaining bacteria was removed from the surface of the clot and the fluorescence was measured. The majority of the labelled bacteria still remained on the surface of the clots and had not travelled through (Figure 37). There were no significant differences between rM1 concentrations.

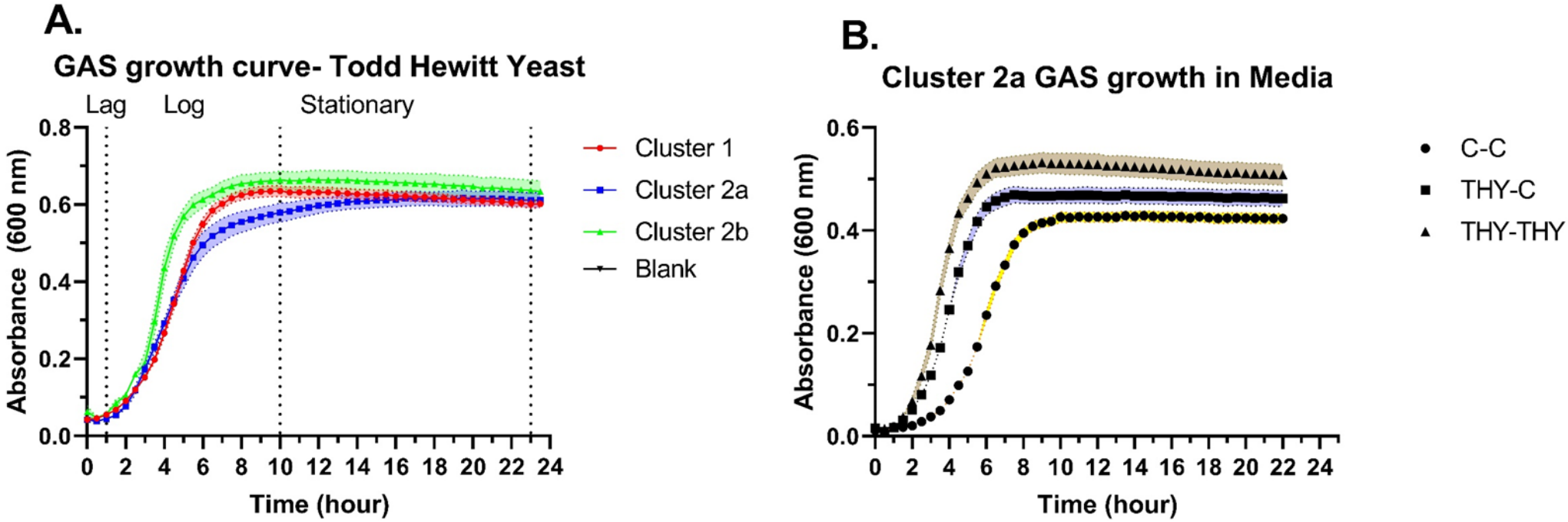

Figure 34 Bacterial fitness by growth curve assays A. Bacterial fitness growth curves of Cluster 1, 2a and 2b Streptococcus pyogenes in THY media over a 22-hour period n=3 Error bar represents SEM **B.** Bacterial fitness growth curves of Streptococcus pyogenes Cluster 2a following overnight culture in C-media then inoculation into C-media • **C-C** , overnight culture in THY media and inoculation in C-media ■ **THY-C** and overnight culture in THY media and inoculation into THY media ▲**THY-THY** n=6 Error bars represent SEM (For more information on buffer formulations, see **Table 1**)

Representative GAS Gram Staining

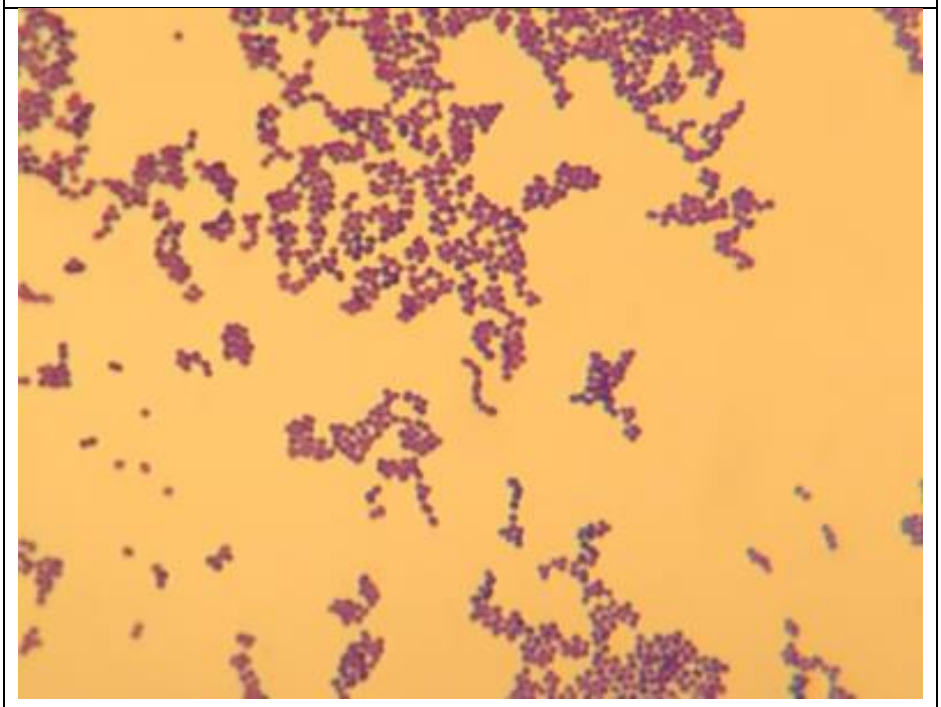

Figure 35 Representative gram staining of Group A Streptococcus Images of Gram-positive (Purple) Group A Streptococci under a x100 lens. Group A Streptococcus can be seen occurring in long chains (>5 cocci), short chains, pairs and individually. No indication of contamination.

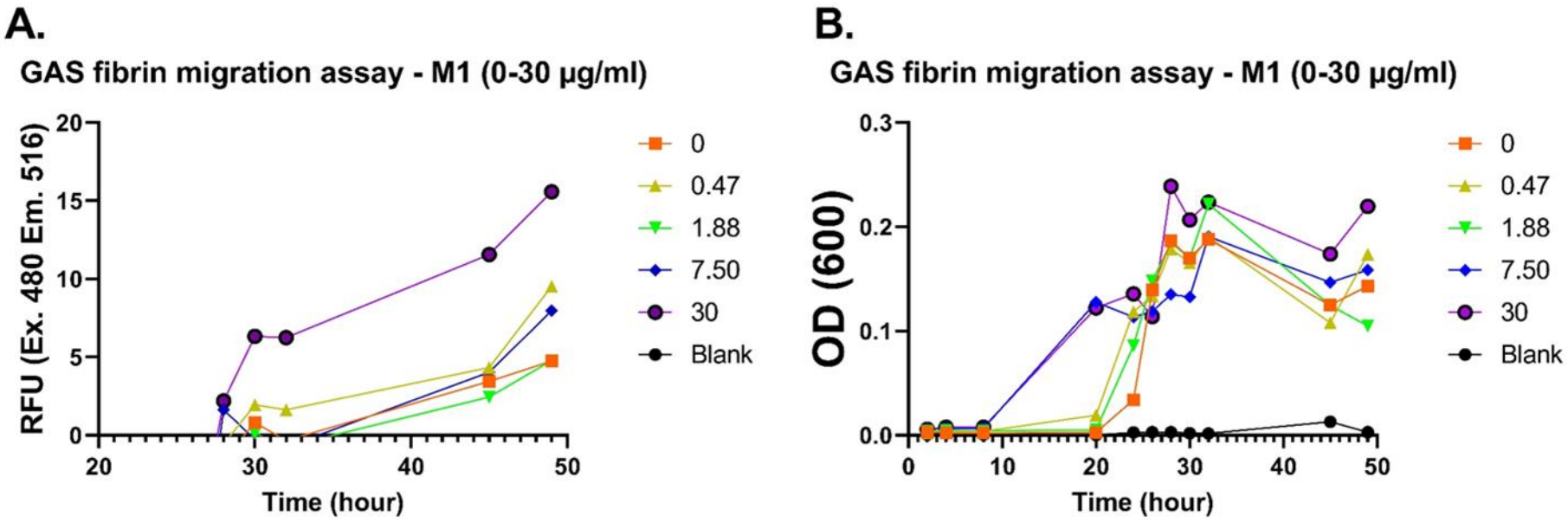

Figure 36 Pilot data from bacterial migration through fibrin clots. Purified fibrin clots, incorporating rM1 (0.47-30 µg/ml), activated with thrombin were formed in Falcon™ Cell Culture Inserts (with 0.8 µm pores) and Probes™ BacLight™ Green labelled bacteria in a poor carbohydrate media was placed on top. The cell culture inserts were placed into a 24-well plate containing 1000 µl rich THY media. Fluorescence (Ex. 480 Em 516) **A**. and absorbance (OD600) **B.** readings were taken from the bottom of each well for up to 49 hours to measure migration of the bacteria through the clot. N=1

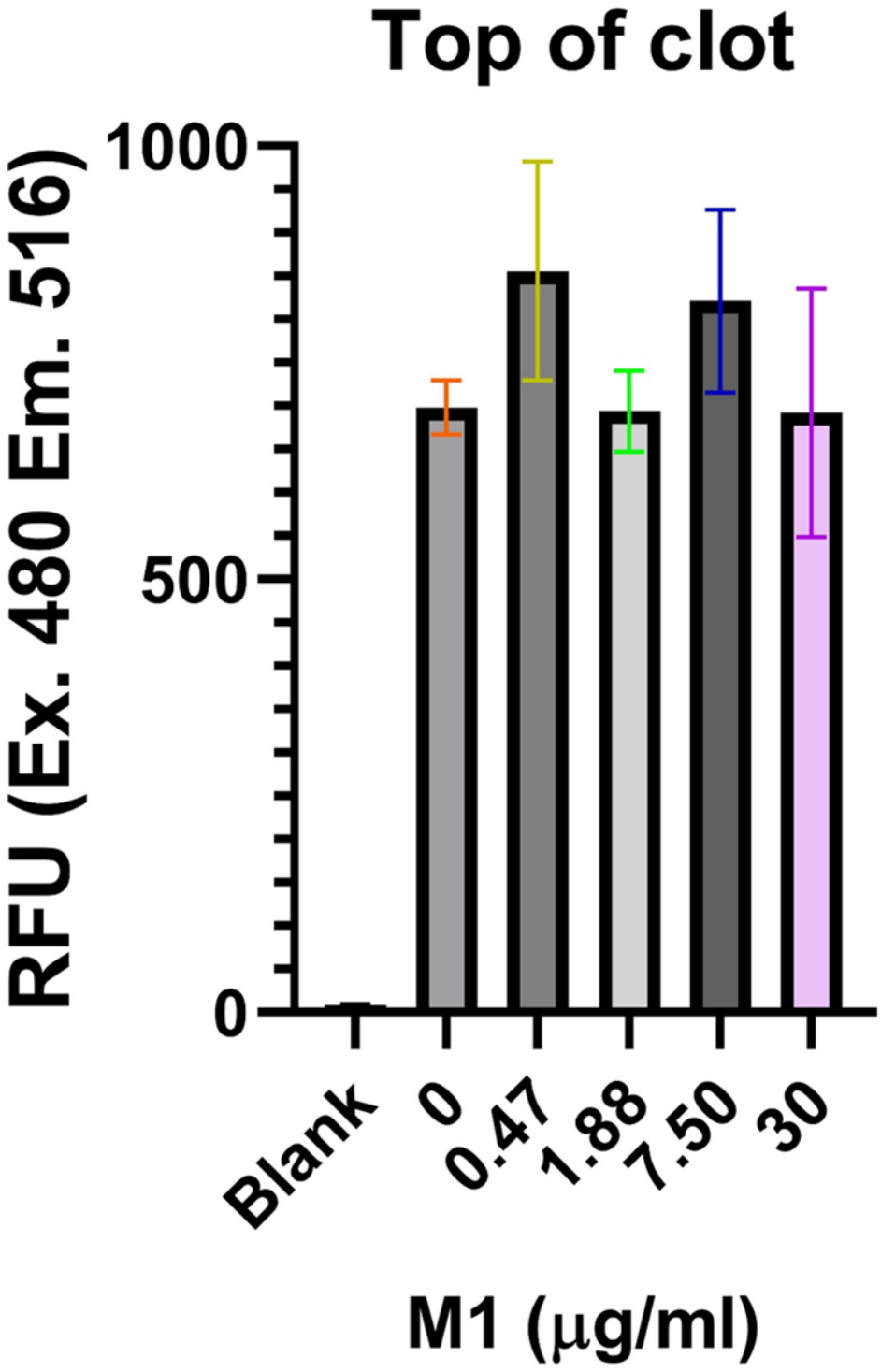

Figure 37 Bacterial migration assays end of experiment labelled bacteria fluorescence. Following the experiment, **Figure 36**, a sample of the bacteria was taken from the surface of the clot (from each M1 concentration) and the fluorescence was measured to quantify the amount of labelled bacteria that had not travelled through the clot N=1

3.4 Discussion

Recent genomic analysis of invasive GAS infections has found that the *emm 1* strain are the most commonly found serotype associated in epidemiological investigations (Gherardi et al., 2018, Nelson et al., 2016, Luca-Harari et al., 2009, O'Grady et al., 2007) . Additionally, since the 1980's a global resurgence of invasive diseases has been attributed to the emergence of novel highly virulent and prevalent mutant strains of GAS such as M1T1 (Aziz and Kotb, 2008, Barnett et al., 2013). These GAS strains contain a cell-bound virulence factor, known as the M1 protein which aids in adherence to epithelial cells (Okada et al., 1995, Ellen and Gibbons, 1972), intracellular invasion of host cells (Cue et al., 2000), immune evasion (Oehmcke et al., 2010) and microcolony formation (Frick et al., 2000). However, the M1 protein is thought to be cleaved from the GAS surface by SpeB (Berge and Bjorck, 1995a) or neutrophil proteinases (Herwald et al., 2004), resulting in functionally active fragments at the site of infection during early infection. M1 protein has been found to bind fibrinogen in solution, constructing pathological supramolecular complexes that are capable of activating neutrophils and inducing vascular leakage, a common symptom of STSS (Macheboeuf et al., 2011). This M1-fibrinogen complex has also been shown to be capable of activating platelets, and subsequently activating neutrophils and monocytes, causing microthrombi to be deposited at local and distant sites (Shannon et al., 2007). The impact of rM1 in terms of fibrin clot formation has not currently been investigated. Fibrin formation is an essential part of innate immunity, providing a scaffold to prevent blood loss and allow repair, forming a protective layer on the surface of blood clots and trapping bacteria within fibrin networks to limit dissemination.

The M1 protein used in this project is from the GAS strain SF370 (Figure 6), which is an ancestral strain to the highly virulent and prevalent M1T1 GAS strain, 5448. The M1T1 GAS clone diverged from the ancestral strain SF370 through horizontal gene transfer mechanisms (Maamary et al., 2012) which lead to the acquisition of two additional virulence factors, the superantigen SpeA and streptodornase Sda1 and increased expression of extracellular toxins NAD^+-glycohydrolase (Nga) and SLO (Cole et al., 2011, Maamary et al., 2012). M1 protein from SF370 strain was used in this project because the strain is well characterised, with the genome first being sequenced in 2001 (Ferretti et al., 2001), and has therefore been widely used in research. Additionally, multiple sequence alignments of SF370 M1 protein with the M1T1 5448 M1 protein (Accession code: AKK71110.1) revealed that the amino acid sequences were 99.8% identical. Therefore, it safe to assume that the findings in this project can translate to the M1T1 5448 binding fibrinogen, and the effects on fibrin clot formation properties.

The M1 protein was recombinantly produced in *E. coli* as described in section 4.3.2. The amino acid sequence with domains is shown in Figure 38. Whilst the Profinity eXact tag is cleaved off precisely, leaving native N-terminal amino acids, the C-terminal histidine tags are for later experiments (Section 4.2.7)

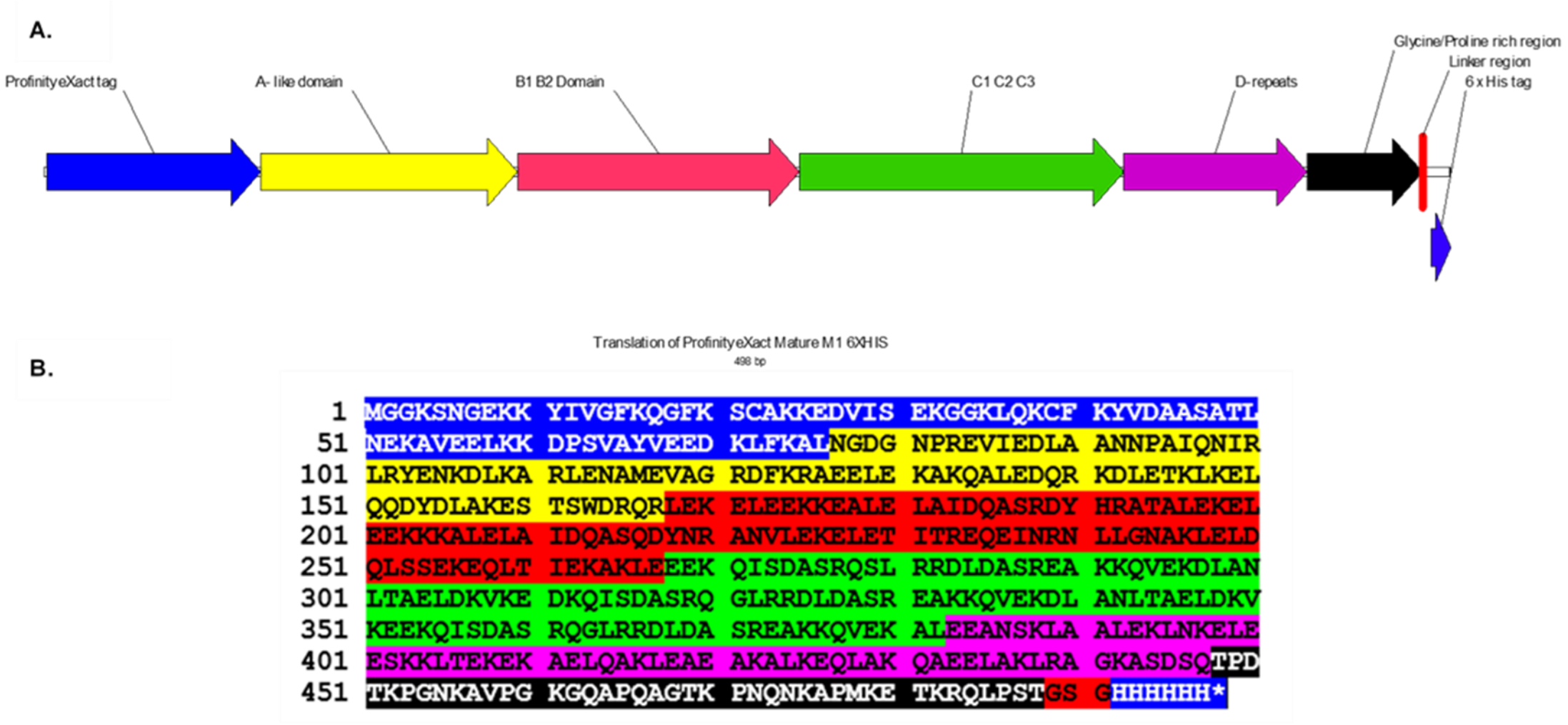

Figure 38 Amino acid sequence for the M1 protein used in this project. (A.) Schematic representation of the rM1 protein with the co-expressed N terminal Profinity eXact tag and C-terminal 6 x Histidine tag. Each set of arrows correlates to the domain sequences shown in **(B.)** The Profinity eXact tag is cleaved off during the purification steps leaving native mature recombinant protein.

3.4.1 rM1 and fibrinogen complex

Reports of M proteins forming insoluble complexes in human plasma date back to 1965, with this being identified as a result of interactions between M proteins and fibrinogen (Kantor, 1965). Since then, much work has been done to characterise this complex including determining the partial crystal structure, which demonstrated that the M1 protein dimer binds via its B1 B2 domains to four fibrinogen D domains, in a cross-like pattern (Macheboeuf et al., 2011). Therefore, it was important to demonstrate that the recombinantly produced M1 protein in this project binds to fibrinogen and is functionally representative of the GAS virulence factor. Pull-down assays (Figure 17A) confirmed that the rM1 protein binds fibrinogen. Additionally, during sample preparation, combining purified fibrinogen and rM1 (without the presence of thrombin), changed the viscosity of the sample to a gel-like consistency. When this viscosity change was observed kinetically (Figure 17B), the change in turbidity presented a similar profile to fibrin clot formation. However, it is important to note that the maximum absorbances observed were always at least 10-fold lower than when fibrin clots were formed by addition of thrombin under the same conditions. Previous studies confirmed that the M1-fibrinogen clustering is not due to thrombin-like cleavage of fibrinogen by adding serine proteinase inhibitors to the complexes (Herwald et al., 2004). The nature of the rM1-fibrinogen complex was further investigated using LSCM (Figure 17C). Consistent with previous SEM imaging (Herwald et al., 2004, Macheboeuf et al., 2011), the LSCM showed dense clusters of rM1- bound fibrinogen and at higher concentrations of rM1, the clusters aggregated forming networks that were distinct from fibrin networks.

Interestingly, previous studies indicated that the M1- fibrinogen complex only formed when both the proteins are in equilibrium (Kantor, 1965). With some studies showing that M1 protein, at 1 µg/ml, in (10%) plasma concentrations of fibrinogen were optimal for complex formation and at higher or lower concentrations the complexes do not form (Herwald et al., 2004, Shannon et al., 2007). However, the experiments conducted during the present study have demonstrated that although the gel might not be visible to the eye, the fibrinogen complexes formation can still be visualised using turbidity and LSCM at varying concentrations. All reagents in this experiment were pre-warmed to 37ºC and maintained at 37ºC during experimental conditions. A recent study demonstrated that PAM does not exist as a dimer at 37ºC, the optimum temperature for GAS growth (Ayinuola et al., 2021a). Therefore, it is highly plausible that the M1 protein also exists as a monomer at this temperature, leading to the observed differences due to different experimental conditions.

3.4.2 Fibrin clot formation

The fibrin clot polymerisation kinetics in the presence of rM1 protein were investigated using turbidimetric assays, KC4 coagulometer and ROTEM analysis. The main parameters derived from the turbidimetric curves was the lag times, which indicates the time required for protofibrils to grow to a sufficient length to begin lateral aggregation, and the maximum absorbance, which reflects the cross-sectional area of the fibrin fibres and the number of protofibrils per fibre (Carr and Hermans, 1978, Wolberg et al., 2002). The maximum absorbance was consistent for both purified (Figure 19C) and plasma conditions (Figure 19D), whereby a dose-dependent decrease in maximum absorbance was observed as rM1 protein concentrations increases; to a maximum of -1.5-fold decrease in the purified conditions and -2.4-fold difference in plasma

condition at 60 µg/ml rM1 protein in comparison to the control (section 3.3.3.1). As discussed in section 1.1.4.4, literature suggests a change in maximum absorbance is usually indicative of a shift in average fibrin fibre diameter. More specifically, a decrease in maximum absorbance has previously been associated with thinner fibrin fibres (Carr and Hermans, 1978). However, in purified samples using the maximum absorbance for fibre diameter predictions depends on the fibrinogen concentration and internal fibrin density remaining constant in all experimental conditions (Pieters et al., 2020). Furthermore, turbidimetric analysis of plasma fibrin clots have suggested that the maximum absorbance in plasma conditions is more strongly associated with the overall clot density, rather than the fibre diameters (Pieters et al., 2020). Therefore, it was clear that further analysis of the clot structure was needed as described in section 3.4.3.

The turbidimetric lag times for the purified fibrinogen (Figure 19A) and plasma samples (Figure 19B) appeared to show conflicting results with increasing concentrations of rM1. Whilst the lag times in purified fibrinogen appeared to decrease with increasing concentrations of rM1 protein (up to a maximum of 6-fold decrease at 15 µg/ml in comparison to the control), thus suggesting an increased rate of lateral aggregation of protofibrils. The plasma condition showed no significant differences between rM1 conditions. The decreased lag time observed with the purified turbidity experiments should be interpreted with caution, due to the immediate fibrinogen-M1 fibrinogen complex formation described in section 3.4.1 and section 3.3.2. Overall, the turbidity experiments provided the first indications that the rM1 protein was modifying the fibrin clot properties and was the starting point of the additional experiments. However, information that can be derived from this technique is limited, with some results

being potentially misleading. For example, it is unclear whether the observed changes in maximum absorbance were due to fibrin diameter changers, or internal fibrin density changes and whether the decrease in lag times were due to increased rate of lateral aggregation of protofibrils or the fibrinogen and M1 complexes.

Fibrin clot formation properties were also investigated using a micro-mechanical clot detection KC4 delta coagulometer, which defines clotting time (s) as the time taken for the fibrin clot to displace the steel ball from the magnetic sensor (section 3.2.2). The purified and plasma fibrin clots were activated using thrombin therefore measuring the final step in the clotting cascade, the conversion of soluble fibrinogen to insoluble fibrin. The results demonstrated that after 7.5 ug/ml rM1, there was a significantly slower clot formation time in both purified and plasma conditions (Figure 20).

ROTEM was utilised to measure the viscoelastic properties of the fibrin clots. ROTEM measures the fibrin clot formation through the resistance to the movement of a rotating sensor pin placed in a cup containing the clotting mixture. More parameters can be derived from this technique as shown by a typical temogram (Figure 9) because, unlike the KC4 delta coagulometer, it does not stop moving once the clot has formed. The main parameter used from the temogram to investigate the kinetics of fibrin clotting was the α-angle. The ROTEM data was consistent with the KC4 delta coagulometer analysis; in purified and whole blood conditions, a decrease in α-angle was observed with increasing concentrations of rM1 (Figure 21). A decrease in α-angle reflects prolonged clot formations times and a decreased clot stability, implying that the coagulation factors are not functioning normally, and initiation of clotting is impaired.

The maximum clot firmness confirms this trend, whereby an increase in rM1 protein lead to a decrease in purified, plasma and whole blood clots stability (Figure 22) .The same trend was observed whether the clots were activated via the intrinsic cascade (INTEM) or the extrinsic cascade (EXTEM) activator. In both conditions, when whole blood clots are formed, the decrease in MCF could be attributed to a decrease in platelet function or platelet concentration. This could potentially be due to rM1- fibrinogen complex binding to the platelet integrins, although activation would not occur due to the absence of IgG antibodies against the rM1 protein (Shannon et al., 2007). However, when platelets were inactivated by cytochalasin D in the FIBTEM assays (Figure 22B), the trend was still observed suggesting that there is also insufficient fibrinogen levels (Cannata et al., 2021). It is important to note that when rPAM, plasminogen binding M protein, was added to the clotting mixture instead of rM1, no significant differences were observed in clot strength (see Appendix 7.2), suggesting it is not a property of all M proteins. The decrease in MCF in the presence of increasing concentrations of M1 is likely due to the formation of the rM1- fibrinogen complexes disrupting the fibrin clot formation. An explanation for the observed reduced stability, in all conditions with increasing concentrations of rM1 could be due to a decrease in cross-linking by FXIIIa.

3.4.3 Fibrin clot structure

Fibrin clots are stabilised by the formation of covalent isopeptide bonds by the plasma transglutaminase, FXIIIa. FXIIIa crosslinks glutamine and lysine residues in the γ chain and α chains of neighbouring fibrin monomers, forming γ -γ dimers, α-γ polymers and α-polymers, which mediates red blood cell retention and increases the clot stiffness (Byrnes et al., 2015). FXIIIa crosslinking has previously been shown to impact clot formation by decreasing

the clot firmness (Jambor et al., 2009), so was investigated as a possible explanation for the observed decrease in ROTEM α-angle and MCF, with increasing rM1 concentrations. Fibrin clots were formed with increasing concentrations of rM1 then reduced and subjected to SDS-PAGE analysis (Figure 24). The α-polymer chains were chosen as an indication of crosslinking due to the close proximity of rM1 to the γ-dimers in molecular weight on the gel. Densitometry analysis of the α-polymer bands (Figure 25A.) revealed at the lower concentrations of rM1 protein (0.48- 1.88 μg/ml), the band intensity was higher than the control condition (0 μg/ml rM1), suggesting an increase in cross-linking is occurring. However, above this concentration (3.75- 60 μg/ml M1) there is a dose-dependent decrease in band intensity until at 60 μg/ml, the band intensity is almost the same as the FXIIIa inhibitor condition (T101) suggesting very little cross-linking is occurring. Visual inspection of the γ-dimers suggests that the rM1 protein is having a smaller effect on the γ-γ crosslinking. However, there is a significantly less intense band at the 60 μg/ml rM1 condition, in comparison to the control (0 μg/ml rM1). FXIIIa cross-links the γ- chains very early in fibrin clot formation (Chen and Doolittle, 1971, Purves et al., 1987), whilst α-polymer chains are cross-linked at a much slower rate (Cottrell et al., 1979, Matsuka et al., 1996, Sobel and Gawinowicz, 1996). Crosslinking of the two chains are believed to play independent roles in fibrin clot formation and structure, with the α- chain influencing the fibre thickness, fibrinolysis rate and clot strength. Whilst the γ-chain plays a role in fibrin fibre appearance time and fibre density (Duval et al., 2014). Thus, suggesting the decrease in α-polymer chains could be an explanation for the decreased clot firmness in the higher concentrations of rM1. A D-dimer ELISA assay was used to confirm the observed decrease in cross-linking with increasing concentrations of rM1. A D-

dimer is a degradation product of cross-linked fibrin clots. A similar trend to the densitometry analysis was observed. At lower concentrations of rM1 (1.88- 15 µg/ml) an increase in D-dimer concentration was observed and at higher concentrations of rM1 (30-60 µg/ml) a dose dependent decrease in D-dimer, in comparison to the control condition (0 µg/ml M1) (Figure 25B). Whilst the D dimer is much higher at 3.75 – 15 µg/ml in these experiments, in comparison to the densitometry analysis, it is important to note that the D-dimer takes into account γ-chain cross-linking, whilst the densitometry was only analysing the α-polymer chains. A FXIIIa activity assay was performed to see if the rM1 was directly inhibiting the FXIIIa activity or indirectly inhibiting the FXIIIa crosslinking due to structural conformation causing inaccessibility of sites. As shown in Figure 26, there was no significant differences observed in the FXIIIa activity with increasing concentrations of rM1.

The decrease observed in the maximum absorbances (turbidimetric experiments), α-angle, MCF (ROTEM) and fibrin clot cross-linking (densitometry and D-dimer) with increasing concentrations of rM1 protein, all suggest a significantly altered clot structure. The Darcy constant, or Ks, were calculated from permeation experiments, which represents the average pore size of the purified or plasma fibrin network (Carr et al., 1977). As shown in Figure 23, a similar profile is observed in both purified (Figure 23A and B) and plasma (Figure 23C and D) conditions; at lower concentrations of rM1 a non-significant decrease in porosity was observed in comparison to the control (0 µg/ml M1), and above concentrations of ~23 µg/ml M1 a significant increase in porosity was observed. The higher concentrations of rM1 caused more inter-experimental variability suggesting that heterogeneous clots were being formed. The porosity data appears to be inversely related to the FXIIIa experiments,

with increased cross-linking at the lower rM1 and decreased cross-linking at the higher rM1 concentrations. This is consistent with previous *in vitro* studies investigating the impact of FXIIIa on fibrin clot porosity which have indicated that purified fibrin clots formed in the presence of FXIIIa had a 2.1-fold decrease in permeability (Ks) in comparison to clots formed in the absence of FXIIIa (Hethershaw et al., 2014).

The fibrin clot architecture in the presence of increasing concentrations of rM1 protein was visualised in both dehydrated and hydrated conditions using SEM and LSCM. Based upon the decreased absorbance with increasing concentrations of rM1 protein, observed in the turbidimetric results (Figure 19C and D), the fibrin clots with rM1 were expected to be denser with thinner fibres in comparison to the control (0 µg/ml M1). As demonstrated in the represented SEM images (Figure 27), upon visual inspection at lower concentrations of rM1 the fibrin clots appeared to be denser and heterogeneous with irregular fibre bundles and compacted fibrin. At the highest concentration of rM1 (60 µg/ml), the overall clot structure was lost. However, there was still evidence of fibrin fibres being formed. The major limitation of SEM is during sample preparation the specimens need to be dehydrated because the imaging is conducted under vacuum. Dehydration leads to fibrin fibre shrinkage that can cause underestimations of diameter and fibre length and overestimates the fibre density (Collet et al., 2000b, Baradet et al., 1995). Additionally, ROTEM has demonstrated that a dramatic decrease in clot firmness is occurring with increasing concentrations of rM1 protein (Figure 22) therefore it is also a possibility that the loss of clot structure observed in the images at the highest concentrations is also a dehydration preparation artefact (the clots are collapsing). The fibrin fibre diameter could not be calculated from the images

due to the presence of plasma proteins coating the fibres. Plans were put into place to repeat the experiments with additional washes to remove these proteins, however due to travel restrictions because of Covid-19 pandemic and time limitations this was not possible.

To overcome the limitation of potential dehydration preparation artefacts observed in SEM imaging, the plasma (Figure 28) and purified (see Appendix 7.1) fibrin clots with increasing concentrations of rM1 were visualised using LSCM. Whilst the resolution is much lower than SEM imaging, LSCM allows clots to be visualised in a fully hydrated native state spiked with a fluorescently labelled fibrinogen, Alexa fluor 594. The LSCM imaging in both purified and plasma samples are consistent with the SEM data (Figure 27) and porosity data (Figure 23), demonstrating the formation of dense clots with irregular fibre bundles at lower concentrations and at higher concentrations the fibrin clots visually show larger pores, irregular clusters and thick fibrin bundles. Interestingly, in plasma conditions, the fibrin fibres in the lowest concentrations of rM1 (1.2- 9.4 μg/ml) appeared to exhibit greater curvature in comparison to the control condition which appeared to be straighter, suggesting the presence of rM1 is causing the formation of less stiff fibres.

Similar fibrin clustering has been reported in other studies such as in the presence of a polymer, known as polyphosphates, which is secreted from activated platelets. Similar to rM1, in the presence of polyphosphates a reduced turbidity was observed and SEM analysis revealed heterogeneous clots, with tight fibrin fibre aggregates interspaced with large pores, in comparison to the control (absence of polyphosphates) which had a homogeneous fibre network (Mutch et al., 2010). However, the polyphosphate does not have any effect on fibrin cross-linking by FXIIIa and the porosity of fibrin clots decreased

suggesting the observed structure differences are due to a different mechanism than in the presence of rM1. rM1 has a calculated net charge of -6.25 at a pH of 7.4 giving it a negative charge (pI = 6.014), polyphosphates are also negatively charged and can bind fibrinogen suggesting some of the observed fibrin characteristics could be due to charge (Mutch et al., 2010).

As described in section (Section 1.2.2) Clfa from *Staphylococcus aureus* is a surface bound protein that is capable of binding to the fibrinogen γ -chain. Similar to M1 protein from S*treptococcus pyogenes*, cell bound Clfa is capable of activating platelets by binding the platelet integrin GPIIb/IIa, mediated by a fibrinogen bridge to GPIIb/IIIa platelet receptor. Clfa binds IgG and the Fc interacts with the platelet Fc receptor FcγRIIa. These interactions result in platelet aggregation and promote thrombus formation (Loughman et al., 2005). On the other hand, M1 protein is thought to be released from the cell surface and form complexes with plasma fibrinogen which bind IgG against the M1 protein and engages the platelet receptors (Shannon et al., 2007). The fibrinogen binding domain of Clfa has previously been isolated and truncated protein was produced to investigate the effect on clot formation properties. Similar to rM1, the addition of increasing concentrations of Clfa resulted in a decreased absorbance in turbidimetric assays, and a decrease in cross-linking by FXIIIa. Although, in relation to the cross-linking Clfa was thought to prevent γ-chain crosslinking (Liu et al., 2005), rather than α-chain cross-linking as observed in this project in the presence of rM1. The Clfa is thought to prevent the formation of fibrin clots through the binding of the C-terminal of fibrinogen γ-chain (Deivanayagam et al., 2002), with antithrombotic effects observed in mice (Liu et al., 2007). Whilst the M1 protein has been shown to bind to α and γ chains on the fibrinogen D domains (as described in section 1.4.2.1), these

interactions are thought to be distant from the γC- globular head that is responsible for platelet integrin binding and contains residues for γ-γ crosslinking (Medved et al., 1997, Macheboeuf et al., 2011), suggesting there is not inhibition of fibrin formation by the same mechanism as Clfa.

3.4.4 Fibrin clot fibrinolytic potential

As described in section 1.1.4.4, changes in the fibrin clot microstructure can affect the clots susceptibility to fibrinolysis by plasmin. For example, Collet *et al* demonstrated that clots with tight conformations and thinner fibres have a much slower lysis times than clots with thick fibres and loose conformations. However, at the individual fibrin fibre level, thinner fibres were found to be cleaved at a faster rate than thicker fibres (Collet et al., 2000a). There have also been many studies on effects of dysfibrinogenemia (coagulation disorders characterised by an abnormal form of fibrinogen), where typically fibrinogen mutations which result in fibrin clots with thin fibres, increased branch points, small pores and are stiffer, are lysed at a slower rate (Weisel and Litvinov, 2008). The permeation of plasmin and plasminogen activators through the fibrin network could play an important role in fibrinolysis rates. Purified clots, incorporating the plasminogen activator streptokinase, with increasing concentrations of rM1 were monitored with turbidimetric assays (Figure 30A), and time to 100% lysis was calculated from the fibrinolysis profile. Despite the observed decrease in clot firmness (ROTEM) and increased porosity at higher concentrations of rM1 (Ks), no significant differences were observed. The same was seen when measuring the mechanical resistance of the clot to calculate lysis time (Figure 30B), where no significant differences were observed with increasing concentrations of rM1. To better represent physiological conditions, a whole blood assay was used with increasing concentrations of rM1. Whole blood clots,

in the presence of rM1, were clotted around the edge of a well with tissue factor. A lysis solution, containing streptokinase was added to the surface and whole blood clot dissolution was measured kinetically using a BMG FluorStar® Omega plate reader. As expected, based upon the previous porosity and clot firmness results, increasing the rM1 protein concentration leads to the faster fibrin clot dissolution times (Figure 30C). ROTEM analysis also confirmed this trend which demonstrated a faster lysis time with increasing concentrations of rM1 (Figure 30D). The presence of red blood cells (RBC) has previously been shown to modify the structural and viscoelastic properties of clots, with high numbers of RBC leading to the formation of thicker fibrin fibres. However, the RBC do not appear to affect the permeability of the clots (Gersh et al., 2009, Carr and Hardin, 1987). The presence of RBC and platelets in the whole blood condition could explain the observed differences between purified and whole blood conditions. Fibrinolysis occurs in two major steps, the first involving the conversion of plasminogen to plasmin by a plasminogen activator. It was therefore of interest to see if the presence of rM1 changed the rates of plasminogen activators leading to the apparent increase in susceptibility to lysis. Fibrin clots were formed with increasing concentrations of rM1 then plasminogen activator and a substrate specific for plasmin was added to the surface of the preformed clot. As plasmin is generated, the chromogenic substrate is cleaved to release a chromophoric group which was monitored kinetically at 405 nm, and the rate is used as a measure of plasminogen activation. However, as shown in Figure 31 increasing the concentration of rM1 bound fibrinogen does not affect the rate of plasmin generation in host plasminogen activators, uPA and tPA, or the streptococcal plasminogen activator, streptokinase (Figure 55). Therefore, suggesting that the differences

in dissolution rates are due to structural changes in the clots with increasing concentrations, rather than the generation of more plasmin by plasminogen activators.

The streptokinase used in this experiment (WHO 3rd International Streptokinase (00/464)) is fibrin independent and does not require fibrin for plasminogen activation (Huish et al., 2017). uPA also does not have a binding sites for fibrin, but tc-uPA has been shown to activate glu-plasminogen at a 10-fold higher rate in the presence of fibrin which is thought to be due to the plasminogen conformational change upon fibrin binding (Cesarman-Maus and Hajjar, 2005). However, tPA binds to fibrin C-terminal lysine residues via the finger domain to activate plasminogen, with the presence of fibrin increasing the tPA activity by 100-1000-fold (de Vries et al., 1991, Rijken et al., 1982, Hoylaerts et al., 1982). It would therefore be of interest to repeat the fibrinolysis experiments with the presence of host plasminogen activators, to see if the dense fibrin clusters and change in fibrin structure reduces the ability of the tPA to bind the fibrin clots.

3.4.5 Fibrin clot biofilm

A recent study demonstrated that the surface of the clot is covered by a protective fibrin film, which encapsulates and helps retain blood cells whilst providing the first line of defence against bacterial invasion. The fibrin film forms during conversion of insoluble fibrinogen to soluble fibrin at the air-liquid interface of the clot and it is distinct from the fibrin network structure underneath (Macrae et al., 2018). The impact on the formation of the fibrin film in the presence of increasing concentrations of rM1 was investigated by LSCM. To begin with a 10 µm z-stack of the fibrin biofilm with and without the presence of rM1 was imaged. The z-stacks were flattened into a 2D-image with maximum intensity projections (Figure 32) The arrow demonstrates the present of the

fibrin film in the control condition (0 µg/ml M1), which appeared to be absent in the presence of rM1 (1.88 µg/ml M1). The advantage of LSCM is the ability to reconstruct z-stacks into 3D images. Therefore, the next steps were to form clots with increasing concentrations of rM1, then image 20 µm z-stacks of each air-liquid interface. The z-stacks were then reconstructed in Imaris software to create a 3D-image of the fibrin film (Figure 33), the clots were pseudo-coloured, as per the key, to represent the intensity of the fibrin. The arrow demonstrates the fibrin film in the control condition, distinct from the fibrin film underneath with the fibrin film at the maximum end of the scale. As the rM1 protein concentration increases, holes or pores begin to form in the film and the intensity begins to decrease. Until at the maximum concentration tested (60 µg/ml M1), the film is no longer distinguishable from the fibrin network underneath.

The proposed mechanism (Figure 39) for fibrin film formation is that upon exposure to air, for example after injury, fibrinogen molecules are absorbed to the air liquid interface forming an organised monolayer. At the same time, tissue factor stimulates fibrin formation via the extrinsic cascade. Fibrin(ogen) continues to rise to the air-liquid interface and begin to form as half-staggered fibrin molecules and the formation of layers of fibrin builds up through A-a knob-hole interactions and the formation of fibres. Which eventually leads to the formation of a continuous layer of fibrin across the clot surface. Additionally, the film can form in the absence of FXIIIa cross-linking (Macrae et al., 2018). The crystal structure of the M1-fibrinogen complex has demonstrated that M1 protein binds fibrinogen D domains in a cross-like pattern (Macheboeuf et al., 2011). This could provide an explanation for increase in fibrin film pores/holes in the presence of rM1, with the film being entirely absent at the highest concentrations. The conformation of the rM1- fibrinogen complex could be

inhibiting the formation of the dense D domains at the air-liquid interface and preventing the rapid rise of fibrinogen molecules to the surface forming an organised monolayer upon exposure to air.

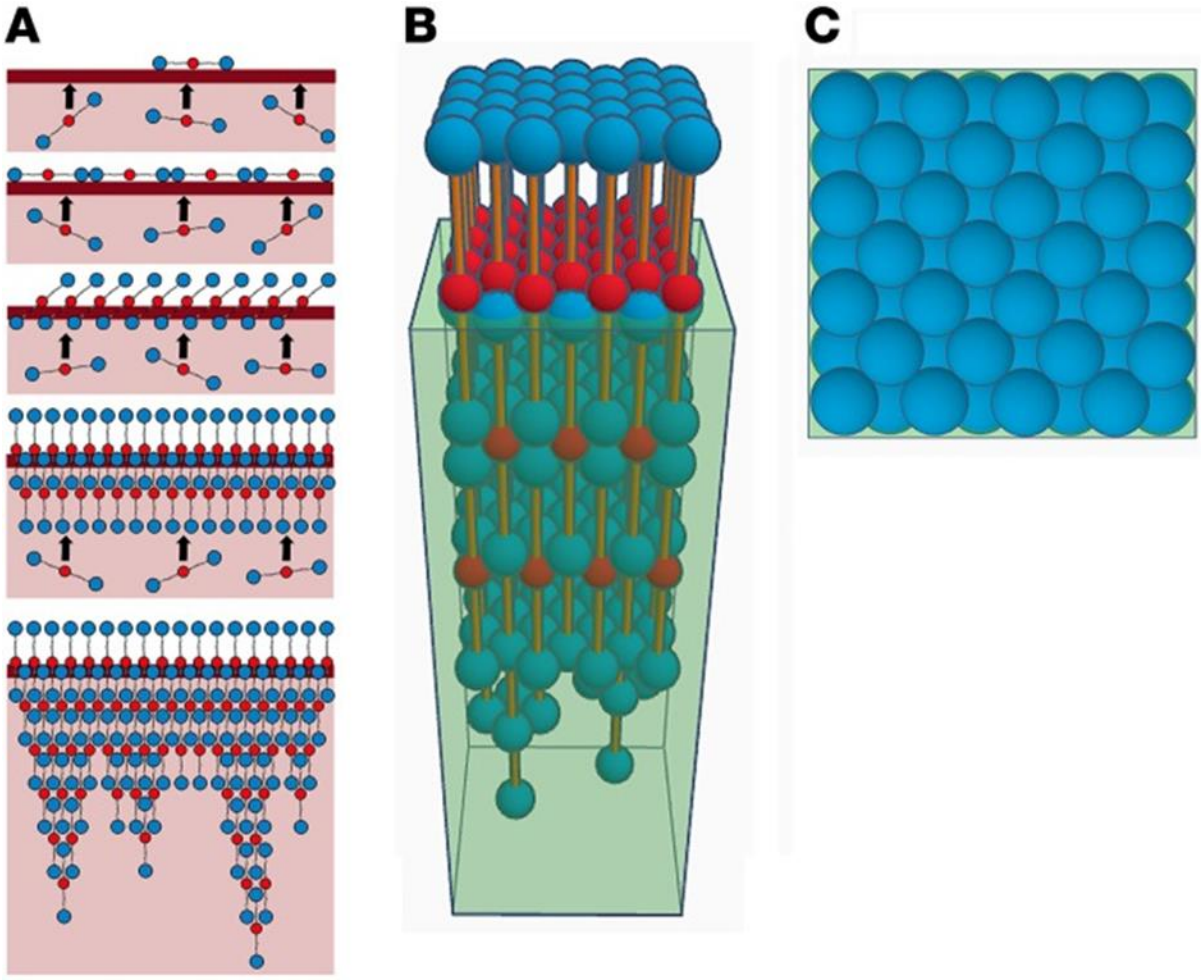

Figure 39 Proposed model for fibrin film formation at the surface of a clot. A. Proposed model in 2D of insoluble fibrin(ogen) rising to the air-liquid interface and forming half-stagged fibrin molecules. D domains are represented with blue spheres, whilst E regions are represented by red spheres. (B.) Side view of proposed 3D-model of the fibrin film with half-staggered fibrin molecules. (C) View from the top of the 3D fibrin model. *Image reused from 'A fibrin biofilm covers blood clots and protects from microbial invasion' © 2018 Macrae et al, (Macrae et al., 2018), is licensed under CC BY 4.0*

3.4.6 Bacterial migration assays

Bacterial migration assays were developed from previous literature (Macrae et al., 2018), in order to investigate the movement of *Streptococcus pyogenes* through fibrin clots with increasing concentrations of rM1 (Figure 16). Purified fibrin clots, with increasing concentrations of rM1, were formed in Falcon™ cell culture inserts. *Streptococcus pyogenes* were fluorescently labelled with Molecular Probes™ BacLight™ Green Bacterial Stain. One of the first changes made to the original protocol was the low nutrient broth that *Streptococcus pyogenes* was resuspended in, and the high nutrient broth that was placed into the wells of each plate. C-media (Table 1) was chosen as a low nutrient broth for *Streptococcus pyogenes*. This is a low glucose media which is thought to represent non-preferred environments encountered by GAS during infection of soft tissues or other environments limiting carbohydrates (Valdes et al., 2018, Gera and McIver, 2013). The high nutrient media placed into the well for the bacteria to disseminate into was a rich THY medium (Table 1). Different growth rates for GAS were observed in the different media, with THY medium demonstrating the fastest growth rates (Figure 34B).

Each fibrin-rM1 clot condition, formed in the cell culture inserts, was placed in the wells as demonstrated in Figure 16. Then fluorescently labelled *Streptococcus pyogenes* suspended in C-media was added to the clot surface. The fluorescence and OD_{600} of the THY media in the well were then measured at different time intervals for up to 49 hours for evidence of bacteria perforation through the clot.

These experiments were performed using different bacteria to the literature migration assays (Macrae et al., 2018), so there were some methodological issues. Early experiments demonstrated no increase in fluorescence through

the fibrin clots, despite an increase in absorbance. The control condition without the presence of bacteria showed no contaminant growth in the media, suggesting the increase in absorbance was GAS in the other conditions (data not shown). To confirm this, all further experiments were supplemented with 20 µg/ml neomycin, which is a selective marker for GAS (Blanchette and Lawrence, 1967). The GAS was also trypsin treated prior to being fluorescently labelled to remove bacterial surface proteins which may be binding to the fibrin and preventing the fluorescently labelled GAS from migrating through the clots (Khakzad et al., 2021). The trypsin was inactivated with fetal bovine serum (FBS), and GAS were washed with PBS before the experiment proceeded to prevent interactions with the fibrin clots.

High concentrations of rM1 caused the formation of clots with increased porosity (Figure 23), decrease clot strength (MCF, Figure 22), decreased FXIII cross-linking (Figure 25) and a decrease in the protective film (Figure 32 and Figure 33). Therefore, GAS was expected to migrate through clots formed with higher concentrations of rM1 at a faster rate in comparison to the control condition (absence of rM1). Pilot studies (n=1, Figure 36) indicated that the GAS migrated through fibrin clots with the two highest concentrations of rM1 tested first (30 and 7.5 µg/ml M1). Whilst the fibrin clots containing low concentrations of rM1 (1.88 µg/ml) and the control clot (0 µg/ml M1), were the last to see bacterial perforation.

The fluorescence increases in comparison to the absorbance increase observed was very low for this experiment again (Figure 36A). At the end of the experiment, the remaining bacteria was removed from the surface of the clots and the fluorescence was measured. The majority of the fluorescently labelled bacteria appears to have not migrated (n=1, Figure 37).

One theory to explain the results of this experiment, could be due GAS ability to form microcolonies (Figure 40). Whilst the M1 protein was removed from the fluorescently labelled bacteria prior to experiment start, by trypsin treatment, there are other GAS cell bound proteins such as the GAS pili which are trypsin resistant (Mora et al., 2005). GAS pili can mediate binding to fibrin surfaces and initiate the formation of biofilms and microcolonies (Fiedler et al., 2015) (Figure 40). These microcolonies provide defence against biological, physical and chemical stress whilst facilitating bacterial growth, before dispersal of bacteria (Vyas et al., 2019). It is highly plausible that a similar mechanism is occurring here, where the initial fluorescently labelled bacteria is mediating binding to surfaces and the resultant unlabelled bacterial growth is the first to disperse through the clots. The first steps to investigate the issue with the fluorescently labelled bacteria would be to visualise the bacterial migration using LSCM. The LSCM could provide information on fluorescently labelled bacteria localisation. Further work with this experiment could involve the introduction of GAS with fluorescent proteins integrated into the genome (Liang et al., 2019, Aymanns et al., 2011), rather than the use of a dye that binds to the membrane and only labels the parent bacteria.

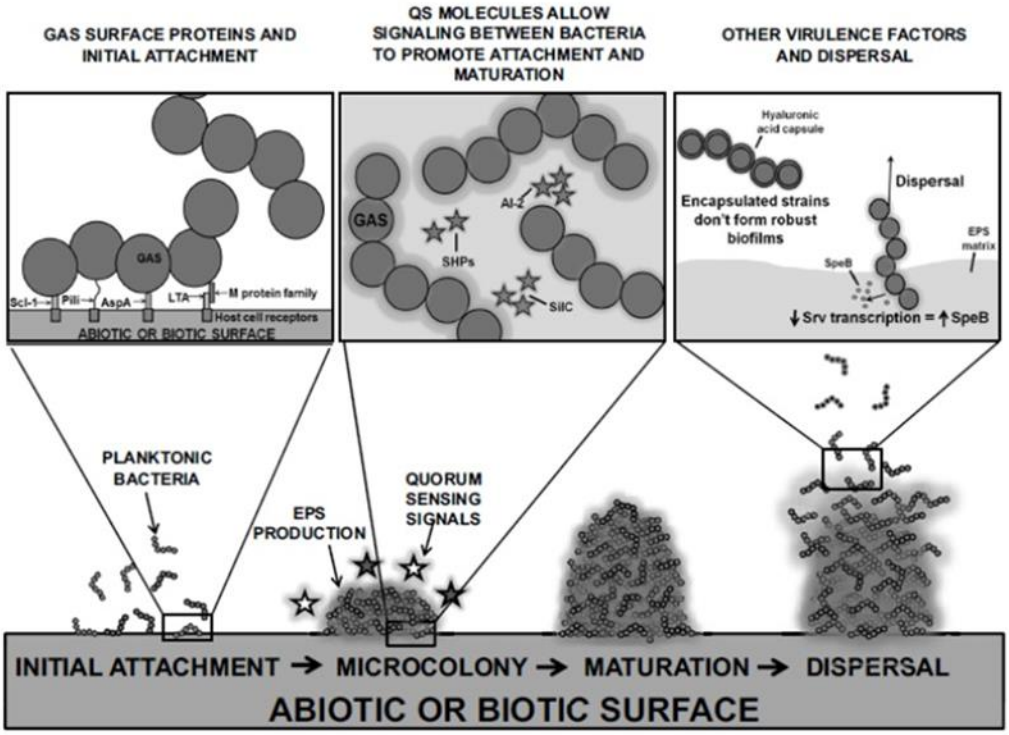

Figure 40 GAS microcolony formation. Many GAS surface proteins aid in the initial attachment to surfaces which is driven by environmental cues (e.g. pH, temperature, nutrients). This includes Streptococcal collagen-like protein (Scl-1), pili, Group A Streptococcus Protein A (AspA), as well as members of the M protein family. Following irreversible attachment, Extracellular Polymeric Substances, consisting of polysaccharides, nucleic acids and lipids are produced forming a meshwork for a biofilm. Microcolonies begin to form. Biofilm maturation induced by quorum sensing signals initiating phenotypical changes and genetic diversification. Enhanced structural defence against biological, physical, and chemical stress. Facilitates reproductive ability. Dispersal of bacteria into host environment occurs due to physical forces or in response to environmental changes (Vyas et al., 2019) *Image reused from 'Current Understanding of Group A Streptococcal Biofilms' © 2019 Bentham Science Publishers (Vyas et al., 2019), is licensed under CC BY-NC 4.0*

3.4.7 Future work

There are further experiments that could be done in the future to complement the findings of the impact of rM1 on fibrin clot properties. During fibrin clot formation, the fibrinopeptide A and B release from fibrinogen in the presence of rM1 could be monitored by high-performance liquid chromatography (HPLC), to further investigate the impact of M1 on polymerisation kinetics (Mutch et al.,

2010, Cooper et al., 2003) Fibrinopeptide B related inhibition can result in structural changes, with B:b knob hole interactions found to impact clot susceptibility to lysis (Section 1.1.3.1).Furthermore, the clotting and lysis could be monitored using LSCM. This would provide an explanation to the lack of fibrin film formation and provide information on whether the fibrinogen-bound-M1 reaches the air-liquid interface but the conformation prevents the formation, or whether the fibrinogen-bound-M1 does not rise to the air-liquid surface at all. Visualising the fibrinolysis could provide an explanation for the observed differences in lysis times between whole blood and purified conditions.

The kinetics of fibrin fibre formation and network formation has been studied extensively in static conditions in this project. In GAS infections, thrombi are often found to occupy diverse tissue locations (Barker et al., 1987, Ashbaugh et al., 1998). There are experiments available to visualise fibrin clot deposition and morphology under shear flow conditions using a microfluidic device, which could be developed to incorporate the rM1 protein. The device flows fibrinogen at a desired shear weight into one channel, whilst introducing thrombin into another channel. The resultant deposited clots are fixed and imaged by electron microscopy (Neeves et al., 2010).

There are other M proteins that are capable of binding fibrinogen in plasma including M5, M6, M12, M14, M18, M19, M23, M54 and M57 (Sanderson-Smith et al., 2014, Glinton et al., 2017). The B repeat regions are responsible for binding fibrinogen, however they do not share a high sequence identity, for examples M5 has only 24% sequence identity to the M1 B-repeat regions (Ringdahl et al., 2000). M3 and M5- protein serotypes have also been found to be capable of forming a complex with fibrinogen and IgG to activate platelets in a similar mechanism to M1 (Palm et al., 2021). Therefore, it would be of interest

to investigate the impact of other fibrinogen binding M proteins on the fibrin clot formation proteins to see if the difference in sequence variation translates to a different impact on clot structures.

Currently the data presented in this thesis is entirely based on *in vitro* experiments. Previous work has demonstrated that M1 protein mediates the formation of platelet-rich thrombi, and M1 has been found to be localised with aggregated platelets in tissue biopsies of a severe soft tissue infection demonstrating these events occur *in vivo* (Shannon et al., 2007). It would therefore be of interest to investigate the fibrin clot structure of these *in vivo* clots formed by M1 by SEM analysis, to see if our results translate.

Chapter 4 Studies on the functional relationship between streptokinase variants, and associated M like proteins

4.1 Introduction

Phylogenetic analysis of streptokinase β-domain from diverse strains of GAS has divided GAS into 3 distinct evolutionary clusters based upon sequence variations (cluster 1, 2a and 2b). The phylogenetic studies also demonstrated that the streptokinase clusters were associated with tissue specific *emm* patterns of the bacterium (Figure 6) (McArthur et al., 2008). The streptokinase protein sequence is highly conserved between the different clusters and displays 85 % amino acid sequence identity to the well characterised Group C streptokinase H46a (SK H46a) used as a thrombolytic drug (Huang et al., 1989). However, the small sequence differences appear to contribute to different plasminogen activation properties. SK 2a is commonly associated with the fibrinogen binding M1 protein, and displays low plasminogen activation levels in solution assays without co-factors, but is maximally stimulated by fibrin (Huish et al., 2017). The significance of M1-bound fibrinogen, either at the cell surface or free in solution following cleavage for plasminogen-activation by SK 2a is not fully understood. Similarly, SK 2b has almost no activity in solution but is greatly enhanced in the presence of its M protein, PAM and further still in the presence of fibrinogen (Cook et al., 2012, McArthur et al., 2008). Cluster 1 streptokinase however behave like Group C streptokinase, whereby cluster 1 can optimally activate plasminogen free in solution and does not appear to coincide with specific M proteins (McArthur et al., 2008). The decrease in SpeB, increases the cell-bound M protein which is proposed to promote cell surface plasmin generation, through the formation of a trimolecular complex with streptokinase, plasminogen and fibrinogen, allowing the bacterium to degrade

through host barriers and disseminate from point of infection (Cole et al., 2011). However, the relationship between streptokinase sequence variations, M-like protein association and bacterial pathogenicity is not fully understood at the molecular level.

The specific objectives were;

1. To research and design expression constructs for an additional streptokinase from cluster 2b, and associated M protein (PAM). To have sequences cloned into vectors by commercial gene synthesis and provided as lyophilised plasmid constructs. To transform these constructs into *E. coli* expression systems. Following trials, to express and purify rSK 2b and rPAM by affinity chromatography.

2. To determine activation kinetics of streptokinase variant rSK 2b without the presence of associated M proteins or cofactors relative to the WHO 3rd IS streptokinase (00/464) and confirm that specific activities of rSK H46a (Group C streptokinase) and rSK 2a are consistent with previously published data

3. To determine plasminogen activation activity of rSK 2b in the presence of fibrin(ogen) and confirm the activities of rSK H46a and rSK 2a are consistent with previously published data by developing chromogenic solution assays to incorporate fibrinogen. To measure plasminogen activation activity upon addition of streptokinase variants to the surface of a preformed clot incorporating a chromogenic substrate specific for plasmin.

4. To investigate the impact of solution and immobilised rM1 protein on streptokinase variants activity, by developing chromogenic solution assays and clot lysis profiles (with plasminogen) incorporating M1 protein. To develop immobilised microtitre plate assays using rM1 protein, with a C-terminal

Histidine tag to mimic cell surface plasmin generation. Fibrinogen will be incorporated into assays to investigate the proposed trimolecular complex formation.

5. To assess the impact of soluble and immobilised rPAM on streptokinase variants activity by developing immobilised microtitre plate using rPAM protein, with a C-terminal Histidine tag to mimic cell surface plasmin generation. To develop chromogenic solution assays (with plasminogen) including rPAM in microtitre plate assays. Fibrinogen will be incorporated into the assays to investigate the proposed trimolecular complex formation.

4.2 Methods

4.2.1 Cloning, protein expression and purification trials

4.2.1.1 Construct design

Expression constructs of recombinant streptokinase 2b (rSK 2b) and recombinant plasminogen binding M-protein (rPAM) were designed in Vector NTI. The gene sequences (from *Streptococcus pyogenes* strain, NS88.2) were obtained from the genetic sequence database (GenBank) using the following accession codes; streptokinase 2b: JX898186 and rPAM: AAQ64526.2

The region encoding the N-terminal signal peptides of rPAM and rSK 2b were removed from both gene sequences and replaced with a Profinity eXact fusion-tag (Biorad). Additionally, for rPAM, the propeptide sequence was removed and a linker region followed by 6 histidine codons was added to the 3' end of the rPAM sequence to produce a flexible C-terminal 6x Histidine tag. A NcoI restriction site was added in front of the N-terminal fusion tag and a NotI restriction site was placed after the stop codon to enable cloning into a pET-27b expression vector (Figure 41).

The sequences, codon optimised for expression in *E. coli*, were generated by commercial gene synthesis and cloned into the pET-27b vector (GenScript Biotech; Piscataway, NJ, USA). The expression constructs were provided as lyophilised plasmids which were reconstituted in double distilled water to a final concentration of 100 ng/ml, ready for transformation into competent cells.

Primers were also designed for rSK 2b as a contingency plan to enable sub-cloning into a SUMOstar vector, to investigate an alternative expression strategy in case there were complications with the Profinity eXact fusion tag that

would require extensive troubleshooting. The SUMOstar fusion tag has shown success with streptokinase 2a in previously published data (Huish et al., 2017).

4.2.1.2 Heat-shock transformation

The rSK 2b and rPAM plasmid constructs were transformed into two different expression strains of *E. coli*: Rosetta™ 2 (DE3) (Merck Millipore) and T7 Express LysY (New England Biolabs). Chemically competent cells of both strains were transformed according to the manufacturers' instructions; 50 µl of Rosetta™ 2 and LysY competent cells were thawed on ice then transferred to a pre-chilled 0.5 ml Eppendorf. Reconstituted plasmid (2 µl of 100 ng/µl from section 4.2.1.1) was added and mixed by tapping the tube. The mixture was returned to ice for 15 minutes before being heat-shocked in a 42ºC water bath for precisely 120 seconds, then returned back to ice for 2 minutes. SOC media was pre-warmed to 37ºC and 800 µl was added to the heat-shocked mixture then placed into a 37ºC incubator shaking at 250 rpm for 60 minutes. The transformation mixture was streaked onto LB agar plate containing 50 µg/ml Kanamycin, then incubated at 37ºC overnight. Plasmids were also transformed into a cloning vector, TOP10 chemically competent *E. coli* cells, using this method. The procedure was repeated twice for each plasmid construct and expression system.

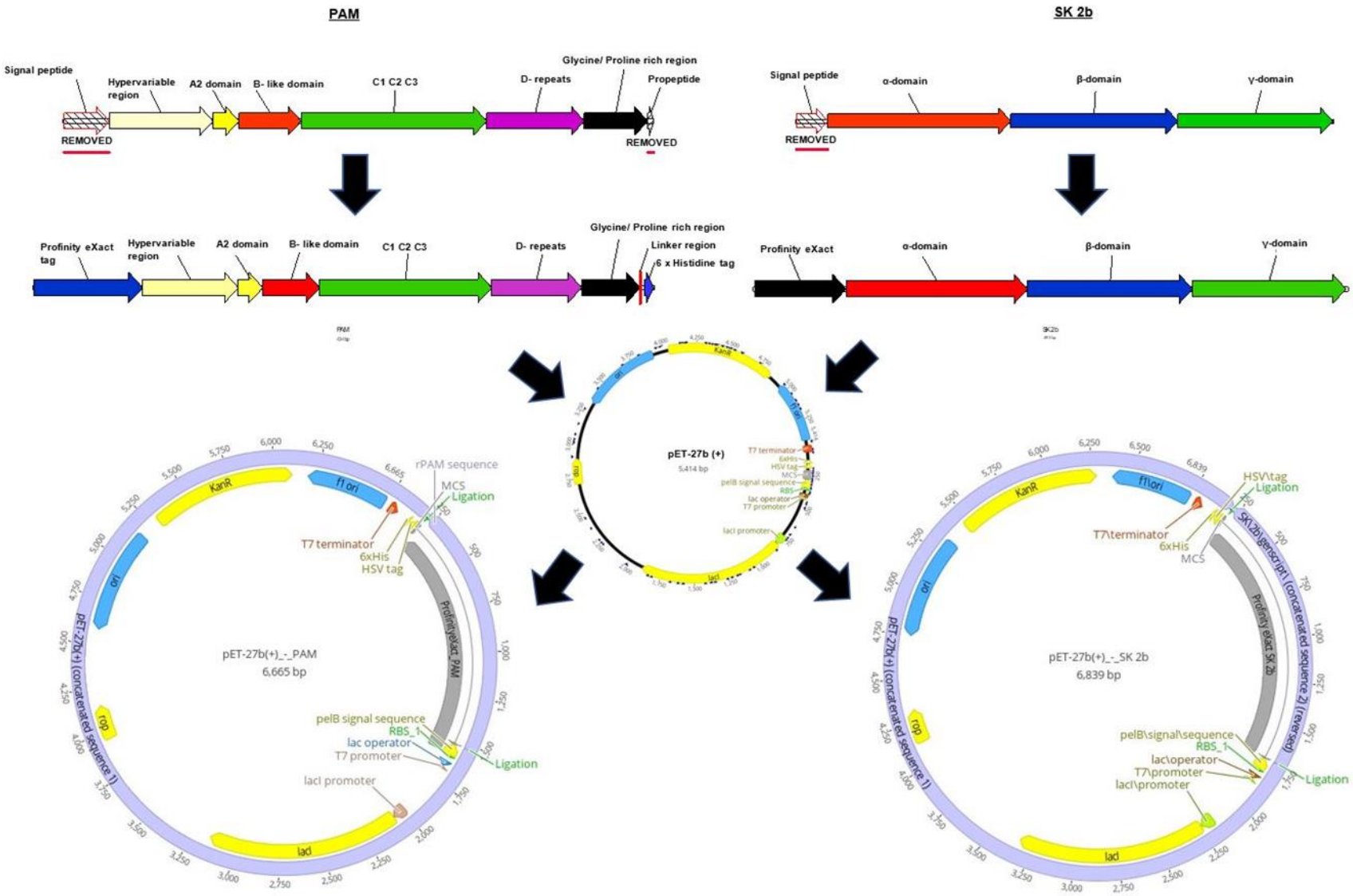

Figure 41 rPAM and rSK 2b construct design. The region encoding the N-terminal signal peptides of rPAM and rSK 2b were removed from both gene sequences and replaced with a Profinity eXact fusion-tag (Biorad). Additionally, for rPAM, the propeptide sequence was removed and a linker region followed by 6 histidine codons was added to the 3' end of the rPAM sequence to produce a flexible C-terminal 6x Histidine tag. A NcoI restriction site was added in front of the N-terminal fusion tag and a NotI restriction site was placed after the stop codon to enable cloning into a pET-27b expression vector. The sequences, codon optimised for expression in *E. coli*, were generated by commercial gene synthesis and cloned into the pET-27b vector (GenScript Biotech; Piscataway, NJ, USA).

4.2.1.3 Expression and solubility screening

Following the transformation (Section 4.2.1.2), two colonies from each LB agar plate were picked and used to inoculate 10 ml of LB broth (containing 50 µg/ml Kanamycin) then incubated overnight at 37ºC (shaking at 250 rpm). Glycerol stocks were prepared as 1 ml stocks from the overnight culture to a final concentration of 15% glycerol and stored at -80ºC. A small scale expression was then performed to check the expression, yield and solubility of each protein in each expression system. Briefly, LB broth (containing 50 µg/ml Kanamycin) was inoculated with the overnight culture, 1:50 ml dilution, and placed shaking at 37ºC until the culture reached an OD_{600} of 0.5-0.7. Recombinant protein expression was induced with the addition of 0.4 mM isopropyl β-D-1-thiogalactopyranoside (IPTG). A non-induced control was also included during the screening process for each condition and expression system. The samples were then either placed in a 37ºC incubator shaking at 250 rpm for a further 4 hours, or placed in an 18ºC incubator, shaking at 250 rpm overnight. The cultures were harvested by centrifugation at 4355 G for 20 minutes at 4ºC and the pellets were stored at -40ºC until further analysis.

The bacterial pellets were lysed by B-PER as described in section 2.4.1. The separated insoluble, soluble, and whole cell (before separation by centrifugation) fragments were reduced and subjected to SDS-PAGE analysis to visualise protein expression, solubility, and yield.

4.2.1.4 Purification trials

Purification trials were conducted using Profinity eXact mini spin columns to check purification conditions and ensure efficient tag removal. Briefly, Profinity eXact wash buffer and Profinity eXact elution buffer (as described in Table 1), were prechilled at 4ºC. The storage buffer from the Profinity eXact spin columns

was removed by centrifugation at 1000 x g for 30 seconds. The resin was equilibrated with 500 µl Profinity eXact wash buffer then centrifuged at 1000 x g for 30 seconds. This step was repeated twice. Following lysis of the bacterial pellets, as per section 4.2.1.3, 600 µl of the insoluble fraction was added to the columns. The lysate was gently mixed with the resin with a pipette then the column was placed on a rocking platform for 20 minutes at 4ºC. The column was then centrifuged at 1000 x g for 30 seconds and the flow through was retained for SDS PAGE analysis. The resin was washed twice with 500 µl of Profinity eXact wash buffer, with centrifugation at 1000 x g for 30 seconds, in-between washes. The native protein was eluted with the addition of 500 µl of Profinity eXact elution buffer. The buffer was mixed into the resin by pipetting and the samples were incubated on a rocking platform at room temperature for 30 minutes. After the 30 minutes, columns were centrifuged at 1000 x g for 30 seconds and the collected fractions were retained for SDS PAGE analysis. The elution step for repeated twice to ensure all protein was collected.

4.2.2 Protein expression and Purification

Recombinant streptokinase 2a (rSK2a) and recombinant M1 (rM1) protein were provided as expression constructs in the form of a glycerol stock by Dr. Craig Thelwell. The expression constructs were designed to produce rSK 2a and rM1 proteins with N-terminal fusion tags (SUMOstar and Profinity eXact respectively). Recombinant streptokinase H46a (rSK H46a) was available as a lyophilised protein in sealed ampoules, value assigned in IU relative to the WHO 3rd international standard for streptokinase (00/464) (WHO 3rd IS Streptokinase (00/464)) by Dr. Sian Huish (Huish et al., 2017).

The large-scale expression and purification of the recombinant proteins were performed as per section 2.4 .

4.2.3 Solution plasminogen activation

Solution plasminogen activation tests were performed as per section 4.2.3. Briefly, the plasminogen activation activity of the streptokinase variants was determined against the WHO 3rd IS SK (00/464) in accordance to the European Pharmacopoeia method (EP)[2]. Plasmin generation was measured using the chromogenic substrate S2251 (Chromogenix), which is cleaved by plasmin to release a chromophoric group, pNa, and can be monitored kinetically. A dilution range of streptokinase (4.8-0.6 IU/ml) was mixed with 100 nM glu-plasminogen (HYPHEN BioMed) and 0.6 mM S2251 substrate. All reactions were made up to a final volume of 100 µl per well. Where stated in the results, amendments were made to this method to investigate the effect of M proteins on streptokinase plasminogen activity. The assays included a dilution range of M protein (0-295.8 µg/ml rPAM or 0-60 µg/ml M1 protein) with 4.8 IU/ml streptokinase or a dilution range of streptokinase (4.8 IU/ml- 0.6 IU/ml) with 3.1 µg/ml M protein. In some experiments, the more readily activatable, Lys-plasminogen (Immuno, Vienna, Austria) was used in replacement to the Glu-plasminogen to a final concentration of 100 nM. Plasminogen activation was measured using a Molecular Devices Thermomax plate reader at OD_{405} at 30 second intervals for 90 minutes at 37ºC.

The raw data generated by Softmax Pro v5.0 (Molecular Devices) software was uploaded to an R script, written by Dr. Colin Longstaff, which calculates zymogen activation rates (Longstaff, 2016b). The initial rates of reaction of plasmin production was calculated from the gradient of transformed plots of

---

[2] [1]Streptokinase concentrated solution 07/2008: 0356 Ph Eur 9th Edition. Strasbourg, France: Council of Europe; 2013

absorbance (where the substrate and plasminogen were less than 10% consumed) verses time^2 (s).

4.2.3.1 Addition of fibrinogen

The plasminogen activation solution assays were also used to investigate the impact of fibrinogen on streptokinase plasminogen activation activity. A dilution range of streptokinase (4.8 – 0.6 IU/ml) was added to 3 mg/ml fibrinogen. Plasminogen activation was initiated through the addition of 100 nM glu-plasminogen and 0.6 mM S2251 substrate. Variations of this assay included keeping the streptokinase a constant concentration (4.8 IU/ml), whilst varying the fibrinogen concentration (5.8 mg/ml- 0 mg/ml). Additionally, where stated in results M1 protein or rPAM was included in this assay. Fibrinogen was obtained from different manufacturers in order to further investigate the effect of fibrinogen on streptokinase and potential fibrinogen contamination. The fibrinogen used in the experiments are included in Table 3. All of the fibrinogen sources were reconstituted in Buffer B (Table 1).

Brand/ Source	Depleted/Free from
Calbiochem®	Plasminogen depleted
Enzyme Research Laboratories	Plasminogen, von Willebrand Factor and Fibronectin depleted
HYPHEN-BioMed	Plasminogen free
University of Leeds	IF-1 purified (free from contaminants)

Table 3 Fibrinogen sources used in the experiments

4.2.3.1.1 Plasminogen contamination test

Due to some unexpected results, the presence of plasminogen contamination was investigated in fibrinogen batches. For a quick test, this was performed as per section 4.2.3.1 with varying concentration of fibrinogen, without the addition

of plasminogen. The initial rates of reaction of plasmin production were calculated from the gradient of transformed plots of absorbance (where the substrate and plasminogen were less than 10% consumed) verses time^2.

4.2.4 Fibrin clot overlay assays

Fibrin clot overlay assays were performed as described in section 2.7.2 with minor adjustments. Fibrin clots were pre-formed in a Corning™ NBS clear 96-well plate to a total volume of 60 µl at 37ºC by combining 3 mg/ml fibrinogen (plasminogen depleted, Calbiochem®) with 5 mM calcium chloride, 100 nM plasminogen and 0.5 IU/ml thrombin (01/578). Where stated in the results a dilution range of rM1 protein (0- 30 µg/ml) was incorporated into the fibrin clots. The clotting reagents were diluted with Buffer D (Table 1) in order to produce clear fibrin clots. Clots were formed at 37ºC for 60 minutes. A dilution range of streptokinase (4.8-0.6 IU/ml) was prepared in a separate microtitre plate, by diluting with Buffer D with the addition of 1 mg/ml HAS. The dilution range was combined with 0.6 mM S2251 and plasminogen activation was initiated by transferring 40 µl of the mixture to the surface of the preformed clots. Reactions were read using a Molecular Devices Thermomax plate reader at two absorbances (OD_{405} and OD_{650}) for 300 minutes with 30 second intervals at 37ºC. The raw data was exported to Microsoft Excel and each well was subtracted by the initial absorbance value from each time point. The normalised absorbance at (3x) 650 nm was then subtracted from the absorbance at 405 nm then uploaded to the R script which calculated the initial rates of reaction of plasmin generation as per section. The potencies and specific activities were then calculated as per section 2.8

4.2.5 Turbidimetric assessment of fibrinolysis by streptokinase variants

Clotting and lysis of fibrin clots was investigated by measuring the turbidity changes of fibrin clots as per section 2.7.3. with minor amendments. Briefly, 0.05 IU/ml thrombin (01/578), 5 mM calcium chloride, 3.1 µg/ml rM1 protein and a dilution range of streptokinase variant (2.4-0.3 IU/ml) was added to a Corning™ NBS clear 96-well plate. The reaction was initiated through the addition of a 3 mg/ml fibrinogen (Calbiochem®) and 100 nM glu-plasminogen solution. Where stated in results, streptokinase was a constant concentration of 0.225 IU/ml and a dilution range of rM1 protein (0- 30 µg/ml) was added. All fibrin clots were formed at 37ºC and to a total volume of 100 µl. Microtitre plates were immediately read for 5 hours, with 30 second intervals, at 37ºC using Molecular Devices Thermomax plate reader software Softmax Pro, v5.0 or v7.1. The data was exported to Microsoft Excel and each well was corrected by subtracting the initial absorbance value from each time point. The data was uploaded to an R script to analysis clotting and lysis parameters (Longstaff, 2016a). The R script can calculate multiple parameters including time between 50% clotting and 50% lysis and time to 100% lysis. Time between clotting and lysis was used to calculate potencies of the streptokinase variants using parallel line bioassay analysis. The specific activities were then calculated by dividing the potencies of each streptokinase by its protein concentration.

4.2.6 Halo assays

Fibrinolysis of whole blood clots in the presence of streptokinase was investigated using a whole blood microtitre plate assay, known as a halo assay, as described in section 2.7.4. Briefly, 5 µl of activation mixture (15% Innovin w/v, 67 mM calcium chloride and 0.62 µg/ml rM1 protein (or buffer B) was

added to the bottom edge of a Falcon® 96-well flat bottom microtitre plate. The activation mixture was then mixed around the bottom edge of the well with the tip of a p100 micropipette containing 25 µl of citrated whole blood. The whole blood clots were formed by incubating at 37ºC for 30 minutes. A dilution range (4.8-0.6 IU/ml, with Buffer C) of the streptokinase variants was prepared then carefully added down the side of each well, to ensure the clots were not dislodged. Reactions were monitored at OD_{510} on a FLUOstar® Omega microplate reader for 300 minutes with 30 second intervals and 5- second orbital shaking at 200 rpm. Each experiment contained a negative control (Lysis mixture without the addition of streptokinase) and a positive control (Blood was not activated with clotting mixture, instead this was substituted with Buffer B). The raw data was exported to Microsoft Excel then uploaded to an R script (Longstaff, 2018b). The R script corrects the data by zeroing each well by its initial time zero absorbance, then calculates several parameters from the raw data such as time to 50% lysis, area under the curve and max absorbance. The max absorbance reflects the time to 100% lysis; therefore, this was used to calculate streptokinase potencies. Potencies were calculated by parallel line bioassay analysis using CombiStats™ as per section 2.8. Specific activities were then calculated by dividing the calculated potencies by each streptokinase concentration.

4.2.7 Immobilised M protein assays

Cell-surface plasmin generation in the presence of M proteins was stimulated by binding the M- proteins, via the C-terminal histidine tag, to a Pierce™ nickel-coated 96-well plate as per section 2.7.5. The maximum binding capacity of the plates (according to the manufacturer's instructions) is ~9 pmol His tagged protein (27 kDa) per well therefore the M protein concentration used for binding

was calculated to be 10 mM rPAM and 11 mM rM1. M protein (10 mM rPAM and 11 mM rM1, 100 µl per well) was bound to the plates by incubating at room temperature with shaking for 1 hour. When M proteins were not included on the plate, the nickel was saturated with 15 µg/ml His-tagged human albumin, (ProSci^{TM}, Poway, CA, USA.). Excess protein was removed, and each well was washed three times with Buffer E (Table 1). Where stated in results, following binding rM1 to the plate, fibrinogen was then bound to the rM1 protein by incubating for 1 hour followed by washes. Where rPAM was immobilised, fibrinogen was included directly in assays without washes. The reaction was initiated through the addition of 0.6 mM S2251, 100 nM glu-plasminogen and a dilution range of streptokinase (4.8-0.6 IU/ml). Where stated in results, 100 nM Lys-plasminogen was used instead of Glu-plasminogen. The reactions were immediately measured at OD_{405} for 90 minutes at 37ºC on a Molecular Devices Thermomax plate reader. The raw data was exported to a Microsoft Excel document then uploaded to a R script that calculates the initial rates of reaction (Longstaff, 2016b). Specific activities were calculated as described in section 2.8.

4.3 Results

4.3.1 Expression and purification screening of rSK 2b and rPAM

The rSK 2b and rPAM pET-27b (+) expression constructs, generated by commercial gene synthesis, were reconstituted, and transformed into two different *E. coli* expression strains (Rosetta 2 (DE3) and T7 Express LysY) purchased as chemically competent cells. Transformed cells were streaked onto LB agar plates (containing appropriate antibiotics) and incubated overnight.

4.3.1.1 Expression and solubility trials

Following transformation, two colonies from each expression system (Rosetta 2 (DE3) and T7 Express LysY) were picked from the LB agar plates and used to inoculate 10 ml of antibiotic containing broth. The cultures were grown to mid-log phase (0.6-0.8, OD600) at 37ºC with shaking and for a further 4 hours following the addition of 0.4 mM IPTG to induce protein expression. Each expression construct included a culture that was not induced to check for leaky expression and to allow *E. coli* proteins to be differentiated from the proteins of interest. To assess the expression yield and determine the solubility of each protein, the cells were harvested, frozen, defrosted then lysed by B-PER bacterial protein extraction reagent. The soluble and insoluble fractions were then reduced and subjected to SDS PAGE analysis. As shown in Figure 42, both rPAM and rSK 2b were expressed as insoluble proteins in both expression systems.

Expression of rSK 2b (Figure 42A) was highest in the Rosetta 2 expression system, as demonstrated by the thick high-density band at approximately 56 kDa. Due to overexpression of the protein subsequently leading to overloading

of the lane, the bands are ‘smiley’ and spread further down the gel than expected. A thinner, less dense band is present in the LysY insoluble fraction indicating a lower yield. The cell lysate containing the rSK 2b plasmid without IPTG induction (uninduced lane) did not show any extra band at 56 kDa.

Expression of rPAM (Figure 42B) was also highest in the Rosetta 2 expression system, as demonstrated by the higher intensity of the band in the insoluble lysate at ~49 kDa in comparison to the LysY expression system. The cell lysate containing the rPAM plasmid without IPTG induction (uninduced lane) did not show any extra band at ~49 kDa.

4.3.1.1.1 Induction at lower temperature

One approach to increase solubility of recombinant proteins expressed in *E. coli*, is lowering temperatures to slow down the translation rate. This has been theorised to provide proteins with increased chance of folding into the correct structures (Mahmoudi et al., 2012, Singha et al., 2017). Therefore, the expression and solubility trials were further investigated in cultures induced at a lower temperature with a longer expression time to optimise the production of soluble protein. Cultures were grown to mid-log phase (OD600: 0.6-0.8) at 37ºC as before, however following induction by IPTG the cultures were placed into a shaking, 18ºC incubator for protein expression overnight. Protein expression yield and solubility were then assessed as above with SDS-PAGE analysis. As shown in Figure 43, the lower expression temperature led to a decrease in overall rSK 2b (Figure 43A) protein yield. The highest rSK 2b expression was seen in the insoluble fraction of Rosetta 2 expression system, with a band at approximately 56 kDa. However, an additional band is also seen in the Rosetta 2 lane, that is not present in the uninduced culture, at approximately 40 kDa suggesting some degradation of rSK 2b. An increase in soluble protein was

seen in both the Rosetta 2 and LysY expression systems, however in comparison to the higher temperature expression (Figure 42), overall protein yield remains low. The cell lysate containing the rSK 2b plasmid without IPTG induction (uninduced lane) did not show any extra band at 56 kDa.

rPAM expressed only as an insoluble protein, however in comparison to the higher temperature expression (Figure 42) the overall protein yield appeared slightly higher. The cell lysate for rPAM without IPTG induction (uninduced lane) did show expression of the protein, with a band visible at approximately 49 kDa, suggesting leaky expression. Tight regulation of the promoter is essential for protein expression because leaky expression can inhibit cell growth and lead to plasmid instability which reduces overall yield of the protein (Singha et al., 2017). Therefore, to minimise the basal level of expression, all further proteins were induced at 37ºC and expressed for 4 hours before being harvested by centrifugation. The insoluble fraction will be solubilised and purified.

4.3.1.2 Small scale purification

Small scale purification of rSK 2b and rPAM was investigated to identify suitable conditions for protein solubilisation, column-binding, and cleavage of the fusion tags. Due to previous success with the Profinity eXact Fusion-Tag system with rM1 used in the project, the same buffers and conditions were used initially. Insoluble pellets containing the protein of interest were solubilised in 4 M urea then successfully diluted to 2 M urea without the formation of insoluble aggregates. The solubilised fractions were loaded on to Profinity eXact mini prep columns and placed on a roller mixer for 20 minutes to allow the proteins to bind to the resin. The flow through was removed and retained for SDS-PAGE analysis. The column was washed before activating the resin's highly specific protease to release the proteins of interest from the Profinity eXact fusion tag,

which remained tightly bound to the resin, whilst the purified protein is eluted. The purification steps were analysed by SDS-PAGE analysis. As shown in Figure 44A, purification of rSK 2b was successful. The resin was slightly oversaturated, as demonstrated by the un-cleaved protein band at ~56 kDa in the flow through well (FT). The elution lanes show a band at ~48 kDa in both elution 1 and 2 lanes of the Rosetta 2 expression systems, indicative of cleaved native protein. Additionally, the extra band at ~56 kDa in the elution 1 lane of Rosetta 2 suggests insufficient washing of the resin and binding of the fusion protein. rSK 2b expressed in LysY *E. coli* had a very faint band at ~48 kDa in the elution 1 lane and a much darker band in the flow through suggesting insufficient binding of the protein to the resin.

rPAM was purified equally well in both expression systems (Figure 44B). The elution lanes in both the Rosetta 2 and LysY show a single band at ~41 kDa indicating successful cleavage of the Profinity tag. The flow through (FT) lane contains the un-cleaved protein, as indicated by the band just above 49 kDa due to oversaturating of the resin.

Whilst rPAM, purified equally well in both expression systems (Figure 44B), rSK 2b expressed in LysY only displayed a faint band suggesting low binding to the column and much higher intensity band in Rosetta 2 (Figure 44A). Additionally, during expression trials, rPAM expressed the highest in Rosetta 2 (Figure 42B). Therefore, all further proteins were expressed using the Rosetta 2 expression system.

4.3.2 Large scale purification

Following the small-scale expression trials, the protein expression was scaled up. Bacteria was recovered from the glycerol stocks by inoculating 10 ml of LB

(with appropriate antibiotic, see Table 2) with a sterile inoculating loop containing a scrape of the frozen stock. This was grown to saturation (overnight at 37ºC, shaking at 250 rpm). Pre-warmed LB (500 ml with appropriate antibiotic) in 2 L shake flasks was inoculated with 10 ml of overnight culture. Recombinant protein expression was induced by the addition of IPTG to a final concentration of 0.4 mM and incubated for a further 4 hours shaking at 250 rpm. The cultures were harvested by centrifugation at 4355 g for 20 minutes at 4°C. The large-scale purification (Section 2.4) was performed using affinity chromatography on a FPLC system. rM1, rPAM, and rSK 2b were expressed with N-terminal Profinity eXact Fusion tags and purified as per section 2.4.1.1. Whilst rSK 2a was expressed with an N-terminal SUMOstar tag and purified as per section 2.4.1.2. The Profinity eXact fusion proteins were cleaved on the column by activating the protease ligand on the resin; the SUMOstar fusion tag associated with rSK 2a required an addition cleavage step following elution to remove the tag. All of the protein sources are listed in Table 2. Typical protein yields of 1- 4 mg of recombinant protein per L of culture were produced, except for rSK 2a, which expressed at 175- 420 µg per L of culture.

Purity and relative molecular weights of the fusion and cleaved proteins were assessed by SDS-PAGE analysis (Figure 45). Several batches of each protein were made and pooled together and estimates of protein concentration were determined by BCA analysis relative to an albumin standard.

.

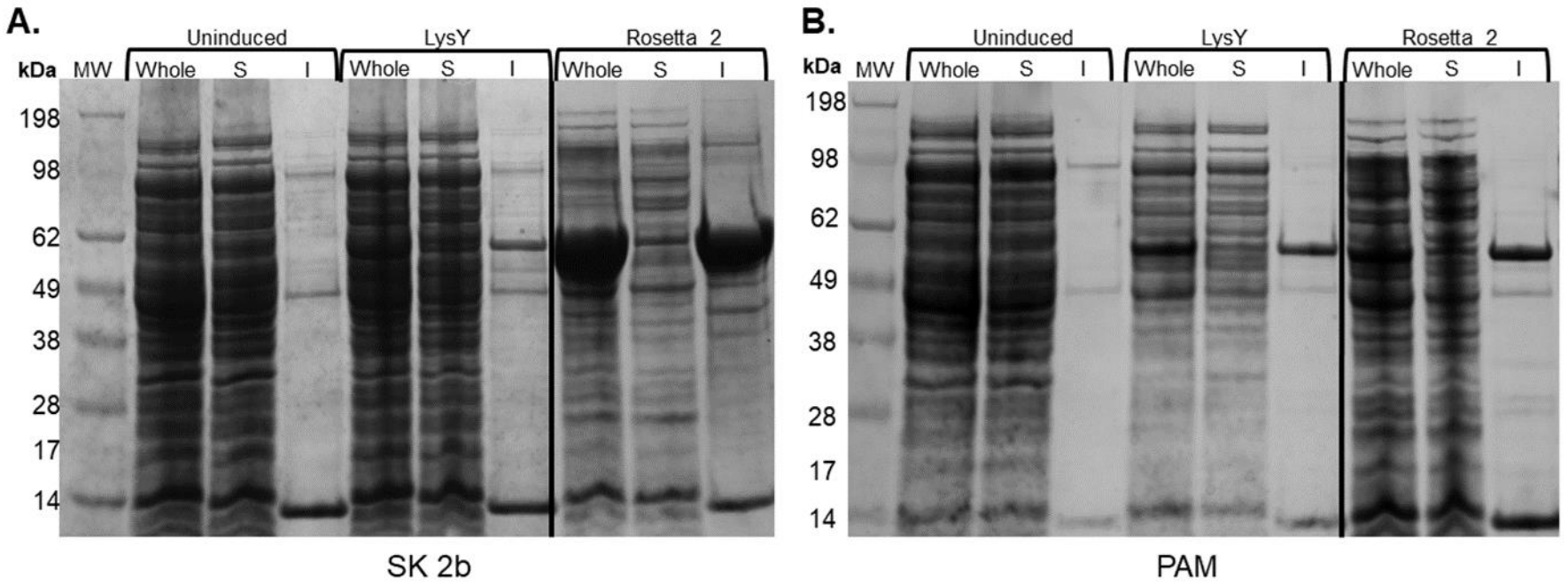

Figure 42 Representative SDS-PAGE analysis of rSK 2b and rPAM expression trials. rSK 2b (A.) and rPAM (B.) DNA constructs were transformed into two *E. coli* expression systems, Rosetta 2 and LysY. Following expression trials at 37ºC for 4 hours, the whole lysate fragment (lanes 2, 5 and 8) and separated, soluble (lanes 3, 6 and 9) and insoluble pellet (lanes 4,7 and 10) was reduced and subjected to SDS-PAGE analysis to quantify the level of protein expression. An uninduced E. coli culture was included to check for leaky expression and to differentiate between *E. coli* proteins and protein of interest (lanes 2,3 and 4). The molecular marker used SeeBlue™ Plus2 Pre-stained Protein Standard.

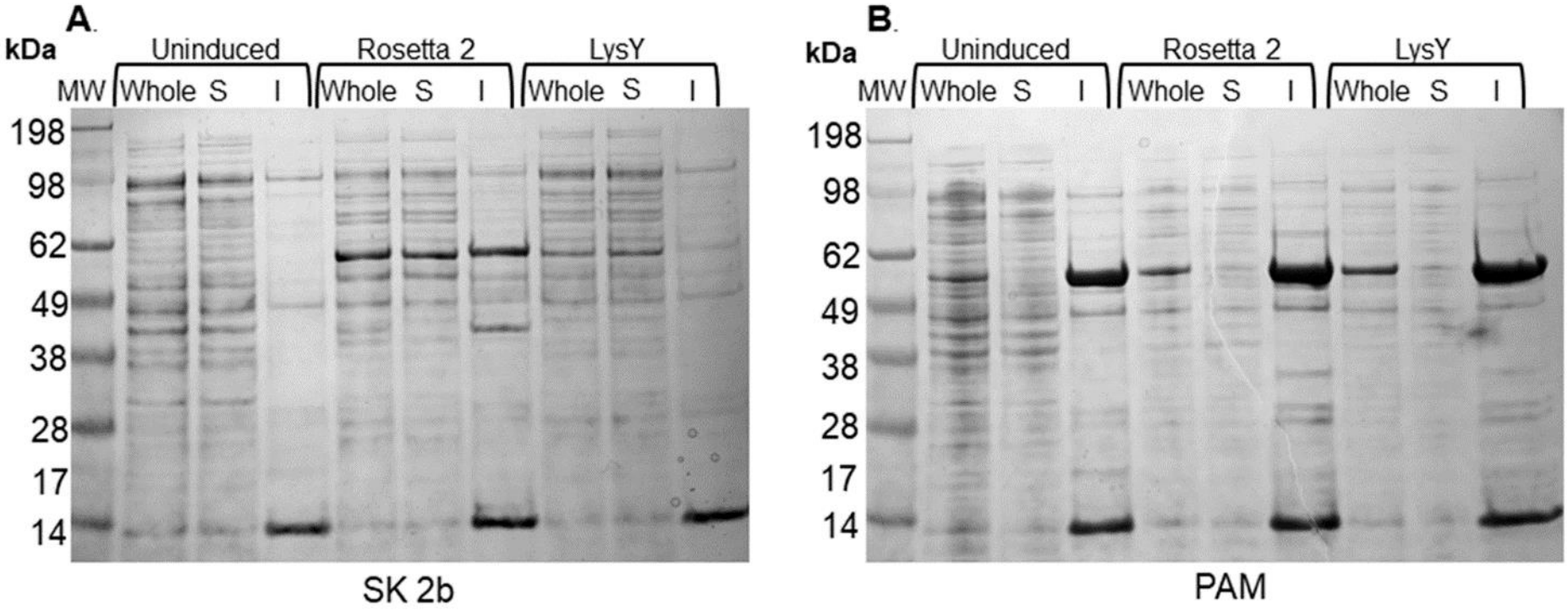

Figure 43 Representative SDS-PAGE analysis of rSK 2b and rPAM expression trials with lower induction temperatures
SK2b (A.) and PAM (B.) DNA constructs were transformed into two *E. coli* expression systems, Rosetta 2 and LysY. Following expression trials at 18ºC, overnight, the whole lysate fragment (lanes 2, 5 and 8) and separated, soluble (lanes 3, 6 and 9) and insoluble pellet (lanes 4,7 and 10) was reduced and subjected to SDS-PAGE analysis to quantify the level of protein expression. An uninduced *E. coli* culture was included to check for leaky expression and to differentiate between *E. coli* proteins and protein of interest (lanes 2,3 and 4). The molecular marker used SeeBlue™ Plus2 Pre-stained Protein Standard.

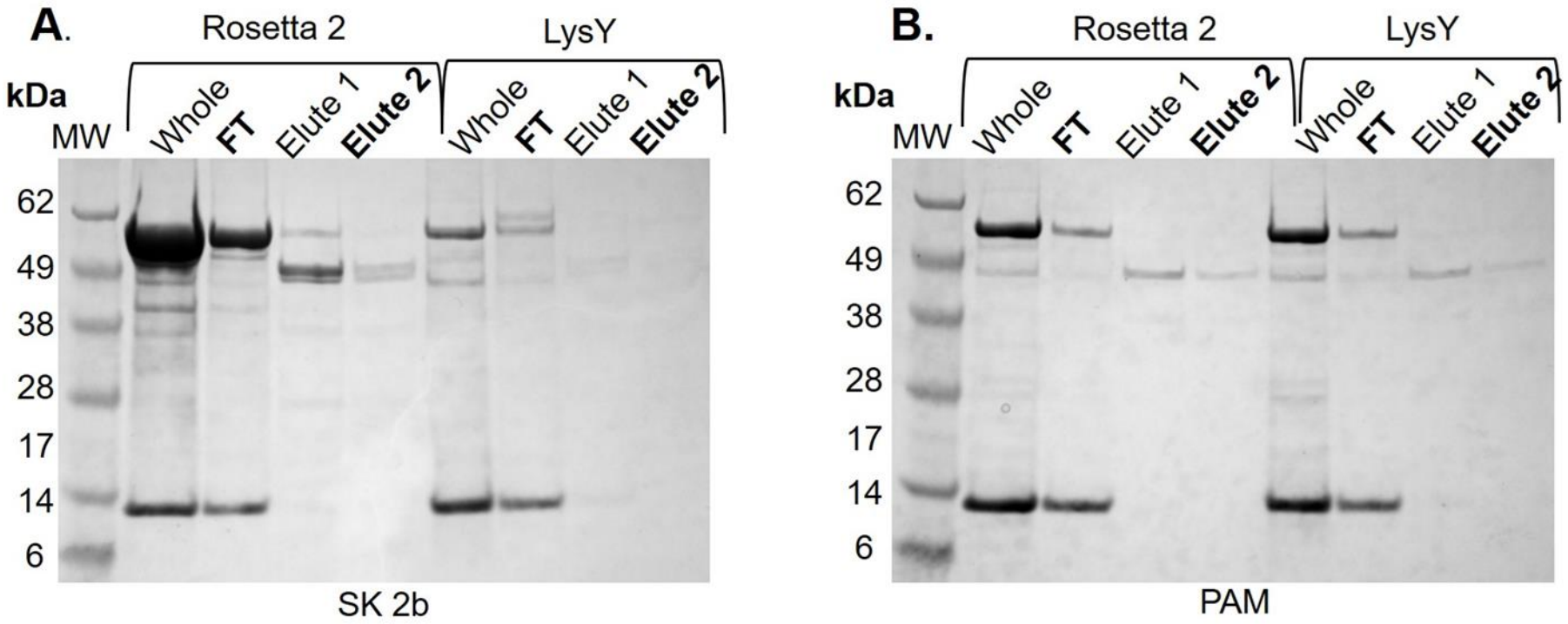

Figure 44 Representative SDS PAGE analysis of small-scale purification trials of Streptokinase 2b (SK 2b) and rPAM. Small scale purification trials of SK 2b (A.) and PAM (B.) in two expression systems were performed using Profinity exact mini prep columns. The 'whole' lane is before purification and flow through is the unbound fraction, contaminating fraction. Elute 1 and Elute 2 are following washes with sodium fluoride, which activates the resins highly specific protease and elutes the native protein from the column. The molecular marker used SeeBlue™ Plus2 Pre-stained Protein Standard.

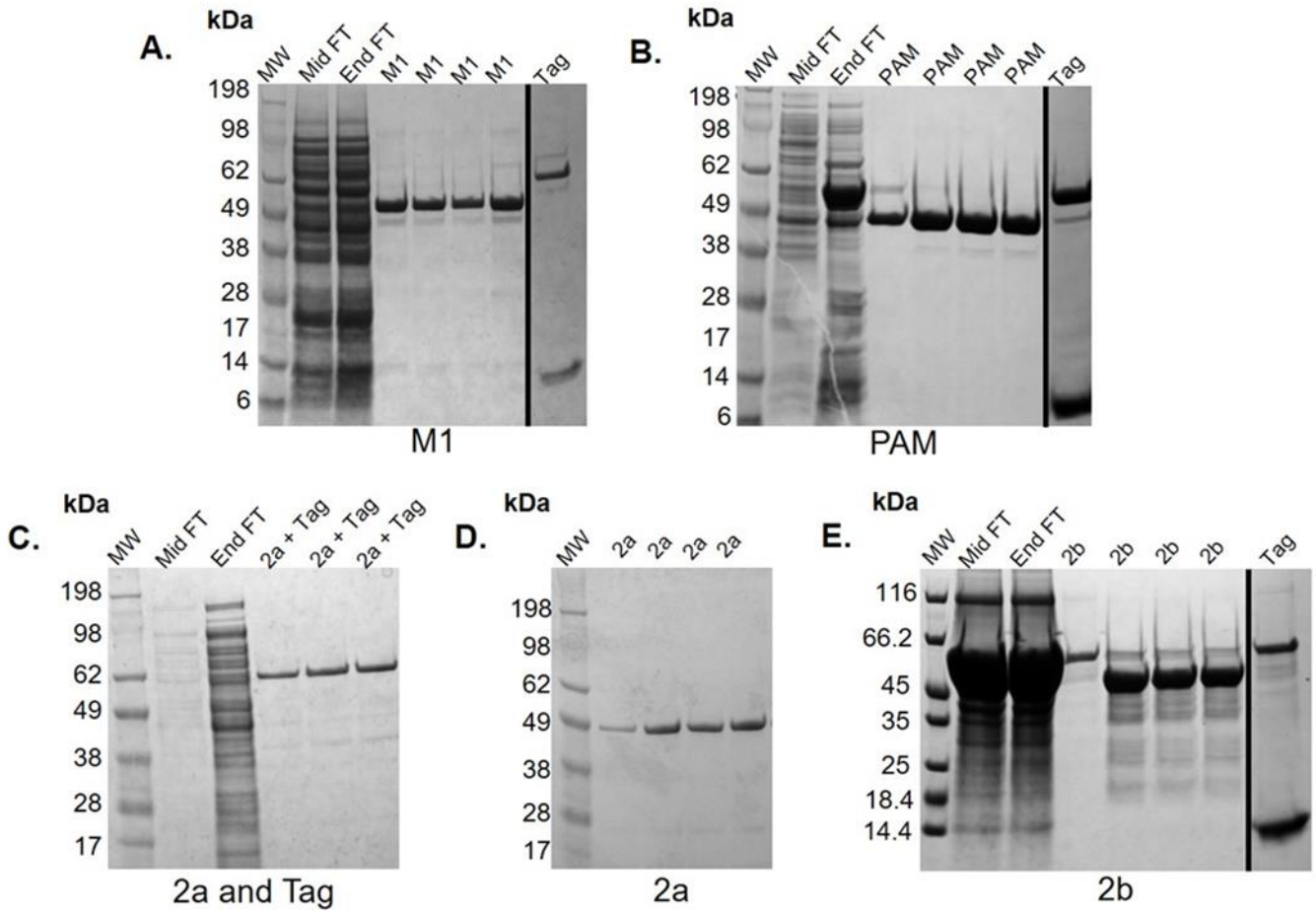

Figure 45 SDS-PAGE analysis of Large-scale purification and tag cleavage. A. B. and **E.** indicate large scale purification of rM1 protein (~54 kDa), rPAM (~41 kDa), and rSK 2b (~48 kDa), respectively. The tag lanes show the presence of un-cleaved protein and the Profinity eXact tag (~8 kDa) after elution from the column **C.** Large scale purification of rSK 2a where the protein was eluted from the column with the SUMOstar tag still present (~62 kDa) **D.** SDS-PAGE analysis of rSK 2a (47 kDa) following tag cleavage step by incubation with SUMOstar protease. All SDS-PAGE gels include a Mid flowthrough (Mid FT) and End flowthrough (End FT) lane which is samples taken from the waste during loading of each protein to the affinity columns.

4.3.3 Investigating the impact of fibrin(ogen) on streptokinase variants activtity

4.3.3.1 Solution plasminogen activation

The activity of streptokinase variants rSK 2a and rSK 2b was first investigated in a chromogenic solution assay, without additional proteins or cofactors. The current EP method was used for this purpose, which was developed for assigning potencies to therapeutic streptokinase products. A dilution range of each streptokinase variant (4.8-0.6 IU/ml, based on initial estimates calculated for each batch of protein) was combined with 100 mM glu-plasminogen and 0.6 mM S2251. Plasmin generation was immediately monitored kinetically at 405 nm using S-2251 substrate, which is cleaved by plasmin to release a chromophoric group. Potencies were calculated relative to the WHO 3rd IS Streptokinase (00/464) using parallel line bioassay analysis, as described in section 2.8. Specific activities were then calculated based on the protein concentrations for each streptokinase preparation. rSK H46a specific activity was previously assigned in IU relative to the WHO 3rd international standard for streptokinase (00/464) (WHO 3rd IS Streptokinase (00/464)) by Dr. Sian Huish (Huish et al., 2017) and used as a comparison in these experiments. As shown in Figure 46, rSK 2a has a specific activity approximately 3.8-fold lower activity than rSK H46a (12.27 ± 1.79 IU/µg verses 47.22 ± 1.59 IU/µg, respectively). The calculated rSK 2a specific activity is consistent with the previously published data (Huish et al., 2017). The rSK 2b variant displayed very little plasminogen activation activity alone in solution, with a calculated specific activity of 0.838 ± 0.31 IU/µg. This is approximately 56.34-fold lower in activity to rSK H46a and 14.6-fold lower activity to rSK 2a.

4.3.3.2 Fibrin(ogen)

The solution plasminogen assay was modified to incorporate 3 mg/ml fibrinogen (plasminogen free) to investigate the relative impact of fibrinogen on rSK 2a and rSK 2b activity. Fibrin clot overlay assays were also used to investigate plasminogen activation rates in the presence of fibrin. Whilst the initial rates of reactions were determined using S2251, as with the solution assays, in this assay system the reaction was measured on the surface of a preformed clot. The data was presented as specific activities (IU/µg) with 95% confidence intervals. The significance of the data was tested using a One-way ANOVA with Tukey post-hoc test. As shown in Figure 47B, rSK 2a demonstrates a significant 2.83-fold increase in activity in the presence of fibrinogen, in comparison to the control (34.74 ± 6.82 IU/µg verses 12.27 ± 1.79 IU/µg, respectively, p= <0.0001). Furthermore, a significant 4.88-fold increase in streptokinase activity was observed in the presence of fibrin in comparison to the control (59.82 ± 10.86 IU/µg verses 12.27 ± 1.79 IU/µg, respectively, p= <0.0001) and a 1.72-fold increase in comparison to the addition of fibrinogen (59.82 ± 10.86 IU/µg verses 34.74 ± 6.82 IU/µg, respectively, p= <0.0001). rSK 2b demonstrated a similar trend (Figure 47C) with a 8.64-fold increase in plasminogen activation activity in the presence of fibrinogen, in comparison to the control (7.24 ± 2.88 IU/µg verses 0.838 ± 0.306 IU/µg, respectively). In the presence of fibrin, a significant 71.97-fold increase was observed in comparison to the control (60.31 ± 14.65 IU/µg verses 0.838 ± 0.306 IU/µg, respectively, p= <0.0001). Additionally, there is a significant 8.3-fold increase in comparison to fibrinogen (60.31 ± 14.65 IU/µg verses 7.24 ± 2.89 IU/µg, p= <0.0001). The presence of fibrin appeared to have no measurable effect on rSK H46a (Figure 47A) in comparison to the solution (49.08 ± 2.49 IU/µg verses 47.22 ± 1.49

IU/µg, respectively.). In the presence of fibrinogen however the specific activity was calculated to be 130.30 (± 17.75) IU/µg, which is approximately 2.76-fold higher than the specific activity of rSK H46a calculated in solution (p= <0.0001). It has been previously reported that Group C streptokinase is not stimulated by fibrinogen (Huish et al., 2017), therefore the plasminogen activation assays were amended to investigate this further.

To investigate the impact of fibrinogen on streptokinase activity further, the solution plasminogen activation assays were repeated with a fixed concentration of streptokinase (4 IU/ml) over a concentration range of fibrinogen. Different fibrinogen lot. numbers of the same commercial fibrinogen and different fibrinogen products with varying levels of purity, were included in these assays to validate the previous potency results. As shown in Figure 48A and B, the native and recombinant Group C streptokinase (rSK H46a and WHO 3rd IS streptokinase (00/464)) are both maximally stimulated at lower levels of fibrinogen. This is demonstrated with an 8-fold maximum increase in plasminogen activation (Figure 48A) at 0.75 mg/ml plasminogen depleted fibrinogen in comparison to the absence of fibrinogen (118.62 Abs/s2 x 1e9 and 14.68 Abs/s2 x 1e9, respectively). Additionally, a 5-fold increase in plasminogen activation activity was observed at 0.21 mg/ml fibronectin (Fn), vWF and plasminogen depleted fibrinogen (Figure 48B) in comparison to the absence of fibrinogen (59.94 Abs/s2 x 1e9 and 11.56 Abs/s2 x 1e9, respectively). Following the maximum stimulation, both Group C streptokinase (Figure 48A and B) display a dose dependant decrease in activity as fibrinogen concentration increases. rSK 2a was also maximally stimulated with 0.75 mg/ml plasminogen depleted fibrinogen (Figure 48A), with a 4-fold increase in activity in comparison to the control (35.09 Abs/s2 x 1e9 and 8.19 Abs/s2 x 1e9, respectively).

Following the maximum stimulation of rSK 2a at 0.75 mg/ml, there was no significant differences in activity with increasing concentrations of fibrinogen.

Plasminogen contamination in the fibrinogen was checked as an explanation for the unexpected stimulation of Group C streptokinase. As shown in Figure 48C and D, both fibrinogen products contain high levels of plasminogen contamination. The plasminogen depleted fibrinogen (Figure 48C) contained the highest level of plasminogen activation, with a maximum activation rate of 28.48 Abs/s2 x 1e9 observed in Lot 1 and 37.95 Abs/s2 x 1e9 in Lot 2. A dilution range of plasminogen was included in the plasminogen depleted fibrinogen assays, a standard curve was plotted, and initial rates were interpolated. There was found to be approximately 70 nM per 1 mg/ml fibrinogen of contaminating plasminogen in lot number 1 and 75 nM per 1 mg/ml fibrinogen of plasminogen in lot number 2. The plasminogen, von Willebrand factor and fibronectin depleted fibrinogen demonstrated lower plasminogen activation with maximum rates of 6.9 Abs/s2 x 1e9. No further experiments were conducted to quantify the plasminogen contamination concentration in this commercial fibrinogen.

Fibrinogen purified using a specific antibody, IF-1, to remove the plasminogen contamination was kindly gifted from the University of Leeds. The assay was then repeated as above to investigate the effect of highly purified fibrinogen on WHO 3rd IS streptokinase (00/464) activity. As shown in Figure 48E, even in the absence of contaminating plasminogen, a dose dependent increase in WHO 3rd IS streptokinase (00/464) activity is observed. At the highest concentration tested (2.8 mg/ml fibrinogen), streptokinase WHO 3rd IS streptokinase (00/464) had increased by almost 17-fold in comparison to the absence of fibrinogen (898.42 Abs/s^{2}x1e9 and 52.85 Abs/s^{2}x1e9, respectively). It is important to note,

due to volume limitations the data is based on 1 independent assay with 2 repeats.

4.3.3.2.1 Fibrinogen, plasminogen free

A commercial fibrinogen product was obtained from HYPHEN BioMed (Fibrinogen, plasminogen free) found to be free of contaminating plasminogen, and the assays above were repeated with all the streptokinase variants. As shown in Figure 49A, for the Group C Streptokinase (WHO 3rd IS streptokinase (00/464)) a dose dependant increase in activity was observed with increasing concentrations of fibrinogen, peaking between 0.7-1.8 mg/ml fibrinogen. The maximum increase observed at 0.7 mg/ml fibrinogen was 6.35-fold higher than without the addition of fibrinogen (284.08 Abs/s2 x 1e9 and 44.75 Abs/s2 x 1e9, respectively). Above 1.8 mg/ml a steady decrease in activity is observed and at the maximum concentration tested, the activity had decreased by 2.27-fold in comparison to the maximum stimulation (125.16 Abs/s2 x 1e9 at 5.4 mg/ml). This trend was also reproduced in Figure 49B, which shows the WHO 3rd IS streptokinase steadily increases in activity with increasing fibrinogen concentrations, peaking at 1.35 mg/ml fibrinogen, which represents a 6.18-fold increase over the activity with no fibrinogen. Above 1.35 mg/ml fibrinogen activity slowly decreases with increasing fibrinogen concentrations. The highest fibrinogen concentration tested (5.4 mg/ml) represents a 2.95-fold increase in activity versus the no-fibrinogen control. rSK 2a displayed a similar trend with a dose dependent increase in activity as fibrinogen concentrations increase. rSK 2a peaks at a slightly higher concentration of 2.7 mg/ml fibrinogen, which represents a 3.83-fold increase in activity in comparison to the control, which decreases to 3.37-fold at 5.4 mg/ml fibrinogen. rSK 2b increases in activity as the fibrinogen concentration increases without peaking within the concentration

range tested. At the maximum concentration of 5.40 mg/ml fibrinogen the streptokinase activity was 19.47-fold higher than without the addition of fibrinogen. It is important to note that without the addition of fibrinogen, rSK 2b has very little activity in solution alone (Figure 35).

When Glu-plasminogen was substituted with the more readily activatable Lys-plasminogen, Group C streptokinase (WHO 3rd IS streptokinase (00/464) and rSK H46a) activation of showed the same profile (Figure 49C). Maximum stimulation of Group C streptokinase activity was observed at 0.675 mg/ml fibrinogen (an increase of 5.92-fold for the international standard and 5.38-fold for rSK H46a) in comparison to the control. Similarly, rSK 2a peaked at 0.675 mg/ml with a 4.47-fold increase in comparison to the control. Above 0.675 mg/ml fibrinogen a rapid decrease in activity was observed with increasing concentrations of fibrinogen, and at the highest concentration of fibrinogen tested (5.40 mg/ml) each streptokinase activity was lower than without the addition of fibrinogen (~0.7-fold).

The experiment was repeated to assess rSK 2b activity against lys-plasminogen, substituting rSK H46a for rSK 2b due to limited space in the microtiter plate. As shown by Figure 49D activation of lys- plasminogen by rSK 2b in the presence of fibrinogen resulted in a similar profile to rSK 2b activation of glu-plasminogen (Figure 49B). A dose dependent increase in rSK 2b activity was observed as fibrinogen concentration increases, and with the highest fibrinogen concentration tested (5.4 mg/ml) a 105.01-fold increase in activity was observed.

In the same experiment the WHO 3rd IS streptokinase (00/464) and rSK 2a produced a different activity profile compared to the previous result (Figure 49C). For the WHO 3rd IS streptokinase (00/464), maximum stimulation of

activity by fibrinogen was observed at 1.35 mg/ml, with a 9.85-fold increase. At the highest fibrinogen concentration (5.40 mg/ml) stimulation of activity was reduced to a 7.99-fold increase, whereas previously activity was comparable to the no-fibrinogen control. For rSK 2a activity only increased with the fibrinogen concentration up to a maximum 7.5-fold at 5.40 mg/ml fibrinogen.

A possible explanation for the difference observed with the WHO IS and rSK 2a is the source of fibrinogen used. Stocks of the commercial plasminogen-free fibrinogen used previously (Figure 49C) were exhausted and so a new batch (with a different Lot number) was purchased and used in the subsequent experiments (Figure 49D). This new fibrinogen Lot was found to contain low levels of contaminating plasminogen which may explain the difference in observed trends.

A.

Streptokinase variant	Specific activity (IU/ µg)	95% CI	N
rSK H46a	47.216	[45.73,48.71]	14
rSK 2a	12.271	[10.48,14.07]	16
rSK 2b	0.838	[0.53,1.14]	17

B.

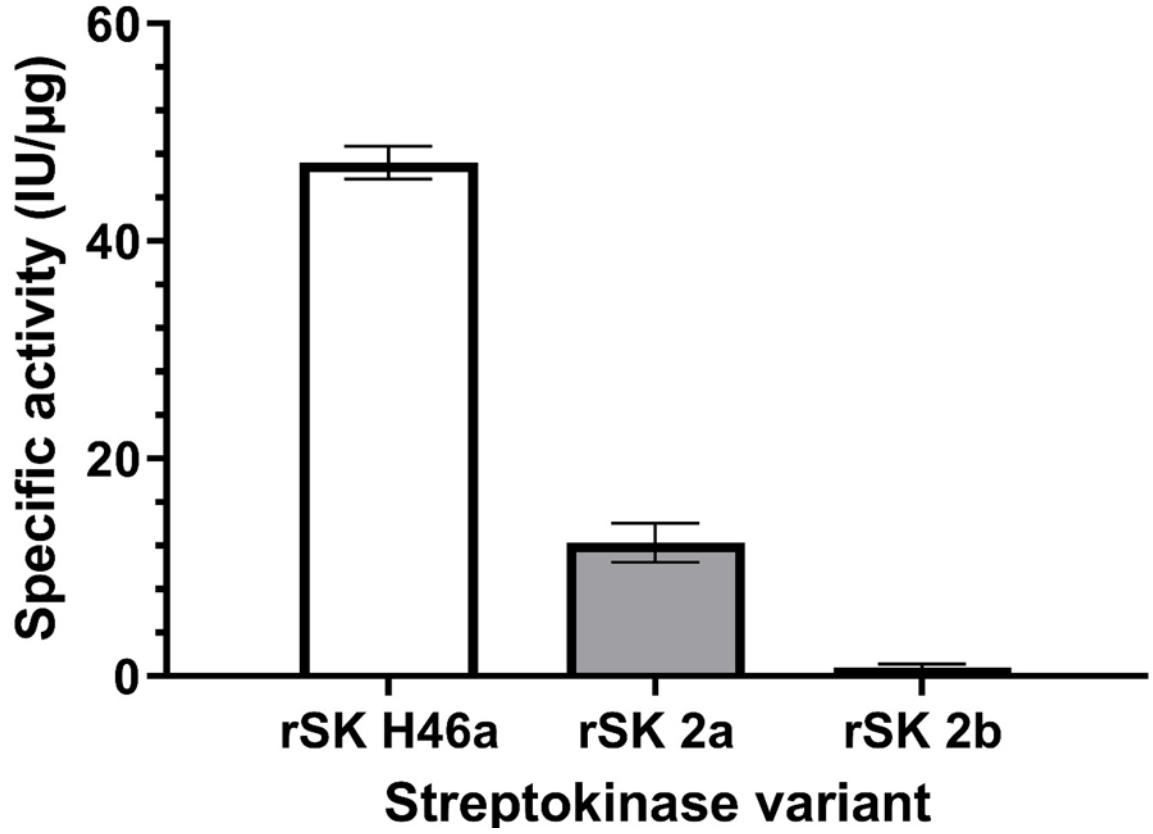

Figure 46 Specific activities of streptokinase variants without addition of co-factors (control). Glu-plasminogen activation activity of streptokinase variants, streptokinase H46a (rSK H46a), streptokinase 2a (rSK 2a) and streptokinase 2b (rSK 2b) was investigated using chromogenic solution assay against S2251, a substrate for specific to plasmin. Potencies were calculated using parallel line bioassay analysis and presented as specific activities, using the concentration of each individual streptokinase as per section 2.8. Error bars represent 95% CI. N=≥14

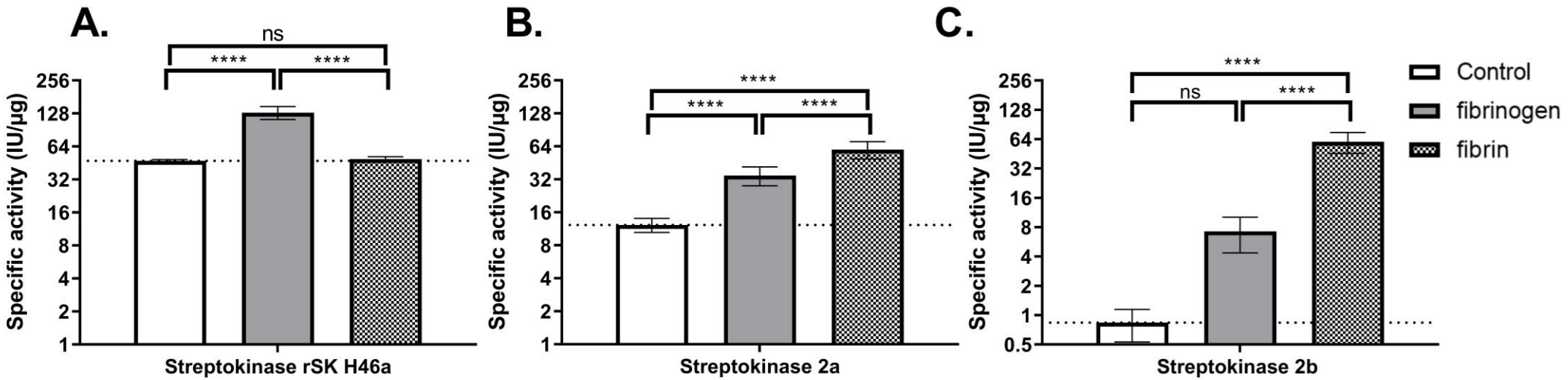

Figure 47 Streptokinase variants in the presence of fibrin(ogen) Glu-plasminogen activation activity of streptokinase variants was investigated using chromogenic solution assay in the presence of purified fibrinogen (HYPHEN BioMed, plasminogen free) and on the surface of a preformed clot (clot overlay). A control (streptokinase alone) was included for comparison purposes for each streptokinase variant and is also represented by the dotted line. Potencies were calculated and presented as specific activities of each variant. Error bars represent 95% CI. (ns = no significance, * $p < 0.05$, ** $p < 0.01$, *** $p < 0.001$, **** $p < 0.0001$, One-way ANOVA with Tukey post-hoc test.). N= ≥ 6

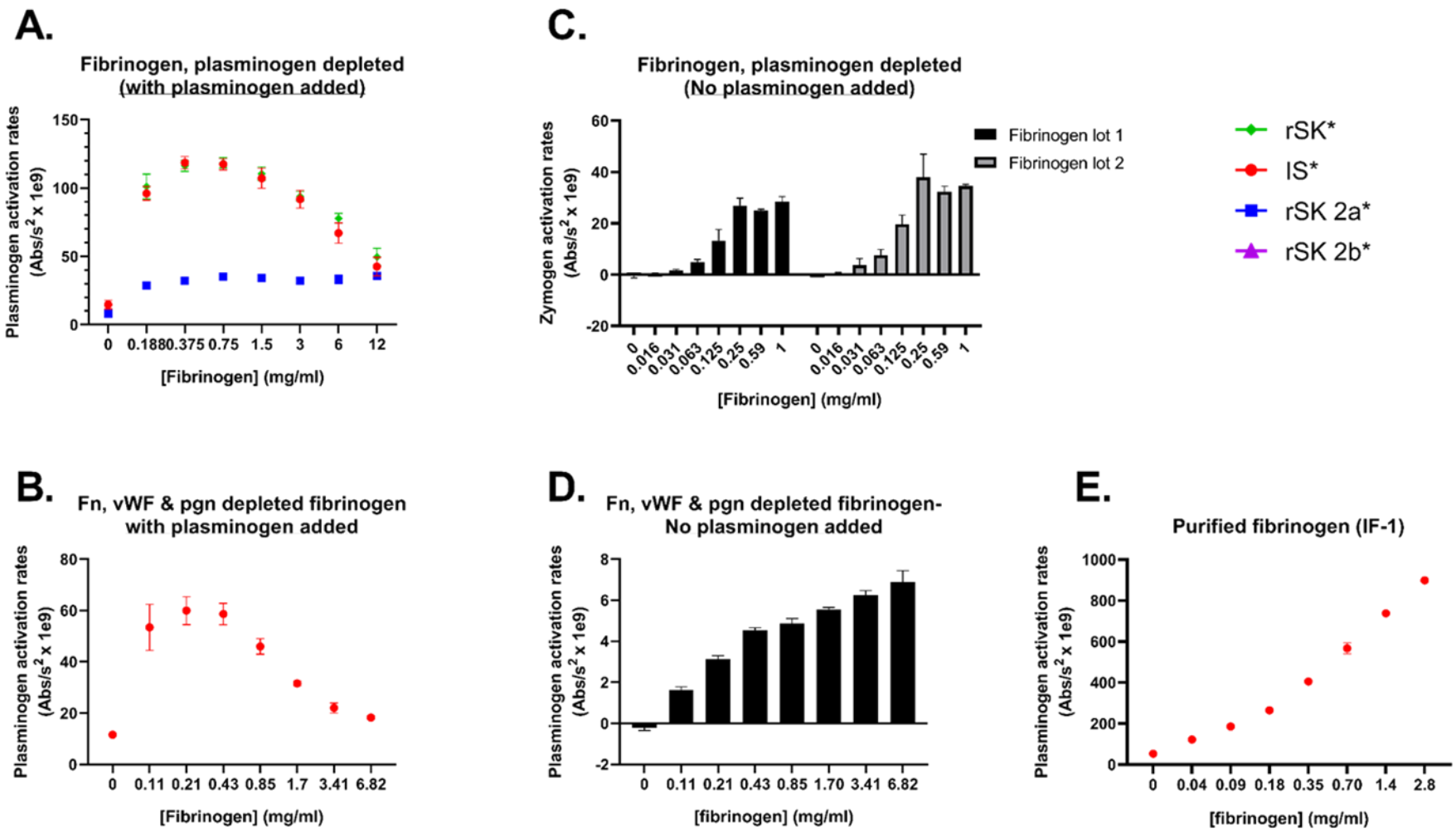

Figure 48 Streptokinase activation in the presence of increasing concentrations of fibrinogen. Glu-plasminogen activity of streptokinase was investigated using chromogenic solution assay in the presence with increasing concentrations of fibrinogen with different purity levels (**A**. Calbiochem: plasminogen depleted (n=4) **B**. HYPHEN BioMed: Fn, vWF and plasminogen depleted (n=4) **E.** University of Leeds: Fibrinogen purified by IF-1 affinity chromatography (n=2) **(C.)** The experiments were also performed without the presence of glu-plasminogen to test the extent of plasminogen contamination with increasing concentrations of Calbiochem: plasminogen depleted fibrinogen (n=2) and **(D.)** HYPHEN, BioMed: Fn, vWF and plasminogen depleted fibrinogen (n=4)

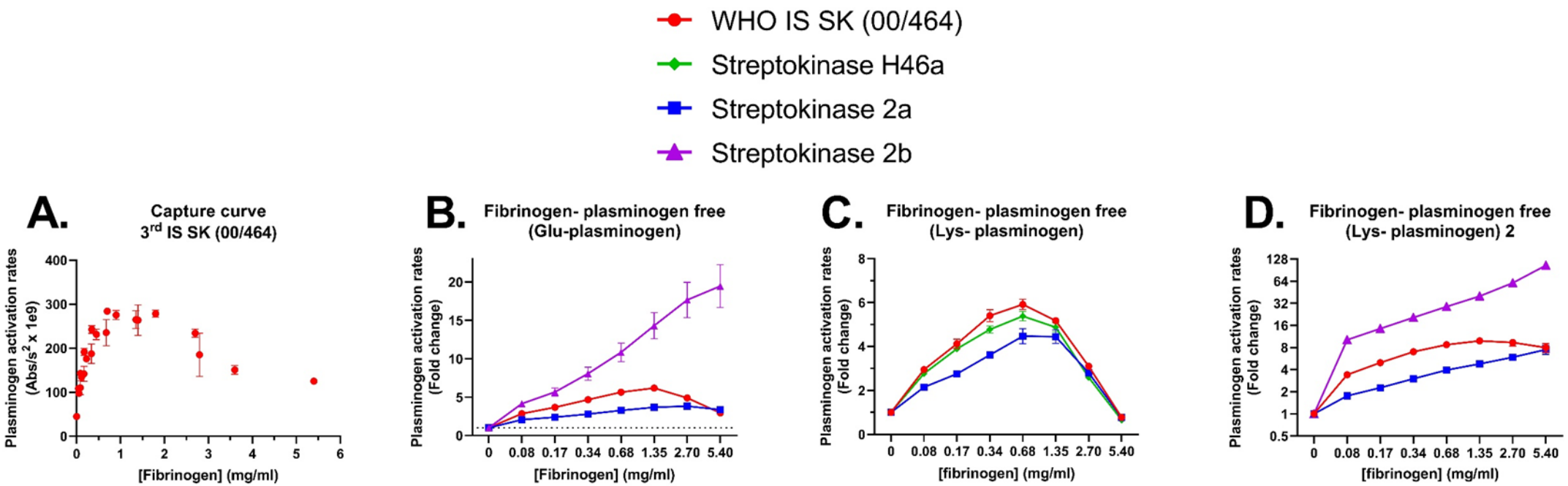

Figure 49 Glu- plasminogen activity of streptokinase variants with increasing concentrations of fibrinogen (HYPHEN BioMed, plasminogen free) Activity of streptokinase variants in the presence of increasing concentrations of fibrinogen (HYPHEN BioMed, plasminogen free) incorporating glu-plasminogen (**A**. and **B.**) or lys-plasminogen (**C.** and **D.**). Experiments conducted in **A., B.,** and **C.** are all performed using the same batch number of commercial fibrinogen, whilst **(D.)** was performed using a new batch number and found to contain small amount of contaminating plasminogen. Error bars represent SEM. N=≥3

4.3.4 Investigating the impact of M1 protein on streptokinase activity

4.3.4.1 Plasminogen activation in the presence of M1 bound fibrinogen

To investigate the effect of rM1 protein on streptokinase activity, the solution assays with and without fibrinogen were adapted to include 3.1 µg/ml rM1 protein. A dilution range of each streptokinase variant (4.8-0.6 IU/ml) was combined with100 mM glu-plasminogen and 0.6 mM S2251. Half of the 96-well plate contained 3.1 µg/ml rM1 protein. Where stated, 3 mg/ml plasminogen-free fibrinogen was included in the assay. Plasmin generation was then immediately monitored kinetically at 405 nm using S-2251 substrate, which is cleaved by plasmin to release a chromophoric group. Specific activities were then calculated for each streptokinase variant, relative to the WHO 3rd IS Streptokinase (00/464), for each condition tested and compared to the control, streptokinase alone. The data was presented as specific activities (IU/µg), with 95% confidence intervals. The validity of the data was assessed using an ordinary one-way ANOVA, with a Tukey post-hoc test (99% confidence interval). As shown in Figure 50A, addition of rM1 protein alone, i.e., no fibrinogen, appeared to have very little effect on rSK H46a activity, increasing only 1.19-fold compared to the control (55.97 ± 4.43 IU/µg and 47.22 IU/µg ± 1.49 IU/µg, respectively). Similarly, rSK 2a (Figure 50B) demonstrated a 1.44-fold increase in activity in the presence of rM1 (17.63 ± 2.02 and 12.27 ± 1.79, respectively), and rSK 2b (Figure 50C) was stimulated 2.63-fold in the presence of rM1 protein alone (2.20 ± 0.55 and 0.84 ± 0.31, respectively).

As described in section 4.3.3.2 (Figure 47), in the presence of fibrinogen a significant increase in plasminogen activation activity in all streptokinase

variants was observed, with a 2.8-fold increase for rSK H46a and rSK 2a and an 8.6-fold increase for rSK 2b.

Because rM1 protein binds fibrinogen, it was of interest to include both proteins in the assay system. It was found that addition of 3.1 µg/ml rM1 and 3 mg/ml fibrinogen, did not stimulate rSK 2a and rSK 2b any further than with the addition of fibrinogen alone. rSK 2a demonstrated a 2.80-fold increase in activity in comparison to the control (34.37 ± 7.43 IU/µg and 12.27 ± 1.794 IU/µg, respectively, p= <0.0001) and rSK 2b activity increased by 7-fold in comparison to the control (5.89 ± 1.60 IU/µg and 0.838 ± 0.31 IU/µg, respectively, p= <0.0001). However, addition of fibrinogen-bound- rM1 protein to rSK H46a further stimulated the plasminogen activator, with a significant increase in activity in comparison to the control and fibrinogen alone. The addition of fibrinogen bound rM1 protein to rSK H46a showed a 7.0-fold increase in plasminogen activation activity in comparison to the control (330.6 ± 93.45 IU/µg and 47.22 ± 1.49 IU/µg, respectively, p= <0.0001) and a 2.54-fold increase in activity in comparison to fibrinogen alone (330.68 ± 93.45 IU/µg and 130.30 ± 17.75 IU/µg, respectively, p<0.0001).

4.3.4.2 Turbidimetric assessment of fibrin clot lysis by streptokinase variants

4.3.4.2.1 Purified fibrin clots

The impact of rM1 on fibrin clot physical dissolution was investigated using turbidimetric assays. Fibrin clots were formed by combining 3 mg/ml fibrinogen, a dilution range of rM1 protein (0.47-30 µg/ml) and a dilution range of streptokinase variants (2.4-0.3 IU/ml) in a microtitre plate. The reaction was initiated with 0.05 IU/ml thrombin (01/578) and 8.2 µg/ml glu-plasminogen. Clot formation and lysis were immediately monitored kinetically by measuring

absorbance changes at 405 nm for up to 5 hours. The time between 50% clotting and 50% lysis and time to 100% lysis were calculated and potency estimates obtained relative to the WHO 3rd IS streptokinase (00/464) using a parallel line bioassay analysis. The data is presented in Figure 51 as fold-change relative to 0 µg/ml rM1 condition. As shown in Figure 51A, each streptokinase variant demonstrated a dose-dependent increase in time between 50% clotting and 50% lysis with increasing concentrations of rM1 protein. At the maximum rM1 protein concentration tested (30 µg/ml) the Group C streptokinase (WHO 3rd IS streptokinase (00/464)) was approximately 1.61-fold slower (p= <0.0001) between 50% clotting and 50% lysis, whilst rSK 2a and rSK 2b rates were 1.94-fold (p= <0.0001) and 2.03-fold slower (p= <0.0001), respectively. However, no trends were observed with the time to reach 100% lysis (Figure 51B).

4.3.4.2.2 Whole blood clots

Physical dissolution of clots in the presence of M1-bound-fibrin was also investigated in whole blood conditions using a microtitre plate assay, known as a halo assay. Whole blood clots (5%) with 0.155 µg/ml rM1 protein (equivalent to 3.1 µg/ml accounting for the whole blood dilution factor) were formed around the edges of a well in a microtitre plate by the addition of an 15% v/v Innovin and 67 mM calcium chloride solution. Once clotting was complete, a lysis solution consisting of a dilution range of streptokinase (2.4- 0.3 IU/ml) was added to the centre of each well. Lysis of the blood clot was monitored at 510 nm for up to 5 hours immediately following the addition of the lysis solution. Time to 100% lysis values were used to calculate potency estimates for each streptokinase variant relative to the WHO 3rd IS streptokinase (00/464) using a parallel line bioassay analysis. Specific activities were calculated in IU/ µg

based on potency estimates and streptokinase protein concentrations. The data was presented as specific activities, with 95% confidence intervals. The significance of the data was tested using an unpaired two-tailed t test (99% confidence limit, definition of statistical significance: $p < 0.1$). As shown in Figure 52 each variant is stimulated, although the differences were not significant by 3.1 µg/ml rM1 (Figure 52 A), a 2.51-fold increase in activity was observed (133.69 ± 75.23 IU/µg and 53.19 ± 11.90 IU/µg, respectively, p= 0.015). Whilst, rSK 2a (Figure 52B) demonstrated a 1.55-fold increase in activity in the presence of rM1 protein (214.68 ± 52.81 µg/ml verses 138.60 ± 20.30 µg/ml control, p= 0.0073) and rSK 2b (Figure 52C) activity increased by 1.38-fold (567.18 ± 186.41 IU/µg and 412.23 ± 91.94 IU/µg, respectively, p = 0.11)).

To further investigate the impact of rM1 on whole blood clot lysis, the halo assays were repeated over a range of rM1 protein concentrations (0.48-30 ug/ml). Lysis was initiated with the addition of 0.6 IU/ml streptokinase to the preformed whole blood clot. The data was presented as time to 100% lysis, with the standard error of the mean, and validity of the data was assessed using an ordinary one-way ANOVA, with a Dunnett's post-hoc test (99% confidence interval). As shown in Figure 53, at rM1 concentrations above 1.88 µg/ml a significant decrease in time to 100% lysis was observed with all streptokinase variants. For rSK H46a with 1.88 µg/ml rM1 (Figure 53A) there was a significant 1.57-fold decrease in time to 100% lysis (2538.75 ± 329.71 seconds and 3990.00 ± 227.56 seconds, respectively, p=0.013) which reduced further with increasing rM1 concentrations up to a maximum of a 3.17-fold decrease at 15 µg/ml compared to the control (1260.00 ± 93.50 seconds and 3990.00 ± 227.55 seconds, respectively, p<0.0001). For rSK 2a with 1.88 µg/ml rM1 protein (Figure 53B) a 1.93-fold decrease in time to 100% lysis time was observed in

comparison to the control (1533.00 ± 205.84 seconds and 2955.00 ± 385.73 seconds, respectively, p=0.0038) which reduced further as the rM1 protein concentration increased, up to a maximum of a 2.64-fold decrease at 7.5 µg/ml rM1 protein (1117.50 ± 113.83 seconds and 2955.00 ± 385.73 seconds, respectively, p<0.0001). rSK 2b followed a similar trend (Figure 53C) but with consistently faster clot lysis times compared to rSK H46A and rSK 2a. The lowest concentration of rM1 protein to show a significant decrease in time to 100% lysis (1.63- fold) for rSK 2b was 3.75 µg/ml in comparison to the control (932.50 ± 112.76 seconds and 1521.00 ± 144.09 seconds, respectively, p=0.0032.). The maximum decrease in time to 100% lysis was observed at 7.5 µg/ml rM1 protein, with a 1.95-fold decrease in comparison to the control (780.00 ± 37.48 seconds and 1521.00 ± 144.09, respectively, p=0.0001).

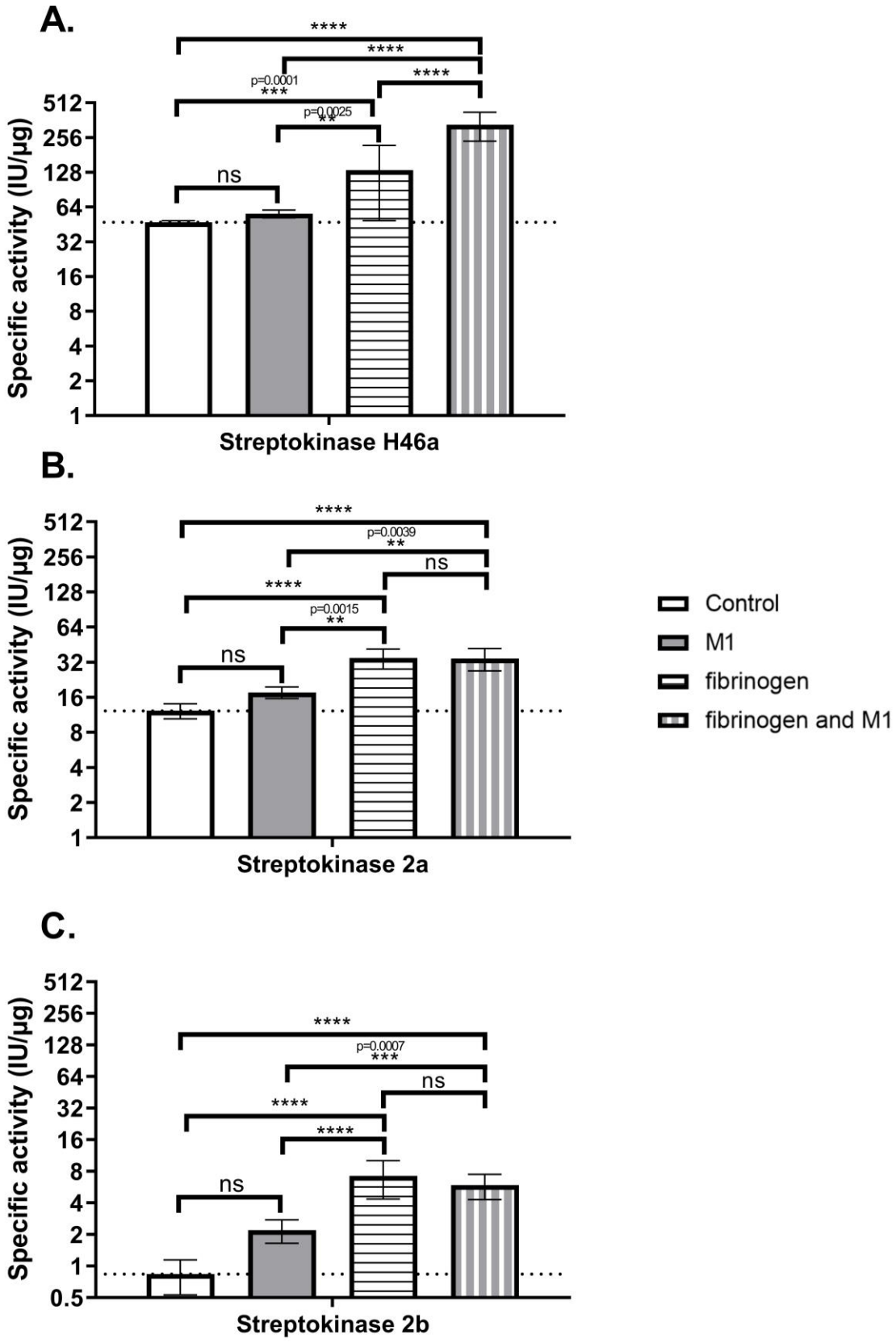

Figure 50 Streptokinase variants in the presence of fibrinogen and rM1 Glu-plasminogen activation activity of rSK H46a (A.), rSK 2a (B.) and rSK 2b (C.) was investigated using chromogenic solution assay in the presence of fibrinogen and M1. A control was included for comparison purposes for each streptokinase variant, streptokinase alone, and is also represented by the dotted line. Data was presented as specific activities (IU/µg) of each variant. Error bars represent 95% CI. (ns = no significance, * $p < 0.05$, ** $p < 0.01$, *** $p < 0.001$, **** $p < 0.0001$, One-way ANOVA with Tukey post-hoc test.). N=≥3

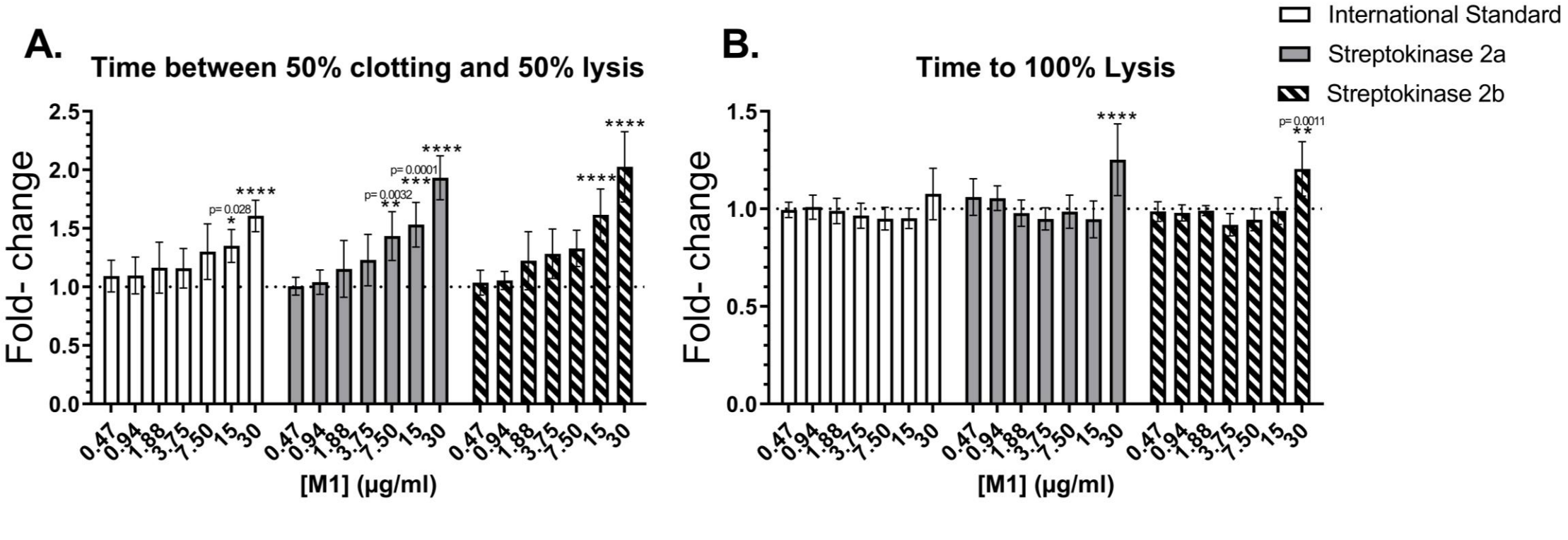

Figure 51 Turbidimetric analysis of fibrin clots by streptokinase variants, in the presence of rM1 protein Time between 50% clotting and 50% lysis (A.) and time to 100% lysis was calculated from fibrinolysis profiles as per (**Figure 18**) in purified samples in the presence of increasing concentrations of rM1 protein for each streptokinase variant (WHO 3rd IS streptokinase (00/464), SK 2a and SK 2b) and presented as fold change. Error bars represent 95% CI. (* $p < 0.05$, ** $p < 0.01$, *** $p < 0.001$, **** $p < 0.0001$, One-way ANOVA with Dunnett post-hoc test, relative to 0 µg/ml M1.) N=10

Figure 52 Specific activity of streptokinase variants in the presence of rM1 protein in a whole blood microtitre plate assay. Dissolution of whole blood clots incorporating 0.155 µg/ml rM1 protein was observed kinetically using a halo assay. A 'halo' ring of whole blood with and without M1 was clotted with TF on the edge of a well. A dilution range of rSK H46a (A.), rSK 2a (B.) or rSK 2b (C.) was added to the centre of the well and clot dissolution was measured kinetically (OD_{510}) in a BMG FluorStar® Omega plate reader. Time to 100% lysis was used to calculate potencies by parallel line bioassay analysis and data was presented as specific activity. Error bars represent 95% CI**.** (Statistically significant at $P < 0.01$, unpaired two-tailed t test). N=≥4

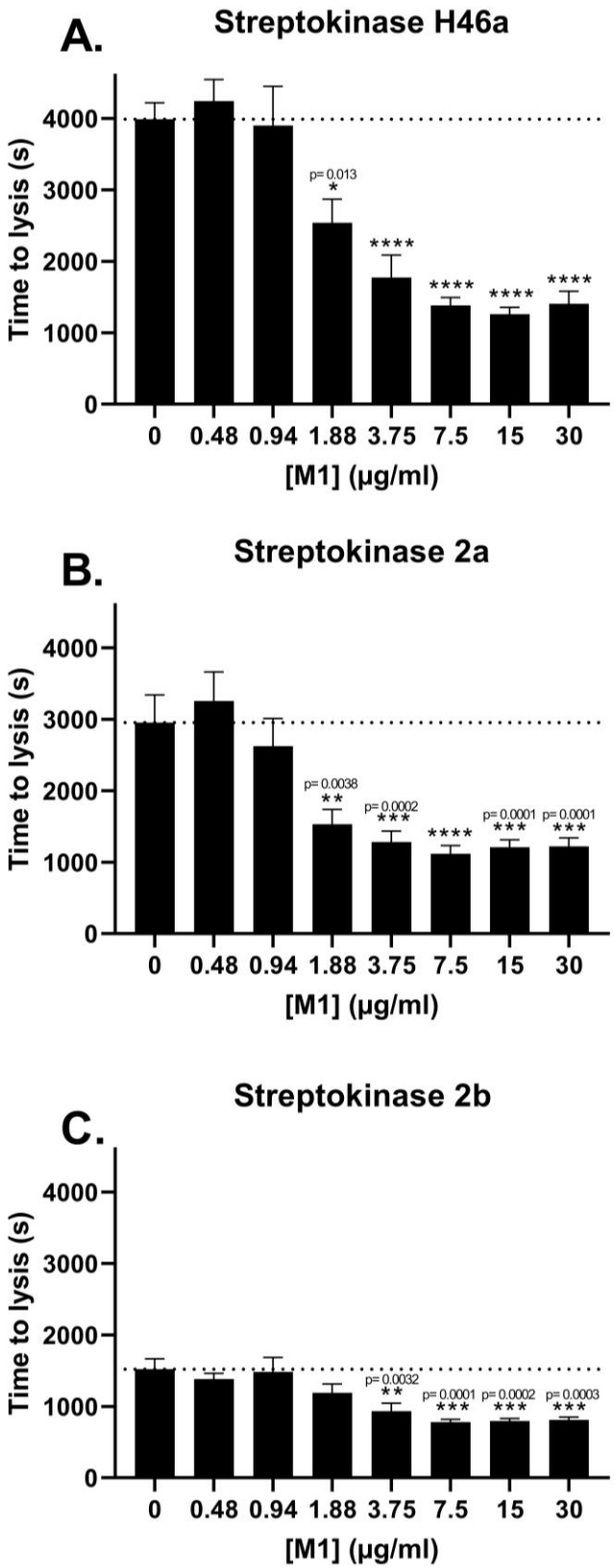

Figure 53 Effect of rM1 on fibrin clot dissolution by streptokinase variants Dissolution of whole blood clots with increasing concentrations of rM1 protein was observed kinetically using a halo assay. A 'halo' ring of whole blood with increasing concentrations of M1 was clotted with TF on the edge of a well. SK H46a (A.), SK 2a (B.) or SK 2b (C.) was added to the centre of the well and clot dissolution was measured kinetically (OD_{510}) in a plate reader. Data is presented as time to 100% lysis (s), Error bars represent SEM (* $p < 0.05$, ** $p < 0.01$, *** $p < 0.001$, **** $p < 0.0001$, One-way ANOVA with Dunnett post-hoc test.) N= ≥8

4.3.4.3 Investigating the impact of M1 protein on plasminogen activation by streptokinase variants

To determine if changes to rates of plasminogen activation contribute to the apparent increase in susceptibility to lysis, plasminogen activation was measured directly using clot overlay assays. Fibrin clots were formed with 3 mg/ml purified fibrinogen, incorporating rM1 protein (3.1 µg/ml) and plasminogen (8.2 µg/ml), by the addition of 0.5 IU/ml thrombin. A dilution range of the streptokinase variants (4.8-0.6 IU/ml) and S2251 (0.6 mM), a substrate for specific plasmin and streptokinase-activated plasminogen, was added to the surface of the pre-formed fibrin clots. Plasmin generation was measured kinetically at 405 nm, and specific activities were derived from potency estimates calculated as described in section 2.8. The data was presented as specific activity, with 95% confidence intervals. The statistical significance of the data was tested using a One-way ANOVA with Tukey post-hoc test. rSK H46a (Figure 54A) showed no significant differences between the control group (47.22 ± 1.49 IU/µg), in presence of fibrin alone (49.08 ± 2.49 IU/µg) or fibrin bound rM1 protein (54.37 ± 26.89 IU/µg). In the presence of fibrin, rSK 2a (Figure 54B) showed a significant 5.4-fold increase in activity in comparison to the control (66.10 ± 10.78 IU/µg and 12.27 ± 1.79 IU/µg, respectively, $p< 0.0001$). However, fibrin-bound rM1 protein did not stimulate the activity further in comparison to fibrinogen alone (64.16 ± 8.22 IU/µg and 66.10 ± 10.78 IU/µg, respectively). rSK 2b (Figure 54C) displayed a similar trend to rSK 2a, reaching similar activity levels, with a 67.8-fold increase in activity upon the addition of fibrin in comparison to the control (56.80 ± 12.57 IU/µg and 0.838 IU/µg ± 0.31, respectively, $p< 0.0001$). Additionally, there was no further stimulation with the

addition of fibrin-bound rM1 protein in comparison to fibrin alone (47.90 ± 33.29 IU/µg and 56.80 ± 12.57).

As M1 is a cell surface-bound protein, cleaved during infection, it is difficult to pinpoint a physiologically relevant concentration. Therefore, the assays were then repeated with a fixed concentration of streptokinase (4.8 IU/ml) over a dilution range of rM1 protein (1.88- 30 µg/ml) to ensure that the streptokinase variants are not stimulated by higher or lower rM1 protein concentrations. As shown in Figure 55, no particular trend was observed for any streptokinase variant activity over the range of rM1 protein concentrations used. The assays were repeated using the host plasminogen activators uPA and tPA as described in section 3.3.5.1, which also showed no significant differences over the range of rM1 protein concentrations (Figure 31). A non-significant 0.88-fold decrease in activity was observed with uPA in comparison to the control, whilst tPA did not show any measurable differences.

4.3.4.3.1 Temperature dependent plasminogen activation with rM1 bound fibrin

During infection Group A *Streptococcus* encounters different environments within the human host. The properties of virulence factors such as the M proteins may change according to the different environmental conditions encountered, such as temperature differences. To investigate if fibrin clot formation in different temperatures, with and without the presence of rM1, impacted streptokinase activity modified fibrin clot overlay assays were performed at two different temperatures. Additionally, the fibrin clot overlay assays were clotted with and without incorporating calcium chloride (Ca2+). Fibrin clots (± 3.1 µg/ml rM1) were formed and assayed at 37ºC, as previously described, or at the lower temperature of 25ºC. rSK 2a was the only variant to be included in these experiments due to M1 being commonly associated with

this streptokinase. The data was presented as specific activities (IU/µg), with 95% confidence intervals. The statistical significance of the data was tested using a mixed-effects model, with a Tukey's multiple comparison post-hoc test Fibrin clots (Ca2+) in the presence of M1 protein, formed and read at 25ºC, demonstrated a 1.39-fold increase in streptokinase activity in comparison to fibrin clots (Ca2+) alone (156.93 ± 51.42 IU/µg and 113.21 ± 29.5 IU/µg, respectively, p= 0.0002). Additionally, fibrin clots without the addition of calcium, but with the addition of M1 also showed a 1.46-fold increase in activity in comparison to fibrin without the addition of calcium or M1 (91.91 ± 23.31 IU/µg and 62.98 ± 8.51 IU/µg, p= 0.020). As expected (Figure 56), fibrin clots formed and read at 37ºC displayed no significant differences in plasminogen activation activity of rSK 2a in any condition. The specific activity of rSK 2a at 37ºC remained at a similar level to the '25ºC fibrin alone' condition (formed without calcium chloride) in all tested conditions (62.98 ± 8.51 IU/µg and 64.21 ± 7.80, respectively)

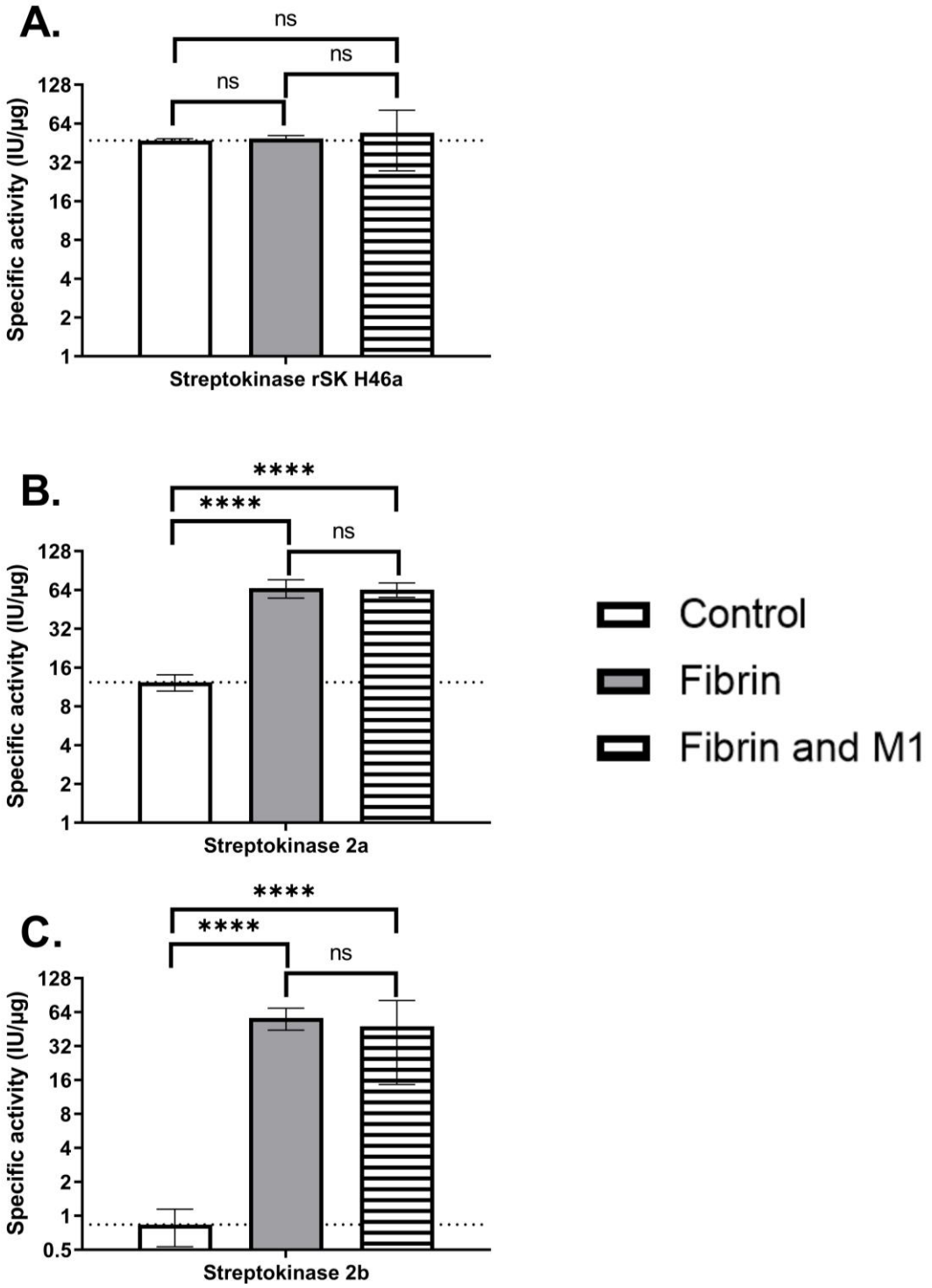

Figure 54 **Streptokinase variants in the presence of fibrin and rM1** Glu-plasminogen activity of streptokinase variants, rSK H46a (A.), rSK 2a (B.), and rSK 2b (C.) was investigated in the presence of 3.1 µg/ml M1 on the surface of a preformed clot. The specific activity was calculated relative to WHO 3rd IS streptokinase (00/464) using parallel line bioassay. Dotted line represents streptokinase alone. Error bar represents 95% CI. (ns = no significance, * $p < 0.05$, ** $p < 0.01$, *** $p < 0.001$, **** $p < 0.0001$, One-way ANOVA with Tukey post-hoc test.) N=≥8

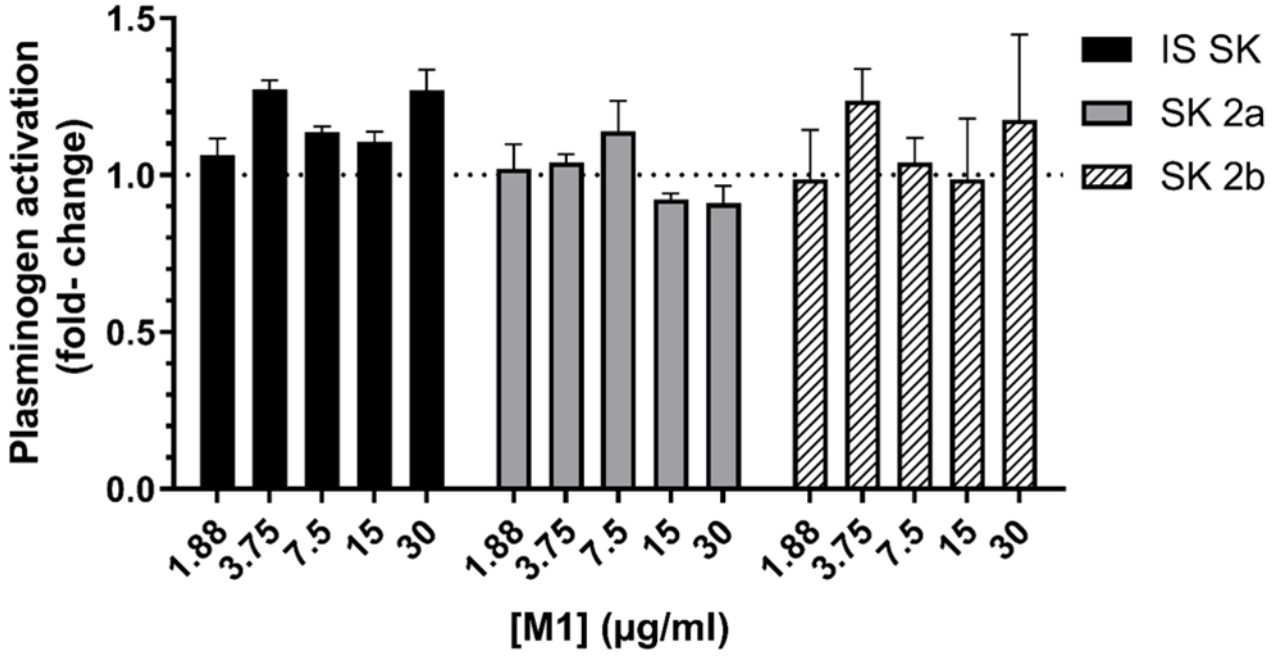

Figure 55 Plasminogen activation activity of streptokinase variants with increasing concentration of rM1 protein Glu-plasminogen activity of streptokinase variants, WHO 3rd IS streptokinase (00/464) (IS SK), rSK 2a (SK 2a) and rSK 2b (SK 2b) was investigated in the presence of increasing concentrations of rM1 (1.88-30 µg/ml) on the surface of a preformed clot using the chromogenic solution assay against S2251. The specific activity was calculated relative to WHO 3rd International Standard streptokinase (00/464) using parallel line bioassay analysis, then presented as fold change. The dotted line indicates streptokinase variants without the presence of rM1. Error bars represent SEM. (No significant differences were shown between M1 concentrations using a One-way ANOVA with a Dunnett post-hoc test) N=≥3

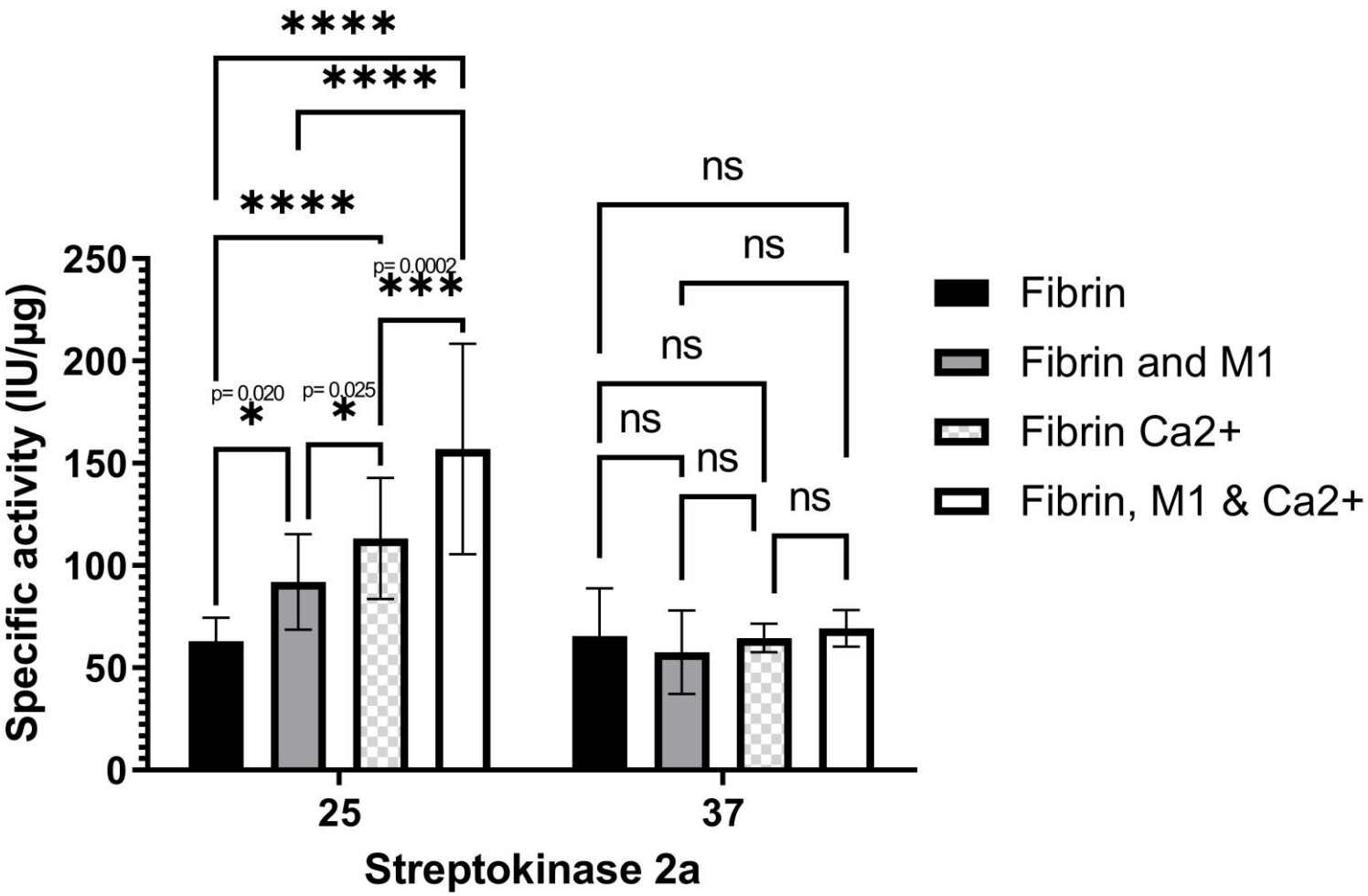

Figure 56 Plasminogen activation activity of rSK 2a in the presence of fibrin with and without rM1 protein, formed at 25ºC or 37ºC Glu-plasminogen activity of streptokinase 2a was investigated in the presence of 3.1 µg/ml M1 on the surface of a preformed clot. Fibrin clots were formed at 25ºC and measured kinetically at 25ºC or formed at 37ºC and measured kinetically at 37ºC The specific activity was calculated relative to WHO 3rd IS streptokinase (00/464) using parallel line bioassay. Error bar represents 95% CI. (ns= no significance, * $p < 0.05$, ** $p < 0.01$, *** $p < 0.001$, **** $p < 0.0001$, Mixed-effects model, with a Tukey's multiple comparison post-hoc test) N=≥3

4.3.5 Assessing the impact of rPAM on streptokinase activity

To investigate the effect of the plasminogen binding M protein (rPAM) on streptokinase activity, the chromogenic solution assay was adapted to include +/-3.1 µg/ml rPAM and +/- 3 mg/ml fibrinogen (HYPHEN BioMed, plasminogen free). A dilution range of each streptokinase variant (4.8- 0.6 IU/ml) was combined with 100 mM glu-plasminogen and 0.6 mM S2251. Plasmin generation was then immediately monitored kinetically at 405 nm. Specific activities were calculated in IU/ µg based on potency estimates and streptokinase protein concentrations. The data was presented as specific activity (IU/µg), with 95% confidence intervals. The statistical significance of the data was tested using a One-way ANOVA with Tukey post-hoc test. As shown in Figure 57A, rSK H46a activity is stimulated 3.06-fold in the presence of rPAM alone (144.362 ± 73.22 IU/µg and 47.21 ± 2.17 IU/µg, respectively). Similarly, rSK 2a activity (Figure 57B) is stimulated 2.99-fold in the presence of rPAM alone in comparison to the control (43.02 ± 32.51 IU/µg and 14.37 ± 1.98 IU/µg, respectively, p= 0.0049). The largest increase observed in the presence of rPAM alone was with rSK 2b (Figure 57C) with a 12.95-fold increase in activity in comparison to the control (9.56 ± 5.55 IU/µg and 0.739 ± 0.369 IU/µg, respectively). However, despite the higher fold increase of rSK 2b activity with rPAM, compared to the other streptokinase variants the specific activity or rSK 2b remains much lower. Consistent with section 4.3.3.2, in the presence of 3 mg/ml fibrinogen rSK H46a (Figure 57A) activity increases by 4.20-fold in comparison to the control (198.26 ± 95.59 IU/µg and 47.21 ± 2.17 IU/µg, respectively, p=0.01). rSK 2a (Figure 57B) was stimulated 2.42-fold in the presence of fibrinogen in comparison to the control (34.74 ± 6.82 IU/µg and 14.37 ± 1.98 IU/µg, respectively, p=0.005) and rSK 2b (Figure 57C) was

stimulated 10.90-fold in activity (8.05 ± 5.48 IU/µg and 0.74 ±0.37 IU/µg, respectively). Addition of both 3 mg/ml fibrinogen and 3.1 µg/ml rPAM did not significantly increase rSK H46a activity further than with fibrinogen or rPAM alone. In comparison to the control condition (without rPAM or fibrinogen) a significant 3.83-fold increase in activity was observed in the presence of fibrinogen and rPAM together (47.21 ± 2.17 IU/µg and 180.71 ± 114.39 IU/µg, respectively, p=0.025). Addition of fibrinogen and rPAM to rSK 2a further stimulated the plasminogen activation activity compared to fibrinogen (3.65- fold increase) and rPAM (2.94-fold increase) alone. In comparison to the control, an overall 8.81-fold increase in activity was observed in the presence of fibrinogen and rPAM (14.37 ± 1.98 IU/µg and 126.67 ± 54.54 IU/µg, respectively, p= <0.0001). Similarly, rSK 2b was further stimulated in the presence of fibrinogen and rPAM in comparison to fibrinogen (4-fold increase) and rPAM (3.59-fold increase) alone. In comparison to the control, addition of fibrinogen and rPAM resulted in a 46.54-fold increase in rSK 2b activity (0.74 ± 0.37 IU/µg and 34.37 ± 13.05 IU/µg, respectively, p= <0.0001).

To investigate the effect of rPAM on the activation of plasminogen by the streptokinase variants further, the solution assays were adapted to include a dilution range of rPAM (0.92- 295.80 µg/ml) and a fixed concentration of streptokinase (4.8 IU/ml). Additionally, the experiment was adapted to include both the closed conformation glu-plasminogen and the more readily activatable lys-plasminogen conformation. The data was presented as mean fold-change (standard error of mean error bars) relative to 0 µg/ml rPAM against a log rPAM concentration range. As shown in Figure 58A with the addition of glu-plasminogen, rSK H46a and rSK 2a continue to increase in a dose-dependent manner as the rPAM concentration increases. At the maximum concentration of

rPAM (295.8 µg/ml), rSK H46a had increased by 5.72-fold (± 0.06), whilst rSK 2a had increased by 8.17-fold (± 0.29) relative to the 0 µg/ml rPAM. A different trend was observed for rSK 2b, which was stimulated to a maximum of 5.70-fold (± 0.31) at 9.2 µg/ml rPAM in comparison to 0 µg/ml. Above 9.2 µg/ml rPAM, rSK 2b activity declined with increasing rPAM concentrations up to the maximum rPAM concentration used (295.80 µg/ml), where the activity was 3.73-fold (± 0.19) higher than 0 µg/ml.

When glu-plasminogen was substituted with lys-plasminogen (Figure 58B), both rSK H46a and rSK 2a displayed a dramatically different trend with increasing concentrations of rPAM. rSK 2a initially increased in lys-plasminogen activation activity, up to a maximum of 1.68-fold (± 0.09) at 9.2 µg/ml, in comparison to the control. Above this concentration rSK 2a activity slowly declines, and at the maximum concentration of rPAM (295.8 µg/ml), the activity had almost returned to baseline levels (1.09-fold ± 0.03). rSK H46a however declines in activity with the increasing rPAM concentrations, at 9.2 µg/ml the activity had reached 0.48-fold (± 0.04) in comparison to the control. At the highest concentration of rPAM tested (295.80 µg/ml), rSK H46a remained at a much lower activity level (0.58-fold) than conditions without rPAM. rSK 2b showed a similar trend to the glu-plasminogen condition, peaking at a slightly lower rPAM concentration of 4.6 µg/ml (4.61- fold ± 0.36) but still remaining relatively high at 9.2 µg/ml rPAM (4.58- fold ±0.35) in comparison to the control. Following these concentrations, a decline in plasminogen activation activity was observed and at the highest concentration of rPAM tested (295.80 µg/ml) the activity of rSK 2b had declined below baseline levels (0.81-fold ± 0.03).

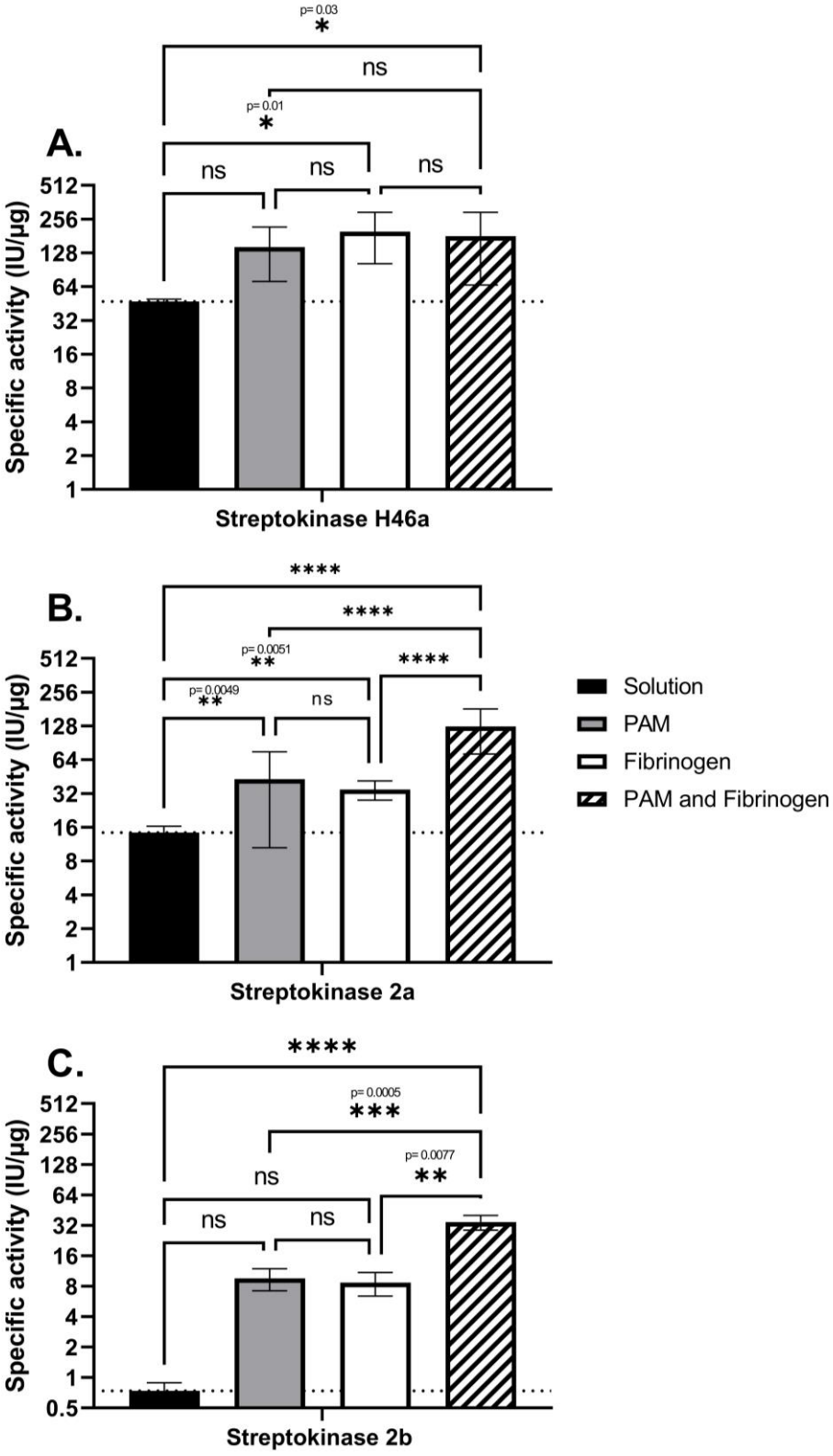

Figure 57 Effect of rPAM and fibrinogen on streptokinase variant activity Glu-plasminogen activation activity of streptokinase variants was investigated using chromogenic solution assay in the presence of 3.1 µg/ml rPAM and 3.0 mg/ml fibrinogen. A control was included for comparison purposes for each streptokinase variant, streptokinase alone, and is also represented by the dotted line. Data was presented as specific activities (IU/µg) of each variant. Error bars represent 95% CI. (ns = no significance, * $p < 0.05$, ** $p < 0.01$, *** $p < 0.001$, **** $p < 0.0001$, One-way ANOVA with Tukey post-hoc test**.)** N=≥3

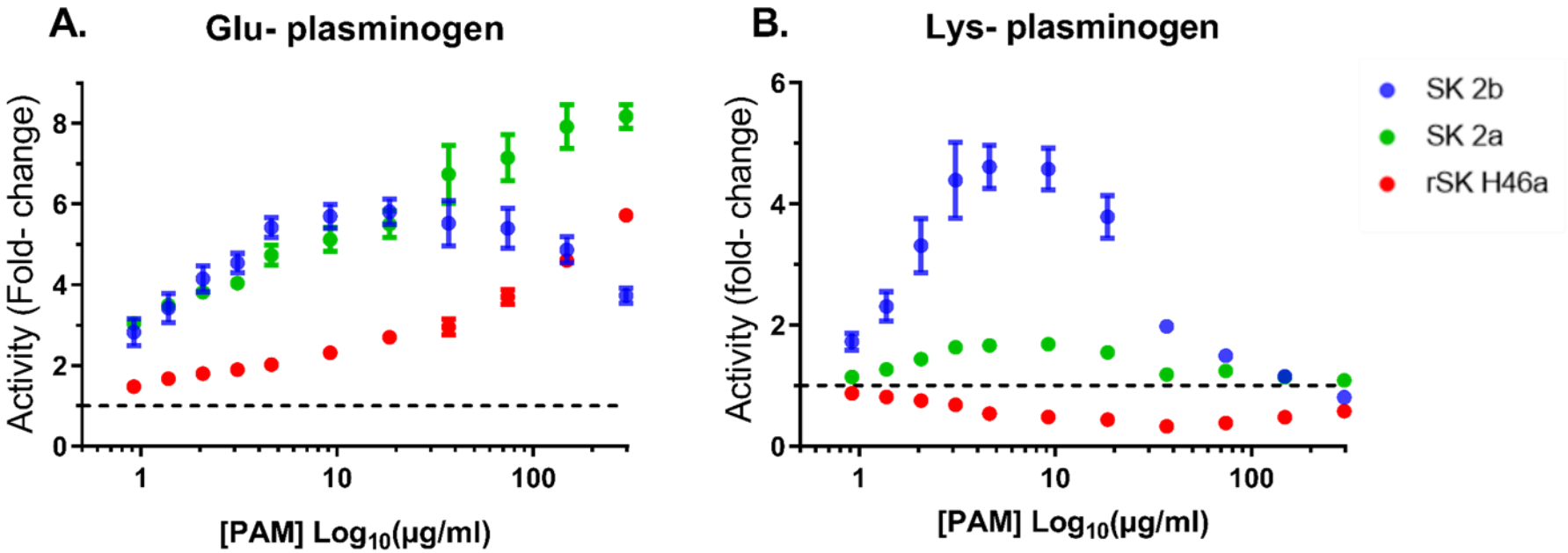

Figure 58 Stimulation of rSK 2b by rPAM is consistent with a template model. Initial activation rates of streptokinase variants, rSK H46a, rSK 2a and rSK 2b, against glu-plasminogen (closed conformation) **(A.)** or lys-plasminogen (open conformation) **(B.)**. Activation rates were determined over a range of rPAM concentrations (0.92 – 295.8 µg/ml) and results are presented as fold-change (relative to 0 µg/ml rPAM) against $\log_{10}$ rPAM concentrations. Error bars represent SEM. N= ≥5

4.3.6 Measuring the impact of Immobilised M proteins on streptokinase plasminogen activation activity

Downregulation of the bacterial protease SpeB, results in a decrease in M protein being cleaved from the cell surface. It was therefore of interest to see if the orientation of the M protein, e.g., cell surface bound M proteins, would influence the streptokinase variants activity. To investigate the effect of the immobilised M protein on streptokinase activity, the chromogenic solution assay was adapted to include +/-immobilised M and +/- 3 mg/ml fibrinogen (HYPHEN BioMed, plasminogen free). M proteins were expressed with a C-terminal histidine tag which was used to immobilise the proteins to the surface of a nickel NTA- microtitre plate. Where included, the fibrinogen was bound to the immobilised rM1 followed by additional washes. No additional washes were performed with immobilised rPAM. A dilution range of streptokinase (4.8-0.6 IU/ml), 100 nM glu- plasminogen and 0.6 mM S2251 were added to initiate the reaction. Plasmin generation was then immediately monitored kinetically at 405 nm. Specific activities were calculated in IU/ µg based on potency estimates and streptokinase protein concentrations, and data was presented as specific activities with 95% CI error bars. The statistical significance of the data was tested using a One-Way ANOVA with a Tukey post-hoc test. Where stated in the results, glu-plasminogen was replaced with lys-plasminogen in the assays. In the absence of M proteins in a well, the Ni-NTA was saturated with Histidine tagged human albumin to minimise non-specific interactions of other proteins.

4.3.6.1 Immobilised rM1

As shown in Figure 59, addition of immobilised rM1 protein alone did not stimulate any of the streptokinase variants. Consistent with section 4.3.3.2, addition of fibrinogen alone stimulated all the streptokinase variants. rSK H46a

(Figure 59A) was stimulated 3.29-fold by fibrinogen in comparison to the control (153.36 ± 29.80 IU/µg and 46.62 ± 1.88 IU/µg, respectively, p= 0.0022). rSK 2a (Figure 59B) activity increased by 3.85-fold (46.51 ± 23.28 IU/µg and 12.09 ± 2.46 IU/µg, respectively, p= <0.0001) and rSK 2b (Figure 59C) increased by 12.59-fold in comparison to the control (11.15 ± 3.93 IU/µg and 0.885 ± 0.30 IU/µg, respectively, p= <0.0001). Addition of fibrinogen-bound-M1 did not stimulate the streptokinase variants any further and displayed no significant differences to the fibrinogen alone condition.

4.3.6.2 Immobilised rPAM

rPAM in solution has previously been shown to stimulate the streptokinase variants, therefore a soluble rPAM condition was included in the assay systems by blocking the binding sites of the Ni-NTA by histidine -tagged albumin. This was to ensure any differences observed were due to the orientation or immobilisation of the rPAM rather than due to different experimental conditions. Consistent with section 4.3.5, all of the streptokinase variants were stimulated by the presence of soluble rPAM. rSK H46a (Figure 60A) demonstrated a 2.86-fold increase in activity in the presence of soluble rPAM in comparison to the control (134.60 ± 81.64 IU/µg and 47.09 ± 1.41 IU/µg, respectively). The presence of immobilised rPAM stimulated the rSK H46a by a further 2.52-fold in comparison to the soluble rPAM condition (339.35 ± 116.94 IU/µg and 134.60 ± 81.637, respectively, p= 0.05). In comparison to the control, rSK H46a activity increased by an overall 7.21-fold increase in the presence of immobilised PAM (p= <0.0001. However, when the glu-plasminogen in these conditions were replaced by lys-plasminogen, the observed increase in activity was lost with a 2.76-fold decrease in activity in comparison to the control (17.06 ± 9.08 IU/µg and 47.09 ± 1.41 IU/µg, respectively).

rSK 2a (Figure 60B) displayed a large increase in activity in the presence of soluble rPAM in these assay systems, with a 19.59-fold increase in activity in comparison to the control (212.76 ± 68.12 IU/µg and 12.86 ± 1.86 IU/µg, respectively, p= 0.0056). When rPAM was immobilised to the Ni-NTA plates, rSK 2a was stimulated a further 1.55-fold than with the soluble rPAM condition (329.70 ± 107.97 IU/µg and 212.76 ± 68.12 IU/µg, respectively) representing a 30.35-fold increase in comparison to the control (p= <0.0001). Similar to rSK H46a, upon substitution of the glu-plasminogen for lys-plasminogen in the immobilised rPAM experiments, rSK 2a displayed no significant differences in comparison to the control (11.28 ± 7.03 IU/µg and 10.86 ± 1.86 IU/µg, respectively).

rSK 2b (Figure 60C) in the presence of soluble rPAM was stimulated by a significant 117.73-fold in comparison to the control (124.21 ± 72.364 IU/µg and 1.06 ± 0.46 IU/µg, respectively, p=0.014). However, rSK 2b was maximally stimulated by the immobilised rPAM with a 237.65-fold increase in activity in comparison to the control (250.72 ± 56.23 IU/µg and 1.06 ± 0.46 IU/µg, respectively, p= <0.0001) and a further 2.02-fold in comparison to soluble rPAM (p= 0.0094). When lys-plasminogen was used in the immobilised rPAM assays instead of glu-plasminogen, a large proportion of the observed stimulation was lost, with a 31.00-fold decrease in activity (8.09 ± 9.19 IU/µg and 250.72 ± 56.23 IU/µg, respectively, (p= 0.0001). However, in comparison to the control, even in the presence of immobilised rPAM with lys-plasminogen a 7.67-fold increase in activity was observed.

4.3.6.3 Immobilised rPAM and fibrinogen

Previous literature has proposed that rSK 2b requires a tri-molecular complex, consisting of cell surface bound PAM, plasminogen, and fibrinogen, in order to

reach full activity (Glinton et al., 2017, Chandrahas et al., 2015, McArthur et al., 2008). To investigate this hypothesis further, the immobilised chromogenic assay systems were adapted to include 3 mg/ml fibrinogen. To ensure that fibrinogen did not interact with the Ni-NTA when rPAM was not included, Histidine-tagged albumin was first bound to the plates to saturate the surface.

As shown in Figure 61, the addition of fibrinogen to immobilised rPAM decreased the activity of each streptokinase variant in comparison to immobilised rPAM alone. rSK H46a (Figure 61A) demonstrated a 3.30-fold decrease in activity in the presence of immobilised rPAM and fibrinogen in comparison to immobilised rPAM alone (102.86 ± 43.86 IU/µg and 339.35 ± 116.94 IU/µg, respectively, p= 0.0014). However, the presence of immobilised rPAM and fibrinogen still stimulated rSK H46a activity 2.18-fold more than the control condition (streptokinase without the additional cofactors/proteins).

Similarly, rSK 2a (Figure 61B) decreased in activity by approximately 1.90-fold in the presence of fibrinogen and immobilised rPAM in comparison to immobilised rPAM alone (173.84 ± 45.85 IU/µg and 329.70 ± 107.97, respectively). However, this was still a 16-fold higher plasminogen activation activity relative to the control condition.

rSK 2b (Figure 61C) also decreased in activity with the addition of fibrinogen and immobilised rPAM in comparison to immobilised rPAM alone with significant 7.38-fold decrease observed (33.97 ± 10.44 IU/µg and 250.72 ± 56.23 IU/µg, respectively, p= <0.0001). In comparison to the control condition, the addition of fibrinogen and immobilised rPAM was a significant 32.20-fold increase in activity due to the lack of rSK 2b activity in solution alone.

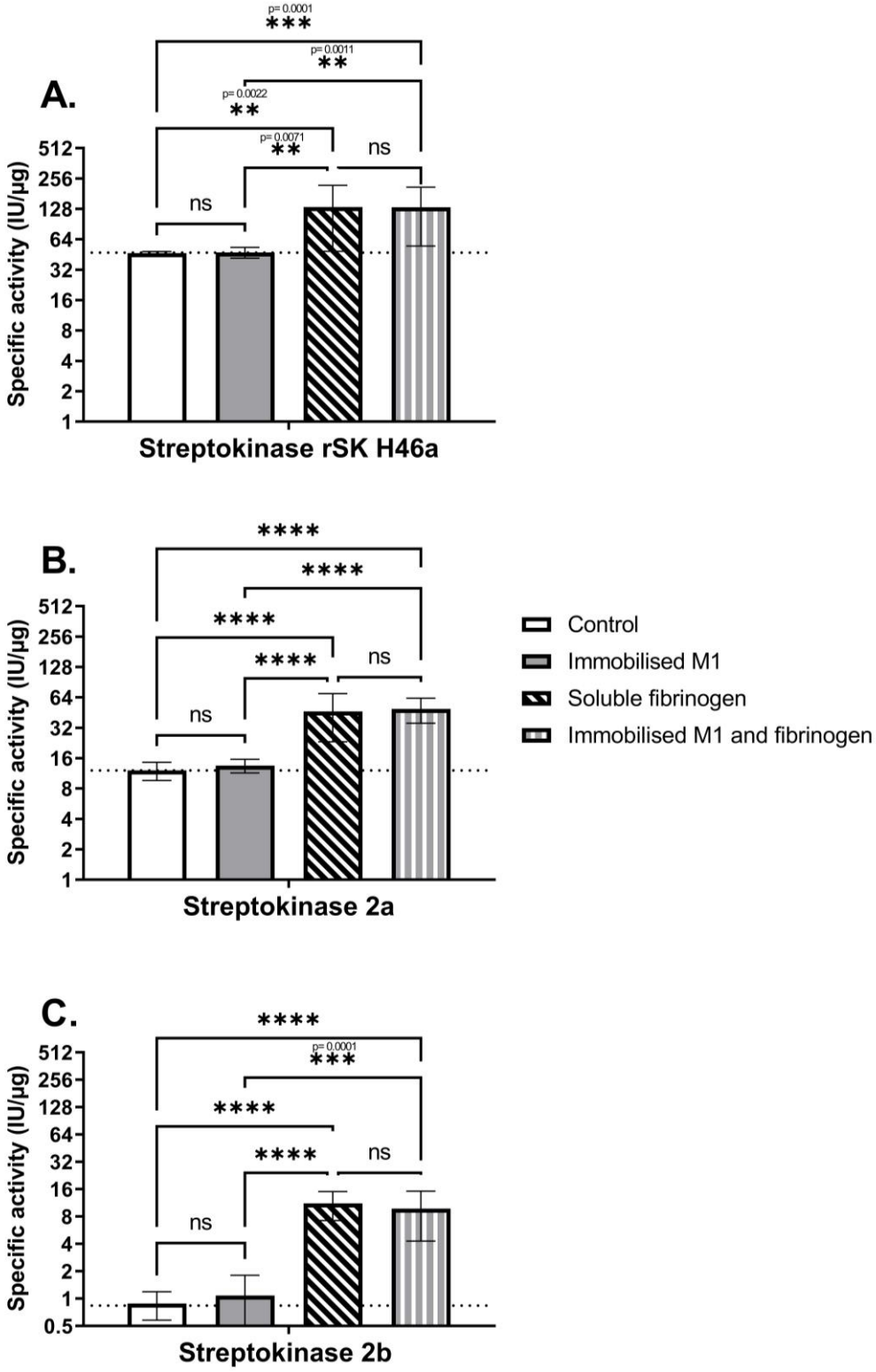

Figure 59 Effect of immobilised rM1 on streptokinase variants M1 protein was immobilised to the 96-well plate via the co-expressed c-terminal 6 x Histidine tag. SK H46a (A.), SK 2a (B.), SK 2b (C.) potencies were calculated relative to the WHO IS SK (00/464) (using a parallel line bioassay) in the presence of immobilised M1, soluble fibrinogen and immobilised M1 with fibrinogen. A control (SK alone) was included for each SK variant and is indicated by a dotted line. Data was presented as specific activities. Error bars represent 95% CI. (ns = no significance, * $p < 0.05$, ** $p < 0.01$, *** $p < 0.001$, **** $p < 0.0001$, One-way ANOVA with Tukey post-hoc test.) N=≥3.

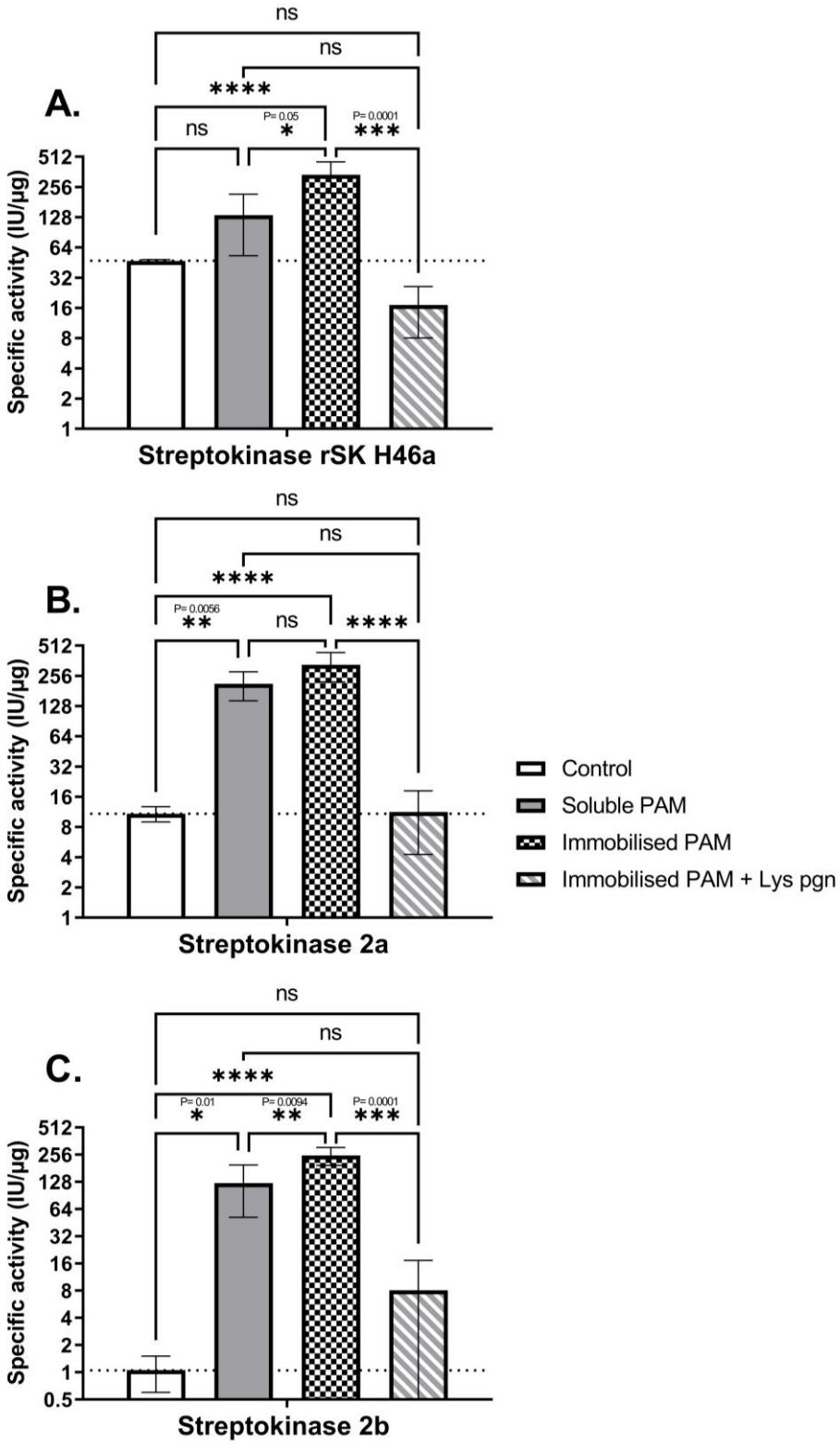

Figure 60 Effect of immobilised rPAM on streptokinase variants with glu and lys-plasminogen PAM protein was immobilised to the 96-well plate via the co-expressed C-terminal 6 x Histidine tag. rSK H46a (A.), rSK 2a (B.), rSK 2b (C.) potencies were calculated relative to the WHO 3rd IS Streptokinase (00/464) (using a parallel line bioassay) in the presence of immobilised PAM, soluble PAM and immobilised PAM with Lys-plasminogen (instead of glu-plasminogen). A control (streptokinase alone) was included for each SK variant and is indicated by a dotted line. Data was presented as specific activities. Error bars represent 95% CI. (ns = no significance, * $p < 0.05$, ** $p < 0.01$, *** $p < 0.001$, **** $p < 0.0001$, One-way ANOVA with Tukey post-hoc test.) N=≥3.

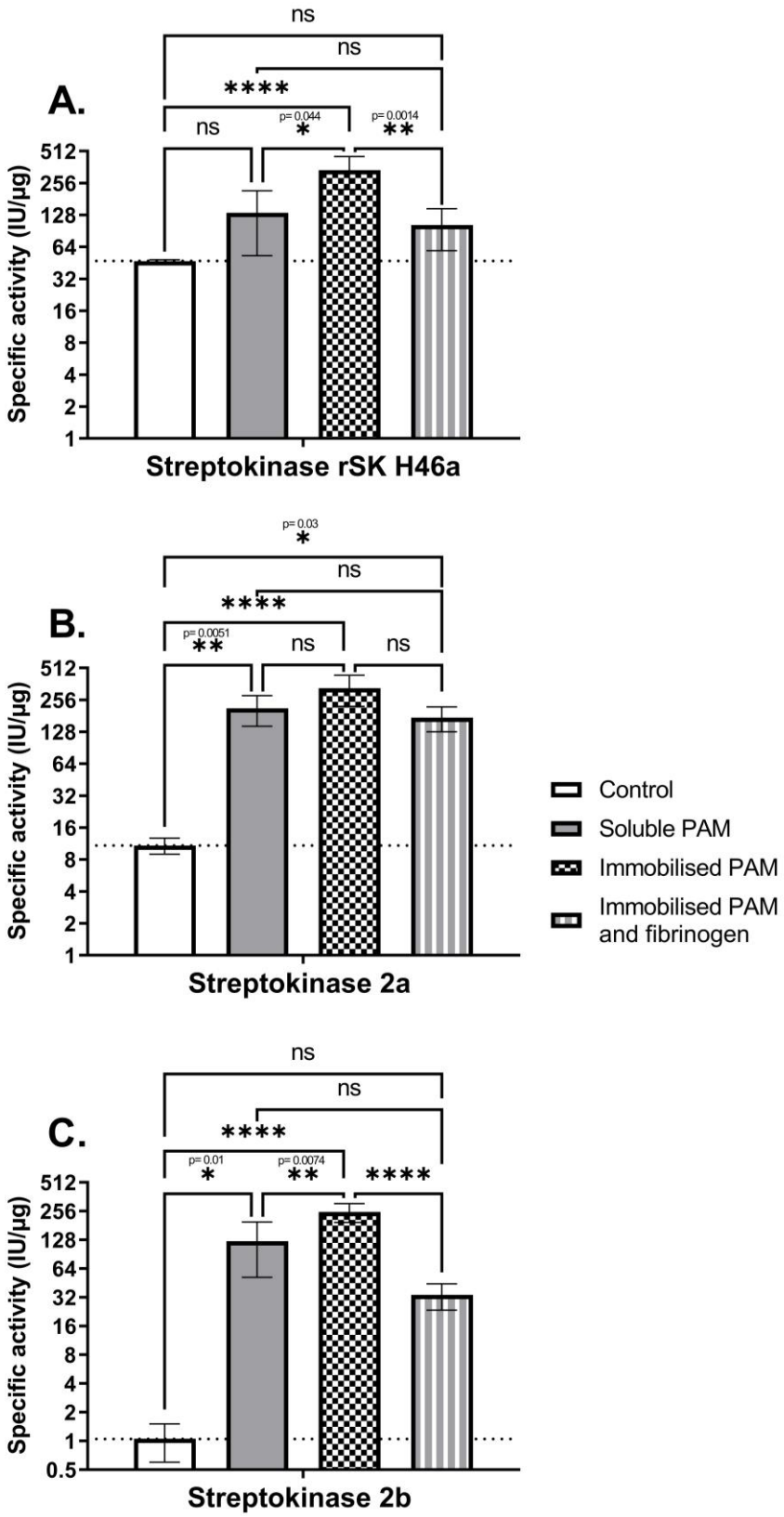

Figure 61 Effect of fibrinogen and immobilised rPAM on streptokinase variants PAM was immobilised to the 96-well plate via the co-expressed C-terminal 6 x Histidine tag. rSK H46a (A.), rSK 2a (B.), rSK 2b (C.) potencies were calculated relative to the WHO 3rd IS Streptokinase (00/464) (using a parallel line bioassay) in the presence of immobilised PAM, soluble fibrinogen and immobilised PAM with fibrinogen. A control (SK alone) was included for each SK variant and is indicated by a dotted line. Data was presented as specific activities. Error bars represent 95% CI. (ns = no significance, * $p < 0.05$, ** $p < 0.01$, *** $p < 0.001$, **** $p < 0.0001$, One-way ANOVA with Tukey post-hoc test.) N=≥4.

4.4 Discussion

A key pathogenic mechanism of invasive bacteria is their ability to express a range of surface- bound and secreted virulence factors. Group A, C and G *Streptococci* secrete a plasminogen activator known as streptokinase which generates plasmin, a serine protease that is capable of degrading fibrin clots, tissue barriers and complement factors (Tewodros et al., 1996, Castellino and Ploplis, 2005, Ploplis and Castellino, 2019). This has been recognised as a critical step in aiding bacterial invasion and evasion of the hosts innate immune response, with streptokinase deficient mutant strains of GAS displaying attenuated virulence in humanised murine models of skin infection (Khil et al., 2003, Sun et al., 2004, Sanderson-Smith et al., 2006). GAS have been divided into three distinct clusters based on phylogenetic analysis of the β-domain of the corresponding streptokinase sequences (Figure 6) 1,2a and 2b) (McArthur et al., 2008, Kalia and Bessen, 2004). Phylogenetic studies have also indicated that the streptokinase clusters are associated with tissue specific *emm* patterns of the bacterium (McArthur et al., 2008). Cluster 2a expressing strains of GAS are nasopharyngeal-specific and are commonly associated with the fibrinogen binding M1 protein, encoded by the *emm 1* gene. The streptokinase 2a has low plasminogen activity in solution however has previously been found to be stimulated by fibrinogen and maximally by fibrin (Huish et al., 2017). The streptokinase 2b is secreted from skin-tropic isolates which express the cell bound plasminogen-binding M proteins, such as PAM (Kalia and Bessen, 2004, Hynes and Sloan, 2016). Streptokinase 2b has very low activity towards plasminogen in solution but this is increased in the presence of plasminogen bound PAM (Zhang et al., 2012). Cluster 1 streptokinase are thought to require no additional co-factors for full plasminogen activity, much like the well

characterised streptokinase from the H46a strain of the Group C *Streptococcus equisimilis* (McArthur et al., 2008).

The streptokinase mechanism of plasminogen activation is mainly understood based upon the therapeutic Group C streptokinase, H46a. Therefore, a recombinantly produced Group C H46a was used in this project, as a comparison with the Cluster 2 streptokinase variants. The streptokinase H46a was previously calibrated to have the same potency and specific activity as the WHO 3rd International standard streptokinase (00/464) and used in previous literature (Huish et al., 2017). The streptokinase variants potencies were calculated using parallel line bioassay analysis relative to the WHO 3rd International standard streptokinase (00/464), which is a native streptokinase protein.

Streptokinase is highly conserved, which was confirmed by multiple sequence alignments (Figure 62) showing 81.7% sequence identity between the three streptokinase variants used in this study (with the sequence identity increasing when comparing two variants; SK 2a SF370 and SK 2b NS88.2: 88.7%, SK 2a SF370 and SK H46a: 88.4%, SK 2b and SK H46a: 85.1%). The first 59 residues of the streptokinase α-domain are thought to be important for plasminogen activation (Boxrud et al., 2001, Cook et al., 2012), with the N-terminal Ile1 residue found to be critical due to the formation of a salt bridge with the Asp740 of plasminogen which induces a conformational change (Wang et al., 1999, Wang et al., 2000) (Figure 62). Although all of the streptokinase variants contain the N-terminal Ile1, the Cluster 2 streptokinase variants contain 11 amino acid differences in the 1-59 region, in comparison to the streptokinase H46a (Figure 62). These sequence differences might prevent the correct conformation for the streptokinase N-terminal within the streptokinase-plasminogen complex,

causing the reduced plasminogen activation activities observed with the Cluster 2 variants. Despite these differences in amino acid sequences, the streptokinase variants have been shown to maintain similar secondary structures (Kapur et al., 1995, Cook et al., 2012). However, the relationship between the streptokinase sequence variations, and the M-protein association is not fully understood at the molecular level.

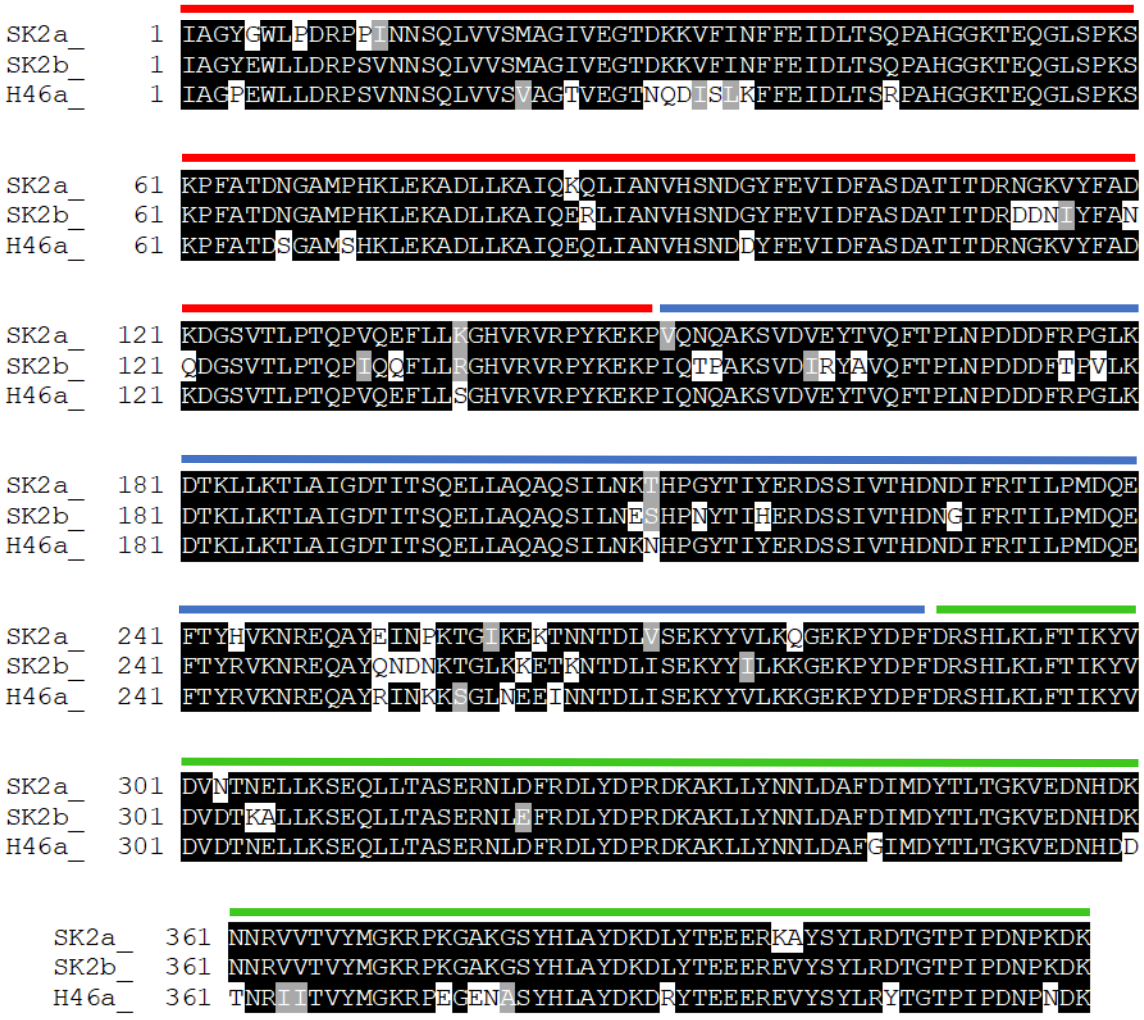

Figure 62 Multiple sequence alignment of streptokinase variants used in this study.). Multiple sequence alignment of SK H46a (H46a, Accession number: K02986.1), SK 2a (SF370, Accession number: AAK34665.1) and SK 2b (NS88.2, Accession number: JX898186) was performed in Vector NTI (InforMax, Bethesda, MD, USA). The SK variants share 81.7% sequence identity (99.3% consensus positions). The line indicates the streptokinase domains, red = α- domain, blue = β- domain and green = γ- domain.

4.4.1 Specific activities of SK variants

The specific activity of rSK 2a was previously calculated to be 12.4 IU/μg by Dr. Sian Huish using solution plasminogen activation assays to calculate potency estimates against the WHO 3rd IS streptokinase (00/464) (Huish et al., 2017). The new batch of rSK 2a produced in this project was consistent with this finding, with a calculated specific activity of 12.27 IU/μg. Potency estimates for rSK 2b in IU have not previously been published, therefore the solution plasminogen activation assay was used to investigate this. The rSK 2b displayed very little activity in solution, with a specific activity of 0.84 IU/μg. This is consistent with previous reports involving culture supernatants, where chromogenic solution assays revealed that SK 2b cannot effectively activate plasminogen in solution (Cook et al., 2012, McArthur et al., 2008). Additionally, SPR analysis revealed SK 2b has an ~30-fold lower affinity for glu-plasminogen in solution suggesting that SK 2b fails to interact with glu-plasminogen and cannot induce an active site in glu-plasminogen (Cook et al., 2014, Cook et al., 2012). The streptokinase Ile1 residue must be positioned within the plasminogen active site so that it can form a salt bridge with (plasminogen) Asp740 in order to form an active site (Wang et al., 1999). The Group C streptokinase, rSK H46a demonstrated significantly higher activity relative to the Cluster 2 SK variants without the presence of co-factors or ligands (Figure 46).

4.4.2 Streptokinase variants in the presence of fibrin(ogen)

Fibrinogen is thought to play an important role in GAS pathogenesis, with many GAS expressing fibrinogen binding M proteins, e.g. M1, on the cell surface that is proposed to provide a template for plasminogen acquisition for SK 2a activation. Additionally, other strains of invasive GAS express plasminogen binding M proteins, e.g. PAM, on the cell-surface that is proposed to require a

trimolecular complex with PAM, plasminogen and fibrinogen for maximal activation by SK 2b (McArthur et al., 2008). It has previously been demonstrated that fibrinogen provides a template for assembly of rSK 2a-plasminogen complex (Huish et al., 2017). Whilst SK 2b has previously been shown to be stimulated in the presence of fibrinogen (McArthur et al., 2008, Cook et al., 2014), experimental evidence that fibrinogen provides a template for rSK 2b is limited due to previous studies using a single concentration of fibrinogen. Chromogenic plasminogen activation assays with increasing concentrations of fibrinogen (HYPHEN BioMed, plasminogen free), used previously to investigate rSK 2a activity, were repeated with rSK 2b. As shown in (Figure 49B and D), the rSK 2b does not show evidence of a bell-shaped profile suggesting that the stimulation is not due to the formation of a template mechanism. The optimum fibrinogen concentration range for rSK 2a stimulation was 3-5 mg/ml (Huish et al., 2017), it is plausible that the rSK 2b activity could begin to decrease with fibrinogen concentrations above 5.4 mg/ml, however, due to the limited availability of plasminogen-free fibrinogen and low concentration of the bulk fibrinogen, these experiments could not be performed. The presence of 3 mg/ml fibrinogen (HYPHEN BioMed, plasminogen free) only increased the specific activity of rSK 2b to ~7.24 IU/µg, a lower activity than rSK 2a plasminogen activity without the presence of co-factors, demonstrating that fibrinogen is a weak stimulator of rSK 2b. The Group C streptokinase activity was also stimulated in the presence of fibrinogen, demonstrating a bell-shaped plot of fold change in activity verses fibrinogen concentration, appearing to follow a template mechanism (Figure 48A, Figure 48C, Figure 49A, Figure 49B and Figure 49C). The observation conflicts with previously published data and the accepted notion that Group C streptokinase is not significantly stimulated by

external factors (Section 1.4.3), although the results for rSK 2a were consistent with the findings of Huish et al., (Huish et al., 2017). Stimulation of rSK 2a activity by fibrinogen was reproduced using different batch numbers of the same commercial fibrinogen and with different fibrinogen products of varying purity. Some commercial fibrinogen products and lot numbers were found to contain contaminating plasminogen (Figure 48C & Figure 48D) which could indicate that stimulation of activity was due to the presence of additional zymogen. However, when plasminogen activation assays were repeated with fibrinogen purified using affinity chromatography with an IF-1 antibody to remove contamination (Figure 48E), a dose-dependent increase in Group C streptokinase activity was observed. At the highest concentration tested, 2.8 mg/ml, the Group C streptokinase activity had increased by almost 17-fold in comparison to the absence of fibrinogen. Whilst this data appears to conflict with previous literature (Huish et al., 2017), the Group C streptokinase has been observed to be enhanced by full length fibrinogen and fibrinogen D domains previously (Chibber et al., 1985, Cook et al., 2014). Additionally, the activation profile was reproduced with both the native (WHO 3rd IS streptokinase (00/464)) and recombinant (rSK H46a) Group C streptokinase, further supporting the conclusion reached that fibrinogen stimulates SK H46a activity (Figure 48A & Figure 49C). Experiments have shown that plasmin cleaves soluble fibrinogen, exposing cryptic sites within the protein and enabling the fibrinogen D-domain to bind with plasminogen (Varadi and Patthy, 1983). The structure of plasminogen conformation is thought to be altered to a more activatable form upon binding or interaction with ligands, which has been shown to enhance the activation rate by streptokinase (Cook et al., 2014). Therefore, the stimulation levels by fibrinogen is likely to reflect the streptokinase variants individual ability to

activate plasminogen free in solution to generate the initial plasmin. For example, rSK 2b cannot effectively generate an active site in solution (77, 92) as evident by the specific activity, 0.84 IU/µg (Figure 46). The small amount of plasmin that is generated by rSK 2b can cleave the fibrinogen providing a binding site for addition plasminogen molecules, relaxing the conformation to a more readily activatable zymogen; thus stimulating rSK 2b activity 8.6-fold (7.24 IU/µg/ml) in the presence of 3 mg/ml fibrinogen.

Previous investigations have found that fibrin is a potent stimulator of rSK 2a activity, displaying a ~14-fold higher activity than rSK H46a in the presence of fibrin (Huish et al., 2017). In the current work, it was also demonstrated that fibrin is a potent stimulator of rSK 2a activity. However, the stimulation was not to the same extent, with specific activities calculated to be ~59.82 IU/µg (Figure 47B), which is similar levels to the published specific activity of rSK H46a in solution, 58.2 IU/µg (Huish et al., 2017) . The difference between observed stimulation between these experiments and previous literature could be due to experimental differences. For example, the local conditions that the present during fibrin polymerisation strongly influences the final clot structure, in the present study, the fibrin clots were activated in the presence of $CaCl_2$ which has previously been shown to decrease clotting time, increase clot fibre density and decrease fibrin fibre diameter (Carr et al., 1986, Hardy et al., 1983, Ryan et al., 1999). Additionally, the clots were kept at 37ºC and monitored at 37ºC, therefore any deviations from this could alter the fibrin structure and thus affect the observed results, such as those in previous study (Huish et al., 2017). For example, Figure 56 demonstrates this effect, where purified fibrin clots formed at 25ºC and monitored at 25 ºC enhanced plasminogen activation of rSK 2a by ~9.23-fold (113.21 IU/µg), relative to activity in solution. Additionally, different

methods were used in this study for calculating the activity of rSK 2a activity. The previous study used turbidimetric analysis of clotting and lysis curves, where streptokinase is incorporated into the forming clot (Huish et al., 2017). In the present study, the activity was measured upon addition of streptokinase and a chromogenic substrate to the surface of a preformed clot. The use of a fibrin-bound plasminogen activation assay may provide more insight into the clot resistance, as it looks specifically at streptokinase activity at the preformed clot surface imitating *in vivo* infection and the way the bacteria may breakthrough the defence.

Fibrin also proved to be a potent stimulator of rSK 2b demonstrated by a 72-fold increase in activity in comparison to solution levels. In the presence of fibrin, rSK 2b plasminogen activation activity is enhanced to similar levels to the Group C streptokinase (Figure 47C). Suggesting that SK 2a and SK 2b would preferentially activate plasminogen in an environment where fibrin is present rather that in solution. Consistent with previous studies that describe Group C streptokinase as fibrin-independent; rSK H46a was not stimulated by fibrin (Figure 47A) (Huish et al., 2017).

4.4.3 Streptokinase variants in the presence of associated M-like proteins

4.4.3.1 Solution rM1

M1 protein can be released from the GAS cell surface through cleavage by SpeB (Berge and Bjorck, 1995b) or neutrophil proteases (Herwald et al., 2004), resulting in functionally active fragments at the site of infection. The M1 protein can bind fibrinogen with a high affinity to form a supramolecular complex (Macheboeuf et al., 2011, Glinton et al., 2017). The M1-fibrinogen complex has been shown to be capable of activating neutrophils and platelets (Section

1.4.2.1), suggesting that the fibrinogen bound to M1 may have different structural properties to cell-bound M1. However, the significance of M1-bound fibrinogen free in solution for plasminogen activation by associated Cluster 2a SK is not fully understood.

4.4.3.1.1 rM1 and fibrinogen

Chromogenic solution plasminogen assays were modified to incorporate rM1 protein then the activity of the rSK H46a, rSK 2a and rSK 2b was calculated using a parallel line bioassay model relative to the WHO 3rd IS streptokinase (00/464). Purified fibrinogen (HYPHEN BioMed, plasminogen free) was added to the assays to investigate if the streptokinase required the formation of a trimolecular complex in solution for maximal activity. In agreement with previous literature (Zhang et al., 2012, Glinton et al., 2017), minimal stimulation of the streptokinase variants was observed in the presence of rM1 alone (Figure 54). However, in contrast to previous findings (Glinton et al., 2017), rSK 2a was not stimulated any further by the presence of rM1 bound fibrinogen, than in the presence of fibrinogen alone (Figure 54B).

Glinton et al. performed chromogenic solution plasminogen activation assays which demonstrated that in the presence of fibrinogen, SK 2a- mediated activation of plasminogen was increased by ~2-fold in comparison to alone, and a further 7-9-fold in the presence of rM1 bound fibrinogen. The conflicting results in comparison to those observed in this project is most likely to be due to experimental conditions. Glinton et al. used a much lower concentration of fibrinogen in these experiments (200 nM = ~0.084 mg/ml). Whereas in the experiments performed in this PhD project, 3 mg/ml fibrinogen was used to better represent physiological concentrations in blood (Section 1.1.3). Fibrinogen is thought to provide a template for rSK 2a by forming a ternary

complex with plasminogen, with optimum stimulation occurring around physiological concentrations of fibrinogen (3 – 5 mg/ml) (Huish et al., 2017). This suggests a relationship might exist between M1 protein and fibrinogen, whereby low concentrations of fibrinogen binding M1 protein stimulate rSK 2a by forming a trimolecular complex, however at optimum concentrations of fibrinogen the presence of M1 does not affect the activity. To confirm this, the experiments would need to be repeated with the same conditions (e.g. buffers) with varying concentrations of rM1 and fibrinogen for any indications of stimulation at different concentrations. rSK 2b demonstrated a similar trend to rSK 2a; no further plasminogen activation activity was observed in the presence of rM1 bound fibrinogen, than with fibrinogen alone (Figure 54C). This is consistent with previous studies which demonstrated that when PAM was replaced with M1, there was no significant activation by rSK 2b (Zhang et al., 2012). Unexpectedly, although not physiologically relevant to *Streptococcus* infection due to Group C streptokinase not associated with M1 protein (McArthur et al., 2008), rSK H46a was further stimulated by rM1 bound fibrinogen. Plasminogen binding sites have been previously been located in the D-domain of fibrinogen (Varadi and Patthy, 1983) and X-ray crystallography has demonstrated that the M1 protein dimer binds 4 fibrinogen D- domains in a cross-like pattern (Section 1.4.2.1). The rSK H46a has previously been shown to optimally activate plasminogen in solution (McArthur et al., 2008), resulting in plasmin generation. M1 bound fibrinogen may result in colocalisation of plasminogen, resulting in enhanced conversion of glu-plasminogen to the more readily activatable conformation, lys-plasminogen, by plasmin (Lahteenmaki et al., 2001) which is more rapidly converted into the proteolytic enzyme (Castellino and Violand, 1979) by rSK H46a.

4.4.3.1.2 rM1 and fibrin

Chapter 3 described the impact of rM1 protein on fibrin clot formation, properties and fibrinolytic potential by the WHO 3rd IS streptokinase and host plasminogen activators, uPA and tPA. The resultant clots displayed significantly different properties in the presence of rM1. Higher concentrations of rM1 formed heterogenous clots with increased porosity, decreased clot strength, decreased cross-linking by FXIIIa and a decrease in the protective fibrin film (Chapter 3). Previous studies have indicated that fragile clots are more susceptible to fibrinolysis (Chapin and Hajjar, 2015), therefore it was hypothesised that the fibrin bound M1 clots would lyse at a faster rate. Whilst, the WHO 3rd IS streptokinase (00/464) used in these experiments displayed no significant differences in time to 100% lysis in purified conditions using ROTEM and turbidimetric analysis. Addition of WHO 3rd IS streptokinase (00/464) to blood clots made with whole blood, with increasing concentrations of rM1 demonstrated faster clot dissolution times in ROTEM and halo microtitre plate assays (section 3.4.4). It is important to note that Group C streptokinase are not associated with the M1 protein therefore this does not represent physiological conditions (McArthur et al., 2008). Therefore, the turbidimetric assays were repeated incorporating rSK 2a, rSK H46a and rSK 2b then time between 50% clotting and 50% lysis and time to 100% lysis was derived from the curves. Whilst the time between 50% clotting and 50% lysis indicated slower rates for all of the streptokinase variants with increasing rM1 (Figure 51A), the time to reach 100% lysis showed no significant differences, except for at 30 µg/ml rM1 which showed a slower lysis time (Figure 51B). Care must be taken when interpreting these results which may be explained by the fibrin clots displaying higher resistance to lysis, or due to the change in the turbidimetric profiles

caused by optical differences in the fibrin rather than being a true reflection of the rate of lysis. The effect of rM1 bound fibrin was investigated further in whole blood using a halo assay. The blood clots incorporating rM1 are clotted around the bottom of the well with TF, and upon addition of the streptokinase containing lysis buffer, clot dissolution is monitored using a BMG FluorStar® Omega plate reader. The use of whole blood in these experiments makes the results more physiologically relevant. Additionally, the assay looks specifically at streptokinase activity at the preformed clot surface imitating *in vivo* infection and the way the bacteria may breakthrough the defences. Consistent with the WHO 3rd IS streptokinase (00/464) data (section 3.4.4), increasing the rM1 protein concentrations leads to faster fibrin dissolution in all streptokinase variant conditions (Figure 53). However, as shown in Figure 54 and Figure 55 when the plasminogen activation rate was measured on the surface of a preformed clot using a chromogenic substrate, the concentration of rM1 bound fibrin does not affect the rate of plasmin generation in rSK H46a, rSK 2a or rSK 2b. Therefore, suggesting that the differences in dissolution rates are due to structural changes described in Chapter 3, rather than the generation of more plasmin by plasminogen activators. These results suggest that the activity of rSK 2a is independent of M1 protein that is cleaved from the cell surface.

It is important to note that the plasminogen activation kinetics of rSK 2a in the presence of rM1 was temperature dependent (Figure 56). When the clots were formed at lower temperatures and monitored kinetically at lower temperatures (25ºC), a stimulation in rSK 2a activity was observed. The M1 protein has previously been shown to have a lower level of α-helices at 37ºC than at 25ºC. This loss in secondary structure causes a dissociation of M1 dimers into monomers, which has also been demonstrated to decrease the binding of

human fibrinogen (Nilson et al., 1995, Cedervall et al., 1997). Whilst 25ºC is not physiologically relevant, the bacterium will encounter different environments during infection. The experiments conducted during this project were carried out at 37ºC, as this is the optimum temperature for GAS growth (Gera and McIver, 2013) and is the average core temperature in humans. However, fever can occur during infection raising the core temperature to above 40ºC (White et al., 2011). Additionally, skin-tropic strains of GAS might encounter much cooler temperatures. All of these variations in temperature have been shown to have an effect on the secondary structure of M-proteins and could aid in the progression of infection.

4.4.3.2 Immobilised rM1

The proposed model for the progression of severe invasive GAS infections suggests that later in infection GAS are selectively pressured towards those with CovRS mutations (section 1.4.1). These mutations result in upregulation of key virulence factors including streptokinase and a repression in the protease, SpeB (Cole et al., 2011). The repression of SpeB results in the retainment of M1 protein on the surface of GAS, which is thought to promote cell surface plasmin generation through the formation of a trimolecular complex with fibrinogen (McArthur et al., 2008, Glinton et al., 2017). Little is currently known about the stimulatory effect that fibrinogen bound M1 has on plasminogen activation by SK 2a. A model of cell-bound M1 protein was used to investigate this, whereby rM1 protein was immobilised on the surface of the wells of a nickel-coated microtiter plate. The rM1 protein was bound to the nickel-coated surface via a C-terminal Histidine tag and plasminogen activation by the streptokinase variants was investigated in the presence of rM1 alone, soluble fibrinogen alone and with rM1 pre-incubated with fibrinogen. Where soluble

fibrinogen was included in the wells, the nickel-coated surface was pre-saturated with histidine tagged albumin to prevent non-specific binding of fibrinogen. As demonstrated in Figure 59, immobilised rM1 does not enhance the activation of glu-plasminogen by rSK H46a, rSK 2a or rSK 2b. Additionally, fibrinogen bound immobilised rM1 does not further stimulate the activation of the streptokinase variants further than in the presence of fibrinogen alone (Figure 47). Based upon these results, it is proposed that the Cluster 2a streptokinase is independent of its associated M1 protein for activation, and preferentially activates plasminogen in the presence of fibrin. Whilst independent to associated SK 2a, cell bound M1 aids in the dissemination of the bacteria by camouflaging the GAS from opsonophagocytic killing (Ringdahl et al., 2000, Carlsson et al., 2005) and promotes cell surface plasmin generation by binding plasminogen to fibrin(ogen) (Glinton et al., 2017). It is not currently known if other bacteria species use a similar mechanism with cell-surface fibrinogen receptors to acquire cell surface plasminogen.

4.4.3.3 Solution rPAM

SK 2b-expressing strains are unique in that they are commonly associated with a plasmin(ogen)-binding M protein known as PAM. SK 2b cannot generate an activate site in glu-plasminogen solution through conformational rearrangement, which is consistent with the specific activities calculated using chromogenic solution plasminogen assays (0.84 IU/µg, section 4.4.1). Current understanding of plasminogen acquisition and activation by SK 2b-expressing strains is limited, with proposed mechanisms suggesting that optimal plasminogen activation requires the formation of a trimolecular complex between the streptokinase-plasminogen-fibrinogen bound to PAM (Zhang et al., 2012, Chandrahas et al., 2015). To further investigate this mechanism chromogenic solution assays were

amended to incorporate 3.1 µg/ml rPAM and 3 mg/ml fibrinogen (Figure 57). Consistent with previous results (Zhang et al., 2012, Chandrahas et al., 2015), PAM stimulates the plasminogen activation activity of rSK 2b ~12.95-fold (Figure 57C). In the presence of rPAM and fibrinogen the activity of rSK 2b is increased by ~46.54-fold, from almost zero in solution assays which are levels comparable to the Group C streptokinase (Figure 57C). Whilst previous studies using culture supernatants (McArthur et al., 2008) have suggested that PAM does not further stimulate the activity of SK 2b, studies using purified conditions are consistent. The experiments that do not observe a stimulation in the presence of PAM use the culture supernatant as a source of SK 2b; which has been shown to contain L-lysine, and analogues, an inhibitor streptokinase-plasminogen formation (Lin et al., 2000). The rSK H46a and rSK 2a was also stimulated ~3-fold in the presence of rPAM (Figure 57A &Figure 57B). However, whilst rSK H46a was not stimulated further by the presence of fibrinogen and rPAM, rSK 2a activity was enhanced by 8.81-fold in comparison to solution activity levels (Figure 57C). The stimulatory effect of rPAM was investigated further by amending the assays to incorporate a dilution range of rPAM in the presence of glu-plasminogen, or lys-plasminogen. The bell-shaped profile of the rSK 2b plots of fold change in activity verses log of the PAM concentration, appears to follow a template mechanism (Figure 58). The increase in rPAM, the template protein, causes an observed increase in plasminogen activation rates up to the optimum rPAM concentration (Figure 63). This suggests that rPAM has a novel binding region for both rSK 2b and plasminogen, allowing the formation of a ternary complex (Figure 63). The optimum stimulation of rSK 2b was observed between 9.2- 36.98 µg/ml rPAM in the presence of glu-plasminogen (Figure 58A) and 3.1 – 18.49 µg/ml rPAM in the presence of lys-

plasminogen (Figure 58B). Binding of rSK 2b-plasminogen and plasminogen to the rPAM surface brings the activator and substrate into close proximity. However, as the rPAM concentration continues to increase, the rSK 2b and plasminogen are likely to bind to different rPAM molecules and the stimulatory effect is lost (Figure 63). PAM is a cell-surface bound M-protein that covers the surface of GAS in a hair-like fimbriae, therefore it is difficult to pinpoint whether these are physiologically relevant concentrations. The rSK H46a and rSK 2a displayed similar levels of glu-plasminogen stimulation in the presence of increasing concentrations of rPAM (Figure 58A). However, upon replacement with lys-plasminogen the Group C Streptokinase, rSK H46a, was not stimulated by rPAM (Figure 58B). This suggests that the stimulation observed with rSK H46a was due to the conformation change of glu-plasminogen binding to rPAM. Recent studies of PAM binding glu-plasminogen lysine binding sites have demonstrated that upon binding, the conformation of the zymogen is relaxed which is more readily activatable (Ayinuola et al., 2021b), thus explaining the loss in stimulation of rSK H46a upon addition of lys-plasminogen. Whilst there was also a dramatic decrease in stimulation rSK 2a in the presence of rPAM bound lys-plasminogen, there is still evidence of a bell-shaped profile, suggesting rSK 2a might also bind to weakly PAM.

This template mechanism is not observed with any of the streptokinase variants in the presence of rM1, suggesting it is specific to rPAM. PAM is a major virulence factor of skin tropic GAS strains, which has previously been shown to bind strongly to Kringle 2 of human plasminogen (~1 nM) via the N terminal A1A2 domains (Wistedt et al., 1998, Wistedt et al., 1995). Mutagenesis studies of the A1A2 domains in PAM have indicated that plasminogen binding occurs via interactions with a Arg His motif. A dramatic reduction in plasminogen

binding is observed upon mutation of these amino acids (Sanderson-Smith et al., 2007, Bhattacharya et al., 2014). The PAM used in this project (NS88.2) is a Class II PAM, which means it only contains the A2 domain, the Arg His motif thought to be responsible for plasmin(ogen) binding is circled in Figure 64. The A2 domain has previously been shown to have a 5-fold higher affinity for plasminogen Kringle 2 domain than the A1 domain (Quek et al., 2019). The M1 protein does not contain any of these consecutive residues, except for in the signal peptide which is removed in the mature protein, possibly explaining the inability for M1 to bind plasminogen (Figure 64) (Qiu et al., 2019). The mature protein sequence of rM1 and rPAM share 60.7% sequence identity, with the C and D domains being the most conserved regions (Figure 64). This mechanism can be further investigated by ensuring other rPAM from different GAS strains demonstrate this template profile. Once confirmed, multiple sequence alignments of rPAM from different GAS strains might identify common motifs in the B-like regions or hypervariable regions of different rPAM for mutagenesis studies and to investigate binding kinetics using SPR.

4.4.3.4 Immobilised rPAM

PAM is not thought to be cleaved by SpeB, as indicated by previous studies investigating the plasminogen binding levels to the GAS surface in culture supernatants which revealed no differences between the presence or absence of the SpeB protease (Agrahari et al., 2013). PAM is thought to be essential for cell-surface plasmin acquisition, providing GAS with a proteolytic coat that can disrupt extracellular matrix and tight junctions, aiding in the dissemination of the bacterium (Sanderson-Smith et al., 2008, Sumitomo et al., 2013, Sumitomo et al., 2016, Lahteenmaki et al., 2000). Whilst PAM is not the only plasminogen receptor on streptococcus (e.g. enolase (Pancholi and Fischetti, 1998) and

GAPDH (Winram and Lottenberg, 1996)). PAM knockout mutants of GAS demonstrated significantly reduced plasmin(ogen) binding suggesting that PAM is the main receptor for cell surface plasmin(ogen) acquisition (Agrahari et al., 2016). Studies on the activation kinetics of plasminogen - cell bound PAM by SK 2b is mainly understood based upon cell culture supernatant activity. Culture supernatants contain L-lysine, and many of its analogues, which has previously been shown to prevent the formation of streptokinase- plasminogen complexes (Zhang et al., 2012), which could impact the observed kinetics. A model of cell-bound PAM was used to investigate this in purified conditions, whereby rPAM was immobilised, via a C-terminal histidine tag, on the surface of the wells of a nickel-coated microtiter plate. As demonstrated in Figure 60C, immobilised rPAM is a potent stimulator of rSK 2b glu-plasminogen activation. In the presence of immobilised rPAM the rSK 2b activity is stimulated ~5.3-fold higher in activity than the rSK H46a in solution. The presence of immobilised rPAM stimulates the rSK 2b ~2-fold more than in the presence of soluble rPAM, suggesting the orientation and colocalisation of glu-plasminogen is important. Consistent with the solution plasminogen activation experiments, in the presence of rPAM (section 4.4.3.3), the rSK H46a and rSK 2a was also stimulated in the presence of immobilised rPAM (Figure 60A and Figure 60B). However, this stimulation was lost when glu-plasminogen was replaced with lys-plasminogen. As described previously, the rSK H46a and rSK 2a stimulation is likely due to the plasminogen binding to ligands, relaxing the conformation to a readily activatable zymogen (Ayinuola et al., 2021b). Whilst rSK 2b also decreased in activity upon addition of lys-plasminogen bound to immobilised rPAM, the levels were still higher than solution activation levels of glu-plasminogen. This suggests the template formation described in section 4.4.3.3

is still occurring and rSK 2b can still generate an active site (Figure 60C). Proposed mechanisms for optimal activation of glu-plasminogen by SK 2b suggest that a trimolecular complex of streptokinase-plasminogen-fibrinogen must be formed bound to PAM (Zhang et al., 2012, Chandrahas et al., 2015). This theory was investigated by amending the immobilised assays to incorporate the presence of fibrinogen. As demonstrated in Figure 61, the addition of fibrinogen to immobilised rPAM decreases the glu-plasminogen activation activity of rSK H46a, rSK 2a and rSK 2b. Thus the pathway proposed for cell-surface plasmin acquisition, involving plasminogen directly interacting with PAM, and enhancing the SK 2b activity (Zhang et al., 2012) appears the most important; with higher glu-plasminogen activation activities observed in the presence of immobilised rPAM alone.

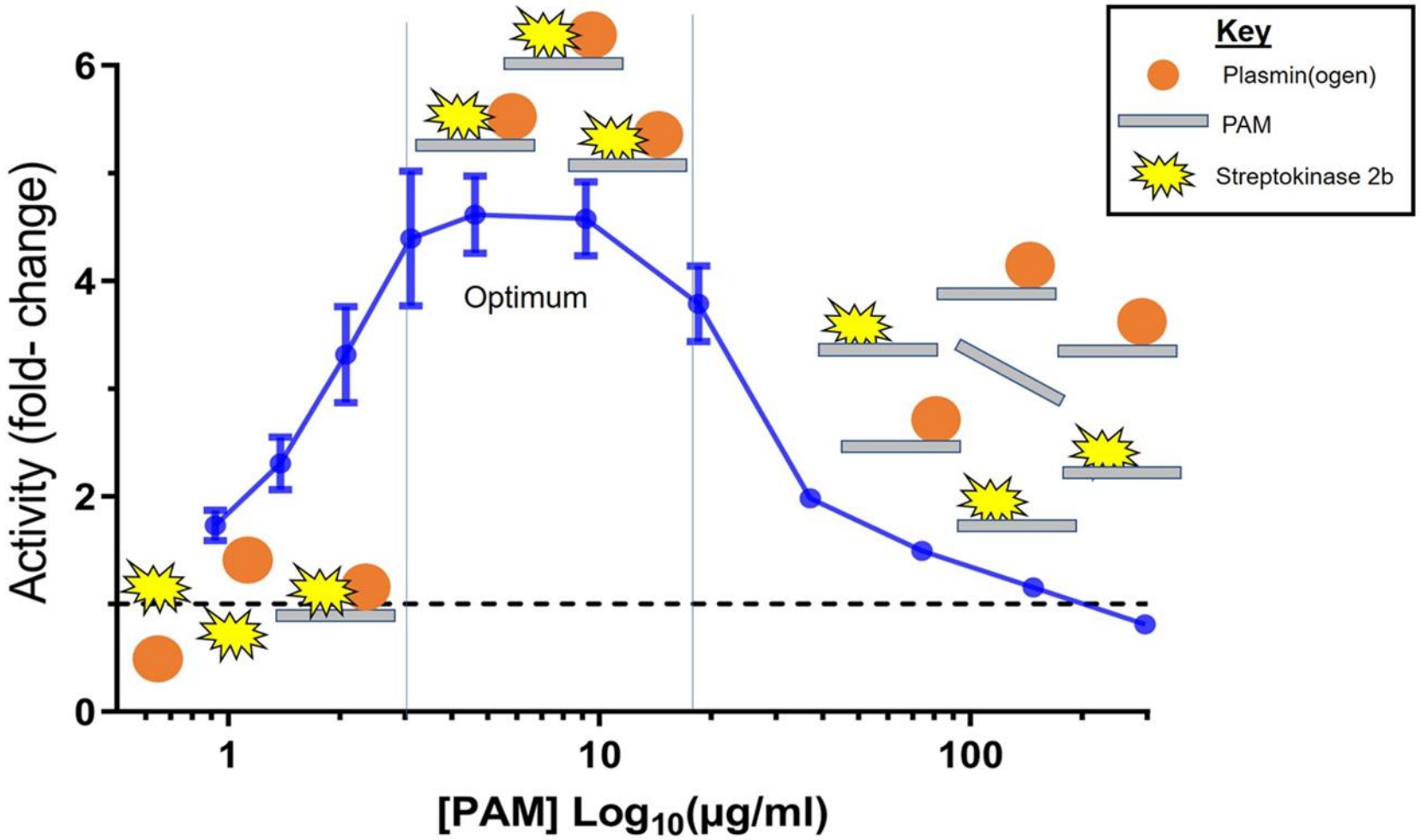

Figure 63 Proposed template mechanism for streptokinase 2b. A bell-shaped profile of the rSK 2b plots of fold change in activity verses log of the PAM concentration, appears to follow a template mechanism. The increase in rPAM causes an observed increase in plasminogen activation rates up to the optimum rPAM concentration. Binding of rSK 2b-plasminogen and plasminogen to the rPAM surface brings the activator and substrate into close proximity. However, as the rPAM concentration continues to increase, the rSK 2b and plasminogen are likely to bind to different rPAM molecules and the stimulatory effect is lost**.**

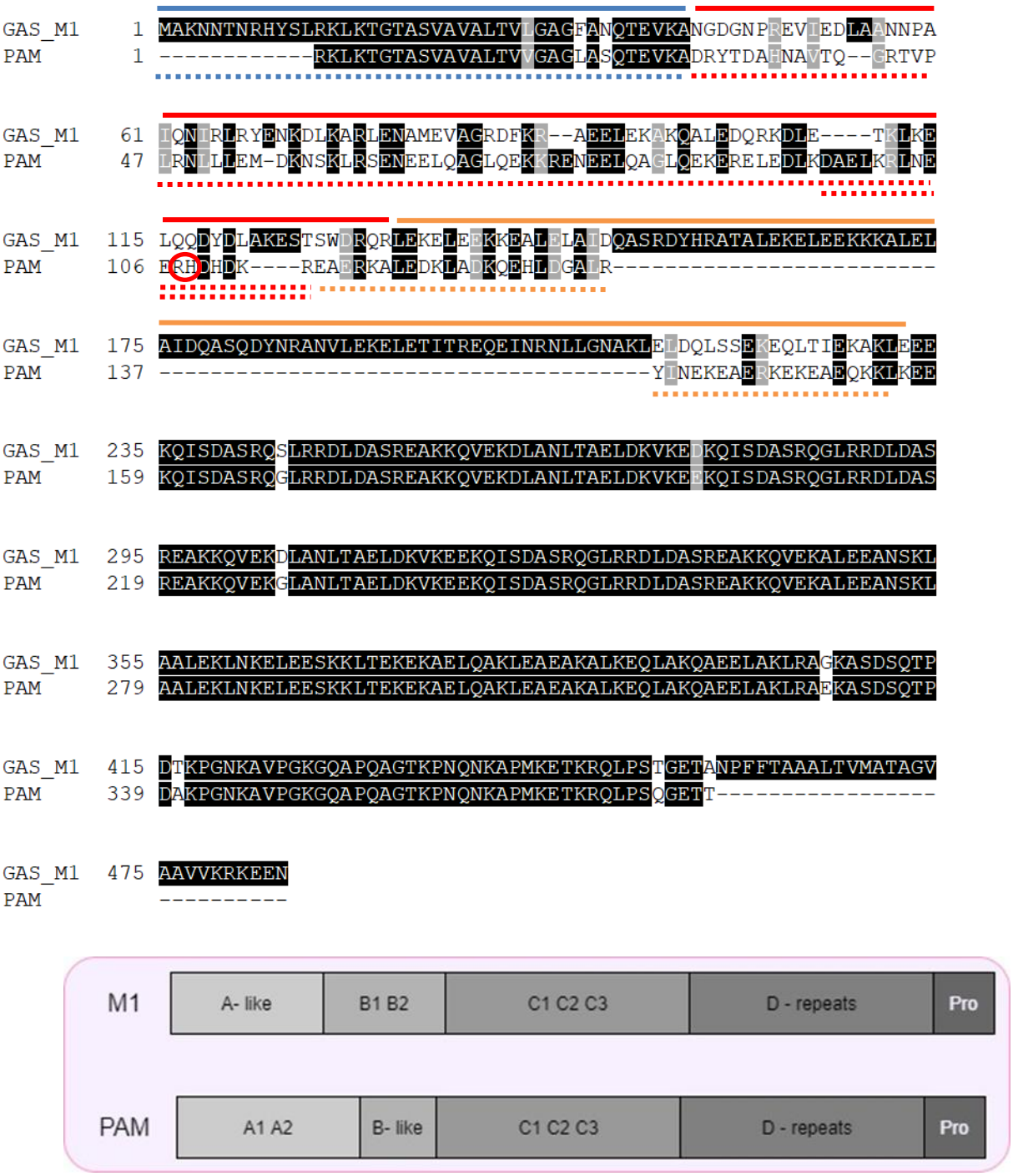

Figure 64 Sequence alignment of M1 protein (SF370) and PAM (NS88.2). Sequence alignment of M1 protein (SF370, Accession number: AAK34694.1) and PAM (NS88.2, Accession number: AAQ64526.2) was performed in Vector NTI (InforMax, Bethesda, MD, USA). The M proteins mature region share 60.7% sequence identity (64.1% consensus positions). Solid lines represent domains in the M1 protein, whilst dash lines represent domains in PAM. Blue is the signal peptide, Red is the A or A-like domains (the double dashed red line indicates the specific A2 domain), Green indicates the B region or B-like region. Circled in the PAM A2 domain sequence is the proposed plasminogen binding residues, Arg and His.

4.4.4 Future work

The data presented in this work suggests that PAM acts as a template for plasmin(ogen) acquisition and contains a binding site for both SK 2b and plasminogen. The PAM used in this work is a Class II PAM, containing only one binding domain for plasminogen (A2). The decision to investigate the mechanism of PAM and SK 2b from GAS strain NS88.2 is because it originates from an invasive blood infection isolate and is found to have a naturally incurring CovS mutation, resulting in an absence in SpeB expression (Maamary et al., 2010). However, other PAM classes contain two binding domains that also originate from invasive GAS strains e.g., invasive skin tropic AP53 GAS strain contains a Class I PAM which binds plasminogen via the A1A2 domain (Qiu et al., 2020). It would be of interest to repeat the experiments with the addition of Class II and III PAM and associated SK 2b to see if the template mechanism is a feature of all PAM. Multiple sequence alignments could provide insights to a common motif in the A or B domain, responsible for binding SK 2b. Previously SPR experiments have been conducted using Biacore to investigate the association and dissociation kinetics of plasminogen binding to PAM (Chandrahas et al., 2015). These experiments could be repeated incorporating SK 2b, SK 2a and SK H46A, with and without the presence of human plasminogen to investigate the presence of a novel binding site specific for SK 2b.

Fibrinogen was also demonstrated to exhibit a template profile for SK 2a activation of glu-plasminogen in previous literature (Huish et al., 2017). However contrary to previous research, both the native and recombinant Group C streptokinase, displayed a similar bell-shaped curve in this project suggesting a similar mechanism is occurring (Figure 48). The use of SPR would also

provide information on the true binding kinetics of the streptokinase variants in fibrinogen, to either rectify or validate the conflicting results.

.

Chapter 5 Summary of Discussions

Streptococcus pyogenes, or GAS, is a strictly human pathogen capable of causing a diverse range of diseases with varying degrees of severity. From mild infections of the skin and throat, such as impetigo and pharyngitis, to severe invasive infections, such as necrotising fasciitis and STSS (section 1.3). GAS is primarily spread through person-to-person transmission through respiratory droplets and with direct contact from broken skin with infected sores (Walker et al., 2014), and can live on the skin and inside the host for several hours to days (Stevens et al., 1989). GAS may encounter many different environments during infection and has evolved secreted and cell surface virulence factors to aid in dissemination.

5.1 Proposed pathogenesis of hypervirulent GAS infections

The pathogenesis of GAS is highly complex, with each GAS serotype having a specific set of virulence factors. A schematic diagram of the proposed pathogenesis of GAS is demonstrated in Figure 65, adapted from (Cole et al., 2011). At the first stages of GAS infection, the bacterium is thought to adhere to host epithelial or mucosal cells via the GAS surface associated carbohydrate, lipoteichoic acid (LTA), binding to fibronectin. This interaction is weak, unspecific and not sufficient to provide tissue tropism, but aids in bringing bacteria and host cells into close proximity (Courtney et al., 2002). A stronger linkage then forms between multiple virulence factors including the HA capsule, pili, and fibronectin-binding protein 1 (SfbI), with M-protein being the most important adhesive (Langshaw et al., 2018, Rohde and Cleary, 2016). A

number of host proteins are involved in this process such as collagen, fibronectin, fibrinogen, laminin and vitronectin providing a binding component for the bacterium adhesins (Rohde and Cleary, 2016). However, the exact cell attachment mechanism is yet to be fully characterised. Once the bacterium is attached, microcolony formation occurs. These microcolonies provide defence against biological, physical and chemical stress whilst facilitating bacterial growth, before dispersal of bacteria (Vyas et al., 2019).

Following colonisation, intracellular dissemination occurs using invasin proteins; SfbI and M proteins are the best-studied which aid in the invasion of epithelial, endothelial and phagocytic cells (Rohde and Cleary, 2016). SfbI is thought to attach to host fibronectin, thus changing the conformation of fibronectin which allows the binding to $\alpha_5\beta_1$ integrins. The integrin and SfbI-fibronectin linkage stimulate recruitment of cell signalling molecules and the rearrangement of the cytoskeleton, forming large invagination in host epithelial cells which ingest the bacteria. The M protein also binds fibronectin directly, allowing fibronectin to interact with surface integrin $\alpha_5\beta_1$, generating a zipper-like structure (Rohde and Cleary, 2016, Castro and Dorfmueller, 2021).

5.1.1 M protein and fibrin(ogen) interaction

Invasive GAS must adapt to the surrounding host environment to establish infection and disseminate into sterile tissues The CovR/S locus is a two-component regulatory system, composed of the response regulator gene (CovR) and sensor kinase gene (CovS). This system responds to environmental stimuli and directly, or indirectly, controls ~15% of the streptococcal genome. The CovRS positively regulates the cysteine protease SpeB, whilst negatively regulating other virulence factors including the HA capsule, streptokinase, SLO,

IgG- degrading enzyme and DNase Sda1 (Levin and Wessels, 1998, Sumby et al., 2006, Vega et al., 2016) (Section 1.4.1).

Whilst establishing infection, SpeB upregulation is thought to hydrolyse a wide range of host and bacterial substrates leading to impaired recognition of GAS by the host immune system and aiding in dissemination. For example, SpeB has been shown to degrade host ECM, epithelial tight junctions, immunoglobulins, complement proteins and chemokines. Whilst also degrading many of GAS virulence factors such as protein H, streptokinase, SdaI and the HA capsule (Nelson et al., 2011).

SpeB and neutrophil proteases have been demonstrated to cleave GAS cell bound M1 protein leading to functionally active M1 at the site of infection. M1 binds host fibrinogen resulting in the formation of a supramolecular complex capable of activating neutrophil β2 integrins (Macheboeuf et al., 2011). This causes the release of heparin binding protein which is an inflammatory mediator that can induce vascular leakage, a common symptom of STSS and necrotising fasciitis (section 1.4.2.1). The M1-fibrinogen complex in the presence of anti-M1 IgG can also activate platelets, via the GPIIb/IIa and FcγRII integrin, causing aggregation and platelet rich thrombi (section 1.4.2.1). The activated platelets release their pro-inflammatory granules then adhere to neutrophils and monocytes; resulting in the activation of both cell types and redistribution of TF creating a hypercoagulable state (Shannon et al., 2007). Additionally, M proteins have been shown to activate the coagulation cascade via the intrinsic and extrinsic pathways (section 1.2.1), with the intrinsic cascade activating at the cell surface and extrinsic being activated by interactions with soluble M proteins (Walker et al., 2014, Oehmcke et al., 2012). Massive dysregulation of the pro- and anti-coagulation equilibrium is a central finding in sepsis and

severe GAS infection (Stevens, 2001) with microthrombi often found at the site of infection and at distant sites. Previous studies have indicated that fibrinogen bound to GAS in human plasma resulted in clots with a drastically different clot morphology; this was attributed to the M proteins because M protein negative mutants displayed normal clot formation (Herwald et al., 2003). The impact of soluble M1 protein on fibrin clot formation properties have not previously been reported. The present study demonstrated that increasing concentrations of rM1 protein resulted in the formation of heterogeneous clots that were more porous, with decreased clot strength, decreased FXIIIa cross-linking and a decrease in the protective fibrin film (Chapter 3). A decrease in cross-linking of fibrin clots would provide an advantage to GAS as FXIIIa has been previously been demonstrated in tissue biopsies of patients with necrotising facciitis to cross-link the bacteria via cell surface bound M1 to fibrin networks (Loof et al., 2011, Deicke et al., 2016). Additionally, FXIIIa deficient mice developed signs of pathologic inflammation at the site of infection and FXIII treatment of wild-type mice demonstrated attenuated bacterial dissemination (Loof et al., 2011). The protective fibrin film on the surface of clots has been proposed to defend the host against microbial invasion (Macrae et al., 2018). However, this film is disrupted in the presence of soluble M1 protein (Section 3.3.6), which would provide an advantage to GAS and allow the proliferation of bacteria and movement through the clot. In whole blood conditions, fibrin clots incorporating M1 protein were more suscepitble to lysis by plasmin. Whilst the plasminogen activators (streptokinase, uPA and tPA) were not further stimulated by the presence of M1 protein (Section 3.3.5.1 and 4.3.4.3), the clots were mechanically weaker (Section 3.3.3.3) and demonstrated faster lysis times in clots formed in whole blood (Section 3.3.5 and 4.3.4.2.2). Whilst establishing

infection, the expression of SpeB has been proposed to degrade streptokinase therefore the GAS would rely on host plasminogen activators to generate plasmin to break down barriers. Humanised mouse models demonstrated that tPA knockout mice showed no difference in bacterial dissemination in comparison to wild-type (Ly et al., 2019). However, a decrease in GAS virulence was observed in uPA knockout mice, with reduced GAS dissemination and cell surface plasmin acquisition (Sanderson-Smith et al., 2013). Additionally, upregulation of uPA expression is correlated with poor patient outcome in sepsis patients (Beyrich et al., 2011, Winkler et al., 2002). It would therefore be of interest to repeat the turbidimetric lysis experiments, incorporating rM1, with the addition of host activators uPA and tPA. Whilst our results demonstrated that the host plasminogen activators are not further stimulated by M1 bound fibrin (Section 3.3.5.1), the structure of the resultant fibrin clots could influence the plasminogen activators ability to generate plasmin. For example, tPA binds to fibrin via C-terminal lysine residues which increases plasminogen activation activity by 100-1000-fold (de Vries et al., 1991, Rijken et al., 1982, Hoylaerts et al., 1982). However, the structural changes observed in M1 bound fibrin could reduce tPA ability to bind fibrin, thus reducing the plasmin generation. On the other hand, uPA contains no binding sites for fibrin and a low affinity for fibrin (Cesarman-Maus and Hajjar, 2005) therefore plasmin generation would be minimally affected by fibrin structure changes. This could possibly explain the reason behind a reduced GAS virulence in the absence of uPA, but not tPA, in streptokinase knockout GAS mutants.

Mutations in the CovS, that reduce the activity of CovR regulator gene, are a common cause of GAS hypervirulence in clinical isolates (Ikebe et al., 2010,

Shea et al., 2011, Maamary et al., 2012, Tatsuno et al., 2013, Garcia et al., 2010, Masuno et al., 2014) and invasive infection models in mice (Sumby et al., 2006, Walker et al., 2007, Mayfield et al., 2014, Engleberg et al., 2001). The exact events leading to and causing a mutation in CovR/S has not yet been determined. However, it has been shown that GAS are selectively pressured towards those clones that lack a fully functioning CovS component when experiencing environmental pressures (Cole et al., 2011). For example, CovRS mutants can be positively selected for in the presence of neutrophils. In mice with normal neutrophil responses, CovS mutants have been demonstrated to outcompete the wild-type bacteria. However, in neutropenic mice the wild-type GAS showed higher survival (Li et al., 2014).

5.1.2 Streptokinase plasminogen activation

An important aspect of CovRS mutations is the downregulation of the bacterial protease, SpeB. This has been observed in culture supernatants, where $CovR^{+}S^{-}$ mutants displayed no detectable SpeB (Maamary et al., 2010). The mutation also allows expression of other virulence factors of GAS (such as streptokinase, SLO and the HA capsule) without degradation by SpeB (Liang et al., 2013). It has been proposed that the $CovS^{-}$ mutants expressing all of the virulence factors are beneficial for GAS in hostile environments (such as in blood), whereas $CovS^{+}$ strains are important for reducing energy burden and aids in colonisation (Vega et al., 2016). The repression of SpeB also results in the retainment of M proteins on the surface of GAS, which is thought to promote cell surface plasmin generation through the formation of a trimolecular complex with fibrinogen-plasminogen-streptokinase (McArthur et al., 2008, Glinton et al., 2017). The plasmin accumulation forms a proteolytic coat surrounding GAS

which can degrade host tissue barriers and fibrin networks leading to systemic dissemination (Walker et al., 2007, Cole et al., 2006).

Streptokinase is a secreted nonproteolytic *Streptococcal* plasminogen activator. The streptokinase binds host plasminogen then the N-terminal Ile1 residue forms a salt bridge with the Asp740 of plasminogen, inducing a conformational change. This complex can then activate further plasminogen molecules to generate the formation of the serine protease, plasmin (Section 1.4.3). Phylogenetic analysis of streptokinase from diverse strains of GAS indicate that β-domain sequence variation can divide the streptokinase into 3 distinct clusters [(Figure 6) 1, 2a and 2b]. Epidemiological studies have demonstrated that type-2b expressing strains are mainly skin-tropic and associated with PAM (plasminogen-binding group A streptococcal M protein) on the cell surface. Whilst type-2a expressing strains are secreted from nasopharyngeal isolates and are commonly associated with a fibrinogen binding M protein such as M1. Cluster 1 streptokinase appear to behave like group C streptokinase, whereby Cluster 1 has no specific tissue tropisms and can activate plasminogen free in solution and does not appear to coincide with particular M- proteins or require co-factors for full activity (Section 1.4.3). However, the relationship between the streptokinase sequence variations, and the M-protein association is not fully understood at the molecular level.

5.1.2.1 SK 2a-expressing GAS and M1

SK 2a expressing GAS strains include the highly prevalent and virulent globally disseminated M1T1 clone (Aziz and Kotb, 2008). The invasive *emm 1* serotype contains the fibrinogen binding M1 protein on the cell surface. Binding fibrinogen to the cell surface of GAS via M1 protein aids dissemination of the bacteria by evading host immune recognition by preventing complement

deposition (Sandin et al., 2006, Carlsson et al., 2005). Additionally, the M1 protein has been shown to acquire cell-surface plasmin through a trimolecular complex with streptokinase-plasminogen-fibrinogen (McArthur et al., 2008). In the present study, SK 2a was weakly stimulated by fibrinogen (Section 4.3.3) and our data and others (Zhang et al., 2012, Glinton et al., 2017), revealed that the presence of M1 protein, immobilised or soluble, does not further stimulate plasmin generation by SK 2a alone or in the presence of fibrinogen (Section 4.3.4). However, a recent study has shown that in the presence of fibrinogen, SK 2a-expressing GAS strains are able to bind plasminogen on their surfaces at similar levels with that of a PAM- expressing strain (Glinton et al., 2017). Thus, formation of trimolecular complex would therefore provide the GAS with a proteolytic coat to overcome host barriers. The surface bound M1 protein has been shown to be cross-linked by FXIIIa to the fibrin network, following activation of the clotting system at the bacterial surface via the intrinsic pathway. The bacteria were observed in tissue biopsies from patients with streptococcal necrotising fasciitis to be cross-linked to the fibrin networks (Loof et al., 2011, Ben Nasr et al., 1995), thereby limiting bacterial invasion. This study (Section 4.3.3.2), and previous literature (Huish et al., 2017), have revealed that fibrin is a potent stimulator of SK 2a. Suggesting that SK 2a would preferentially activate plasminogen in an environment where fibrin is present rather than in solution. Additionally, fibrin can also prevent host immune responses by acting as a shield on the surface of SK 2a -expressing GAS (Ploplis and Castellino, 2019).

SK 2a in complex with (fibrin)ogen, M1 or alone can also activate soluble plasminogen in solution without inactivation by the host inhibitor a2 -antiplasmin (Grella and Castellino, 1997). Therefore, plasmin generation at the site of

infection (soluble or at the cell surface) can function as a defence against the immune responses. Plasmin acquisition enables GAS to penetrate epithelial cells, endothelial cells, and tight junctions. Additionally, plasmin can activate host matrix metalloproteinases which degrade ECM and basement membrane, further facilitating systemic spread of GAS into sterile sites (Sun et al., 2004, Hynes and Sloan, 2016).

The M1 protein appears to have different functions at different stages of infection. For example, M1 aids in colonisation by binding fibronectin, evades the immune system by binding complement proteins and promotes cell surface plasmin acquisition. At certain stages of infection, the M1 is cleaved from the surface where it can activate neutrophils, platelets and monocytes resulting in a hypercoagulable state (Section 5.1.1). However, in tissue biopsies specimens from patients with invasive *Streptococcus pyogenes* infections, it has also been demonstrated that GAS and platelets are colocalised in microthrombi at sites of infection (Shannon et al., 2007), suggesting that cell bound M1 fibrinogen complexes can also activate platelets. Therefore, cell bound M1 may retain some of the functionalities of soluble M1, resulting in consumption of clotting factors and platelet depletion, as observed in Streptococcal sepsis (Reglinski and Sriskandan, 2014).

5.1.2.2 SK 2b-expressing GAS and PAM

The present study is consistent with previously published data that SK 2b cannot conformationally induce an active site in soluble glu-plasminogen without the presence of co-factors (Section 4.3.3.1), with a calculated specific activity of 0.84 IU/μg. SK 2b is commonly associated with PAM, an M protein that can directly bind to the lysine binding sites of plasminogen K2 domain (Wistedt et al., 1998, Wistedt et al., 1995). Whilst PAM is not the only

plasminogen binding protein on GAS (enolase and GADPH), it has been shown that that other plasminogen receptors do not affect the generation of the streptokinase – plasminogen complex and PAM is the main receptor for plasminogen acquisition (Agrahari et al., 2016, Cook et al., 2014). The importance of PAM for GAS pathogenesis has previously been demonstrated using knockout PAM mutants in humanised mice models. Inactivation of the PAM gene reduced bacterial virulence and increased survival rates of mice to ~60% after 10 days in comparison to wild-type GAS strains (<20% survival rate) (Chandrahas et al., 2015). It has been proposed that PAM is co-inherited with the SK 2b (McArthur et al., 2008, Kalia and Bessen, 2004, Zhang et al., 2012). In the current work, a template mechanism was observed for plasminogen activation with increasing concentrations of PAM, suggesting that PAM has a novel binding site for SK 2b (Section 4.4.3.3). If this is confirmed with further studies, this would support that PAM is coinherited with the SK 2b. The present study demonstrated that SK 2b preferentially activates glu-plasminogen bound to immobilised PAM (Section 4.4.3.4) or fibrin clots (Section 4.4.2). However, the addition of fibrinogen to the immobilised PAM assays reduced the plasminogen activation activity of SK 2b (Section 4.4.3.4). Previous studies have indicated that, unlike SK 2a, the SK 2b is inhibited by α_2-antiplasmin when the activator is in complex with plasmin, plasminogen-PAM, or plasminogen-fibrinogen. However, the SK 2b was found to be resistant to α_2-antiplasmin when plasminogen was bound to fibrin or when a trimolecular complex is formed between fibrinogen-plasminogen-PAM (Cook et al., 2014). Therefore, it is likely that in the presence of inhibitors, the SK 2b will be limited by the presence or availability of additional cofactors and activity would be restricted to certain microenvironments. The SK 2b would preferentially activate

plasminogen bound to fibrin or to cell-bound PAM and fibrinogen in a trimolecular complex. SK 2b displays some similarities to staphylokinase, a plasminogen activator secreted from the ubiquitous skin coloniser, *Staphylococcus aureus*. Staphylokinase has a low affinity for plasminogen and cannot activate glu-plasminogen directly (Section 1.2). Additionally, similar to SK 2b the staphylokinase-plasmin complex can be inhibited by a2 -antiplasmin (Grella and Castellino, 1997). These characteristics could attenuate GAS dissemination due to restricted plasminogen activation kinetics. Where the SK 2b activation complexes are protected from inhibition by a2 -antiplasmin only at sites with fibrin or at the cell surface leading to more localised host proteolysis by plasmin. However, it has been suggested that the cell surface plasminogen binding capacity of PAM may be beneficial for long term colonisation of the skin (Kinnby et al., 2008, Cook et al., 2014). The cell surface plasmin acquisition can aid in evasion of the innate immune defences whilst preventing bacteria from becoming entrapped in a fibrin coagulum (Sun et al., 2004, Law et al., 2013).

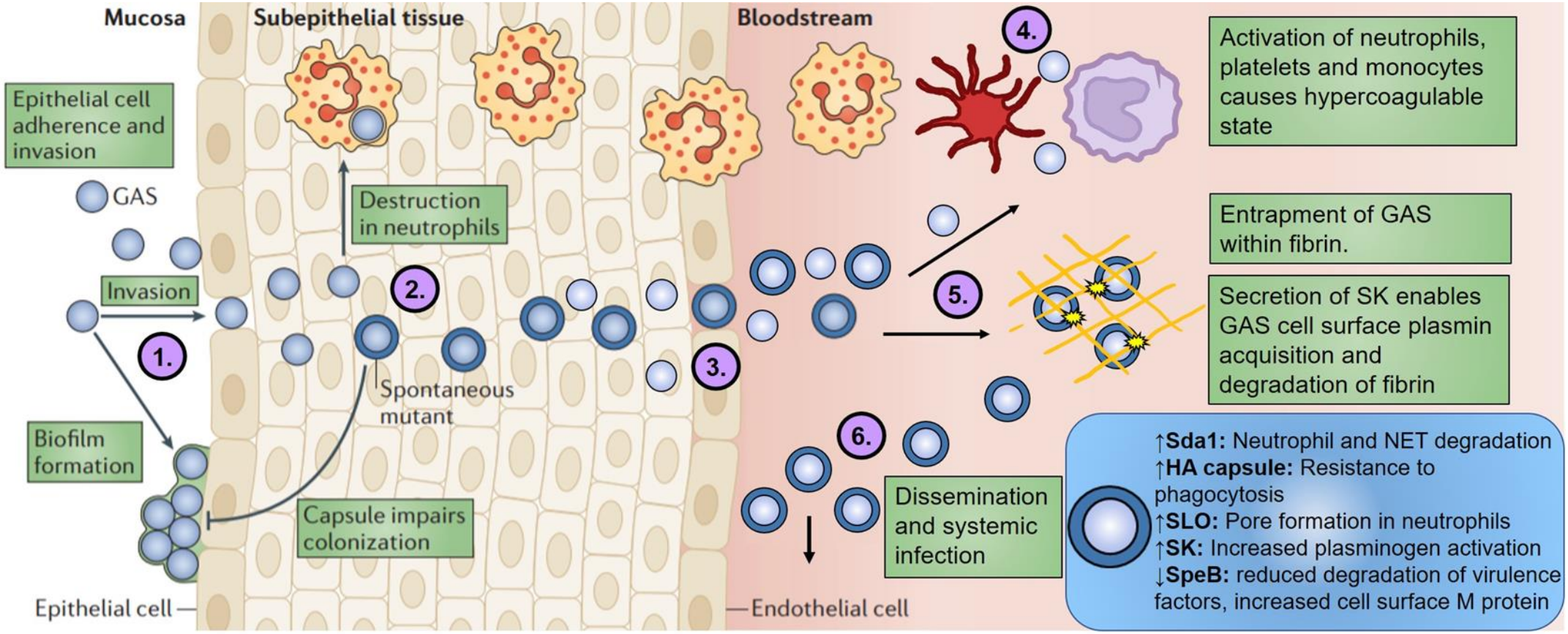

Figure 65 Proposed pathogenesis of GAS (1.) Wild-type GAS adhere, form microcolonies then invade epithelial cells. **(2.)** Selective pressure on GAS results in spontaneous mutations in the CovRS regulon **(3.)** A mixed population of wild-type and mutant GAS break through host barriers into the bloodstream through secretion of bacterial proteases e.g., SpeB **(4.)** Fibrinogen binding M proteins (e.g., M1) from wild-type GAS is cleaved by SpeB and neutrophil proteases forms supramolecular complexes with fibrinogen activating platelets, neutrophils and monocytes creating hypercoagulable state. M1 protein impacts fibrin clot formation, structure, and fibrinolytic potential **(5.)** Mutated GAS is cross-linked into fibrin clots by FXIIIa, secreted streptokinase (SK) generates cell surface plasmin degrading host fibrin. SK 2a associated with M1 protein binds fibrinogen, generating cell surface plasmin but preferentially activates plasminogen in the presence of fibrin. SK 2b is associated with plasminogen binding M protein, PAM. SK 2b preferentially activates plasminogen at the cell surface or in the presence of fibrin **(6.)** Decrease in SpeB results in cell surface plasmin generation and aids in hiding from the host immune system allowing dissemination and systemic infection. Some GAS serotypes do not go through all these steps, for example PAM is not thought to be cleaved from the surface and is reliant on cell surface plasmin generation throughout pathogenesis.*(Imaged adapted from (Cole et al., 2011) with permission from Springer Nature; Licence number: 5256051386270)*

5.2 Future perspectives

Despite over 100 years of research, currently no vaccination for GAS exists. An increased understanding of GAS pathogenesis and virulence mechanisms might uncover therapeutic targets for the treatment of GAS diseases and sequalae. Studies such as these provide detailed information on the molecular interactions of host proteins and bacterial virulence factors, which could identify key proteins that lead to invasive diseases. For example, this work demonstrated that host fibrin could play a key role in GAS pathogenesis, being a potent stimulator of both SK 2a and SK 2b activity (Section 4.4.2). Furthermore, fibrinogen has also been shown to interact extensively with cell-surface bound M proteins, such as M1, which has been shown to activate platelets, neutrophils and create a hypercoagulable state, whilst also enabling the bacterium to hide from the host immune system and aiding in cell surface plasmin acquisition (Section 1.4.2.1). Therefore, disruption of the fibrin(ogen)-GAS interaction could potentially reduce the virulence of the bacterium.

Additionally, the virulence factors could be exploited for new therapeutics. For example, streptokinase from the Group C *Streptococci*, H46a, has been used as a thrombolytic agent since 1987 (Adivitiya and Khasa, 2017). However, unlike tPA and pro-uPA, SK H46a has no fibrin specificity thus increasing the risk of bleeding complications. However streptokinase is still widely used, due to the high cost of human plasminogen activators (Adivitiya and Khasa, 2017). Other bacterial activators with fibrin specificity have been proposed as potential thrombolytic therapeutic such as staphylokinase (Collen, 1998). These are attractive targets due to the fibrin specificity and rapid inactivation by a2 -antiplasmin when not in complex with fibrin. In the current study, fibrin was also

a potent stimulator of SK 2b, and was previously been found to be inactivated by a2 -antiplasmin in solution (Grella and Castellino, 1997). Unlike staphylokinase, SK 2b does not require trace plasmin to be present for activation of plasminogen and can activate plasminogen bound fibrin. Additionally, in the presence of fibrin, the SK 2b displayed similar activity to the SK H46a (Section 4.4.2), but the activity would be limited to the fibrin clot, reducing the risk of bleeding complications. Therefore, SK 2b could be a useful plasminogen activator for therapeutic applications.

It is important to note that the data collected in this study was entirely based on *in vitro* studies. These mechanisms should be further investigated *in vivo* to ensure the results correlate with living organisms. There have been many murine Streptococcal infection models developed, including human plasminogen transgenic mice which can be used to further investigate the findings in the current study (Khil et al., 2003, Sun et al., 2004, Sanderson-Smith et al., 2006, Herwald et al., 2004, Watson et al., 2016). Additionally, patient tissue biopsies of *Streptococcus pyogenes* infection might provide further insight. For example, M1 protein and platelet aggregation was previously shown in tissue biopsies of severe soft tissue infection (Shannon et al., 2007). Patient tissue biopsies could provide insight on microthrombi deposition and platelet rich thrombi incorporating M1 protein and further investigate the impact of M1 protein on fibrin clot formation properties. Additionally, whilst the data presented provides good insight into these invasive strains, there are currently ~230 serotypes of GAS. Whilst extensive research has previously been conducted on the highly prevalent M1T1 strain, there is a clear need to continue investigating how these findings translate to other invasive GAS isolates.

5.3 Conclusion

GAS expresses an arsenal of cell surface bound and secreted virulence factors which interact with the host immune and haemostatic system to aid in bacterial dissemination. The current study focussed on cell surface bound M proteins and secreted plasminogen activator, streptokinase.

M1-bound fibrinogen produces clots with remarkably different structures and properties. Increasing the rM1 protein concentration produced heterogeneous clots with irregular fibre bundles and compacted fibrin that lacked mechanical strength. At rM1 concentrations above 23 μg/ml, the fibrin network was more porous with increased fluid permeability. The protective fibrin biofilm at the clot surface was also disrupted, with increasing numbers of pores/holes, and the biofilm was entirely absent at the higher rM1 concentrations. Whilst the purified fibrinogen showed no significant differences in lytic susceptibility in the presence of rM1, whole blood conditions demonstrated an observed increase in susceptibility to lysis. GAS strains of M1-type are commonly associated with invasive infections, the impact of M1 on fibrin structure may contribute to the severity of infection by compromising the fibrin barrier that limits bacterial proliferation and migration. Sepsis and invasive GAS infection are often associated with massive dysregulation of haemostasis resulting in the deposition of microthrombi and consumption of coagulation factors, with secondary risk of bleeding (Stevens, 2001). Therefore, the structure and mechanical properties of fibrin may translate to the *in vivo* consequences of infection such as microthrombi or thrombus formation.

Streptokinase variants share a high amino acid sequence identity, with rSK H46a, rSK 2a and rSK 2b showing 81.7% sequence identity. However, these variations translate to significant mechanistic differences at the molecular level.

At 37ºC, rSK 2a is completely independent of its M-like protein for activity but is maximally stimulated in the presence of fibrin. Whilst fibrin is also a potent stimulator of rSK 2b, rSK 2b is maximally stimulated in the presence of its immobilised M-like protein, rPAM suggesting an important role for cell-surface plasmin generation. A template mechanism is observed with increasing concentration of rPAM, suggesting a binding site exists on rPAM for rSK 2b. Fibrinogen is a weak stimulator of rSK 2b, however appears to provide a template for plasminogen activation for Group C streptokinase (recombinant, rSK H46a and native, 3rd WHO IS streptokinase). Previous literature has also indicated that fibrinogen also provides a template for rSK 2a activation of plasminogen (Huish et al., 2017).

Chapter 6 References

ADAMS, T. E. & HUNTINGTON, J. A. 2016. Structural transitions during prothrombin activation: On the importance of fragment 2. *Biochimie,* 122**,** 235-42.

ADIVITIYA & KHASA, Y. P. 2017. The evolution of recombinant thrombolytics: Current status and future directions. *Bioengineered,* 8**,** 331-358.

AGILENT. *E. coli Cell Culture Concentration from OD600 Calculator* [Online]. Available: https://www.agilent.com/store/biocalculators/calcODBacterial.jsp?_requestid=91940 [Accessed].

AGRAHARI, G., LIANG, Z., GLINTON, K., LEE, S. W., PLOPLIS, V. A. & CASTELLINO, F. J. 2016. Streptococcus pyogenes Employs Strain-dependent Mechanisms of C3b Inactivation to Inhibit Phagocytosis and Killing of Bacteria. *J Biol Chem,* 291**,** 9181-9.

AGRAHARI, G., LIANG, Z., MAYFIELD, J. A., BALSARA, R. D., PLOPLIS, V. A. & CASTELLINO, F. J. 2013. Complement-mediated opsonization of invasive group A Streptococcus pyogenes strain AP53 is regulated by the bacterial two-component cluster of virulence responder/sensor (CovRS) system. *J Biol Chem,* 288**,** 27494-504.

AKESSON, P., SCHMIDT, K. H., COONEY, J. & BJORCK, L. 1994. M1 protein and protein H: IgGFc- and albumin-binding streptococcal surface proteins encoded by adjacent genes. *Biochem J,* 300 (Pt 3)**,** 877-86.

ASHBAUGH, C. D., WARREN, H. B., CAREY, V. J. & WESSELS, M. R. 1998. Molecular analysis of the role of the group A streptococcal cysteine protease, hyaluronic acid capsule, and M protein in a murine model of human invasive soft-tissue infection. *J Clin Invest,* 102**,** 550-60.

AVIRE, N. J., WHILEY, H. & ROSS, K. 2021. A Review of Streptococcus pyogenes: Public Health Risk Factors, Prevention and Control. *Pathogens,* 10**,** 248.

AYINUOLA, O., AYINUOLA, Y. A., QIU, C., LEE, S. W., PLOPLIS, V. A. & CASTELLINO, F. J. 2021a. Binding of the kringle-2 domain of human plasminogen to streptococcal PAM-type M-protein causes dissociation of PAM dimers. *Microbiologyopen,* 10**,** e1252.

AYINUOLA, Y. A., BRITO-ROBINSON, T., AYINUOLA, O., BECK, J. E., CRUZ-TOPETE, D., LEE, S. W., PLOPLIS, V. A. & CASTELLINO, F. J. 2021b. Streptococcus co-opts a conformational lock in human plasminogen to facilitate streptokinase cleavage and bacterial virulence. *J Biol Chem,* 296**,** 100099.

AYMANNS, S., MAUERER, S., VAN ZANDBERGEN, G., WOLZ, C. & SPELLERBERG, B. 2011. High-level fluorescence labeling of gram-positive pathogens. *PLoS One,* 6**,** e19822.

AZIZ, R. K. & KOTB, M. 2008. Rise and persistence of global M1T1 clone of Streptococcus pyogenes. *Emerg Infect Dis,* 14**,** 1511-7.

BAETEN, K. M., RICHARD, M. C., KANSE, S. M., MUTCH, N. J., DEGEN, J. L. & BOOTH, N. A. 2010. Activation of single-chain urokinase-type

plasminogen activator by platelet-associated plasminogen: a mechanism for stimulation of fibrinolysis by platelets. *J Thromb Haemost,* 8**,** 1313-22.
BAO, Y. J., LIANG, Z., MAYFIELD, J. A., DONAHUE, D. L., CAROTHERS, K. E., LEE, S. W., PLOPLIS, V. A. & CASTELLINO, F. J. 2016. Genomic Characterization of a Pattern D Streptococcus pyogenes emm53 Isolate Reveals a Genetic Rationale for Invasive Skin Tropicity. *J Bacteriol,* 198**,** 1712-24.
BARADET, T. C., HASELGROVE, J. C. & WEISEL, J. W. 1995. Three-dimensional reconstruction of fibrin clot networks from stereoscopic intermediate voltage electron microscope images and analysis of branching. *Biophys J,* 68**,** 1551-60.
BARKER, F. G., LEPPARD, B. J. & SEAL, D. V. 1987. Streptococcal Necrotizing Fasciitis - Comparison between Histological and Clinical-Features. *Journal of Clinical Pathology,* 40**,** 335-41.
BARNETT, T. C., BOWEN, A. C. & CARAPETIS, J. R. 2018. The fall and rise of Group A Streptococcus diseases. *Epidemiol Infect***,** 1-6.
BARNETT, T. C., LIEBL, D., SEYMOUR, L. M., GILLEN, C. M., LIM, J. Y., LAROCK, C. N., DAVIES, M. R., SCHULZ, B. L., NIZET, V., TEASDALE, R. D. & WALKER, M. J. 2013. The globally disseminated M1T1 clone of group A Streptococcus evades autophagy for intracellular replication. *Cell Host Microbe,* 14**,** 675-82.
BEN NASR, A., OLSEN, A., SJOBRING, U., MULLERESTERL, W. & BJORCK, L. 1996. Assembly of human contact phase proteins and release of bradykinin at the surface of curli-expressing Escherichia coli. *Molecular Microbiology,* 20**,** 927-35.
BEN NASR, A. B., HERWALD, H., MULLER-ESTERL, W. & BJORCK, L. 1995. Human kininogens interact with M protein, a bacterial surface protein and virulence determinant. *Biochem J,* 305 (Pt 1)**,** 173-80.
BENNASR, A., HERWALD, H., SJOBRING, U., RENNE, T., MULLERESTERL, W. & BJORCK, L. 1997. Absorption of kininogen from human plasma by Streptococcus pyogenes is followed by the release of bradykinin. *Biochemical Journal,* 326**,** 657-60.
BERGE, A. & BJORCK, L. 1995a. Streptococcal Cysteine Proteinase Releases Biologically-Active Fragments of Streptococcal Surface-Proteins. *Journal of Biological Chemistry,* 270**,** 9862-7.
BERGE, A. & BJORCK, L. 1995b. Streptococcal cysteine proteinase releases biologically active fragments of streptococcal surface proteins. *J Biol Chem,* 270**,** 9862-7.
BESSEN, D. E. 2016. Molecular Basis of Serotyping and the Underlying Genetic Organization of Streptococcus pyogenes. *In:* FERRETTI, J. J., STEVENS, D. L. & FISCHETTI, V. A. (eds.) *Streptococcus pyogenes : Basic Biology to Clinical Manifestations.* University of Oklahoma Health Sciences Center, Oklahoma City (OK).
BESSEN, D. E., SOTIR, C. M., READDY, T. L. & HOLLINGSHEAD, S. K. 1996. Genetic correlates of throat and skin isolates of group A streptococci. *J Infect Dis,* 173**,** 896-900.
BEYRICH, C., LOFFLER, J., KOBSAR, A., SPEER, C. P., KNEITZ, S. & EIGENTHALER, M. 2011. Infection of human coronary artery endothelial cells by group B streptococcus contributes to dysregulation of apoptosis, hemostasis, and innate immune responses. *Mediators Inflamm,* 2011**,** 971502.

BHAKDI, S., TRANUM-JENSEN, J. & SZIEGOLEIT, A. 1985. Mechanism of membrane damage by streptolysin-O. *Infect Immun,* 47**,** 52-60.
BHATTACHARYA, S., LIANG, Z., QUEK, A. J., PLOPLIS, V. A., LAW, R. & CASTELLINO, F. J. 2014. Dimerization is not a determining factor for functional high affinity human plasminogen binding by the group A streptococcal virulence factor PAM and is mediated by specific residues within the PAM a1a2 domain. *J Biol Chem,* 289**,** 21684-93.
BJERKETORP, J., JACOBSSON, K. & FRYKBERG, L. 2004. The von Willebrand factor-binding protein (vWbp) of Staphylococcus aureus is a coagulase. *FEMS Microbiology Letters,* 234**,** 309-14.
BJERKETORP, J., NILSSON, M., LJUNGH, A., FLOCK, J. I., JACOBSSON, K. & FRYKBERG, L. 2002. A novel von Willebrand factor binding protein expressed by Staphylococcus aureus. *Microbiology,* 148**,** 2037-44.
BLANCHETTE, L. P. & LAWRENCE, C. 1967. Group A streptococcus screening with neomycin blood agar. *Am J Clin Pathol,* 48**,** 441-3.
BLOMBACK, B., CARLSSON, K., HESSEL, B., LILJEBORG, A., PROCYK, R. & ASLUND, N. 1989. Native fibrin gel networks observed by 3D microscopy, permeation and turbidity. *Biochim Biophys Acta,* 997**,** 96-110.
BLOMBACK, B., HESSEL, B., HOGG, D. & THERKILDSEN, L. 1978. A two-step fibrinogen--fibrin transition in blood coagulation. *Nature,* 275**,** 501-5.
BLOMBACK, B. & OKADA, M. 1982. Fibrin gel structure and clotting time. *Thromb Res,* 25**,** 51-70.
BODE, W. & HUBER, R. 1976. Induction of the bovine trypsinogen-trypsin transition by peptides sequentially similar to the N-terminus of trypsin. *FEBS Lett,* 68**,** 231-6.
BONNARD, T., LAW, L. S., TENNANT, Z. & HAGEMEYER, C. E. 2017. Development and validation of a high throughput whole blood thrombolysis plate assay. *Sci Rep,* 7**,** 2346.
BOOTH, N. A., WALKER, E., MAUGHAN, R. & BENNETT, B. 1987. Plasminogen-Activator in Normal Subjects after Exercise and Venous Occlusion - T-Pa Circulates as Complexes with C1-Inhibitor and Pai-1. *Blood,* 69**,** 1600-4.
BOWLEY, S. R., OKUMURA, N. & LORD, S. T. 2009. Impaired protofibril formation in fibrinogen gamma N308K is due to altered D:D and "A:a" interactions. *Biochemistry,* 48**,** 8656-63.
BOXRUD, P. D., FAY, W. P. & BOCK, P. E. 2000. Streptokinase binds to human plasmin with high affinity, perturbs the plasmin active site, and induces expression of a substrate recognition exosite for plasminogen. *J Biol Chem,* 275**,** 14579-89.
BOXRUD, P. D., VERHAMME, I. M. & BOCK, P. E. 2004. Resolution of conformational activation in the kinetic mechanism of plasminogen activation by streptokinase. *J Biol Chem,* 279**,** 36633-41.
BOXRUD, P. D., VERHAMME, I. M., FAY, W. P. & BOCK, P. E. 2001. Streptokinase triggers conformational activation of plasminogen through specific interactions of the amino-terminal sequence and stabilizes the active zymogen conformation. *J Biol Chem,* 276**,** 26084-9.
BRICKER, A. L., CYWES, C., ASHBAUGH, C. D. & WESSELS, M. R. 2002. NAD(+)-glycohydrolase acts as an intracellular toxin to enhance the extracellular survival of group A streptococci. *Molecular Microbiology,* 44**,** 257-69.

BRINKMANN, V., REICHARD, U., GOOSMANN, C., FAULER, B., UHLEMANN, Y., WEISS, D. S., WEINRAUCH, Y. & ZYCHLINSKY, A. 2004. Neutrophil extracellular traps kill bacteria. *Science,* 303**,** 1532-5.

BROOK, I. 2013. Penicillin failure in the treatment of streptococcal pharyngo-tonsillitis. *Curr Infect Dis Rep,* 15**,** 232-5.

BROWN, J. H., VOLKMANN, N., JUN, G., HENSCHEN-EDMAN, A. H. & COHEN, C. 2000. The crystal structure of modified bovine fibrinogen. *Proc Natl Acad Sci U S A,* 97**,** 85-90.

BUGGE, T. H., FLICK, M. J., DANTON, M. J., DAUGHERTY, C. C., ROMER, J., DANO, K., CARMELIET, P., COLLEN, D. & DEGEN, J. L. 1996. Urokinase-type plasminogen activator is effective in fibrin clearance in the absence of its receptor or tissue-type plasminogen activator. *Proc Natl Acad Sci U S A,* 93**,** 5899-904.

BYRNES, J. R., DUVAL, C., WANG, Y., HANSEN, C. E., AHN, B., MOOBERRY, M. J., CLARK, M. A., JOHNSEN, J. M., LORD, S. T., LAM, W. A., MEIJERS, J. C., NI, H., ARIENS, R. A. & WOLBERG, A. S. 2015. Factor XIIIa-dependent retention of red blood cells in clots is mediated by fibrin alpha-chain crosslinking. *Blood,* 126**,** 1940-8.

CAMPBELL, R. A., OVERMYER, K. A., SELZMAN, C. H., SHERIDAN, B. C. & WOLBERG, A. S. 2009. Contributions of extravascular and intravascular cells to fibrin network formation, structure, and stability. *Blood,* 114**,** 4886-96.

CANNATA, G., MARIOTTI ZANI, E., ARGENTIERO, A., CAMINITI, C., PERRONE, S. & ESPOSITO, S. 2021. TEG((R)) and ROTEM((R)) Traces: Clinical Applications of Viscoelastic Coagulation Monitoring in Neonatal Intensive Care Unit. *Diagnostics (Basel),* 11.

CARAPETIS, J. R., STEER, A. C., MULHOLLAND, E. K. & WEBER, M. 2005. The global burden of group A streptococcal diseases. *Lancet Infect Dis,* 5**,** 685-94.

CARLSSON, F., SANDIN, C. & LINDAHL, G. 2005. Human fibrinogen bound to Streptococcus pyogenes M protein inhibits complement deposition via the classical pathway. *Mol Microbiol,* 56**,** 28-39.

CARMELIET, P., SCHOONJANS, L., KIECKENS, L., REAM, B., DEGEN, J., BRONSON, R., DE VOS, R., VAN DEN OORD, J. J., COLLEN, D. & MULLIGAN, R. C. 1994. Physiological consequences of loss of plasminogen activator gene function in mice. *Nature,* 368**,** 419-24.

CARR, M. E. 1988. Fibrin formed in plasma is composed of fibers more massive than those formed from purified fibrinogen. *Thromb Haemost,* 59**,** 535-9.

CARR, M. E. & ALVING, B. M. 1995. Effect of Fibrin Structure on Plasmin-Mediated Dissolution of Plasma Clots. *Blood Coagulation & Fibrinolysis,* 6**,** 567-73.

CARR, M. E., JR., GABRIEL, D. A. & MCDONAGH, J. 1986. Influence of Ca2+ on the structure of reptilase-derived and thrombin-derived fibrin gels. *Biochem J,* 239**,** 513-6.

CARR, M. E., JR. & HARDIN, C. L. 1987. Fibrin has larger pores when formed in the presence of erythrocytes. *Am J Physiol,* 253**,** H1069-73.

CARR, M. E., JR. & HERMANS, J. 1978. Size and density of fibrin fibers from turbidity. *Macromolecules,* 11**,** 46-50.

CARR, M. E., JR., SHEN, L. L. & HERMANS, J. 1977. Mass-length ratio of fibrin fibers from gel permeation and light scattering. *Biopolymers,* 16**,** 1-15.

CASTELLINO, F. J. & PLOPLIS, V. A. 2005. Structure and function of the plasminogen/plasmin system. *Thromb Haemost,* 93**,** 647-54.
CASTELLINO, F. J. & VIOLAND, B. N. 1979. The fibrinolytic system--basic considerations. *Prog Cardiovasc Dis,* 21**,** 241-54.
CASTRO, S. A. & DORFMUELLER, H. C. 2021. A brief review on Group A Streptococcus pathogenesis and vaccine development. *R Soc Open Sci,* 8**,** 201991.
CEDERVALL, T., JOHANSSON, M. U. & AKERSTROM, B. 1997. Coiled-coil structure of group A streptococcal M proteins. Different temperature stability of class A and C proteins by hydrophobic-nonhydrophobic amino acid substitutions at heptad positions a and d. *Biochemistry,* 36**,** 4987-94.
CESARMAN-MAUS, G. & HAJJAR, K. A. 2005. Molecular mechanisms of fibrinolysis. *Br J Haematol,* 129**,** 307-21.
CHANDRAHAS, V., GLINTON, K., LIANG, Z., DONAHUE, D. L., PLOPLIS, V. A. & CASTELLINO, F. J. 2015. Direct Host Plasminogen Binding to Bacterial Surface M-protein in Pattern D Strains of Streptococcus pyogenes Is Required for Activation by Its Natural Coinherited SK2b Protein. *J Biol Chem,* 290**,** 18833-42.
CHAPIN, J. C. & HAJJAR, K. A. 2015. Fibrinolysis and the control of blood coagulation. *Blood Rev,* 29**,** 17-24.
CHEN, R. & DOOLITTLE, R. F. 1971. - cross-linking sites in human and bovine fibrin. *Biochemistry,* 10**,** 4487-91.
CHENG, A. G., MCADOW, M., KIM, H. K., BAE, T., MISSIAKAS, D. M. & SCHNEEWIND, O. 2010. Contribution of coagulases towards Staphylococcus aureus disease and protective immunity. *PLoS Pathog,* 6**,** e1001036.
CHERNYSH, I. N., NAGASWAMI, C. & WEISEL, J. W. 2011. Visualization and identification of the structures formed during early stages of fibrin polymerization. *Blood,* 117**,** 4609-14.
CHIBBER, B. A., MORRIS, J. P. & CASTELLINO, F. J. 1985. Effects of human fibrinogen and its cleavage products on activation of human plasminogen by streptokinase. *Biochemistry,* 24**,** 3429-34.
CHRISTEN, M. T., FRANK, P., SCHALLER, J. & LLINAS, M. 2010. Human plasminogen kringle 3: solution structure, functional insights, phylogenetic landscape. *Biochemistry,* 49**,** 7131-50.
CHURCHWARD, G. 2007. The two faces of Janus: virulence gene regulation by CovR/S in group A streptococci. *Mol Microbiol,* 64**,** 34-41.
CLAES, J., DITKOWSKI, B., LIESENBORGHS, L., VELOSO, T. R., ENTENZA, J. M., MOREILLON, P., VANASSCHE, T., VERHAMME, P., HOYLAERTS, M. F. & HEYING, R. 2018. Assessment of the Dual Role of Clumping Factor A in S. Aureus Adhesion to Endothelium in Absence and Presence of Plasma. *Thromb Haemost,* 118**,** 1230-41.
CLAES, J., LIESENBORGHS, L., PEETERMANS, M., VELOSO, T. R., MISSIAKAS, D., SCHNEEWIND, O., MANCINI, S., ENTENZA, J. M., HOYLAERTS, M. F., HEYING, R., VERHAMME, P. & VANASSCHE, T. 2017. Clumping factor A, von Willebrand factor-binding protein and von Willebrand factor anchor Staphylococcus aureus to the vessel wall. *J Thromb Haemost,* 15**,** 1009-19.
CLAUSHUIS, T. A., DE STOPPELAAR, S. F., STROO, I., ROELOFS, J. J., OTTENHOFF, R., VAN DER POLL, T. & VAN'T VEER, C. 2017. Thrombin contributes to protective immunity in pneumonia-derived sepsis

via fibrin polymerization and platelet-neutrophil interactions. *J Thromb Haemost,* 15**,** 744-57.
CLEMETSON, K. J. 2012. Platelets and primary haemostasis. *Thromb Res,* 129**,** 220-4.
COLE, J. N., BARNETT, T. C., NIZET, V. & WALKER, M. J. 2011. Molecular insight into invasive group A streptococcal disease. *Nat Rev Microbiol,* 9**,** 724-36.
COLE, J. N., MCARTHUR, J. D., MCKAY, F. C., SANDERSON-SMITH, M. L., CORK, A. J., RANSON, M., ROHDE, M., ITZEK, A., SUN, H., GINSBURG, D., KOTB, M., NIZET, V., CHHATWAL, G. S. & WALKER, M. J. 2006. Trigger for group A streptococcal M1T1 invasive disease. *FASEB J,* 20**,** 1745-7.
COLE, J. N., PENCE, M. A., VON KOCKRITZ-BLICKWEDE, M., HOLLANDS, A., GALLO, R. L., WALKER, M. J. & NIZET, V. 2010. M protein and hyaluronic acid capsule are essential for in vivo selection of covRS mutations characteristic of invasive serotype M1T1 group A Streptococcus. *MBio,* 1**,** e00191-10.
COLLEN, D. 1998. Staphylokinase: a potent, uniquely fibrin-selective thrombolytic agent. *Nat Med,* 4**,** 279-84.
COLLEN, D., SCHLOTT, B., ENGELBORGHS, Y., VAN HOEF, B., HARTMANN, M., LIJNEN, H. R. & BEHNKE, D. 1993. On the mechanism of the activation of human plasminogen by recombinant staphylokinase. *J Biol Chem,* 268**,** 8284-9.
COLLET, J. P., MOEN, J. L., VEKLICH, Y. I., GORKUN, O. V., LORD, S. T., MONTALESCOT, G. & WEISEL, J. W. 2005. The alphaC domains of fibrinogen affect the structure of the fibrin clot, its physical properties, and its susceptibility to fibrinolysis. *Blood,* 106**,** 3824-30.
COLLET, J. P., PARK, D., LESTY, C., SORIA, J., SORIA, C., MONTALESCOT, G. & WEISEL, J. W. 2000a. Influence of fibrin network conformation and fibrin fiber diameter on fibrinolysis speed - Dynamic and structural approaches by confocal microscopy. *Arteriosclerosis Thrombosis and Vascular Biology,* 20**,** 1354-61.
COLLET, J. P., PARK, D., LESTY, C., SORIA, J., SORIA, C., MONTALESCOT, G. & WEISEL, J. W. 2000b. Influence of fibrin network conformation and fibrin fiber diameter on fibrinolysis speed: dynamic and structural approaches by confocal microscopy. *Arterioscler Thromb Vasc Biol,* 20**,** 1354-61.
COLLET, J. P., SORIA, J., MIRSHAHI, M., HIRSCH, M., DAGONNET, F. B., CAEN, J. & SORIA, C. 1993. Dusart Syndrome - a New Concept of the Relationship between Fibrin Clot Architecture and Fibrin Clot Degradability - Hypofibrinolysis Related to an Abnormal Clot Structure. *Blood,* 82**,** 2462-9.
COLMAN, R. W. & SCHMAIER, A. H. 1997. Contact system: a vascular biology modulator with anticoagulant, profibrinolytic, antiadhesive, and proinflammatory attributes. *Blood,* 90**,** 3819-43.
COOK, S. M., SKORA, A., GILLEN, C. M., WALKER, M. J. & MCARTHUR, J. D. 2012. Streptokinase variants from Streptococcus pyogenes isolates display altered plasminogen activation characteristics - implications for pathogenesis. *Mol Microbiol,* 86**,** 1052-62.
COOK, S. M., SKORA, A., WALKER, M. J., SANDERSON-SMITH, M. L. & MCARTHUR, J. D. 2014. Site-restricted plasminogen activation mediated by group A streptococcal streptokinase variants. *Biochem J,* 458**,** 23-31.

COOPER, A. V., STANDEVEN, K. F. & ARIENS, R. A. 2003. Fibrinogen gamma-chain splice variant gamma' alters fibrin formation and structure. *Blood,* 102**,** 535-40.
COTTRELL, B. A., STRONG, D. D., WATT, K. W. & DOOLITTLE, R. F. 1979. Amino acid sequence studies on the alpha chain of human fibrinogen. Exact location of cross-linking acceptor sites. *Biochemistry,* 18**,** 5405-10.
COURTNEY, H. S., HASTY, D. L. & DALE, J. B. 2002. Molecular mechanisms of adhesion, colonization, and invasion of group A streptococci. *Ann Med,* 34**,** 77-87.
CRAWLEY, J. T., ZANARDELLI, S., CHION, C. K. & LANE, D. A. 2007. The central role of thrombin in hemostasis. *J Thromb Haemost,* 5 Suppl 1**,** 95-101.
CROSBY, H. A., KWIECINSKI, J. & HORSWILL, A. R. 2016. Staphylococcus aureus Aggregation and Coagulation Mechanisms, and Their Function in Host-Pathogen Interactions. *Adv Appl Microbiol,* 96**,** 1-41.
CUE, D., SOUTHERN, S. O., SOUTHERN, P. J., PRABHAKAR, J., LORELLI, W., SMALLHEER, J. M., MOUSA, S. A. & CLEARY, P. P. 2000. A nonpeptide integrin antagonist can inhibit epithelial cell ingestion of Streptococcus pyogenes by blocking formation of integrin alpha 5 beta 1-fibronectin-M1 protein complexes. *Proceedings of the National Academy of Sciences of the United States of America,* 97**,** 2858-63.
CUNNINGHAM, M. W. 2000. Pathogenesis of group A streptococcal infections. *Clin Microbiol Rev,* 13**,** 470-511.
DALE, J. B., WASHBURN, R. G., MARQUES, M. B. & WESSELS, M. R. 1996. Hyaluronate capsule and surface M protein in resistance to opsonization of group A streptococci. *Infection and Immunity,* 64**,** 1495-501.
DALTON, T. L. & SCOTT, J. R. 2004. CovS inactivates CovR and is required for growth under conditions of general stress in Streptococcus pyogenes. *J Bacteriol,* 186**,** 3928-37.
DAVIE, E. W. & RATNOFF, O. D. 1964. Waterfall Sequence for Intrinsic Blood Clotting. *Science,* 145**,** 1310-2.
DAVIES, M. R., MCINTYRE, L., MUTREJA, A., LACEY, J. A., LEES, J. A., TOWERS, R. J., DUCHENE, S., SMEESTERS, P. R., FROST, H. R., PRICE, D. J., HOLDEN, M. T. G., DAVID, S., GIFFARD, P. M., WORTHING, K. A., SEALE, A. C., BERKLEY, J. A., HARRIS, S. R., RIVERA-HERNANDEZ, T., BERKING, O., CORK, A. J., TORRES, R., LITHGOW, T., STRUGNELL, R. A., BERGMANN, R., NITSCHE-SCHMITZ, P., CHHATWAL, G. S., BENTLEY, S. D., FRASER, J. D., MORELAND, N. J., CARAPETIS, J. R., STEER, A. C., PARKHILL, J., SAUL, A., WILLIAMSON, D. A., CURRIE, B. J., TONG, S. Y. C., DOUGAN, G. & WALKER, M. J. 2019. Atlas of group A streptococcal vaccine candidates compiled using large-scale comparative genomics. *Nat Genet,* 51**,** 1035-43.
DE VRIES, C., VEERMAN, H., NESHEIM, M. E. & PANNEKOEK, H. 1991. Kinetic characterization of tissue-type plasminogen activator (t-PA) and t-PA deletion mutants. *Thromb Haemost,* 65**,** 280-5.
DEICKE, C., CHAKRAKODI, B., PILS, M. C., DICKNEITE, G., JOHANSSON, L., MEDINA, E. & LOOF, T. G. 2016. Local activation of coagulation factor XIII reduces systemic complications and improves the survival of mice after Streptococcus pyogenes M1 skin infection. *Int J Med Microbiol,* 306**,** 572-79.

DEIVANAYAGAM, C. C., WANN, E. R., CHEN, W., CARSON, M., RAJASHANKAR, K. R., HOOK, M. & NARAYANA, S. V. 2002. A novel variant of the immunoglobulin fold in surface adhesins of Staphylococcus aureus: crystal structure of the fibrinogen-binding MSCRAMM, clumping factor A. *EMBO J,* 21**,** 6660-72.

DEMURI, G. P., STERKEL, A. K., KUBICA, P. A., DUSTER, M. N., REED, K. D. & WALD, E. R. 2017. Macrolide and Clindamycin Resistance in Group a Streptococci Isolated From Children With Pharyngitis. *Pediatr Infect Dis J,* 36**,** 342-44.

DEMURI, G. P. & WALD, E. R. 2014. The Group A Streptococcal Carrier State Reviewed: Still an Enigma. *J Pediatric Infect Dis Soc,* 3**,** 336-42.

DICKNEITE, G., HERWALD, H., KORTE, W., ALLANORE, Y., DENTON, C. P. & MATUCCI CERINIC, M. 2015. Coagulation factor XIII: a multifunctional transglutaminase with clinical potential in a range of conditions. *Thromb Haemost,* 113**,** 686-97.

DISCIPIO, R. G. 1982. The activation of the alternative pathway C3 convertase by human plasma kallikrein. *Immunology,* 45**,** 587-95.

DOMINGUES, M. M., MACRAE, F. L., DUVAL, C., MCPHERSON, H. R., BRIDGE, K. I., AJJAN, R. A., RIDGER, V. C., CONNELL, S. D., PHILIPPOU, H. & ARIENS, R. A. 2016. Thrombin and fibrinogen gamma' impact clot structure by marked effects on intrafibrillar structure and protofibril packing. *Blood,* 127**,** 487-95.

DOMINIECKI, M. E. & WEISS, J. 1999. Antibacterial action of extracellular mammalian group IIA phospholipase A2 against grossly clumped Staphylococcus aureus. *Infect Immun,* 67**,** 2299-305.

DOOLITTLE, R. F. & PANDI, L. 2006. Binding of synthetic B knobs to fibrinogen changes the character of fibrin and inhibits its ability to activate tissue plasminogen activator and its destruction by plasmin. *Biochemistry,* 45**,** 2657-67.

DRAKE, T. A., MORRISSEY, J. H. & EDGINGTON, T. S. 1989. Selective cellular expression of tissue factor in human tissues. Implications for disorders of hemostasis and thrombosis. *Am J Pathol,* 134**,** 1087-97.

DUVAL, C., ALLAN, P., CONNELL, S. D., RIDGER, V. C., PHILIPPOU, H. & ARIENS, R. A. 2014. Roles of fibrin alpha- and gamma-chain specific cross-linking by FXIIIa in fibrin structure and function. *Thromb Haemost,* 111**,** 842-50.

DUVAL, C., PROFUMO, A., APRILE, A., SALIS, A., MILLO, E., DAMONTE, G., GAUER, J. S., ARIENS, R. A. S. & ROCCO, M. 2020. Fibrinogen alphaC-regions are not directly involved in fibrin polymerization as evidenced by a "Double-Detroit" recombinant fibrinogen mutant and knobs-mimic peptides. *J Thromb Haemost,* 18**,** 802-14.

EASTMAN, D., WURM, F. M., VANREIS, R. & HIGGINS, D. L. 1992. A Region of Tissue Plasminogen-Activator That Affects Plasminogen Activation Differentially with Various Fibrin(Ogen)-Related Stimulators. *Biochemistry,* 31**,** 419-22.

ELGUE, G., SANCHEZ, J., FATAH, K., OLSSON, P. & BLOMBACK, B. 1994. The effect of plasma antithrombin concentration on thrombin generation and fibrin gel structure. *Thromb Res,* 75**,** 203-12.

ELLEN, R. P. & GIBBONS, R. J. 1972. M protein-associated adherence of Streptococcus pyogenes to epithelial surfaces: prerequisite for virulence. *Infect Immun,* 5**,** 826-30.

ENGLEBERG, N. C., HEATH, A., MILLER, A., RIVERA, C. & DIRITA, V. J. 2001. Spontaneous mutations in the CsrRS two-component regulatory system of Streptococcus pyogenes result in enhanced virulence in a murine model of skin and soft tissue infection. *J Infect Dis,* 183**,** 1043-54.
ERICKSON, H. P. & FOWLER, W. E. 1983. Electron microscopy of fibrinogen, its plasmic fragments and small polymers. *Ann N Y Acad Sci,* 408**,** 146-63.
EVERSE, S. J., SPRAGGON, G., VEERAPANDIAN, L., RILEY, M. & DOOLITTLE, R. F. 1998. Crystal structure of fragment double-D from human fibrin with two different bound ligands. *Biochemistry,* 37**,** 8637-42.
FACKLAM, R. F., MARTIN, D. R., LOVGREN, M., JOHNSON, D. R., EFSTRATIOU, A., THOMPSON, T. A., GOWAN, S., KRIZ, P., TYRRELL, G. J., KAPLAN, E. & BEALL, B. 2002. Extension of the Lancefield classification for group A streptococci by addition of 22 new M protein gene sequence types from clinical isolates: emm103 to emm124. *Clin Infect Dis,* 34**,** 28-38.
FATAH, K., SILVEIRA, A., TORNVALL, P., KARPE, F., BLOMBACK, M. & HAMSTEN, A. 1996. Proneness to formation of tight and rigid fibrin gel structures in men with myocardial infarction at a young age. *Thrombosis and Haemostasis,* 76**,** 535-40.
FERRETTI, J. J., MCSHAN, W. M., AJDIC, D., SAVIC, D. J., SAVIC, G., LYON, K., PRIMEAUX, C., SEZATE, S., SUVOROV, A. N., KENTON, S., LAI, H. S., LIN, S. P., QIAN, Y., JIA, H. G., NAJAR, F. Z., REN, Q., ZHU, H., SONG, L., WHITE, J., YUAN, X., CLIFTON, S. W., ROE, B. A. & MCLAUGHLIN, R. 2001. Complete genome sequence of an M1 strain of Streptococcus pyogenes. *Proc Natl Acad Sci U S A,* 98**,** 4658-63.
FERRY, J. D. & MORRISON, P. R. 1947. Preparation and properties of serum and plasma proteins; the conversion of human fibrinogen to fibrin under various conditions. *J Am Chem Soc,* 69**,** 388-400.
FIEDLER, T., KOLLER, T. & KREIKEMEYER, B. 2015. Streptococcus pyogenes biofilms-formation, biology, and clinical relevance. *Front Cell Infect Microbiol,* 5**,** 15.
FISCHETTI, V. A. 1989. Streptococcal M protein: molecular design and biological behavior. *Clin Microbiol Rev,* 2**,** 285-314.
FLECK, R. A., RAO, L. V., RAPAPORT, S. I. & VARKI, N. 1990. Localization of human tissue factor antigen by immunostaining with monospecific, polyclonal anti-human tissue factor antibody. *Thromb Res,* 59**,** 421-37.
FLICK, M. J., DU, X., PRASAD, J. M., RAGHU, H., PALUMBO, J. S., SMEDS, E., HOOK, M. & DEGEN, J. L. 2013. Genetic elimination of the binding motif on fibrinogen for the S. aureus virulence factor ClfA improves host survival in septicemia. *Blood,* 121**,** 1783-94.
FOGELSON, A. L. & KEENER, J. P. 2010. Toward an understanding of fibrin branching structure. *Phys Rev E Stat Nonlin Soft Matter Phys,* 81**,** 051922.
FOWLER, W. E. & ERICKSON, H. P. 1979. Trinodular structure of fibrinogen. Confirmation by both shadowing and negative stain electron microscopy. *J Mol Biol,* 134**,** 241-9.
FRICK, I. M., MORGELIN, M. & BJORCK, L. 2000. Virulent aggregates of Streptococcus pyogenes are generated by homophilic protein-protein interactions. *Mol Microbiol,* 37**,** 1232-47.
FRIEDRICH, R., PANIZZI, P., FUENTES-PRIOR, P., RICHTER, K., VERHAMME, I., ANDERSON, P. J., KAWABATA, S., HUBER, R.,

BODE, W. & BOCK, P. E. 2003. Staphylocoagulase is a prototype for the mechanism of cofactor-induced zymogen activation. *Nature,* 425**,** 535-9.
FROEHLICH, B. J., BATES, C. & SCOTT, J. R. 2009. Streptococcus pyogenes CovRS mediates growth in iron starvation and in the presence of the human cationic antimicrobial peptide LL-37. *J Bacteriol,* 191**,** 673-7.
FUCHS, H., WALLICH, R., SIMON, M. M. & KRAMER, M. D. 1994. The Outer Surface Protein-a of the Spirochete Borrelia-Burgdorferi Is a Plasmin(Ogen) Receptor. *Proceedings of the National Academy of Sciences of the United States of America,* 91**,** 12594-8.
GABRIEL, D. A., MUGA, K. & BOOTHROYD, E. M. 1992. The Effect of Fibrin Structure on Fibrinolysis. *Journal of Biological Chemistry,* 267**,** 24259-63.
GAERTNER, F. & MASSBERG, S. 2016. Blood coagulation in immunothrombosis-At the frontline of intravascular immunity. *Semin Immunol,* 28**,** 561-69.
GALANAKIS, D. K., LANE, B. P. & SIMON, S. R. 1987. Albumin modulates lateral assembly of fibrin polymers: evidence of enhanced fine fibril formation and of unique synergism with fibrinogen. *Biochemistry,* 26**,** 2389-400.
GALE, A. J. 2011. Continuing education course #2: current understanding of hemostasis. *Toxicol Pathol,* 39**,** 273-80.
GAO, R. & STOCK, A. M. 2009. Biological insights from structures of two-component proteins. *Annu Rev Microbiol,* 63**,** 133-54.
GARCIA, A. F., ABE, L. M., ERDEM, G., CORTEZ, C. L., KURAHARA, D. & YAMAGA, K. 2010. An insert in the covS gene distinguishes a pharyngeal and a blood isolate of Streptococcus pyogenes found in the same individual. *Microbiology,* 156**,** 3085-95.
GEBBINK, M. F. 2011. Tissue-type plasminogen activator-mediated plasminogen activation and contact activation, implications in and beyond haemostasis. *J Thromb Haemost,* 9 Suppl 1**,** 174-81.
GERA, K. & MCIVER, K. S. 2013. Laboratory growth and maintenance of Streptococcus pyogenes (the Group A Streptococcus, GAS). *Curr Protoc Microbiol,* 30**,** 9D 2 1-9D 2 13.
GERSH, K. C., NAGASWAMI, C. & WEISEL, J. W. 2009. Fibrin network structure and clot mechanical properties are altered by incorporation of erythrocytes. *Thromb Haemost,* 102**,** 1169-75.
GHERARDI, G., VITALI, L. A. & CRETI, R. 2018. Prevalent emm Types among Invasive GAS in Europe and North America since Year 2000. *Frontiers in Public Health,* 6.
GHOSH, P. 2018. Variation, Indispensability, and Masking in the M protein. *Trends Microbiol,* 26**,** 132-44.
GIFFARD, P. M., TONG, S. Y. C., HOLT, D. C., RALPH, A. P. & CURRIE, B. J. 2019. Concerns for efficacy of a 30-valent M-protein-based Streptococcus pyogenes vaccine in regions with high rates of rheumatic heart disease. *PLoS Negl Trop Dis,* 13**,** e0007511.
GLINTON, K., BECK, J., LIANG, Z., QIU, C., LEE, S. W., PLOPLIS, V. A. & CASTELLINO, F. J. 2017. Variable region in streptococcal M-proteins provides stable binding with host fibrinogen for plasminogen-mediated bacterial invasion. *J Biol Chem,* 292**,** 6775-85.
GRAILHE, P., NIEUWENHUIZEN, W. & ANGLESCANO, E. 1994. Study of Tissue-Type Plasminogen-Activator Binding-Sites on Fibrin Using Distinct Fragments of Fibrinogen. *European Journal of Biochemistry,* 219**,** 961-7.

GRAU, E. & MOROZ, L. A. 1989. Fibrinolytic activity of normal human blood monocytes. *Thromb Res,* 53**,** 145-62.
GREBE, T. & HAKENBECK, R. 1996. Penicillin-binding proteins 2b and 2x of Streptococcus pneumoniae are primary resistance determinants for different classes of beta-lactam antibiotics. *Antimicrob Agents Chemother,* 40**,** 829-34.
GRELLA, D. K. & CASTELLINO, F. J. 1997. Activation of human plasminogen by staphylokinase. Direct evidence that preformed plasmin is necessary for activation to occur. *Blood,* 89**,** 1585-9.
GROVER, S. P. & MACKMAN, N. 2018. Tissue Factor: An Essential Mediator of Hemostasis and Trigger of Thrombosis. *Arterioscler Thromb Vasc Biol,* 38**,** 709-25.
GUGGENBERGER, C., WOLZ, C., MORRISSEY, J. A. & HEESEMANN, J. 2012. Two distinct coagulase-dependent barriers protect Staphylococcus aureus from neutrophils in a three dimensional in vitro infection model. *PLoS Pathogens,* 8**,** e1002434.
HALL, C. E. & SLAYTER, H. S. 1959. The fibrinogen molecule: its size, shape, and mode of polymerization. *J Biophys Biochem Cytol,* 5**,** 11-6.
HAN, E. D., MACFARLANE, R. C., MULLIGAN, A. N., SCAFIDI, J. & DAVIS, A. E., 3RD 2002. Increased vascular permeability in C1 inhibitor-deficient mice mediated by the bradykinin type 2 receptor. *J Clin Invest,* 109**,** 1057-63.
HARDY, J. J., CARRELL, N. A. & MCDONAGH, J. 1983. Calcium ion functions in fibrinogen conversion to fibrin. *Ann N Y Acad Sci,* 408**,** 279-87.
HERWALD, H., COLLIN, M., MULLER-ESTERL, W. & BJORCK, L. 1996. Streptococcal cysteine proteinase releases kinins: a virulence mechanism. *J Exp Med,* 184**,** 665-73.
HERWALD, H., CRAMER, H., MORGELIN, M., RUSSELL, W., SOLLENBERG, U., NORRBY-TEGLUND, A., FLODGAARD, H., LINDBOM, L. & BJORCK, L. 2004. M protein, a classical bacterial virulence determinant, forms complexes with fibrinogen that induce vascular leakage. *Cell,* 116**,** 367-79.
HERWALD, H., MORGELIN, M., DAHLBACK, B. & BJORCK, L. 2003. Interactions between surface proteins of Streptococcus pyogenes and coagulation factors modulate clotting of human plasma. *Journal of Thrombosis and Haemostasis,* 1**,** 284-291.
HERWALD, H., MORGELIN, M., OLSEN, A., RHEN, M., DAHLBACK, B., MULLER-ESTERL, W. & BJORCK, L. 1998. Activation of the contact-phase system on bacterial surfaces--a clue to serious complications in infectious diseases. *Nat Med,* 4**,** 298-302.
HETHERSHAW, E. L., CILIA LA CORTE, A. L., DUVAL, C., ALI, M., GRANT, P. J., ARIENS, R. A. & PHILIPPOU, H. 2014. The effect of blood coagulation factor XIII on fibrin clot structure and fibrinolysis. *J Thromb Haemost,* 12**,** 197-205.
HIGGINS, J., LOUGHMAN, A., VAN KESSEL, K. P. M., VAN STRIJP, J. A. G. & FOSTER, T. J. 2006. Clumping factor A of Staphylococcus aureus inhibits phagocytosis by human polymorphonuclear leucocytes. *Fems Microbiology Letters,* 258**,** 290-6.
HIROTA-KAWADOBORA, M., TERASAWA, F., SUZUKI, T., TOZUKA, M., SANO, K. & OKUMURA, N. 2004. Comparison of thrombin-catalyzed fibrin polymerization and factor XIIIa-catalyzed cross-linking of fibrin

among three recombinant variant fibrinogens, gamma 275C, gamma 275H, and gamma 275A. *J Thromb Haemost,* 2**,** 1359-67.
HOLINSTAT, M. 2017. Normal platelet function. *Cancer Metastasis Rev,* 36**,** 195-98.
HOLLINGSHEAD, S. K., FISCHETTI, V. A. & SCOTT, J. R. 1986. Complete nucleotide sequence of type 6 M protein of the group A Streptococcus. Repetitive structure and membrane anchor. *J Biol Chem,* 261**,** 1677-86.
HOLVOET, P., LIJNEN, H. R. & COLLEN, D. 1985. A monoclonal antibody specific for Lys-plasminogen. Application to the study of the activation pathways of plasminogen in vivo. *J Biol Chem,* 260**,** 12106-11.
HONDA-OGAWA, M., OGAWA, T., TERAO, Y., SUMITOMO, T., NAKATA, M., IKEBE, K., MAEDA, Y. & KAWABATA, S. 2013. Cysteine proteinase from Streptococcus pyogenes enables evasion of innate immunity via degradation of complement factors. *J Biol Chem,* 288**,** 15854-64.
HOYLAERTS, M., RIJKEN, D. C., LIJNEN, H. R. & COLLEN, D. 1982. Kinetics of the activation of plasminogen by human tissue plasminogen activator. Role of fibrin. *J Biol Chem,* 257**,** 2912-9.
HUAI, Q., MAZAR, A. P., KUO, A., PARRY, G. C., SHAW, D. E., CALLAHAN, J., LI, Y., YUAN, C., BIAN, C., CHEN, L., FURIE, B., FURIE, B. C., CINES, D. B. & HUANG, M. 2006. Structure of human urokinase plasminogen activator in complex with its receptor. *Science,* 311**,** 656-9.
HUANG, T. T., MALKE, H. & FERRETTI, J. J. 1989. The streptokinase gene of group A streptococci: cloning, expression in Escherichia coli, and sequence analysis. *Mol Microbiol,* 3**,** 197-205.
HUDSON, N. E. 2017. Biophysical Mechanisms Mediating Fibrin Fiber Lysis. *Biomed Res Int,* 2017**,** 2748340.
HUISH, S., THELWELL, C. & LONGSTAFF, C. 2017. Activity Regulation by Fibrinogen and Fibrin of Streptokinase from Streptococcus Pyogenes. *PLoS One,* 12**,** e0170936.
HYNES, W. & SLOAN, M. 2016. Secreted Extracellular Virulence Factors. *In:* FERRETTI, J. J., STEVENS, D. L. & FISCHETTI, V. A. (eds.) *Streptococcus pyogenes : Basic Biology to Clinical Manifestations.* Oklahoma City (OK).
ICHINOSE, A., FUJIKAWA, K. & SUYAMA, T. 1986. The activation of pro-urokinase by plasma kallikrein and its inactivation by thrombin. *J Biol Chem,* 261**,** 3486-9.
IKEBE, T., ATO, M., MATSUMURA, T., HASEGAWA, H., SATA, T., KOBAYASHI, K. & WATANABE, H. 2010. Highly frequent mutations in negative regulators of multiple virulence genes in group A streptococcal toxic shock syndrome isolates. *PLoS Pathog,* 6**,** e1000832.
IMAMURA, T., POTEMPA, J., PIKE, R. N. & TRAVIS, J. 1995. Dependence of vascular permeability enhancement on cysteine proteinases in vesicles of Porphyromonas gingivalis. *Infect Immun,* 63**,** 1999-2003.
IMAMURA, T., TANASE, S., SZMYD, G., KOZIK, A., TRAVIS, J. & POTEMPA, J. 2005. Induction of vascular leakage through release of bradykinin and a novel kinin by cysteine proteinases from Staphylococcus aureus. *Journal of Experimental Medicine,* 201**,** 1669-76.
JACKSON, K. W. & TANG, J. 1978. The amino-terminal sequence of streptokinase and its functional implications in plasminogen activation. *Thromb Res,* 13**,** 693-9.
JAMBOR, C., REUL, V., SCHNIDER, T. W., DEGIACOMI, P., METZNER, H. & KORTE, W. C. 2009. In vitro inhibition of factor XIII retards clot formation,

reduces clot firmness, and increases fibrinolytic effects in whole blood. *Anesth Analg,* 109**,** 1023-8.
JOHNSON, D. R., KAPLAN, E. L., VANGHEEM, A., FACKLAM, R. R. & BEALL, B. 2006. Characterization of group A streptococci (Streptococcus pyogenes): correlation of M-protein and emm-gene type with T-protein agglutination pattern and serum opacity factor. *J Med Microbiol,* 55**,** 157-64.
KALIA, A. & BESSEN, D. E. 2004. Natural selection and evolution of streptococcal virulence genes involved in tissue-specific adaptations. *J Bacteriol,* 186**,** 110-21.
KANNEMEIER, C., SHIBAMIYA, A., NAKAZAWA, F., TRUSHEIM, H., RUPPERT, C., MARKART, P., SONG, Y., TZIMA, E., KENNERKNECHT, E., NIEPMANN, M., VON BRUEHL, M. L., SEDDING, D., MASSBERG, S., GUNTHER, A., ENGELMANN, B. & PREISSNER, K. T. 2007. Extracellular RNA constitutes a natural procoagulant cofactor in blood coagulation. *Proc Natl Acad Sci U S A,* 104**,** 6388-93.
KANTOR, F. S. 1965. Fibrinogen Precipitation by Streptococcal M Protein. I. Identity of the Reactants, and Stoichiometry of the Reaction. *J Exp Med,* 121**,** 849-59.
KAPRAL, F. A. 1966. Clumping of Staphylococcus aureus in the peritoneal cavity of mice. *J Bacteriol,* 92**,** 1188-95.
KAPUR, V., KANJILAL, S., HAMRICK, M. R., LI, L. L., WHITTAM, T. S., SAWYER, S. A. & MUSSER, J. M. 1995. Molecular population genetic analysis of the streptokinase gene of Streptococcus pyogenes: mosaic alleles generated by recombination. *Mol Microbiol,* 16**,** 509-19.
KATONA, E., PENZES, K., MOLNAR, E. & MUSZBEK, L. 2012. Measurement of factor XIII activity in plasma. *Clin Chem Lab Med,* 50**,** 1191-202.
KEARNEY, K. J., ARIENS, R. A. S. & MACRAE, F. L. 2021a. The Role of Fibrin(ogen) in Wound Healing and Infection Control. *Semin Thromb Hemost*.
KEARNEY, K. J., BUTLER, J., POSADA, O. M., WILSON, C., HEAL, S., ALI, M., HARDY, L., AHNSTROM, J., GAILANI, D., FOSTER, R., HETHERSHAW, E., LONGSTAFF, C. & PHILIPPOU, H. 2021b. Kallikrein directly interacts with and activates Factor IX, resulting in thrombin generation and fibrin formation independent of Factor XI. *Proc Natl Acad Sci U S A,* 118.
KHAKZAD, H., HAPPONEN, L., KARAMI, Y., CHOWDHURY, S., BERGDAHL, G. E., NILGES, M., NHIEU, G. T. V., MALMSTROM, J. & MALMSTROM, L. 2021. Structural determination of Streptococcus pyogenes M1 protein interactions with human immunoglobulin G using integrative structural biology. *Plos Computational Biology,* 17.
KHIL, J., IM, M., HEATH, A., RINGDAHL, U., MUNDADA, L., CARY ENGLEBERG, N. & FAY, W. P. 2003. Plasminogen enhances virulence of group A streptococci by streptokinase-dependent and streptokinase-independent mechanisms. *J Infect Dis,* 188**,** 497-505.
KIMURA, S. & AOKI, N. 1986. Cross-linking site in fibrinogen for alpha 2-plasmin inhibitor. *J Biol Chem,* 261**,** 15591-5.
KINNBY, B., BOOTH, N. A. & SVENSATER, G. 2008. Plasminogen binding by oral streptococci from dental plaque and inflammatory lesions. *Microbiology (Reading),* 154**,** 924-931.

KOHLER, S., SCHMID, F. & SETTANNI, G. 2015. The Internal Dynamics of Fibrinogen and Its Implications for Coagulation and Adsorption. *PLoS Comput Biol,* 11**,** e1004346.
KORHONEN, T. K., HAIKO, J., LAAKKONEN, L., JARVINEN, H. M. & WESTERLUND-WIKSTROM, B. 2013. Fibrinolytic and coagulative activities of Yersinia pestis. *Front Cell Infect Microbiol,* 3**,** 35.
KORHONEN, T. K., LAHTEENMAKI, K., KUKKONEN, M., POUTTU, R., HYNONEN, U., SAVOLAINEN, K., WESTERLUNDWIKSTROM, B. & VIRKOLA, R. 1997. Plasminogen receptors - Turning Salmonella and Escherichia coli into proteolytic organisms. *Mechanisms in the Pathogenesis of Enteric Diseases,* 412**,** 185-92.
KOSTELANSKY, M. S., BETTS, L., GORKUN, O. V. & LORD, S. T. 2002. 2.8 A crystal structures of recombinant fibrinogen fragment D with and without two peptide ligands: GHRP binding to the "b" site disrupts its nearby calcium-binding site. *Biochemistry,* 41**,** 12124-32.
KRISHER, K. & CUNNINGHAM, M. W. 1985. Myosin: a link between streptococci and heart. *Science,* 227**,** 413-5.
KUKKONEN, M., SAARELA, S., LAHTEENMAKI, K., HYNONEN, U., WESTERLUND-WIKSTROM, B., RHEN, M. & KORHONEN, T. K. 1998. Identification of two laminin-binding fimbriae, the type 1 fimbria of Salmonella enterica serovar typhimurium and the G fimbria of Escherichia coli, as plasminogen receptors. *Infection and Immunity,* 66**,** 4965-70.
KURNIAWAN, N. A., VAN KEMPEN, T. H. S., SONNEVELD, S., ROSALINA, T. T., VOS, B. E., JANSEN, K. A., PETERS, G. W. M., VAN DE VOSSE, F. N. & KOENDERINK, G. H. 2017. Buffers Strongly Modulate Fibrin Self-Assembly into Fibrous Networks. *Langmuir,* 33**,** 6342-52.
LAHTEENMAKI, K., KUUSELA, P. & KORHONEN, T. K. 2000. Plasminogen activation in degradation and penetration of extracellular matrices and basement membranes by invasive bacteria. *Methods,* 21**,** 125-32.
LAHTEENMAKI, K., KUUSELA, P. & KORHONEN, T. K. 2001. Bacterial plasminogen activators and receptors. *FEMS Microbiol Rev,* 25**,** 531-52.
LAHTEENMAKI, K., WESTERLUND, B., KUUSELA, P. & KORHONEN, T. K. 1993. Immobilization of Plasminogen on Escherichia-Coli Flagella. *Fems Microbiology Letters,* 106**,** 309-14.
LAMBA, D., BAUER, M., HUBER, R., FISCHER, S., RUDOLPH, R., KOHNERT, U. & BODE, W. 1996. The 2.3 A crystal structure of the catalytic domain of recombinant two-chain human tissue-type plasminogen activator. *J Mol Biol,* 258**,** 117-35.
LANCEFIELD, R. C. 1933. A Serological Differentiation of Human and Other Groups of Hemolytic Streptococci. *J Exp Med,* 57**,** 571-95.
LANE, D. A., PHILIPPOU, H. & HUNTINGTON, J. A. 2005. Directing thrombin. *Blood,* 106**,** 2605-12.
LANGSHAW, E. L., PANDEY, M. & GOOD, M. F. 2018. Cellular interactions of covR/S mutant group A Streptococci. *Microbes Infect,* 20**,** 531-535.
LARSSON, L. I., SKRIVER, L., NIELSEN, L. S., GRONDAHL-HANSEN, J., KRISTENSEN, P. & DANO, K. 1984. Distribution of urokinase-type plasminogen activator immunoreactivity in the mouse. *J Cell Biol,* 98**,** 894-903.
LAW, R. H., CARADOC-DAVIES, T., COWIESON, N., HORVATH, A. J., QUEK, A. J., ENCARNACAO, J. A., STEER, D., COWAN, A., ZHANG, Q., LU, B. G., PIKE, R. N., SMITH, A. I., COUGHLIN, P. B. & WHISSTOCK, J. C.

2012. The X-ray crystal structure of full-length human plasminogen. *Cell Rep,* 1**,** 185-90.
LAW, R. H. P., ABU-SSAYDEH, D. & WHISSTOCK, J. C. 2013. New insights into the structure and function of the plasminogen/plasmin system. *Current Opinion in Structural Biology,* 23**,** 836-841.
LEVIN, E. G. & DEL ZOPPO, G. J. 1994. Localization of tissue plasminogen activator in the endothelium of a limited number of vessels. *Am J Pathol,* 144**,** 855-61.
LEVIN, J. C. & WESSELS, M. R. 1998. Identification of csrR/csrS, a genetic locus that regulates hyaluronic acid capsule synthesis in group A Streptococcus. *Molecular Microbiology,* 30**,** 209-19.
LI, J., LIU, G., FENG, W., ZHOU, Y., LIU, M., WILEY, J. A. & LEI, B. 2014. Neutrophils select hypervirulent CovRS mutants of M1T1 group A Streptococcus during subcutaneous infection of mice. *Infect Immun,* 82**,** 1579-90.
LIANG, Z., CAROTHERS, K., HOLMES, A., DONAHUE, D., LEE, S. W., CASTELLINO, F. J. & PLOPLIS, V. A. 2019. Stable genetic integration of a red fluorescent protein in a virulent Group A Streptococcus strain. *Access Microbiol,* 1**,** e000062.
LIANG, Z., ZHANG, Y., AGRAHARI, G., CHANDRAHAS, V., GLINTON, K., DONAHUE, D. L., BALSARA, R. D., PLOPLIS, V. A. & CASTELLINO, F. J. 2013. A natural inactivating mutation in the CovS component of the CovRS regulatory operon in a pattern D Streptococcal pyogenes strain influences virulence-associated genes. *J Biol Chem,* 288**,** 6561-73.
LIJNEN, H. R., VAN HOEF, B., DE COCK, F., OKADA, K., UESHIMA, S., MATSUO, O. & COLLEN, D. 1991a. On the mechanism of fibrin-specific plasminogen activation by staphylokinase. *J Biol Chem,* 266**,** 11826-32.
LIJNEN, H. R., VANHOEF, B., DECOCK, F., MATSUO, O. & COLLEN, D. 1991b. On the Mechanism of Fibrin-Specific Plasminogen Activation by Staphylokinase. *Thrombosis and Haemostasis,* 65**,** 11826-32.
LIN, L. F., HOUNG, A. Y. & REED, G. L. 2000. Epsilon amino caproic acid inhibits streptokinase-plasminogen activator complex formation and substrate binding through kringle-dependent mechanisms. *Biochemistry,* 39**,** 4740-4745.
LINDER, A., CHRISTENSSON, B., HERWALD, H., BJORCK, L. & AKESSON, P. 2009. Heparin-binding protein: an early marker of circulatory failure in sepsis. *Clin Infect Dis,* 49**,** 1044-50.
LITVINOV, R. I., PIETERS, M., DE LANGE-LOOTS, Z. & WEISEL, J. W. 2021. Fibrinogen and Fibrin. *Subcell Biochem,* 96**,** 471-501.
LIU, C. Z., HUANG, T. F., TSAI, P. J., TSAI, P. J., CHANG, L. Y. & CHANG, M. C. 2007. A segment of Staphylococcus aureus clumping factor A with fibrinogen-binding activity (ClfA221-550) inhibits platelet-plug formation in mice. *Thromb Res,* 121**,** 183-91.
LIU, C. Z., SHIH, M. H. & TSAI, P. J. 2005. ClfA(221-550), a fibrinogen-binding segment of Staphylococcus aureus clumping factor A, disrupts fibrinogen function. *Thromb Haemost,* 94**,** 286-94.
LONGSTAFF, C. 2016a. *Shiny App for calculating clot lysis times, version 0.91b* [Online]. Available: https://drclongstaff.shinyapps.io/clotlysisCL/

https://onlinelibrary.wiley.com/doi/pdfdirect/10.1111/jth.13656?download=true [Accessed 2020-06-23].

LONGSTAFF, C. 2016b. *Shiny App for calculating zymogen activation rates, version 0.6* [Online]. Available: https://drclongstaff.shinyapps.io/zymogenactnCL/ [Accessed 28/08/18].
LONGSTAFF, C. 2018a. Measuring fibrinolysis: from research to routine diagnostic assays. *J Thromb Haemost,* 16**,** 652-62.
LONGSTAFF, C. 2018b. *Shiny App for calculating halo assay lysis times, version 0.35* [Online]. Available: https://drclongstaff.shinyapps.io/HalolysisCL [Accessed].
LONGSTAFF, C. & KOLEV, K. 2015. Basic mechanisms and regulation of fibrinolysis. *J Thromb Haemost,* 13 Suppl 1**,** 98-105.
LONGSTAFF, C., THELWELL, C., WILLIAMS, S. C., SILVA, M. M., SZABO, L. & KOLEV, K. 2011. The interplay between tissue plasminogen activator domains and fibrin structures in the regulation of fibrinolysis: kinetic and microscopic studies. *Blood,* 117**,** 661-8.
LONGSTAFF, C. & WHITTON, C. M. 2004. A proposed reference method for plasminogen activators that enables calculation of enzyme activities in SI units. *J Thromb Haemost,* 2**,** 1416-21.
LOOF, T. G., MORGELIN, M., JOHANSSON, L., OEHMCKE, S., OLIN, A. I., DICKNEITE, G., NORRBY-TEGLUND, A., THEOPOLD, U. & HERWALD, H. 2011. Coagulation, an ancestral serine protease cascade, exerts a novel function in early immune defense. *Blood,* 118**,** 2589-98.
LOTTENBERG, R., DESJARDIN, L. E., WANG, H. & BOYLE, M. D. 1992. Streptokinase-producing streptococci grown in human plasma acquire unregulated cell-associated plasmin activity. *J Infect Dis,* 166**,** 436-40.
LOUGHMAN, A., FITZGERALD, J. R., BRENNAN, M. P., HIGGINS, J., DOWNER, R., COX, D. & FOSTER, T. J. 2005. Roles for fibrinogen, immunoglobulin and complement in platelet activation promoted by Staphylococcus aureus clumping factor A. *Molecular Microbiology,* 57**,** 804-18.
LUCA-HARARI, B., DARENBERG, J., NEAL, S., SILJANDER, T., STRAKOVA, L., TANNA, A., CRETI, R., EKELUND, K., KOLIOU, M., TASSIOS, P. T., VAN DER LINDEN, M., STRAUT, M., VUOPIO-VARKILA, J., BOUVET, A., EFSTRATIOU, A., SCHALEN, C., HENRIQUES-NORMARK, B., JASIR, A. & GRP, S.-E. S. 2009. Clinical and Microbiological Characteristics of Severe Streptococcus pyogenes Disease in Europe. *Journal of Clinical Microbiology,* 47**,** 1155-65.
LUO, D., SZABA, F. M., KUMMER, L. W., PLOW, E. F., MACKMAN, N., GAILANI, D. & SMILEY, S. T. 2011. Protective roles for fibrin, tissue factor, plasminogen activator inhibitor-1, and thrombin activatable fibrinolysis inhibitor, but not factor XI, during defense against the gram-negative bacterium Yersinia enterocolitica. *J Immunol,* 187**,** 1866-76.
LY, D., DONAHUE, D., WALKER, M. J., PLOPLIS, V. A., MCARTHUR, J. D., RANSON, M., CASTELLINO, F. J. & SANDERSON-SMITH, M. L. 2019. Characterizing the role of tissue-type plasminogen activator in a mouse model of Group A streptococcal infection. *Microbes Infect*.
MAAMARY, P. G., BEN ZAKOUR, N. L., COLE, J. N., HOLLANDS, A., AZIZ, R. K., BARNETT, T. C., CORK, A. J., HENNINGHAM, A., SANDERSON-SMITH, M., MCARTHUR, J. D., VENTURINI, C., GILLEN, C. M., KIRK, J. K., JOHNSON, D. R., TAYLOR, W. L., KAPLAN, E. L., KOTB, M., NIZET, V., BEATSON, S. A. & WALKER, M. J. 2012. Tracing the evolutionary history of the pandemic group A streptococcal M1T1 clone. *FASEB J,* 26**,** 4675-84.

MAAMARY, P. G., SANDERSON-SMITH, M. L., AZIZ, R. K., HOLLANDS, A., COLE, J. N., MCKAY, F. C., MCARTHUR, J. D., KIRK, J. K., CORK, A. J., KEEFE, R. J., KANSAL, R. G., SUN, H., TAYLOR, W. L., CHHATWAL, G. S., GINSBURG, D., NIZET, V., KOTB, M. & WALKER, M. J. 2010. Parameters governing invasive disease propensity of non-M1 serotype group A streptococci. *J Innate Immun,* 2**,** 596-606.

MAAS, C., OSCHATZ, C. & RENNE, T. 2011. The plasma contact system 2.0. *Semin Thromb Hemost,* 37**,** 375-81.

MACHEBOEUF, P., BUFFALO, C., FU, C. Y., ZINKERNAGEL, A. S., COLE, J. N., JOHNSON, J. E., NIZET, V. & GHOSH, P. 2011. Streptococcal M1 protein constructs a pathological host fibrinogen network. *Nature,* 472**,** 64-8.

MACHLUS, K. R., CARDENAS, J. C., CHURCH, F. C. & WOLBERG, A. S. 2011. Causal relationship between hyperfibrinogenemia, thrombosis, and resistance to thrombolysis in mice. *Blood,* 117**,** 4953-63.

MACKMAN, N. 2004. Role of tissue factor in hemostasis, thrombosis, and vascular development. *Arterioscler Thromb Vasc Biol,* 24**,** 1015-22.

MACRAE, F. L., DUVAL, C., PAPAREDDY, P., BAKER, S. R., YULDASHEVA, N., KEARNEY, K. J., MCPHERSON, H. R., ASQUITH, N., KONINGS, J., CASINI, A., DEGEN, J. L., CONNELL, S. D., PHILIPPOU, H., WOLBERG, A. S., HERWALD, H. & ARIENS, R. A. 2018. A fibrin biofilm covers blood clots and protects from microbial invasion. *J Clin Invest,* 128**,** 3356-68.

MADISON, E. L. & SAMBROOK, J. E. 1993. Probing structure-function relationships of tissue-type plasminogen activator by oligonucleotide-mediated site-specific mutagenesis. *Methods Enzymol,* 223**,** 249-71.

MADRAZO, J., BROWN, J. H., LITVINOVICH, S., DOMINGUEZ, R., YAKOVLEV, S., MEDVED, L. & COHEN, C. 2001. Crystal structure of the central region of bovine fibrinogen (E5 fragment) at 1.4-A resolution. *Proc Natl Acad Sci U S A,* 98**,** 11967-72.

MAHMOUDI, S., ABTAHI, H., BAHADOR, A., MOSAYEBI, G., SALMANIAN, A. H. & TEYMURI, M. 2012. Optimizing of Nutrients for High Level Expression of Recombinant Streptokinase Using pET32a Expression System. *Maedica (Buchar),* 7**,** 241-6.

MALACHOWA, N., KOBAYASHI, S. D., PORTER, A. R., BRAUGHTON, K. R., SCOTT, D. P., GARDNER, D. J., MISSIAKAS, D. M., SCHNEEWIND, O. & DELEO, F. R. 2016. Contribution of Staphylococcus aureus Coagulases and Clumping Factor A to Abscess Formation in a Rabbit Model of Skin and Soft Tissue Infection. *PLoS One,* 11**,** e0158293.

MALKE, H. & FERRETTI, J. J. 1984. Streptokinase: cloning, expression, and excretion by Escherichia coli. *Proc Natl Acad Sci U S A,* 81**,** 3557-61.

MALKE, H., ROE, B. & FERRETTI, J. J. 1985. Nucleotide sequence of the streptokinase gene from Streptococcus equisimilis H46A. *Gene,* 34**,** 357-62.

MANCHANDA, N. & SCHWARTZ, B. S. 1990. Lipopolysaccharide-induced modulation of human monocyte urokinase production and activity. *J Immunol,* 145**,** 4174-80.

MANCHANDA, N. & SCHWARTZ, B. S. 1991. Single Chain Urokinase - Augmentation of Enzymatic-Activity Upon Binding to Monocytes. *Journal of Biological Chemistry,* 266**,** 14580-4.

MARCHI, R. C., CARVAJAL, Z., BOYER-NEUMANN, C., ANGLES-CANO, E. & WEISEL, J. W. 2006. Functional characterization of fibrinogen Bicetre II:

a gamma 308 Asn-->Lys mutation located near the fibrin D:D interaction sites. *Blood Coagul Fibrinolysis,* 17**,** 193-201.
MARKUS, G., PRIORE, R. L. & WISSLER, F. C. 1979. The binding of tranexamic acid to native (Glu) and modified (Lys) human plasminogen and its effect on conformation. *J Biol Chem,* 254**,** 1211-6.
MARTIN, J. 2016. The Streptococcus pyogenes Carrier State. *In:* FERRETTI, J. J., STEVENS, D. L. & FISCHETTI, V. A. (eds.) *Streptococcus pyogenes : Basic Biology to Clinical Manifestations.* Oklahoma City (OK).
MASSELL, B. F., HONIKMAN, L. H. & AMEZCUA, J. 1969. Rheumatic fever following streptococcal vaccination. Report of three cases. *JAMA,* 207**,** 1115-9.
MASUNO, K., OKADA, R., ZHANG, Y., ISAKA, M., TATSUNO, I., SHIBATA, S. & HASEGAWA, T. 2014. Simultaneous isolation of emm89-type Streptococcus pyogenes strains with a wild-type or mutated covS gene from a single streptococcal toxic shock syndrome patient. *J Med Microbiol,* 63**,** 504-507.
MATSUKA, Y. V., MEDVED, L. V., MIGLIORINI, M. M. & INGHAM, K. C. 1996. Factor XIIIa-catalyzed cross-linking of recombinant alpha C fragments of human fibrinogen. *Biochemistry,* 35**,** 5810-6.
MATTSSON, E., HERWALD, H., CRAMER, H., PERSSON, K., SJOBRING, U. & BJORCK, L. 2001. Staphylococcus aureus induces release of bradykinin in human plasma. *Infect Immun,* 69**,** 3877-82.
MAYFIELD, J. A., LIANG, Z., AGRAHARI, G., LEE, S. W., DONAHUE, D. L., PLOPLIS, V. A. & CASTELLINO, F. J. 2014. Mutations in the control of virulence sensor gene from Streptococcus pyogenes after infection in mice lead to clonal bacterial variants with altered gene regulatory activity and virulence. *PLoS One,* 9**,** e100698.
MCADOW, M., KIM, H. K., DEDENT, A. C., HENDRICKX, A. P., SCHNEEWIND, O. & MISSIAKAS, D. M. 2011. Preventing Staphylococcus aureus sepsis through the inhibition of its agglutination in blood. *PLoS Pathog,* 7**,** e1002307.
MCADOW, M., MISSIAKAS, D. M. & SCHNEEWIND, O. 2012. Staphylococcus aureus secretes coagulase and von Willebrand factor binding protein to modify the coagulation cascade and establish host infections. *J Innate Immun,* 4**,** 141-8.
MCARTHUR, J. D., MCKAY, F. C., RAMACHANDRAN, V., SHYAM, P., CORK, A. J., SANDERSON-SMITH, M. L., COLE, J. N., RINGDAHL, U., SJOBRING, U., RANSON, M. & WALKER, M. J. 2008. Allelic variants of streptokinase from Streptococcus pyogenes display functional differences in plasminogen activation. *FASEB J,* 22**,** 3146-53.
MCDEVITT, D., NANAVATY, T., HOUSEPOMPEO, K., BELL, E., TURNER, N., MCINTIRE, L., FOSTER, T. & HOOK, M. 1997. Characterization of the interaction between the Staphylococcus aureus clumping factor (ClfA) and fibrinogen. *European Journal of Biochemistry,* 247**,** 416-24.
MCKEE, P. A., MATTOCK, P. & HILL, R. L. 1970. Subunit structure of human fibrinogen, soluble fibrin, and cross-linked insoluble fibrin. *Proc Natl Acad Sci U S A,* 66**,** 738-44.
MEDVED, L., LITVINOVICH, S., UGAROVA, T., MATSUKA, Y. & INGHAM, K. 1997. Domain structure and functional activity of the recombinant human fibrinogen gamma-module (gamma148-411). *Biochemistry,* 36**,** 4685-93.

MEDVED, L., WEISEL, J. W., FIBRINOGEN, FACTOR, X. S. O. S. S. C. O. I. S. O. T. & HAEMOSTASIS 2009. Recommendations for nomenclature on fibrinogen and fibrin. *J Thromb Haemost,* 7**,** 355-9.

MOLLA, A., YAMAMOTO, T., AKAIKE, T., MIYOSHI, S. & MAEDA, H. 1989. Activation of Hageman-Factor and Prekallikrein and Generation of Kinin by Various Microbial Proteinases. *Journal of Biological Chemistry,* 264**,** 10589-94.

MONROE, D. M., MACKMAN, N. & HOFFMAN, M. 2010. Wound healing in hemophilia B mice and low tissue factor mice. *Thromb Res,* 125 Suppl 1**,** S74-7.

MORA, M., BENSI, G., CAPO, S., FALUGI, F., ZINGARETTI, C., MANETTI, A. G., MAGGI, T., TADDEI, A. R., GRANDI, G. & TELFORD, J. L. 2005. Group A Streptococcus produce pilus-like structures containing protective antigens and Lancefield T antigens. *Proc Natl Acad Sci U S A,* 102**,** 15641-6.

MOSES, A. E., WESSELS, M. R., ZALCMAN, K., ALBERTI, S., NATANSONYARON, S., MENES, T. & HANSKI, E. 1997. Relative contributions of hyaluronic acid capsule and M protein to virulence in a mucoid strain of the group A Streptococcus. *Infection and Immunity,* 65**,** 64-71.

MOSESSON, M. W., DIORIO, J. P., SIEBENLIST, K. R., WALL, J. S. & HAINFELD, J. F. 1993. Evidence for a second type of fibril branch point in fibrin polymer networks, the trimolecular junction. *Blood,* 82**,** 1517-21.

MULLARKY, I. K., SZABA, F. M., BERGGREN, K. N., PARENT, M. A., KUMMER, L. W., CHEN, W., JOHNSON, L. L. & SMILEY, S. T. 2005. Infection-stimulated fibrin deposition controls hemorrhage and limits hepatic bacterial growth during listeriosis. *Infect Immun,* 73**,** 3888-95.

MULLER, F., GAILANI, D. & RENNE, T. 2011. Factor XI and XII as antithrombotic targets. *Curr Opin Hematol,* 18**,** 349-55.

MULLER, F., MUTCH, N. J., SCHENK, W. A., SMITH, S. A., ESTERL, L., SPRONK, H. M., SCHMIDBAUER, S., GAHL, W. A., MORRISSEY, J. H. & RENNE, T. 2009. Platelet polyphosphates are proinflammatory and procoagulant mediators in vivo. *Cell,* 139**,** 1143-56.

MULLIN, J. L., BRENNAN, S. O., GANLY, P. S. & GEORGE, P. M. 2002. Fibrinogen Hillsborough: a novel gammaGly309Asp dysfibrinogen with impaired clotting. *Blood,* 99**,** 3597-601.

MUTCH, N. J. & BOOTH, N. A. 2016. Plasmin-Antiplasmin System. *In:* GONZALEZ, E., MOORE, H. B. & MOORE, E. E. (eds.) *Trauma Induced Coagulopathy.* Cham: Springer International Publishing.

MUTCH, N. J., ENGEL, R., UITTE DE WILLIGE, S., PHILIPPOU, H. & ARIENS, R. A. 2010. Polyphosphate modifies the fibrin network and down-regulates fibrinolysis by attenuating binding of tPA and plasminogen to fibrin. *Blood,* 115**,** 3980-8.

NAIR, C. H., SHAH, G. A. & DHALL, D. P. 1986. Effect of temperature, pH and ionic strength and composition on fibrin network structure and its development. *Thromb Res,* 42**,** 809-16.

NASKI, M. C. & SHAFER, J. A. 1991. A kinetic model for the alpha-thrombin-catalyzed conversion of plasma levels of fibrinogen to fibrin in the presence of antithrombin III. *J Biol Chem,* 266**,** 13003-10.

NEEVES, K. B., ILLING, D. A. & DIAMOND, S. L. 2010. Thrombin flux and wall shear rate regulate fibrin fiber deposition state during polymerization under flow. *Biophys J,* 98**,** 1344-52.

NELSON, D. C., GARBE, J. & COLLIN, M. 2011. Cysteine proteinase SpeB from Streptococcus pyogenes - a potent modifier of immunologically important host and bacterial proteins. *Biol Chem,* 392**,** 1077-88.
NELSON, G. E., PONDO, T., TOEWS, K. A., FARLEY, M. M., LINDEGREN, M. L., LYNFIELD, R., ARAGON, D., ZANSKY, S. M., WATT, J. P., CIESLAK, P. R., ANGELES, K., HARRISON, L. H., PETIT, S., BEALL, B. & VAN BENEDEN, C. A. 2016. Epidemiology of Invasive Group A Streptococcal Infections in the United States, 2005-2012. *Clin Infect Dis,* 63**,** 478-86.
NEMERSON, Y. & REPKE, D. 1985. Tissue factor accelerates the activation of coagulation factor VII: the role of a bifunctional coagulation cofactor. *Thromb Res,* 40**,** 351-8.
NICKEL, K. F. & RENNE, T. 2012. Crosstalk of the plasma contact system with bacteria. *Thromb Res,* 130 Suppl 1**,** 78-83.
NILSON, B. H., FRICK, I. M., AKESSON, P., FORSEN, S., BJORCK, L., AKERSTROM, B. & WIKSTROM, M. 1995. Structure and stability of protein H and the M1 protein from Streptococcus pyogenes. Implications for other surface proteins of gram-positive bacteria. *Biochemistry,* 34**,** 13688-98.
NOLAN, M., BOULDIN, S. D. & BOCK, P. E. 2013. Full time course kinetics of the streptokinase-plasminogen activation pathway. *J Biol Chem,* 288**,** 29482-93.
NORRMAN, B., WALLEN, P. & RANBY, M. 1985. Fibrinolysis mediated by tissue plasminogen activator. Disclosure of a kinetic transition. *Eur J Biochem,* 149**,** 193-200.
NOUBOUOSSIE, D. F., HENDERSON, M. W., MOOBERRY, M., ILICH, A., ELLSWORTH, P., PIEGORE, M., SKINNER, S. C., PAWLINSKI, R., WELSBY, I., RENNE, T., HOFFMAN, M., MONROE, D. M. & KEY, N. S. 2020. Red blood cell microvesicles activate the contact system, leading to factor IX activation via 2 independent pathways. *Blood,* 135**,** 755-765.
O'GRADY, K. A. F., KELPIE, L., ANDREWS, R. M., CURTIS, N., NOLAN, T. M., SELVARAJ, G., PASSMORE, J. W., OPPEDISANO, F., CARNIE, J. A. & CARAPETIS, J. R. 2007. The epidemiology of invasive group A streptococcal disease in Victoria, Australia. *Medical Journal of Australia,* 186**,** 565-69.
OEHMCKE, S., MORGELIN, M., MALMSTROM, J., LINDER, A., CHEW, M., THORLACIUS, H. & HERWALD, H. 2012. Stimulation of blood mononuclear cells with bacterial virulence factors leads to the release of pro-coagulant and pro-inflammatory microparticles. *Cell Microbiol,* 14**,** 107-19.
OEHMCKE, S., SHANNON, O., MORGELIN, M. & HERWALD, H. 2010. Streptococcal M proteins and their role as virulence determinants. *Clin Chim Acta,* 411**,** 1172-80.
OKADA, N., LISZEWSKI, M. K., ATKINSON, J. P. & CAPARON, M. 1995. Membrane cofactor protein (CD46) is a keratinocyte receptor for the M protein of the group A streptococcus. *Proc Natl Acad Sci U S A,* 92**,** 2489-93.
PALM, F., CHOWDHURY, S., WETTEMARK, S., MALMSTROM, J., HAPPONEN, L. & SHANNON, O. 2021. Distinct serotypes of streptococcal M proteins mediate fibrinogen-dependent platelet activation and pro-inflammatory effects. *Infect Immun***,** IAI0046221.

PANCHOLI, V. & FISCHETTI, V. A. 1998. alpha-enolase, a novel strong plasmin(ogen) binding protein on the surface of pathogenic streptococci. *J Biol Chem,* 273**,** 14503-15.
PANIZZI, P., FRIEDRICH, R., FUENTES-PRIOR, P., BODE, W. & BOCK, P. E. 2004. The staphylocoagulase family of zymogen activator and adhesion proteins. *Cell Mol Life Sci,* 61**,** 2793-8.
PANIZZI, P., FRIEDRICH, R., FUENTES-PRIOR, P., RICHTER, K., BOCK, P. E. & BODE, W. 2006. Fibrinogen substrate recognition by staphylocoagulase.(pro)thrombin complexes. *J Biol Chem,* 281**,** 1179-87.
PARKKINEN, J., HACKER, J. & KORHONEN, T. K. 1991. Enhancement of Tissue Plasminogen Activator-Catalyzed Plasminogen Activation by Escherichia-Coli S-Fimbriae Associated with Neonatal Septicemia and Meningitis. *Thrombosis and Haemostasis,* 65**,** 483-6.
PARRY, M. A. A., ZHANG, X. C. & BODE, W. 2000. Molecular mechanisms of plasminogen activation: bacterial cofactors provide clues. *Trends in Biochemical Sciences,* 25**,** 53-59.
PASSALI, D., LAURIELLO, M., PASSALI, G. C., PASSALI, F. M. & BELLUSSI, L. 2007. Group A streptococcus and its antibiotic resistance. *Acta Otorhinolaryngol Ital,* 27**,** 27-32.
PASTURAL, E., MCNEIL, S. A., MACKINNON-CAMERON, D., YE, L., LANGLEY, J. M., STEWART, R., MARTIN, L. H., HURLEY, G. J., SALEHI, S., PENFOUND, T. A., HALPERIN, S. & DALE, J. B. 2020. Safety and immunogenicity of a 30-valent M protein-based group a streptococcal vaccine in healthy adult volunteers: A randomized, controlled phase I study. *Vaccine,* 38**,** 1384-92.
PENNICA, D., HOLMES, W. E., KOHR, W. J., HARKINS, R. N., VEHAR, G. A., WARD, C. A., BENNETT, W. F., YELVERTON, E., SEEBURG, P. H., HEYNEKER, H. L., GOEDDEL, D. V. & COLLEN, D. 1983. Cloning and expression of human tissue-type plasminogen activator cDNA in E. coli. *Nature,* 301**,** 214-21.
PIETERS, M., GUTHOLD, M., NUNES, C. M. & DE LANGE, Z. 2020. Interpretation and Validation of Maximum Absorbance Data Obtained from Turbidimetry Analysis of Plasma Clots. *Thromb Haemost,* 120**,** 44-54.
PIETROCOLA, G., NOBILE, G., GIANOTTI, V., ZAPOTOCZNA, M., FOSTER, T. J., GEOGHEGAN, J. A. & SPEZIALE, P. 2016. Molecular Interactions of Human Plasminogen with Fibronectin-binding Protein B (FnBPB), a Fibrinogen/Fibronectin-binding Protein from Staphylococcus aureus. *Journal of Biological Chemistry,* 291**,** 18148-62.
PING, L., HUANG, L., CARDINALI, B., PROFUMO, A., GORKUN, O. V. & LORD, S. T. 2011. Substitution of the human alphaC region with the analogous chicken domain generates a fibrinogen with severely impaired lateral aggregation: fibrin monomers assemble into protofibrils but protofibrils do not assemble into fibers. *Biochemistry,* 50**,** 9066-75.
PIRO, O. & BROZE, G. J., JR. 2005. Comparison of cell-surface TFPIalpha and beta. *J Thromb Haemost,* 3**,** 2677-83.
PLOPLIS, V. A. & CASTELLINO, F. J. 2019. Host Pathways of Hemostasis that Regulate Group A Streptococcus Pyogenes Pathogenicity. *Curr Drug Targets*.
PLOW, E. F. & COLLEN, D. 1981. The presence and release of alpha 2-antiplasmin from human platelets. *Blood,* 58**,** 1069-74.

POSMA, J. J., POSTHUMA, J. J. & SPRONK, H. M. 2016. Coagulation and non-coagulation effects of thrombin. *J Thromb Haemost,* 14**,** 1908-16.
PROTOPOPOVA, A. D., BARINOV, N. A., ZAVYALOVA, E. G., KOPYLOV, A. M., SERGIENKO, V. I. & KLINOV, D. V. 2015. Visualization of fibrinogen alphaC regions and their arrangement during fibrin network formation by high-resolution AFM. *J Thromb Haemost,* 13**,** 570-9.
PROTOPOPOVA, A. D., LITVINOV, R. I., GALANAKIS, D. K., NAGASWAMI, C., BARINOV, N. A., MUKHITOV, A. R., KLINOV, D. V. & WEISEL, J. W. 2017. Morphometric characterization of fibrinogen's alphaC regions and their role in fibrin self-assembly and molecular organization. *Nanoscale,* 9**,** 13707-16.
PROUD, D. & KAPLAN, A. P. 1988. Kinin formation: mechanisms and role in inflammatory disorders. *Annu Rev Immunol,* 6**,** 49-83.
PRYZDIAL, E. L. G., LEE, F. M. H., LIN, B. H., CARTER, R. L. R., TEGEGN, T. Z. & BELLETRUTTI, M. J. 2018. Blood coagulation dissected. *Transfus Apher Sci,* 57**,** 449-57.
PUBLIC HEALTH ENGLAND. 2020. *Group A streptococcal infections: first report on seasonal activity in England, 2019/20* [Online]. Health Protection Report: Public Health England. Available: https://assets.publishing.service.gov.uk/government/uploads/system/uploads/attachment_data/file/865263/hpr0320_GAS_Version_2__crrctd-3_.pdf [Accessed 2021].
PURVES, L., PURVES, M. & BRANDT, W. 1987. Cleavage of fibrin-derived D-dimer into monomers by endopeptidase from puff adder venom (Bitis arietans) acting at cross-linked sites of the gamma-chain. Sequence of carboxy-terminal cyanogen bromide gamma-chain fragments. *Biochemistry,* 26**,** 4640-6.
QIU, C., YUAN, Y., LEE, S. W., PLOPLIS, V. A. & CASTELLINO, F. J. 2020. A local alpha-helix drives structural evolution of streptococcal M-protein affinity for host human plasminogen. *Biochem J,* 477**,** 1613-30.
QIU, C., YUAN, Y., LIANG, Z., LEE, S. W., PLOPLIS, V. A. & CASTELLINO, F. J. 2019. Variations in the secondary structures of PAM proteins influence their binding affinities to human plasminogen. *J Struct Biol,* 206**,** 193-203.
QIU, C., YUAN, Y., ZAJICEK, J., LIANG, Z., BALSARA, R. D., BRITO-ROBIONSON, T., LEE, S. W., PLOPLIS, V. A. & CASTELLINO, F. J. 2018. Contributions of different modules of the plasminogen-binding Streptococcus pyogenes M-protein that mediate its functional dimerization. *J Struct Biol***,** 151-64.
QUEK, A. J. H., MAZZITELLI, B. A., WU, G., LEUNG, E. W. W., CARADOC-DAVIES, T. T., LLOYD, G. J., JEEVARAJAH, D., CONROY, P. J., SANDERSON-SMITH, M., YUAN, Y., AYINUOLA, Y. A., CASTELLINO, F. J., WHISSTOCK, J. C. & LAW, R. H. P. 2019. Structure and Function Characterization of the a1a2 Motifs of Streptococcus pyogenes M Protein in Human Plasminogen Binding. *J Mol Biol***,** 3804-13.
RAABE, V. N. & SHANE, A. L. 2019. Group B Streptococcus (Streptococcus agalactiae). *Microbiol Spectr,* 7.
RALPH, A. P. & CARAPETIS, J. R. 2013. Group a streptococcal diseases and their global burden. *Curr Top Microbiol Immunol,* 368**,** 1-27.
RANBY, M., BERGSDORF, N. & NILSSON, T. 1982. Enzymatic properties of the one- and two-chain form of tissue plasminogen activator. *Thromb Res,* 27**,** 175-83.

RATNOFF, O. D. & COLOPY, J. E. 1955. A familial hemorrhagic trait associated with a deficiency of a clot-promoting fraction of plasma. *J Clin Invest,* 34**,** 602-13.
REGLINSKI, M. & SRISKANDAN, S. 2014. The contribution of group A streptococcal virulence determinants to the pathogenesis of sepsis. *Virulence,* 5**,** 127-36.
RENNE, T., SCHMAIER, A. H., NICKEL, K. F., BLOMBACK, M. & MAAS, C. 2012. In vivo roles of factor XII. *Blood,* 120**,** 4296-303.
RIEDEL, T., SUTTNAR, J., BRYNDA, E., HOUSKA, M., MEDVED, L. & DYR, J. E. 2011. Fibrinopeptides A and B release in the process of surface fibrin formation. *Blood,* 117**,** 1700-6.
RIJKEN, D. C., HOYLAERTS, M. & COLLEN, D. 1982. Fibrinolytic properties of one-chain and two-chain human extrinsic (tissue-type) plasminogen activator. *J Biol Chem,* 257**,** 2920-5.
RINGDAHL, U., SVENSSON, H. G., KOTARSKY, H., GUSTAFSSON, M., WEINEISEN, M. & SJOBRING, U. 2000. A role for the fibrinogen-binding regions of streptococcal M proteins in phagocytosis resistance. *Mol Microbiol,* 37**,** 1318-26.
RIOS-STEINER, J. L., SCHENONE, M., MOCHALKIN, I., TULINSKY, A. & CASTELLINO, F. J. 2001. Structure and binding determinants of the recombinant kringle-2 domain of human plasminogen to an internal peptide from a group A Streptococcal surface protein. *J Mol Biol,* 308**,** 705-19.
RITCHIE, H., LAWRIE, L. C., CROMBIE, P. W., MOSESSON, M. W. & BOOTH, N. A. 2000. Cross-linking of plasminogen activator inhibitor 2 and alpha 2-antiplasmin to fibrin(ogen). *J Biol Chem,* 275**,** 24915-20.
RITCHIE, H., LAWRIE, L. C., MOSESSON, M. W. & BOOTH, N. A. 2001. Characterization of crosslinking sites in fibrinogen for plasminogen activator inhibitor 2 (PAI-2). *Ann N Y Acad Sci,* 936**,** 215-8.
ROBBINS, K. C., SUMMARIA, L., HSIEH, B. & SHAH, R. J. 1967. The peptide chains of human plasmin. Mechanism of activation of human plasminogen to plasmin. *J Biol Chem,* 242**,** 2333-42.
ROHDE, M. & CLEARY, P. P. 2016. Adhesion and invasion of Streptococcus pyogenes into host cells and clinical relevance of intracellular streptococci. *In:* FERRETTI, J. J., STEVENS, D. L. & FISCHETTI, V. A. (eds.) *Streptococcus pyogenes : Basic Biology to Clinical Manifestations.* Oklahoma City (OK).
ROTHFORK, J. M., DESSUS-BABUS, S., VAN WAMEL, W. J., CHEUNG, A. L. & GRESHAM, H. D. 2003. Fibrinogen depletion attenuates Staphyloccocus aureus infection by preventing density-dependent virulence gene up-regulation. *J Immunol,* 171**,** 5389-95.
RYAN, E. A., MOCKROS, L. F., WEISEL, J. W. & LORAND, L. 1999. Structural origins of fibrin clot rheology. *Biophys J,* 77**,** 2813-26.
SAKATA, Y. & AOKI, N. 1980. Cross-linking of alpha 2-plasmin inhibitor to fibrin by fibrin-stabilizing factor. *J Clin Invest,* 65**,** 290-7.
SAKSELA, O. 1985. Plasminogen activation and regulation of pericellular proteolysis. *Biochim Biophys Acta,* 823**,** 35-65.
SANDERSON-SMITH, M., BATZLOFF, M., SRIPRAKASH, K. S., DOWTON, M., RANSON, M. & WALKER, M. J. 2006. Divergence in the plasminogen-binding group a streptococcal M protein family: functional conservation of binding site and potential role for immune selection of variants. *J Biol Chem,* 281**,** 3217-26.

SANDERSON-SMITH, M., DE OLIVEIRA, D. M. P., GUGLIELMINI, J., MCMILLAN, D. J., VU, T., HOLIEN, J. K., HENNINGHAM, A., STEER, A. C., BESSEN, D. E., DALE, J. B., CURTIS, N., BEALL, B. W., WALKER, M. J., PARKER, M. W., CARAPETIS, J. R., VAN MELDEREN, L., SRIPRAKASH, K. S., SMEESTERS, P. R. & GRP, M. P. S. 2014. A Systematic and Functional Classification of Streptococcus pyogenes That Serves as a New Tool for Molecular Typing and Vaccine Development. *Journal of Infectious Diseases,* 210**,** 1325-38.

SANDERSON-SMITH, M. L., DINKLA, K., COLE, J. N., CORK, A. J., MAAMARY, P. G., MCARTHUR, J. D., CHHATWAL, G. S. & WALKER, M. J. 2008. M protein-mediated plasminogen binding is essential for the virulence of an invasive Streptococcus pyogenes isolate. *FASEB J,* 22**,** 2715-22.

SANDERSON-SMITH, M. L., DOWTON, M., RANSON, M. & WALKER, M. J. 2007. The plasminogen-binding group A streptococcal M protein-related protein Prp binds plasminogen via arginine and histidine residues. *J Bacteriol,* 189**,** 1435-40.

SANDERSON-SMITH, M. L., ZHANG, Y., LY, D., DONAHUE, D., HOLLANDS, A., NIZET, V., RANSON, M., PLOPLIS, V. A., WALKER, M. J. & CASTELLINO, F. J. 2013. A key role for the urokinase plasminogen activator (uPA) in invasive Group A streptococcal infection. *PLoS Pathog,* 9**,** e1003469.

SANDIN, C., CARLSSON, F. & LINDAHL, G. 2006. Binding of human plasma proteins to Streptococcus pyogenes M protein determines the location of opsonic and non-opsonic epitopes. *Mol Microbiol,* 59**,** 20-30.

SEKULOSKI, S., BATZLOFF, M. R., GRIFFIN, P., PARSONAGE, W., ELLIOTT, S., HARTAS, J., O'ROURKE, P., MARQUART, L., PANDEY, M., RUBIN, F. A., CARAPETIS, J., MCCARTHY, J. & GOOD, M. F. 2018. Evaluation of safety and immunogenicity of a group A streptococcus vaccine candidate (MJ8VAX) in a randomized clinical trial. *PLoS One,* 13**,** e0198658.

SELA, S. & BARZILAI, A. 1999. Why do we fail with penicillin in the treatment of group A streptococcus infections? *Ann Med,* 31**,** 303-7.

SHAH, G. A., NAIR, C. H. & DHALL, D. P. 1987. Comparison of fibrin networks in plasma and fibrinogen solution. *Thromb Res,* 45**,** 257-64.

SHANNON, O., HERTZEN, E., NORRBY-TEGLUND, A., MORGELIN, M., SJOBRING, U. & BJORCK, L. 2007. Severe streptococcal infection is associated with M protein-induced platelet activation and thrombus formation. *Mol Microbiol,* 65**,** 1147-57.

SHEA, P. R., BERES, S. B., FLORES, A. R., EWBANK, A. L., GONZALEZ-LUGO, J. H., MARTAGON-ROSADO, A. J., MARTINEZ-GUTIERREZ, J. C., REHMAN, H. A., SERRANO-GONZALEZ, M., FITTIPALDI, N., AYERS, S. D., WEBB, P., WILLEY, B. M., LOW, D. E. & MUSSER, J. M. 2011. Distinct signatures of diversifying selection revealed by genome analysis of respiratory tract and invasive bacterial populations. *Proc Natl Acad Sci U S A,* 108**,** 5039-44.

SHIGEMATSU, S., ISHIDA, S., GUTE, D. C. & KORTHUIS, R. J. 2002. Bradykinin-induced proinflammatory signaling mechanisms. *Am J Physiol Heart Circ Physiol,* 283**,** H2676-86.

SILVA, M. M., THELWELL, C., WILLIAMS, S. C. & LONGSTAFF, C. 2012. Regulation of fibrinolysis by C-terminal lysines operates through

plasminogen and plasmin but not tissue-type plasminogen activator. *J Thromb Haemost,* 10**,** 2354-60.
SINGHA, T. K., GULATI, P., MOHANTY, A., KHASA, Y. P., KAPOOR, R. K. & KUMAR, S. 2017. Efficient genetic approaches for improvement of plasmid based expression of recombinant protein in Escherichia coli: A review. *Process Biochemistry,* 55**,** 17-31.
SMITH, S. A., TRAVERS, R. J. & MORRISSEY, J. H. 2015. How it all starts: Initiation of the clotting cascade. *Crit Rev Biochem Mol Biol,* 50**,** 326-36.
SOBEL, J. H. & GAWINOWICZ, M. A. 1996. Identification of the alpha chain lysine donor sites involved in factor XIIIa fibrin cross-linking. *J Biol Chem,* 271**,** 19288-97.
SPRAGGON, G., EVERSE, S. J. & DOOLITTLE, R. F. 1997. Crystal structures of fragment D from human fibrinogen and its crosslinked counterpart from fibrin. *Nature,* 389**,** 455-62.
STALDER, M., HAUERT, J., KRUITHOF, E. K. & BACHMANN, F. 1985. Release of vascular plasminogen activator (v-PA) after venous stasis: electrophoretic-zymographic analysis of free and complexed v-PA. *Br J Haematol,* 61**,** 169-76.
STANDEVEN, K. F., CARTER, A. M., GRANT, P. J., WEISEL, J. W., CHERNYSH, I., MASOVA, L., LORD, S. T. & ARIENS, R. A. 2007. Functional analysis of fibrin {gamma}-chain cross-linking by activated factor XIII: determination of a cross-linking pattern that maximizes clot stiffness. *Blood,* 110**,** 902-7.
STEVENS, D. L. 2001. Invasive streptococcal infections. *Journal of Infection and Chemotherapy,* 7**,** 69-80.
STEVENS, D. L. & BRYANT, A. E. 2016. Severe Group A Streptococcal Infections. *In:* FERRETTI, J. J., STEVENS, D. L. & FISCHETTI, V. A. (eds.) *Streptococcus pyogenes : Basic Biology to Clinical Manifestations.* Oklahoma City (OK).
STEVENS, D. L., TANNER, M. H., WINSHIP, J., SWARTS, R., RIES, K. M., SCHLIEVERT, P. M. & KAPLAN, E. 1989. Severe group A streptococcal infections associated with a toxic shock-like syndrome and scarlet fever toxin A. *N Engl J Med,* 321**,** 1-7.
STEWART, R. J., FREDENBURGH, J. C. & WEITZ, J. I. 1998. Characterization of the interactions of plasminogen and tissue and vampire bat plasminogen activators with fibrinogen, fibrin, and the complex of D-dimer noncovalently linked to fragment E. *Journal of Biological Chemistry,* 273**,** 18292-9.
SUENSON, E., LUTZEN, O. & THORSEN, S. 1984. Initial plasmin-degradation of fibrin as the basis of a positive feed-back mechanism in fibrinolysis. *Eur J Biochem,* 140**,** 513-22.
SUH, T. T., HOLMBACK, K., JENSEN, N. J., DAUGHERTY, C. C., SMALL, K., SIMON, D. I., POTTER, S. & DEGEN, J. L. 1995. Resolution of spontaneous bleeding events but failure of pregnancy in fibrinogen-deficient mice. *Genes Dev,* 9**,** 2020-33.
SUMBY, P., WHITNEY, A. R., GRAVISS, E. A., DELEO, F. R. & MUSSER, J. M. 2006. Genome-wide analysis of group A streptococci reveals a mutation that modulates global phenotype and disease specificity. *Plos Pathogens,* 2**,** 41-49.
SUMITOMO, T., NAKATA, M., HIGASHINO, M., TERAO, Y. & KAWABATA, S. 2013. Group A Streptococcal Cysteine Protease Cleaves Epithelial

Junctions and Contributes to Bacterial Translocation. *Journal of Biological Chemistry,* 288**,** 13317-24.
SUMITOMO, T., NAKATA, M., HIGASHINO, M., YAMAGUCHI, M. & KAWABATA, S. 2016. Group A Streptococcus exploits human plasminogen for bacterial translocation across epithelial barrier via tricellular tight junctions. *Sci Rep,* 7**,** 20069.
SUN, H., RINGDAHL, U., HOMEISTER, J. W., FAY, W. P., ENGLEBERG, N. C., YANG, A. Y., ROZEK, L. S., WANG, X., SJOBRING, U. & GINSBURG, D. 2004. Plasminogen is a critical host pathogenicity factor for group A streptococcal infection. *Science,* 305**,** 1283-6.
SUN, H., WANG, X., DEGEN, J. L. & GINSBURG, D. 2009. Reduced thrombin generation increases host susceptibility to group A streptococcal infection. *Blood,* 113**,** 1358-64.
TATSUNO, I., OKADA, R., ZHANG, Y., ISAKA, M. & HASEGAWA, T. 2013. Partial loss of CovS function in Streptococcus pyogenes causes severe invasive disease. *BMC Res Notes,* 6**,** 126.
TEWODROS, W., KARLSSON, I. & KRONVALL, G. 1996. Allelic variation of the streptokinase gene in beta-hemolytic streptococci group C and G isolates of human origin. *FEMS Immunol Med Microbiol,* 13**,** 29-34.
THELWELL, C. & LONGSTAFF, C. 2014. Biosimilars: the process is the product. The example of recombinant streptokinase. *J Thromb Haemost,* 12**,** 1229-33.
THOMAS, S., LIU, W., ARORA, S., GANESH, V., KO, Y. P. & HOOK, M. 2019. The Complex Fibrinogen Interactions of the Staphylococcus aureus Coagulases. *Front Cell Infect Microbiol,* 9**,** 106.
THOMER, L., SCHNEEWIND, O. & MISSIAKAS, D. 2013. Multiple ligands of von Willebrand factor-binding protein (vWbp) promote Staphylococcus aureus clot formation in human plasma. *J Biol Chem,* 288**,** 28283-92.
THOMER, L., SCHNEEWIND, O. & MISSIAKAS, D. 2016. Pathogenesis of Staphylococcus aureus Bloodstream Infections. *Annu Rev Pathol,* 11**,** 343-64.
TIMMER, A. M., TIMMER, J. C., PENCE, M. A., HSU, L. C., GHOCHANI, M., FREY, T. G., KARIN, M., SALVESEN, G. S. & NIZET, V. 2009. Streptolysin O Promotes Group A Streptococcus Immune Evasion by Accelerated Macrophage Apoptosis. *Journal of Biological Chemistry,* 284**,** 862-71.
TORBET, J. 1986. Fibrin assembly in human plasma and fibrinogen/albumin mixtures. *Biochemistry,* 25**,** 5309-14.
TSURUPA, G., MAHID, A., VEKLICH, Y., WEISEL, J. W. & MEDVED, L. 2011. Structure, stability, and interaction of fibrin alphaC-domain polymers. *Biochemistry,* 50**,** 8028-37.
TURNER, C. E., BUBBA, L. & EFSTRATIOU, A. 2019. Pathogenicity Factors in Group C and G Streptococci. *Microbiol Spectr,* 7.
UCHIYAMA, S., ANDREONI, F., ZURCHER, C., SCHILCHER, K., ENDER, M., MADON, J., MATT, U., GHOSH, P., NIZET, V., SCHUEPBACH, R. A. & ZINKERNAGEL, A. S. 2013. Coiled-coil irregularities of the M1 protein structure promote M1-fibrinogen interaction and influence group A Streptococcus host cell interactions and virulence. *J Mol Med (Berl),* 91**,** 861-9.
ULLBERG, M., KUUSELA, P., KRISTIANSEN, B. E. & KRONVALL, G. 1992. Binding of Plasminogen to Neisseria-Meningitidis and Neisseria-

Gonorrhoeae and Formation of Surface-Associated Plasmin. *Journal of Infectious Diseases,* 166**,** 1329-34.
US FOOD AND DRUG ADMINISTRATION, H. 2005. Status of Specific Products; Group A Streptococcus. Federal Register.
VALDES, K. M., SUNDAR, G. S., BELEW, A. T., ISLAM, E., EL-SAYED, N. M., LE BRETON, Y. & MCIVER, K. S. 2018. Glucose Levels Alter the Mga Virulence Regulon in the Group A Streptococcus. *Sci Rep,* 8**,** 4971.
VANASSCHE, T., PEETERMANS, M., VAN AELST, L. N., PEETERMANS, W. E., VERHAEGEN, J., MISSIAKAS, D. M., SCHNEEWIND, O., HOYLAERTS, M. F. & VERHAMME, P. 2013. The role of staphylothrombin-mediated fibrin deposition in catheter-related Staphylococcus aureus infections. *J Infect Dis,* 208**,** 92-100.
VANASSCHE, T., VERHAEGEN, J., PEETERMANS, W. E., J, V. A. N. R., CHENG, A., SCHNEEWIND, O., HOYLAERTS, M. F. & VERHAMME, P. 2011. Inhibition of staphylothrombin by dabigatran reduces Staphylococcus aureus virulence. *J Thromb Haemost,* 9**,** 2436-46.
VANNICE, K. S., RICALDI, J., NANDURI, S., FANG, F. C., LYNCH, J. B., BRYSON-CAHN, C., WRIGHT, T., DUCHIN, J., KAY, M., CHOCHUA, S., VAN BENEDEN, C. A. & BEALL, B. 2020. Streptococcus pyogenes pbp2x Mutation Confers Reduced Susceptibility to beta-Lactam Antibiotics. *Clin Infect Dis,* 71**,** 201-4.
VARADI, A. & PATTHY, L. 1983. Location of plasminogen-binding sites in human fibrin(ogen). *Biochemistry,* 22**,** 2440-6.
VARJU, I., LONGSTAFF, C., SZABO, L., FARKAS, A. Z., VARGA-SZABO, V. J., TANKA-SALAMON, A., MACHOVICH, R. & KOLEV, K. 2015. DNA, histones and neutrophil extracellular traps exert anti-fibrinolytic effects in a plasma environment. *Thromb Haemost,* 113**,** 1289-98.
VEGA, L. A., MALKE, H. & MCIVER, K. S. 2016. Virulence-Related Transcriptional Regulators of Streptococcus pyogenes. *In:* FERRETTI, J. J., STEVENS, D. L. & FISCHETTI, V. A. (eds.) *Streptococcus pyogenes : Basic Biology to Clinical Manifestations.* Oklahoma City (OK).
VISSER, M., VAN OERLE, R., TEN CATE, H., LAUX, V., MACKMAN, N., HEITMEIER, S. & SPRONK, H. M. H. 2020. Plasma Kallikrein Contributes to Coagulation in the Absence of Factor XI by Activating Factor IX. *Arterioscler Thromb Vasc Biol,* 40**,** 103-111.
VYAS, H. K. N., PROCTOR, E. J., MCARTHUR, J., GORMAN, J. & SANDERSON-SMITH, M. 2019. Current Understanding of Group A Streptococcal Biofilms. *Curr Drug Targets,* 20**,** 982-993.
WALKER, M. J., BARNETT, T. C., MCARTHUR, J. D., COLE, J. N., GILLEN, C. M., HENNINGHAM, A., SRIPRAKASH, K. S., SANDERSON-SMITH, M. L. & NIZET, V. 2014. Disease manifestations and pathogenic mechanisms of Group A Streptococcus. *Clin Microbiol Rev,* 27**,** 264-301.
WALKER, M. J., HOLLANDS, A., SANDERSON-SMITH, M. L., COLE, J. N., KIRK, J. K., HENNINGHAM, A., MCARTHUR, J. D., DINKLA, K., AZIZ, R. K., KANSAL, R. G., SIMPSON, A. J., BUCHANAN, J. T., CHHATWAL, G. S., KOTB, M. & NIZET, V. 2007. DNase Sda1 provides selection pressure for a switch to invasive group A streptococcal infection. *Nat Med,* 13**,** 981-5.
WANG, M., ZAJICEK, J., GEIGER, J. H., PROROK, M. & CASTELLINO, F. J. 2010a. Solution structure of the complex of VEK-30 and plasminogen kringle 2. *J Struct Biol,* 169**,** 349-59.

WANG, S., REED, G. L. & HEDSTROM, L. 1999. Deletion of Ile1 changes the mechanism of streptokinase: evidence for the molecular sexuality hypothesis. *Biochemistry,* 38**,** 5232-40.
WANG, S., REED, G. L. & HEDSTROM, L. 2000. Zymogen activation in the streptokinase-plasminogen complex. Ile1 is required for the formation of a functional active site. *Eur J Biochem,* 267**,** 3994-4001.
WANG, W., BOFFA, M. B., BAJZAR, L., WALKER, J. B. & NESHEIM, M. E. 1998a. A study of the mechanism of inhibition of fibrinolysis by activated thrombin-activable fibrinolysis inhibitor. *J Biol Chem,* 273**,** 27176-81.
WANG, X., LIN, X., LOY, J. A., TANG, J. & ZHANG, X. C. 1998b. Crystal structure of the catalytic domain of human plasmin complexed with streptokinase. *Science,* 281**,** 1662-5.
WANG, Z., WILHELMSSON, C., HYRSL, P., LOOF, T. G., DOBES, P., KLUPP, M., LOSEVA, O., MORGELIN, M., IKLE, J., CRIPPS, R. M., HERWALD, H. & THEOPOLD, U. 2010b. Pathogen entrapment by transglutaminase--a conserved early innate immune mechanism. *PLoS Pathog,* 6**,** e1000763.
WATSON, M. E., JR., NEELY, M. N. & CAPARON, M. G. 2016. Animal Models of Streptococcus pyogenes Infection. *In:* FERRETTI, J. J., STEVENS, D. L. & FISCHETTI, V. A. (eds.) *Streptococcus pyogenes : Basic Biology to Clinical Manifestations.* Oklahoma City (OK).
WEISEL, J. W. 2005. Fibrinogen and fibrin. *Adv Protein Chem,* 70**,** 247-99.
WEISEL, J. W. & LITVINOV, R. I. 2008. The biochemical and physical process of fibrinolysis and effects of clot structure and stability on the lysis rate. *Cardiovasc Hematol Agents Med Chem,* 6**,** 161-80.
WEISEL, J. W. & LITVINOV, R. I. 2017. Fibrin Formation, Structure and Properties. *Subcell Biochem,* 82**,** 405-56.
WEISEL, J. W. & MEDVED, L. 2001. The structure and function of the alpha C domains of fibrinogen. *Ann N Y Acad Sci,* 936**,** 312-27.
WEISEL, J. W. & NAGASWAMI, C. 1992. Computer modeling of fibrin polymerization kinetics correlated with electron microscope and turbidity observations: clot structure and assembly are kinetically controlled. *Biophys J,* 63**,** 111-28.
WEISEL, J. W., STAUFFACHER, C. V., BULLITT, E. & COHEN, C. 1985. A model for fibrinogen: domains and sequence. *Science,* 230**,** 1388-91.
WEISEL, J. W., VEKLICH, Y. & GORKUN, O. 1993. The sequence of cleavage of fibrinopeptides from fibrinogen is important for protofibril formation and enhancement of lateral aggregation in fibrin clots. *J Mol Biol,* 232**,** 285-97.
WESSELS, M. R., MOSES, A. E., GOLDBERG, J. B. & DICESARE, T. J. 1991. Hyaluronic-Acid Capsule Is a Virulence Factor for Mucoid Group-a Streptococci. *Proceedings of the National Academy of Sciences of the United States of America,* 88**,** 8317-21.
WHITE, M. D., BOSIO, C. M., DUPLANTIS, B. N. & NANO, F. E. 2011. Human body temperature and new approaches to constructing temperature-sensitive bacterial vaccines. *Cell Mol Life Sci,* 68**,** 3019-31.
WILCOX, J. N., SMITH, K. M., SCHWARTZ, S. M. & GORDON, D. 1989. Localization of tissue factor in the normal vessel wall and in the atherosclerotic plaque. *Proc Natl Acad Sci U S A,* 86**,** 2839-43.
WILF, J., GLADNER, J. A. & MINTON, A. P. 1985. Acceleration of fibrin gel formation by unrelated proteins. *Thromb Res,* 37**,** 681-8.

WILLIAMS, R. C. 1981. Morphology of bovine fibrinogen monomers and fibrin oligomers. *J Mol Biol,* 150**,** 399-408.
WIMAN, B. 1980. On the reaction of plasmin or plasmin-streptokinase complex with aprotinin or alpha 2-antiplasmin. *Thromb Res,* 17**,** 143-52.
WINKLER, F., KASTENBAUER, S., KOEDEL, U. & PFISTER, H. W. 2002. Role of the urokinase plasminogen activator system in patients with bacterial meningitis. *Neurology,* 59**,** 1350-5.
WINRAM, S. B. & LOTTENBERG, R. 1996. The plasmin-binding protein Plr of group A streptococci is identified as glyceraldehyde-3-phosphate dehydrogenase. *Microbiology-Sgm,* 142**,** 2311-2320.
WISTEDT, A. C., KOTARSKY, H., MARTI, D., RINGDAHL, U., CASTELLINO, F. J., SCHALLER, J. & SJOBRING, U. 1998. Kringle 2 mediates high affinity binding of plasminogen to an internal sequence in streptococcal surface protein PAM. *J Biol Chem,* 273**,** 24420-4.
WISTEDT, A. C., RINGDAHL, U., MULLER-ESTERL, W. & SJOBRING, U. 1995. Identification of a plasminogen-binding motif in PAM, a bacterial surface protein. *Mol Microbiol,* 18**,** 569-78.
WOLBERG, A. S. 2007. Thrombin generation and fibrin clot structure. *Blood Rev,* 21**,** 131-42.
WOLBERG, A. S. & CAMPBELL, R. A. 2008. Thrombin generation, fibrin clot formation and hemostasis. *Transfus Apher Sci,* 38**,** 15-23.
WOLBERG, A. S., GABRIEL, D. A. & HOFFMAN, M. 2002. Analyzing fibrin clot structure using a microplate reader. *Blood Coagul Fibrinolysis,* 13**,** 533-9.
WOLBERG, A. S., MONROE, D. M., ROBERTS, H. R. & HOFFMAN, M. 2003. Elevated prothrombin results in clots with an altered fiber structure: a possible mechanism of the increased thrombotic risk. *Blood,* 101**,** 3008-13.
WOLLEIN WALDETOFT, K., SVENSSON, L., MORGELIN, M., OLIN, A. I., NITSCHE-SCHMITZ, D. P., BJORCK, L. & FRICK, I. M. 2012. Streptococcal surface proteins activate the contact system and control its antibacterial activity. *J Biol Chem,* 287**,** 25010-8.
WORLD HEALTH ORGANISATION. 2005. *The Current Evidence for the Burden of Group A Streptococcal Diseases.* [Online]. Discussion papers on Child Health. Department of Child and Adolescent Health and Development: World Health Organisation. Available: http://whqlibdoc.who.int/hq/2005/WHO_FCH_CAH_05.07.pdf [Accessed 2021].
XUE, Y., BODIN, C. & OLSSON, K. 2012. Crystal structure of the native plasminogen reveals an activation-resistant compact conformation. *J Thromb Haemost,* 10**,** 1385-96.
YANG, Z., MOCHALKIN, I. & DOOLITTLE, R. F. 2000. A model of fibrin formation based on crystal structures of fibrinogen and fibrin fragments complexed with synthetic peptides. *Proc Natl Acad Sci U S A,* 97**,** 14156-61.
YEE, V. C., PRATT, K. P., COTE, H. C., TRONG, I. L., CHUNG, D. W., DAVIE, E. W., STENKAMP, R. E. & TELLER, D. C. 1997. Crystal structure of a 30 kDa C-terminal fragment from the gamma chain of human fibrinogen. *Structure,* 5**,** 125-38.
YU, W., KIM, H. K., RAUCH, S., SCHNEEWIND, O. & MISSIAKAS, D. 2017. Pathogenic conversion of coagulase-negative staphylococci. *Microbes Infect,* 19**,** 101-9.

YUAN, Y., AYINUOLA, Y. A., SINGH, D., AYINUOLA, O., MAYFIELD, J. A., QUEK, A., WHISSTOCK, J. C., LAW, R. H. P., LEE, S. W., PLOPLIS, V. A. & CASTELLINO, F. J. 2019. Solution structural model of the complex of the binding regions of human plasminogen with its M-protein receptor from Streptococcus pyogenes. *J Struct Biol***,** 18-29.

YUN, S. H., SIM, E. H., GOH, R. Y., PARK, J. I. & HAN, J. Y. 2016. Platelet Activation: The Mechanisms and Potential Biomarkers. *Biomed Res Int,* 2016**,** 9060143.

ZEERLEDER, S. 2011. C1-inhibitor: more than a serine protease inhibitor. *Semin Thromb Hemost,* 37**,** 362-74.

ZHANG, Y., LIANG, Z., HSUEH, H. T., PLOPLIS, V. A. & CASTELLINO, F. J. 2012. Characterization of streptokinases from group A Streptococci reveals a strong functional relationship that supports the coinheritance of plasminogen-binding M protein and cluster 2b streptokinase. *J Biol Chem,* 287**,** 42093-103.

ZHANG, Y., MAYFIELD, J. A., PLOPLIS, V. A. & CASTELLINO, F. J. 2014. The beta-domain of cluster 2b streptokinase is a major determinant for the regulation of its plasminogen activation activity by cellular plasminogen receptors. *Biochem Biophys Res Commun,* 444**,** 595-8.

ZHMUROV, A., BROWN, A. E., LITVINOV, R. I., DIMA, R. I., WEISEL, J. W. & BARSEGOV, V. 2011. Mechanism of fibrin(ogen) forced unfolding. *Structure,* 19**,** 1615-24.

ZHMUROV, A., PROTOPOPOVA, A. D., LITVINOV, R. I., ZHUKOV, P., MUKHITOV, A. R., WEISEL, J. W. & BARSEGOV, V. 2016. Structural Basis of Interfacial Flexibility in Fibrin Oligomers. *Structure,* 24**,** 1907-17.

ZSCHIEDRICH, C. P., KEIDEL, V. & SZURMANT, H. 2016. Molecular Mechanisms of Two-Component Signal Transduction. *J Mol Biol,* 428**,** 3752-75.

ZUEV, Y. F., LITVINOV, R. I., SITNITSKY, A. E., IDIYATULLIN, B. Z., BAKIROVA, D. R., GALANAKIS, D. K., ZHMUROV, A., BARSEGOV, V. & WEISEL, J. W. 2017. Conformational Flexibility and Self-Association of Fibrinogen in Concentrated Solutions. *J Phys Chem B,* 121**,** 7833-43.

Chapter 7 Appendices

7.1 LSCM of purified fibrin fibres

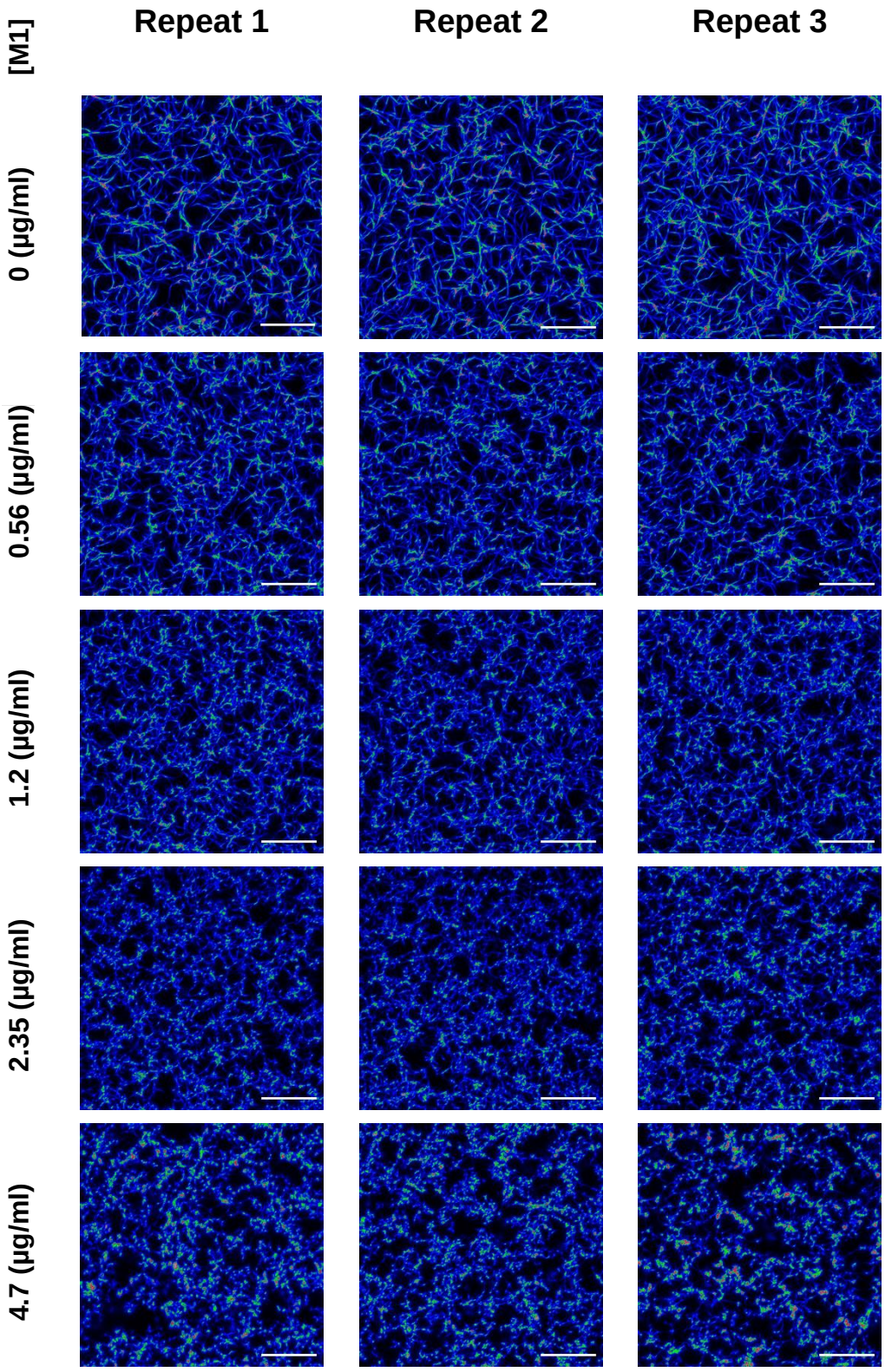

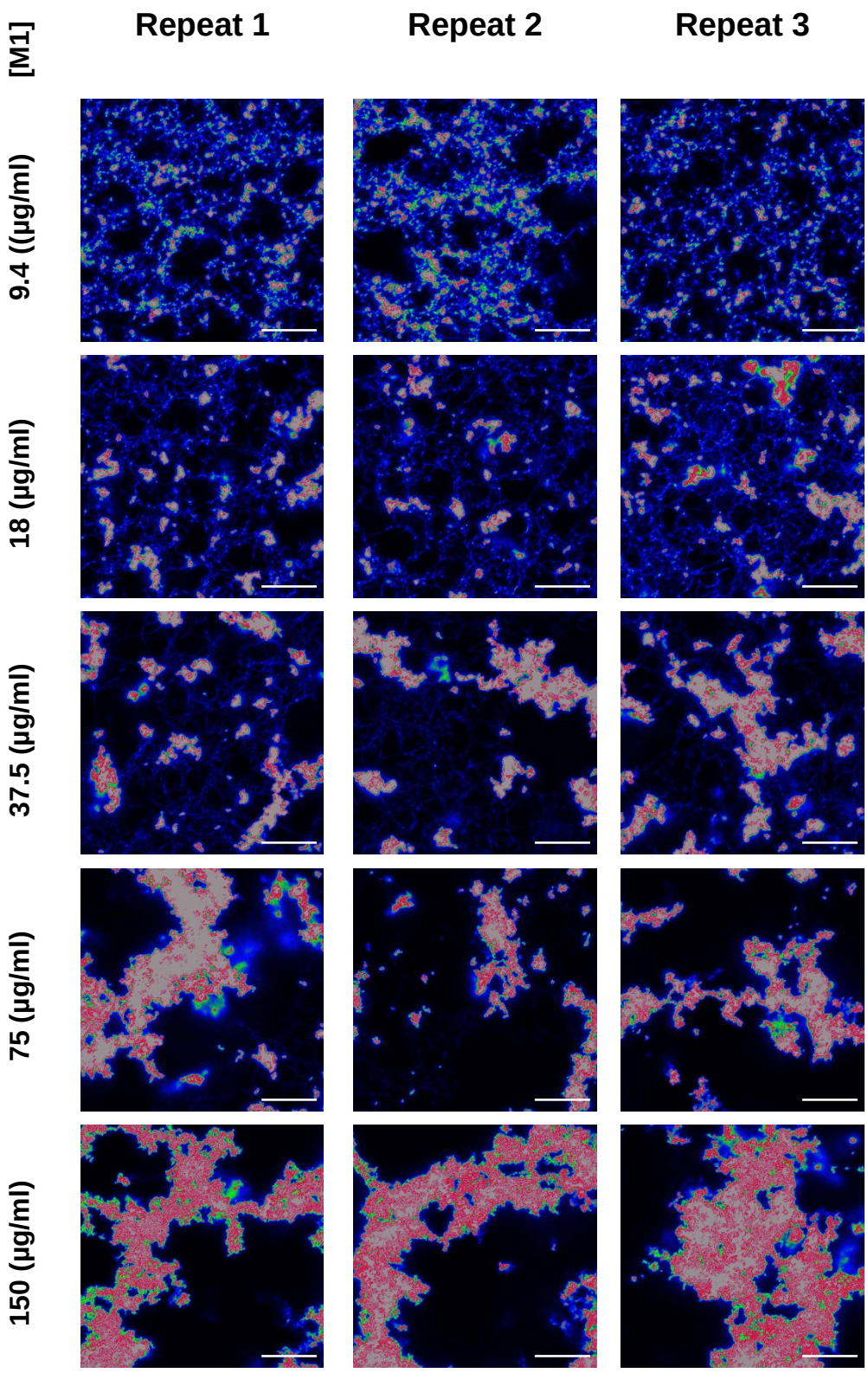

Fibrin fibres were formed through the addition of thrombin ((01/578) 0.2 IU/ml) and calcium (5 mM) in the presence of varying concentrations of rM1 protein (0-150 µg/ml). Fibrinogen (3 mg/ml) was fluorescently labelled with Alexa fluor 594 (0.05 mg/ml). All dilutions were performed in Buffer B (Table 1) Scale bar: 20 µm

7.2 MCF of purified fibrin clots in the presence of increasing concentrations of rM1 and rPAM (1.88- 60 µg/ml)

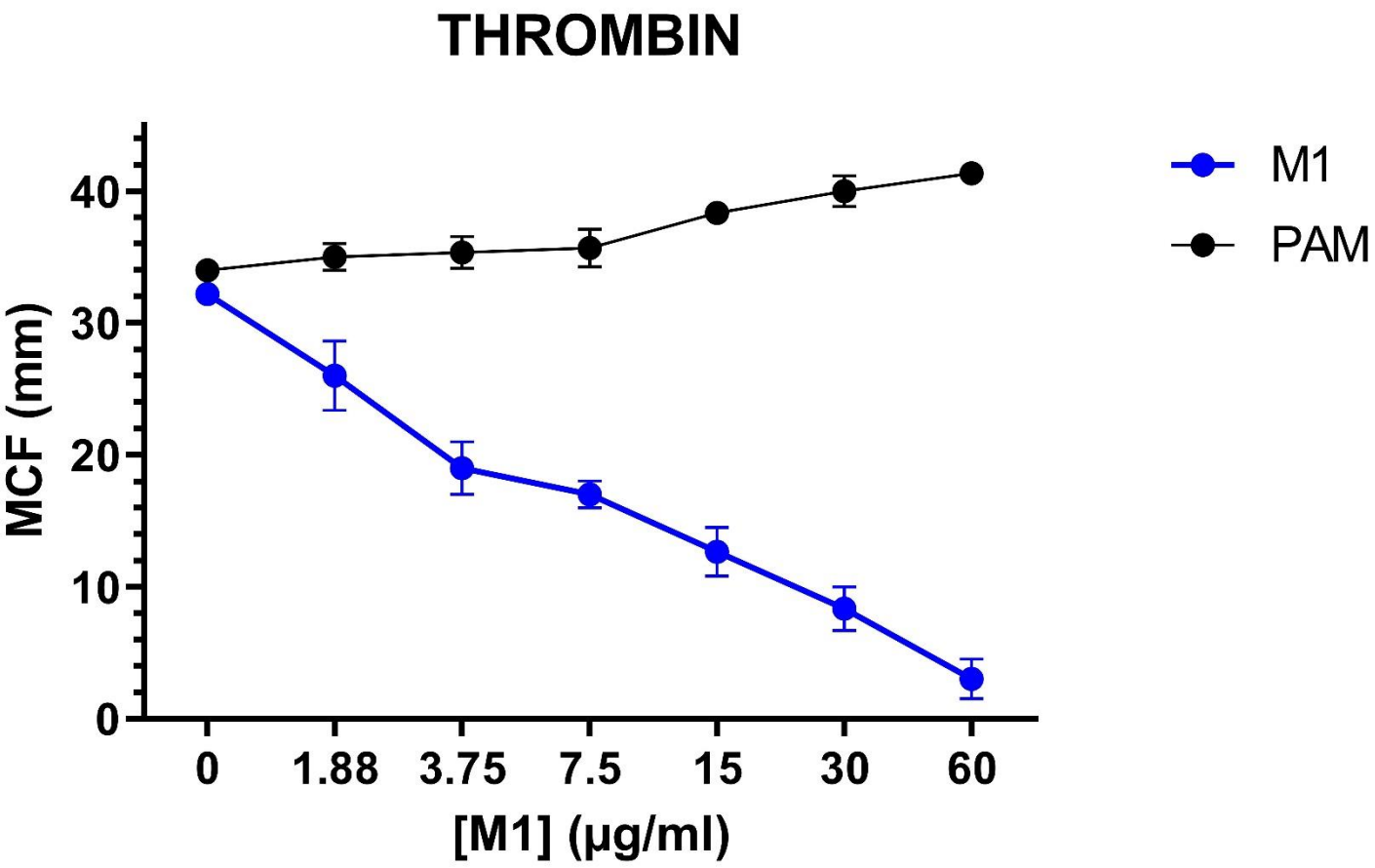

Physical strength of clots incorporating rM1 or rPAM (0-60 µg/ml) were measured with the addition of thrombin (00/578), 0.5 IU/ml) and calcium (5 mM). All dilutions were in Buffer B (Table 1), performed using ROTEM ®. Maximum clot formation (MCF) after 1 hour is shown. Error bars represent SEM